IOWA STATE UNIVERSITY
Digital Repository

Retrospective Theses and Dissertations

Iowa State University Capstones, Theses and Dissertations

1992

Theoretical and experimental methods for in situ infrared spectroelectrochemistry of organic monomolecular films

Darwin David Popenoe
Iowa State University

Follow this and additional works at: https://lib.dr.iastate.edu/rtd

 Part of the Analytical Chemistry Commons, and the Physical Chemistry Commons

Recommended Citation
Popenoe, Darwin David, "Theoretical and experimental methods for in situ infrared spectroelectrochemistry of organic monomolecular films " (1992). *Retrospective Theses and Dissertations*. 10386.
https://lib.dr.iastate.edu/rtd/10386

This Dissertation is brought to you for free and open access by the Iowa State University Capstones, Theses and Dissertations at Iowa State University Digital Repository. It has been accepted for inclusion in Retrospective Theses and Dissertations by an authorized administrator of Iowa State University Digital Repository. For more information, please contact digirep@iastate.edu.

www.manaraa.com

INFORMATION TO USERS

This manuscript has been reproduced from the microfilm master. UMI films the text directly from the original or copy submitted. Thus, some thesis and dissertation copies are in typewriter face, while others may be from any type of computer printer.

The quality of this reproduction is dependent upon the quality of the copy submitted. Broken or indistinct print, colored or poor quality illustrations and photographs, print bleedthrough, substandard margins, and improper alignment can adversely affect reproduction.

In the unlikely event that the author did not send UMI a complete manuscript and there are missing pages, these will be noted. Also, if unauthorized copyright material had to be removed, a note will indicate the deletion.

Oversize materials (e.g., maps, drawings, charts) are reproduced by sectioning the original, beginning at the upper left-hand corner and continuing from left to right in equal sections with small overlaps. Each original is also photographed in one exposure and is included in reduced form at the back of the book.

Photographs included in the original manuscript have been reproduced xerographically in this copy. Higher quality 6" x 9" black and white photographic prints are available for any photographs or illustrations appearing in this copy for an additional charge. Contact UMI directly to order.

U·M·I

University Microfilms International
A Bell & Howell Information Company
300 North Zeeb Road, Ann Arbor, MI 48106-1346 USA
313/761-4700 800/521-0600

Order Number 9302014

Theoretical and experimental methods for *in situ* infrared spectroelectrochemistry of organic monomolecular films

Popenoe, Darwin David, Ph.D.

Iowa State University, 1992

U·M·I
300 N. Zeeb Rd.
Ann Arbor, MI 48106

Theoretical and experimental methods for in situ infrared spectroelectrochemistry of organic monomolecular films

by

Darwin David Popenoe

A Dissertation Submitted to the
Graduate Faculty in Partial Fulfillment of the
Requirements for the Degree of
DOCTOR OF PHILOSOPHY

Department: Chemistry
Major: Analytical Chemistry

Approved:

Signature was redacted for privacy.

In Charge of Major Work

Signature was redacted for privacy.

For the Major Department

Signature was redacted for privacy.

For the Graduate College

Iowa State University
Ames, Iowa

1992

DEDICATION

This dissertation is dedicated to my father, Paul Popenoe, and to the memory of my mother, Norma Jaekel Popenoe (1919-1979). Without their guidance, love, and support early in my life, I would not have made it to this point today.

TABLE OF CONTENTS

ACKNOWLEDGMENTS

I wish to express thanks to Dr. Marc Porter, major professor and research adviser, for his extensive tutelage. I give tremendous gratitude to my wife, Flora Mbasha Popenoe, for her editing help, moral support, and extreme patience. Also, I express appreciation to Janey Spangler, Russell Hoffman, Martha Stewart, and many other friends in the Ames community who made the stay here enjoyable, productive, and mentally healthy.

The receipt of a graduate fellowship from BP America I gratefully acknowledge. This work was performed at Ames Laboratory under contract no. W-7405-eng-82 with the U. S. Department of Energy. The United States government has assigned the DOE Report number IS-T 1607 to this thesis.

GENERAL INTRODUCTION

1. Some Background Concerning the Study of Liquid-Solid Interfaces

In the broad, expanding, and interdisciplinary field of surface science, the use of ordered monomolecular films assembled at the surface of an electrode or other substrate has proven invaluable for tailoring model surfaces. When assembled at a liquid-solid interface, these ordered monolayer films constitute versatile tools for studying interfacial phenomena. They can, for example, serve as models of polymer surfaces exposed to liquids, of biomaterials implanted in living tissue, of coatings used for reducing corrosion or friction, and of surfaces of suspended colloids or solid particles in solutions. Those "real-life" systems are very complex and disordered, but creating a model experimental system allows us to vary one aspect of the interface at a time and to examine the effect of that one variable upon the structure and chemical behavior of the entire interface.

To illustrate the type of system studied in my research, Figure 1 shows a generic diagram of a self-assembled monolayer film at a liquid-solid interface. To maintain a high degree of order and create a barrier film, the body of the adsorbate molecule is usually a linear alkyl chain. Some head group other than methyl is necessary to bind the adsorbate to the surface. In addition, the end group may be manipulated to bring about different interactions between the liquid and the film. The surrounding liquid, in general, may be aqueous or non-aqueous, conducting or non-conducting.

Specifically, my co-workers and I have emphasized the study of the structure and chemical reactivity of spontaneously adsorbed monolayers of alkanethiolates and derivatized analogs, in which the head group is a sulfur atom, at gold electrodes.[1,2,3,4,5,6,7,8,9,10,11,12] Alkanethiols have been shown to adsorb onto Au with

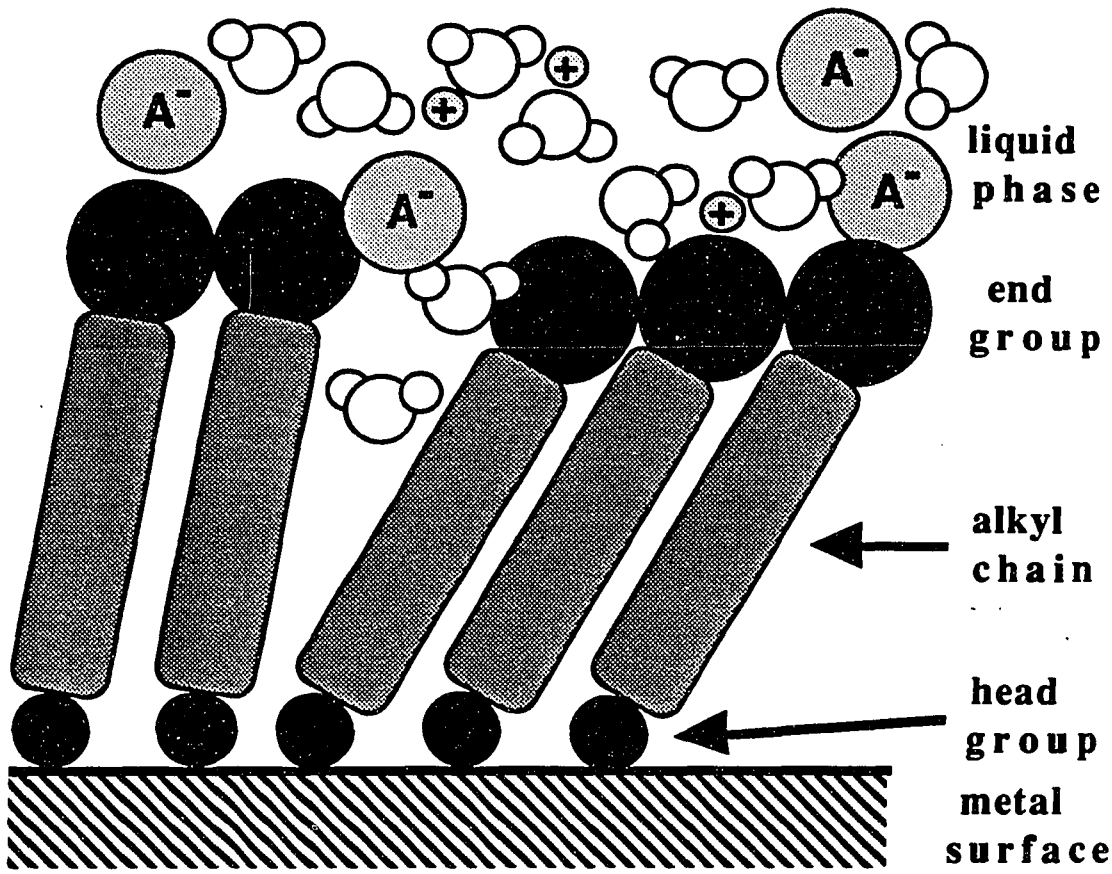

Figure 1. General depiction of a monolayer at a liquid-solid interface. For simplicity, the hydration spheres of the electrolyte ions are not shown.

loss of a proton to form a gold alkanethiolate.[12,13,14] Alkanethiolate monolayer films, illustrated in Figure 2, form as densely packed structures with a well-defined composition, thickness, and orientation—properties that have led to their extensive use as a model molecular system for examining chemical and electrochemical processes at surfaces in contact with aqueous solutions (e.g. wetting[5,6,7] and heterogeneous electron

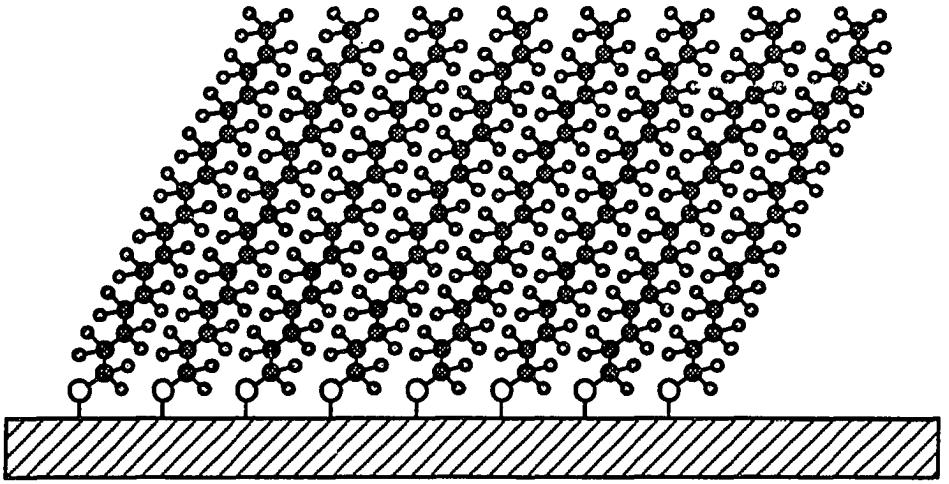

Figure 2. Depiction of an alkanethiolate monolayer at gold.

transfer[8,9,10,11,12,15,16,17,18]). Long-chain alkanethiolate monolayers exposed to air have been shown to have an all-trans chain conformation with a tilt of ~30° from the surface normal[9] and to form with $\left(\sqrt{3}\times\sqrt{3}\right)$ R 30° packing at the Au(111) sites typical of evaporated gold films.[19]

Many analytical techniques have been developed to investigate monolayers at liquid-solid interfaces. Some spectroscopic investigations of electrode surfaces involve generating a surface species in solution, emersing the electrode, and scanning a spectrum of the surface in air or N_2; these are designated as *ex situ* techniques. However, measuring a spectrum of an electrode surface while it is still in contact with the liquid—known as *in situ* spectroscopy—is more useful because it avoids the possibility of changes to the interface during emersion.

Infrared reflection-absorption spectroscopy (IRRAS), when coupled with electrochemical and polarization-modulation techniques, is an invaluable tool for probing

molecular transformations in situ at electrode surfaces.[20,21,22,23,24,25,26,27,28] The modulation techniques discriminate the small absorbances associated with monolayer quantities of adsorbates from the large background absorbances of thin (~2-10 μm) overlayers of electrolytic solutions. The application of electrochemical modulation reveals potential-dependent interfacial changes. In contrast, polarization-modulation techniques harness the enhancement of p-polarized light over s-polarized light at reflective metallic surfaces to produce a difference spectrum with a strong interfacial component.

The IRRAS technique works well for many interfacial systems, but when probing the interactions between methyl-terminated alkanethiolate monolayers and a thin aqueous overlayer, application of the technique is very difficult experimentally. Unfortunately, the spectroscopic and chemical properties of these polymethylene-dominated structures decrease the utility of the noted modulation techniques for examining the reflection spectrum of the monolayer film if an aqueous overlayer is present. Electrochemical modulation is precluded since alkanethiolates at gold exhibit a structural dependence only at applied voltages that induce oxidative or reductive desorption.[12] On the other hand, optical polarization modulation is hindered by the spectral distortions that result from overlap of the principal spectroscopic signatures of alkyl chains (in the C–H stretching region of the spectrum) with the tail of the O–H stretching mode of aqueous solutions,[29] complicating a structural interpretation of the data. This dilemma led Marc Porter, Scott Stole, and me to develop a new form of in situ IRRAS to study these systems.

The technique of in situ external-reflection IRRAS of a liquid-solid interface is illustrated in Figure 3. In our work, a thin layer of solution is sandwiched between an IR-transmitting window and a metal surface at which the monolayer is adsorbed. In this method, the IR beam traverses the window, goes through the liquid at a nearly grazing angle of incidence, reflects off the surface where its electric field interacts with the

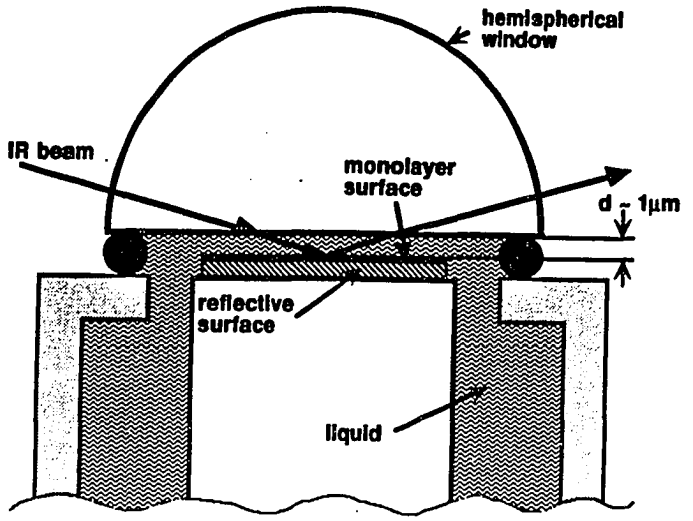

Figure 3. Illustration of the technique of in situ infrared reflection-absorption spectroscopy (IRRAS).

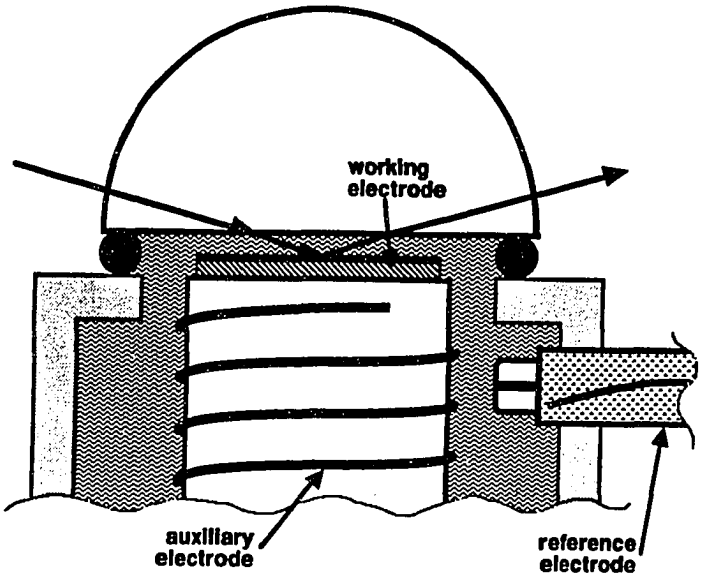

Figure 4. Illustration of the technique of in situ infrared spectroelectrochemistry (IRSEC).

monolayer, and proceeds to exit the cell. Much of the work described herein is concerned with developing this technique and applying it to studies of monolayers at the interface with aqueous solutions. The aqueous layer is useful as an electrolyte and to model real-world situations, but, as noted earlier, it poses an experimental challenge because of its strong absorption and dispersion of the IR beam passing through it. Sections II and III address this problem in detail.

In many cases, monolayers are used to modify the surface of an electrode in an electrochemical cell. For instance, coating the surface with a monolayer may be used to modify the rate or selectivity of an electron-transfer reaction of a species in solution—in order to elucidate redox processes occurring at the surface, or in order to effect electron-transfer reactions of the adsorbed film itself. Notwithstanding the discussion above, in cases where the monolayer film itself is electroactive, the utility of IRRAS for studying the interface may be extended by controlling the potential of the coated surface during acquisition of a spectrum, as illustrated in Figure 4. This potential control is done by attaching the monolayer-coated (working) electrode to a potentiostat and adding reference and auxiliary electrodes to the cell. This dissertation refers to the combination of IRRAS with any type of electrochemical modulation as infrared spectroelectrochemistry (IRSEC). In summary, the research described herein is largely concerned with in situ IRRAS and IRSEC of alkanethiolate films self-assembled at Au.

2. An Explanation of the Dissertation Organization

To complete this introductory chapter, a discussion of the organization of this dissertation follows. The dissertation is divided into individual sections, and each covers one project, set of experiments, or topic area. The sections are similar to manuscripts that would be published in the chemical literature, but with the exception of Section IV, they are not papers that have been submitted for publication in their present form. Following

this introduction, two other preliminary chapters give (1) a review of recent literature in related areas and (2) the theoretical background used in calculations and models in subsequent sections.

In the body of the dissertation, Section I addresses the methods of determining optical functions and experimental results of this determination for compounds used in my research group. Section II presents calculations of mean square electric field (MSEF) for the in situ cell used in this work. Section III presents the theoretical and experimental analysis of in situ IRRAS of an octadecanethiolate monolayer at the aqueous/metal interface. Section IV consists of a paper discussing the examination, by in situ IRRAS combined with electrochemical modulation, of a monolayer derivatized with ferrocene. Section V offers some preliminary results and prospects for in situ study of an electroactive monolayer derivatized with a flavin. Finally, an overall summary and prospects for future work in this area conclude the body of the dissertation.

Among the supplementary material included at the end are a glossary of abbreviations used throughout and the list of references. Two appendices give some additional data for reference. Appendix 1 lists the source code in FORTRAN (actually in the form of listing files created by Microsoft FORTRAN Version 4.1) for the computer programs used in this work. Appendix 2 gives in tabular form the data for optical functions of materials presented in Section II.

Each of the sections describing experimental work has its own subsection presenting the experimental details; these sections are organized in a fashion similar to individual articles in technical journals. Much of the work presented in this dissertation has been published previously, primarily in a book chapter and two articles.[30,31,32] Because the dissertation adds material not included in these publications, all the sections except Section IV are organized logically around a central theme, rather than being

presented in their as-published form. Only the paper on the ferrocene-derivatized monolayers appears verbatim in the actual form which was accepted for publication in *Langmuir*,[32] since it forms a coherent whole in the context of this dissertation. The second and third authors of that work are Randall S. Deinhammer and Marc D. Porter. The results of electrochemical studies by Deinhammer are included in this dissertation because they support—and provide additional information about—the IRRAS studies of the ferrocenyl monolayer. Section V, which presents the study of the flavin-derivatized alkanethiolate monolayer film, constitutes preliminary work that Porter and I may submit for publication later in a revised and expanded form. For the most part, results included here represent my contribution to the respective publications; I have acknowledged the work of others where appropriate.

THE RECENT LITERATURE OF IN SITU IR REFLECTION SPECTROCHEMICAL TECHNIQUES FOR STUDIES OF SURFACE FILMS

1. Introduction

This chapter summarizes some of the recent literature about in situ IRRAS and IRSEC; this literature is related to the central focus of this dissertation. Literature in this area published through 1989 has been reviewed by Porter, Stole, and me in two previous publications.[30,33] Here I summarize the breadth of only those in situ studies of adsorbed films reported since the earlier reviews; however, this summary is not intended to be an exhaustive list of all publications. In situ Raman spectroscopic studies of interfaces form another large body of work and are not reviewed here; however, I have included a few novel vibrational spectroscopic techniques which are not strictly IR spectroscopy.

Much of the early work involving in situ IRSEC concerned small molecules or ions, such as CO or CN^-, adsorbed at metal surfaces. Recently, the technique has been extended to study thin films of polymers, especially redox-active and electrically conductive polymers, at metal and semiconductor surfaces. Therefore, this summary is divided between discussions of studies of monolayer and polymer films—in that order.

2. General Review Articles

A few general reviews of in situ IRRAS appeared in the last two years. A review article by Rajeshwar, Lezna and de Tacconi focuses on novel ways of combining electrochemistry and spectroscopy. Most of this article focuses on photoelectrochemistry and other techniques, but IR studies of adsorbed methanol at electrode surfaces are briefly discussed.[34]

A paper by Kunimatsu, one of the early workers in the field, discusses application of electrochemically modulated IRRAS to many different experimental problems. Adsorption of methanol at Pt, H_2O at Au, and HSO_4^- and SO_4^- at Pt are discussed. The application of polarization-modulation IRRAS to study CO on Pt is also described. The roles of in situ IRRAS and ellipsometry in electrochemistry are described in a review by Hamnett, et al.[35]

3. Monolayer Film Systems

a. Instrumentation/new techniques

This review of specific topics surrounding in situ spectrochemical research begins with reports of significantly new techniques to study adsorbed films of approximately monolayer thickness. The use of infrared-visible sum-frequency spectroscopy to study a non-electroactive monolayer formed by 16-methoxyhexadecanethiol at Au under various solvents was reported by Bain and coworkers. This technique permits examination of C–H stretching frequencies even in the presence of a large amount of solvent having a broad O–H stretching band nearby, similar to the problem addressed by our technique discussed in Section III.[36]

The combination of a flow cell with in situ external reflection IRSEC allowed Roth and Weaver to distinguish between spectral bands arising from the electrode-solution interface and those from the bulk solution. Separate papers discuss the experimental setup[37] and application of the technique to adsorption of azide and cyanate ion at polycrystalline silver.[38]

A method for in situ photothermal spectroscopy using a polyvinylidene fluoride pyroelectric film detector was developed and applied to investigations of anodic oxide formation at a nickel electrode.[39] A new ATR technique for IRSEC employing multiple

internal reflections and thin Au or Ag coatings on Si crystals used as optically transparent electrodes is reported in the dissertation by Parry.[40]

Concerning the *theory* of in situ spectroscopy, which is particularly relevant to this work, Faguy and Fawcett present calculations of the effects of experimental parameters on in situ IRRA spectra, complementary to my discussion in Section III.[41] One important difference is that they examined the ν(CN) mode, rather than the ν(CH) modes discussed herein. In addition, my method of calculating mean square electric fields shows how the electric field is distributed in space in the cell. This description adds to the information available from calculations of reflectances and spectra by providing insight into the physical factors affecting reflectivity changes. Further, I have extended the scope of our study beyond that of their work by presenting experimental data to confirm my predictions.

b. Small molecules

In situ IR spectroscopic techniques have been used to study many systems involving small molecules adsorbed at metal and semiconductor surfaces. The following is a summary of recent work on many such systems. Unless otherwise noted, these studies all employed in situ IRRAS combined with electrochemical modulation of one type or another. The majority of studies involved CO adsorbed at the surface of one of the noble metals, in which case the C–O stretching band at ~2000 cm^{-1} provides a useful indicator of the type of surface bonding. The CO is either adsorbed from solution or the gas phase or is electrochemically generated from methanol or other species.

i. CO and methanol

Weaver and coworkers published two papers discussing in situ IRRAS results for CO adsorbed at ordered Pt(110)/aqueous interfaces.[42,43] A subsequent paper presents absolute in situ IRRA spectra for CO adsorbed on ordered Rh(100) as a function of CO

coverage and electrode potential.[44] That group also reported in situ IRRA spectra in the C–O stretching region for CO at an Ir(111) electrode in aqueous solutions as a function of the same variables.[45] They used the aforementioned Pt and Rh systems to compare the behavior of metal/solution and metal/ultrahigh-vacuum interfaces and discussed the prospects for utilizing IR spectroscopy to interconnect more generally the structural properties of these two types of interfaces.[46] A very recent publication by Weaver's group discusss the use of in situ IRSEC to probe the influence of the double-layer cation upon ν(C–O) frequencies and binding geometries of saturated CO adlayers on polycrystalline Pt and their dependence upon applied voltage.[47] Another paper describes the use of in situ IRRAS and scanning tunneling microscopy to yield detailed atomic-level adlayer structures for saturated coverages of CO at Rh(111) in aqueous solutions.[48]

Electrochemical oxidation of α-D(+)-glucose at polycrystalline Pt in aqueous solutions is the subject of several papers by Yeager and coworkers. Oxidation in 0.1M $HClO_4$ resulted in linearly adsorbed CO, which inhibited the electrode reaction.[49] The oxidation of α-D(+)-glucose at Pt in 0.1 M NaOH was found to result in surface adsorption of linear CO and bridged CO.[50]

Adsorbed CO formed by electroreduction of CO_2 on Pt, Au, and glassy carbon electrodes was investigated in acetonitrile and different reduction products were found for each of the three surfaces.[51] The same reaction was studied on Pt in perchloric acid solutions by Scherson, et al.[52] This group further studied the modifications in the mode of bonding of CO on Pt in perchloric acid electrolytes induced by the presence of Sn(IV).[53]

Anderson and Huang examined CO on polycrystalline Pt in the presence of acetonitrile solutions with various electrolytes by IRSEC. They determined that: (1) near-monolayer coverage can be obtained from solutions saturated with CO, (2) the coverage stays constant over roughly the entire double-layer region, (3) the CO adsorbs to the Pt

surface exclusively in the linear bonded site, (4) the position of the C–O stretching band is linearly dependent upon the applied voltage, and (5) the dependence of the peak position on applied voltage is strongly related to the size of the electrolyte cation.[54]

The adsorption of CO at Ru was studied by Beden and coworkers: steady-state CO electrooxidation was observed in acid solution but not in alkaline solution, due to the presence of an inactive ruthenium oxide in the latter case.[55] A review article by McQuillan concentrates on his studies of electrochemical reactions of methanol at Pt surfaces and films adsorbed at TiO_2 electrodes.[56] Kunimatsu also studied electrooxidation of methanol at Pt.[57]

The group of Pham, Lacaze, and others applied their in situ multiple-internal-reflection FTIR spectroscopic technique to study the intermediates and final products of the electrochemical oxidation of methanol at Pt in H_2SO_4 solutions.[58] Others reported some experimental problems with the above technique due to spalling of the Pt film off the internal-reflection element.[59]

ii. other small adsorbed molecules

In addition to CO and methanol, several other small molecular adsorbates were studied at metal surfaces. The oxidation of formaldehyde at Pt in alkaline solutions was studied by Olivi et al.[60] The electroreduction of dioxygen on Au electrodes in alkaline solutions was studied by Christensen, Paliteiro, and Hamnett.[61] Oxidation of 1-propanol at Pt was examined by Sun and coworkers, who found that the reactive intermediates are mainly propanoic acid and the final product of oxidation is CO_2.[62] The absorption of ethyl xanthate was monitored at Au, Ag, and Cu surfaces by Talonen and coworkers.[63]

c. Self-assembled monolayers (e.g. alkanethiolates)

A few studies examined in situ self-assembled monolayer films, including those of alkanethiolates, which is particularly relevant to this work. Monolayers of 2,5-

dihydroxythiophenol at Au were studied by Scherson and others by in situ IRSEC. Oxidation of this monolayer appeared to produce the quinone form of the adsorbate, and both forms exhibited a small angle with respect to the surface.[64] Electrochemical reactions of monolayers formed from chemisorption of several thiophenols at Ir electrodes were examined by Bothwell and Soriaga.[65]

One application of in situ IRSEC to examine redox self-assembled monolayers on gold, similar to the work described in Section IV, was reported by Bae, et al. Monolayers of N-ethyl-N'-octadecyl-4,4'-bipyridinium self-assembled at Au were studied, and positive-going potential-dependent absorbance peaks were attributed to vibronically based charge oscillation of monomeric and dimeric forms of the bipyridinium moiety. The spectroscopic data yields details of the orientation of the film as a function of potential.[66]

d. Other monolayer systems and adsorbed species

A study by Sariciftci, Mehring, and Neugebauer applied in situ IRSEC to charge-transfer reactions of a zwitterion-viologen system in both formamide and acetonitrile solutions. Interestingly, they observed some changes in the IR spectra using acetonitrile electrolyte in a region where no electrochemical reaction occurs.[67] One IRSEC study of the benzoquinone/benzohydroquinone couple indicated that a hemiketal intermediate may be produced in the redox reaction.[68] Evidence from IRSEC combined with XPS showed that prussian blue is an adsorption product in the hexacyanoferrate redox system in neutral aqueous solution at Pt, according to Datta and Datta.[69] Subsequent work on cyanide adsorbed at Pt in K_2SO_4 solution indicated that CN^- is oxidized to OCN^-.[70]

e. Corrosion and reactions of the metal electrode surface

Several reports appeared of using in situ IRRAS to study corrosion and formation of oxide and other layers at oxide and semiconductor surfaces. While such films are not necessarily monomolecular, discussion of them is appropriate in this section. Two papers

by Neugebauer and coworkers describe application of several modes of IRSEC to probing electrochemical reactions of Fe electrodes in alkaline solutions. Both external and internal (ATR) reflection techniques were used.[71] Photo-corrosion of n-silicon in ammonium fluoride solutions at pH 4.5 was studied by ATR spectroscopy by Pons, et al. Interestingly, the results of this study imply the formation of a porous silicon layer during illumination, which then dissolved slowly in the dark.[72] A similar system was studied by Chazalviel, et al. (see below). Electrochemical oxide formation at Fe surfaces was also studied in alkaline solutions by Bewick, et al., who detected different oxide structures formed depending on the OH concentration of the electrolyte.[73]

f. Electrochromism

The electrochromic reactions of tungsten trioxide films were examined by Habib and Maheswari at various stages of reduction (coloration) using in situ IRRAS. Changes in the vibrational intensities of W:O, W–O, and W–O–H bands indicated the incorporation of water into the layer and the formation of H_xWO_3 bronze during coloration.[74]

g. Miscellaneous studies of adsorbates

A few other miscellaneous in situ studies of monolayer-thick films appeared in the literature. The mechanism of reduction of nitrate ion at Au pretreated by underpotential deposition of Cd was studied with the help of in situ IRRAS.[75] An unusual study by Mandal, Ozanam, and Chazalviel studied absorption of hydrogen *into* a surface. IRSEC was used to examine the electrochemical incorporation of hydrogen into cathodically treated silicon and germanium. The position and polarization dependence of a band at 2000 cm^{-1} indicate it is associated with hydrogen inside the semiconductor lattice.[76] This group published two other papers examining the porous layer formation of a silicon surface in hydrofluoric acid.[77,78]

4. Conductive Polymer Film Systems And Electropolymerization

a. Polypyrrole and polythiophene

As mentioned earlier, use of in situ IR spectrochemical techniques to study conductive polymers is relatively new. Nonetheless, the emergence of this application is significant, since these techniques allow generating the film and probing its structure and composition practically at the same time.

Christensen and Hamnett used in situ ellipsometry and IRSEC to probe the growth, electrochemical cycling, and overoxidation of polypyrrole in perchlorate solution. The charge carriers are identified as polarons or bipolarons, depending on the potentials applied. Overoxidation (oxidation of the polymer with an excessive amount of charge to produce an irreversible chemical degradation) of the film produces pyrrolinones, which are eventually oxidized to CO_2 without destroying the mechanical integrity of the polymer.[79]

In situ IRSEC was used by Vielstich and others to investigate the polymerization, cycling behavior, and overoxidation of polypyrrole (PPy) in propylene carbonate (PC), as described in a monograph.[80] They published a subsequent paper covering the irreversible oxidation of thin PPy layers in PC electrolyte containing 0.5M $LiClO_4$. It was found that trace products from the anodic oxidation of PC attack the doped PPy chains, leaving a non-conjugated overoxidized film.[81] Electrochemical synthesis and redox properties of poly-N-methylpyrrole and copolymers of it with PPy were also studied.[82] The same group extended this work, in combination with on-line mass spectrometry, to probe the anodic stability of propylene carbonate at Pt electrolytes at potentials above 4 V (vs. Li/Li^+).[83] They further investigated the influence of trace amounts of H_2O on propylene carbonate oxidation.[84] The electropolymerization of thiophene at Pt in a PC electrolyte was also examined by Vielstich and coworkers.[85]

b. Poly(1-naphthol)

Several studies of poly(1-naphthol) using in situ spectroscopies were made by Pham et al. In one study, potential-step techniques were used to study the electrochemical doping-undoping process of this system.[86] In situ multiple-internal-reflection FTIR spectroscopy was used to investigate the electrochemical oxidation of 2-naphthol on graphite and Pt in a solution of $LiAsF_6$ in acetonitrile.[87] Pham et al. further studied the electrochemical redox processes of a poly(1-naphthol)-coated electrode in the same solution.[88] The same technique was used to examine the electrochemical immobilization of heteropolyanions (HPAs) in poly(1-naphthol)-coated electrodes when the HPAs are present during electropolymerization. The HPA $P_2W_{18}O_{62}^{6-}$ was observed to be distributed unevenly throughout the polymer, with a larger amount at the metal-film interface. Spectral data revealed that the presence of the HPA did not affect the structural change occurring during the redox processes of the film.[89]

c. Other systems

Pham et al. applied a multiple-internal-reflection spectroscopic technique to examine the growth mechanism of polyphenylene during electrooxidation of biphenyl in methylene chloride at Pt.[90] In another report, they used the technique to investigate the polymer chain orientation of films electrochemically deposited on Fe by oxidation of *o*-hydroxypropiophenone.[91]

The electropolymerization of 2,6-dimethylphenol at Au was studied with a linear-potential-sweep IRSEC technique by Zhou.[92] In work by Sariciftci, et al., the structural and electronic transitions in polyaniline were studied by in situ IRSEC and other techniques. Intercalation and deintercalation of anions were observed, depending on the potential and whether the electrolyte was organic or aqueous.[93]

Korzeniewski and others used in situ IRSEC to probe polymer-dopant interactions in polyaniline-modified electrodes. The electrochemical response of the film depended on the pH of the deposition solution. IR spectroscopic data revealed that cross-linked structures may be responsible for the fact that films that displayed voltammetry typical of the para-substituted phenyleneamineimine structure decomposed to *p*-benzoquinone at positive potentials, while other films did not show evidence of this decomposition product.[94]

THE THEORETICAL BASIS FOR SPECTRAL CALCULATIONS AND DATA ANALYSIS APPLICABLE TO IR REFLECTION SPECTROSCOPIC TECHNIQUES

1. Propagation of Electromagnetic Radiation

Much of the work in this dissertation concentrates on studying the mechanism and optimization of in situ IRRAS. To assist readers in examining results presented later, this section explains those portions of classical electromagnetic theory that govern IR spectroscopy and that are used as the basis of model calculations. Following the sub-sections about theory as applied to IRRAS, another sub-section discusses the nature of the electric field at a reflecting interface.

Electromagnetic radiation in a uniform isotropic medium, as shown in Figure 1, is typically depicted as a plane-polarized wave propagating at a phase velocity equal to c/n, where c is the velocity of light in a vacuum, and n is the index of refraction of the medium. The instantaneous magnitude of the oscillating electric field vector $\hat{\mathbf{E}}$, which is found from the time-dependent solution of Maxwell's equations, is

$$\hat{\mathbf{E}} = E^0 \exp\left[i\left(\omega t - \frac{2\pi n}{\lambda} \mathbf{s}\cdot\mathbf{r} \right) \right], \qquad (1)$$

where E° is the maximum amplitude of the wave, λ is the wavelength in a vacuum, ω is the angular frequency, s is a unit vector in the direction of propagation, and r is a position vector. The wavelength λ is related to the wavenumber, ν, as

$$\nu = 1/\lambda. \qquad (2)$$

The wavelength is also related to the angular frequency ω by $\omega = 2\pi c/\lambda = 2\pi c\nu$. Thus, the periodicity of both the electric field and magnetic field are defined in time and space by λ

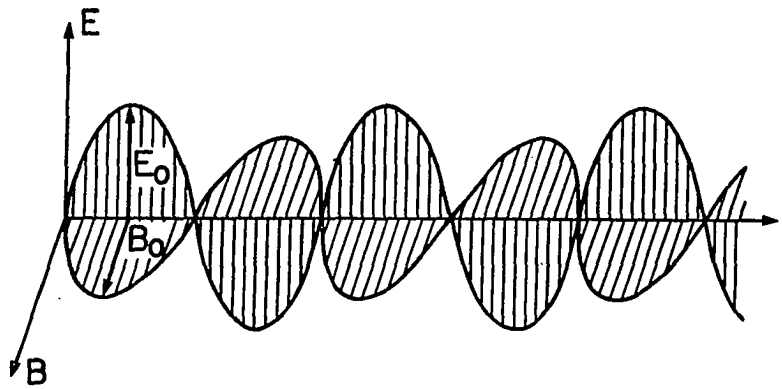

Figure 1. Plane-polarized electromagnetic wave.

and ν. Values of λ, frequency in Hz, and ν and the equivalent energy in electron volts are given in Table 1 for representative electronic and molecular transitions.

As shown in Equation 1, $\hat{\mathbf{E}}$ is typically treated as a complex-valued function of time and of the spatial coordinates x, y, and z. This format is more convenient for mathematical manipulations than the use of a real-valued trigonometric function. An expression similar to Equation 1 can also be written for the magnetic field vector $\hat{\mathbf{H}}$.

Table 1. Representative Values for the Energies of Various Molecular and Electronic Excitations

Transition	$\lambda(\AA)$	frequency (Hz)	$\nu(cm^{-1})$	energy (eV)[a]
Electronic ($p \rightarrow p^*$)	2540	1.8×10^{15}	39370	4.88
Vibrational (ν(C=O) for carboxylic acid)	57803	5.19×10^{13}	1730	0.214
Rotational ($J=1 \rightarrow J=2$ for HCl)	2.40×10^{6}	1.25×10^{10}	41.7	5.18×10^{-3}

[a] 1 eV ~ 8065.5 cm^{-1}

In an absorbing medium, the plane wave undergoes an exponential attenuation with increasing propagation distance and is represented as

$$\hat{\mathbf{E}} = E^0 \exp\left[i\left(\omega t - \frac{2\pi n}{\lambda}\mathbf{s}\cdot\mathbf{r}\right)\right]\exp\left(-\frac{2\pi k}{\lambda}\mathbf{s}\cdot\mathbf{r}\right), \tag{3}$$

where k is the absorption index and is restricted to $k \geq 0$. If a complex refractive index

$$\hat{n} = n + ik \tag{4}$$

is introduced, Equation 3 can be recast to resemble Equation 1, giving

$$\hat{\mathbf{E}} = E^0 \exp\left[i\left(\omega t - \frac{2\pi \hat{n}}{\lambda}\mathbf{s}\cdot\mathbf{r}\right)\right]. \tag{5}$$

Since the refractive index is related to the dielectric constant $\hat{\varepsilon}$ by

$$\hat{n} = \sqrt{\mu\hat{\varepsilon}}, \tag{6}$$

and the magnetic permeability μ equals unity at optical frequencies, $\hat{\varepsilon}$ for absorbing materials is complex and can be written as

$$\hat{\varepsilon} = \hat{n}^2 = \varepsilon' - i\varepsilon'', \tag{7}$$

where ε' and ε'' are linked to n and k as

$$\varepsilon' = n^2 - k^2 \tag{8}$$

$$\varepsilon'' = 2nk. \tag{9}$$

The intensity and direction of energy flow for a plane wave are given by the Poynting vector S:

$$\mathbf{S} = \frac{1}{\mu}\mathbf{E}\times\mathbf{H}. \tag{10}$$

For a discrete optical transition, the attenuation of a propagating wave with intensity I is given by the Lambert law

$$I = I^\circ \exp(-\alpha z), \tag{11}$$

where I° is the initial light intensity, α is the absorption coefficient, and z is the distance of penetration into the absorbing medium. The absorption index k is related to α by

$$\alpha = \frac{4\pi k}{\lambda}. \tag{12}$$

The penetration depth, often referred to as the skin depth, of the radiation into the medium is defined as $1/\alpha$, i.e., the distance at which the beam intensity has decreased by 63% of its initial value.

For infrared spectroscopy, the optical properties of each phase are completely defined by a set of optical functions: n and k, or ε' and ε''. Physically, ε' and ε'' are respectively related to the frequency-dependent polarizability and the conductivity of the medium. A single complex function, as in either of the following equations, completely defines the optical properties of a homogeneous isotropic medium:

$$\hat{n}(\nu) = n(\nu) + ik(\nu) \tag{13}$$

$$\hat{\varepsilon}(\nu) = \varepsilon'(\nu) + i\varepsilon''(\nu). \tag{14}$$

2. Optical Theory for Reflection Spectroscopy

In a reflection spectroscopy experiment, electromagnetic radiation interacts with more than one optical medium. In its simplest approximation, such an experiment can be depicted by a stratified medium, with two optically isotropic phases that are separated by a plane boundary, as shown in Figure 2. The entry phase is transparent, whereas the optical functions of the second phase may be complex. The components of both the incident and reflected radiation are defined with respect to the plane of propagation. The E_x and E_z components are in the plane of propagation (p-polarization), and the E_y component is perpendicular to the plane of propagation (s-polarization). The E_x and E_y components are parallel to the interface between the two phases, whereas E_z is

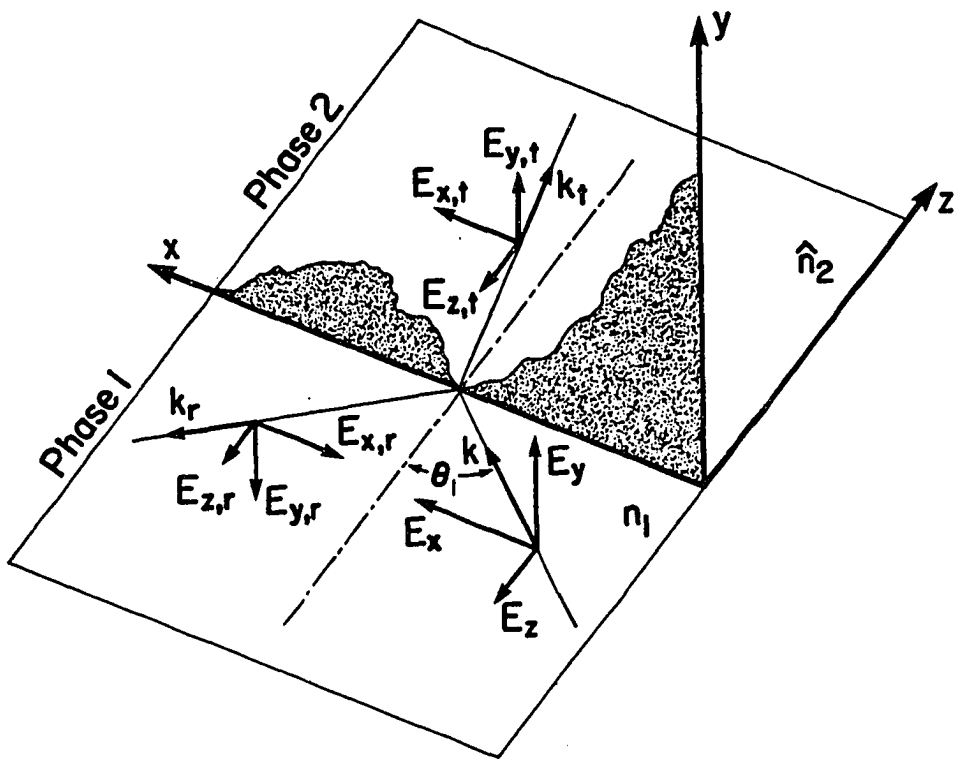

Figure 2. The electric field vectors for plane-polarized light incident on a phase boundary in a two-phase medium.

perpendicular to this interface. The angle of incidence θ_1 is measured from the surface normal.

In a three-phase stratified medium, as shown in Figure 3, phase 2 may represent an interfacial structure, consisting, for example, of a polymeric or monomolecular film of thickness, *d*. An *n*-phase medium representing a multilayered system, which is exemplified by the Gouy-Chapman model of the electrical double layer, is given is Figure 4.

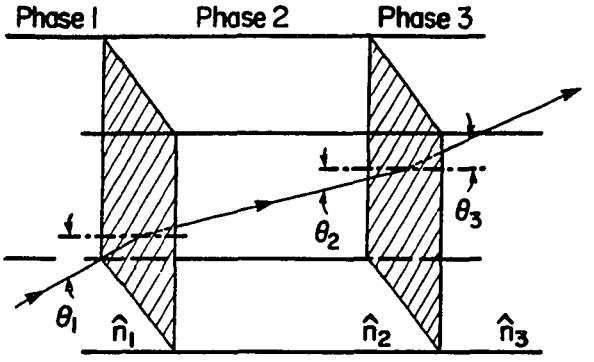

Figure 3. Radiation incident upon a three-phase medium. Rays for reflected light are omitted for clarity.

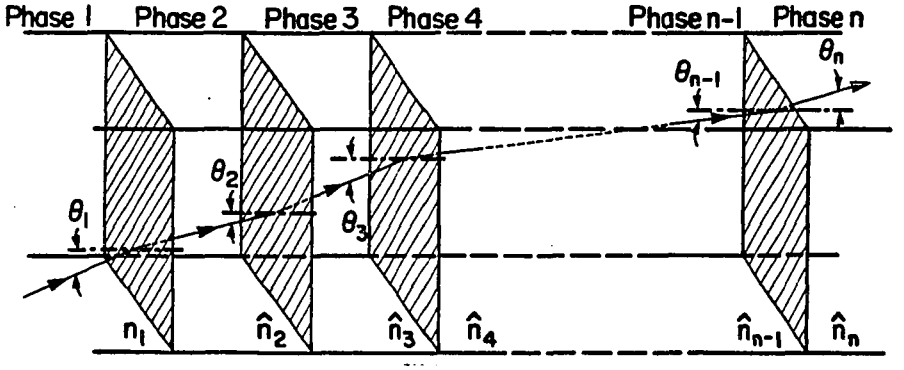

Figure 4. Radiation incident upon an n-phase medium. Rays for reflected light are omitted for clarity.

The characteristics of the three- and n-phase media are defined by the optical functions of each phase j as

$$\hat{n}_j = n_j + ik_j \tag{15}$$

and thicknesses of the intermediate phases d_j. The Fresnel coefficients quantify the magnitudes of the transmitted and reflected waves emanating from a phase boundary. These coefficients are defined as the ratio of the complex amplitudes of the electric field vectors of the incident wave to that of the reflected or transmitted wave and are a function of the angle of incidence and polarization of the incident beam. Before calculating these coefficients, it is useful to define the refractive coefficient ξ_j for phase j as

$$\xi_j = \hat{n}_j \cos\hat{\theta}_j . \tag{16}$$

If phase j is absorbing, $\hat{\theta}_j$ is complex. By Snell's law, ξ_j can be related to the angle of incidence and real refractive index of phase 1 as

$$\xi_j = \left(\hat{n}_j^2 - n_1^2 \sin^2\theta_1\right)^{1/2}. \tag{17}$$

The complex Fresnel coefficients for reflection r_{jk}, and transmission t_{jk}, at the boundary of phases j and k for radiation polarized parallel and perpendicular to the plane of propagation are then given as

$$r_{\perp jk} = \frac{\xi_j - \xi_k}{\xi_j + \xi_k} \qquad t_{\perp jk} = \frac{2\xi_j}{\xi_j + \xi_k} \tag{18}$$

$$r_{\parallel jk} = \frac{\hat{n}_k^2\xi_j - \hat{n}_j^2\xi_k}{\hat{n}_k^2\xi_j + \hat{n}_j^2\xi_k} \qquad t_{\parallel jk} = \frac{2\hat{n}_j\hat{n}_k\xi_j}{\hat{n}_k^2\xi_j + \hat{n}_j^2\xi_k} \tag{19}$$

Again, μ for all phases equals unity. These coefficients are derived from Maxwell's equations by applying the continuity requirements of $\hat{\mathbf{E}}$ and $\hat{\mathbf{H}}$ at the phase boundary.

Plane-polarized light, described by $E_{\perp}$ and $E_{||}$, undergoes a change in amplitude and phase upon reflection at a phase boundary. This change in phase is related to the real and imaginary parts of the Fresnel coefficients by

$$\delta_{jk}^{r} = \arg(r_{jk}) = \tan^{-1}\left[\frac{\mathrm{Im}(r_{jk})}{\mathrm{Re}(r_{jk})}\right]. \qquad (20)$$

If the time dependence of the field is $e^{-i\omega t}$, both $\mathrm{Im}(r_{jk})$ and $\mathrm{Re}(r_{jk})$ must be ≥ 0.

From Equations 18 and 19, the reflectivity of each phase boundary, R_{jk}, can be calculated as

$$R_{jk} = \left|r_{jk}\right|^2 = r_{jk} r_{jk}^{*}, \qquad (21)$$

where r_{jk}^{*} is the complex conjugate of r_{jk}. For the two-phase medium in Figure 3, the reflectivities of the perpendicular and parallel components of the reflected radiation are given as

$$R_{\perp 12} = \left|\frac{\xi_1 - \xi_2}{\xi_1 + \xi_2}\right|^2 \qquad R_{\| 12} = \left|\frac{\hat{n}_2^2 \xi_1 - \hat{n}_1^2 \xi_2}{\hat{n}_2^2 \xi_1 + \hat{n}_1^2 \xi_2}\right| \qquad (22)$$

For the three-phase medium, r_{123} has

$$r_{\perp} = \frac{r_{\perp 12} + r_{\perp 23}\, e^{-2i\beta}}{1 + r_{\perp 12} \cdot r_{\perp 23}\, e^{-2i\beta}} \qquad r_{\|} = \frac{r_{\| 12} + r_{\| 23}\, e^{-2i\beta}}{1 + r_{\| 12} \cdot r_{\| 23}\, e^{-2i\beta}} \qquad (23)$$

with $R_{\| ,123} = r_{\| ,123} \cdot r_{\| ,123}^{*}$ and $R_{\perp,123} = r_{\perp,123} \cdot r_{\perp,123}^{*}$. The phase angle term, β, represents the beam attenuation in phase 2 and equals

$$\beta = 2\pi(d/\lambda)\, \xi_2 \qquad (24)$$

Similar expressions, based on matrix manipulations, have been devised for the n-phase optical medium.[95,96,97,98,99,100]

In IRRAS, the spectrum arises from the change in reflectance between that, R, of a sample measurement and the reflectance, R_0, of a background measurement in which the

absorbing material is not present or does not interact with the reflected beam. Spectra are normally measured as reflectance-absorbance (RA):

$$\mathrm{RA} = -\log\frac{R}{R_0} \tag{25}$$

or as differential reflectance, $(R - R_0)/R$.

3. Mean-Square Electric Field Strengths at a Reflecting Interface and Their Relation to Detectability

Having examined the origin of a spectrum in physical optical terms, let us look at the role of the electric field near the surface in giving rise to spectra. In a reflection spectroscopy experiment, the sensitivity of the measurement is a strong function of the optical properties of the substrate and the angle of incidence and polarization of the incident light. For an in situ experiment, such as one to examine an electrochemical interface, the sensitivity is further affected by the thickness and optical properties of the solvent and electrolyte.[23,24,25,26,27] As we shall see, the intensity of the electric field generated in the sample cell will give useful measures of detectability.

In air, the detectability of a thin film is governed to a large extent by the boundary conditions imposed by the free electrons of the substrate. For metal substrates, the electrical conductivity approaches that of its DC value (σ(esu) $\approx 10^{-17}$ s^{-1}) and leads to a high infrared reflectivity (near unity). The dependence of the reflectivity, and hence, the intensity of the mean-square electric field (MSEF) at the surface is elucidated by examining the relationships between an oscillating $\hat{\mathbf{E}}$ and the free conductive electrons in a metal. From the standpoint of physical optics, a reflecting metal surface acts as a collection of charges that are free to move within the metal but are prevented from moving beyond the surface (i.e. outside) of the metal. The incident radiation gives rise to an oscillating electric field vector $\hat{\mathbf{E}}$ at the surface, causing the incident radiation to interact

with the metal. The component of $\hat{\mathbf{E}}$ parallel to the surface induces an image dipole in the metal that opposes the incident field (Figure 5a) whereas the component of $\hat{\mathbf{E}}$ perpendicular to the surface induces an image dipole that is aligned with the incident component (Figure 5b). The phase change of the reflected wave then results from the orientational difference between the incident electric field and the induced dipole. Figure 6 illustrates the phase shift for light polarized both perpendicular to and parallel to the plane of propagation at a large angle of incidence. For perpendicular-polarized light (Figure 6a), the incident $\hat{\mathbf{E}}$ is parallel to the surface, leading to a phase shift of $\sim -180°$, as discussed above. This effectively holds for all angles of incidence.

On the other hand, parallel-polarized light at large incident angles has a large portion of its electric field oriented perpendicular to the surface (Figure 6b). The resulting induced dipole has a normal component parallel to and reinforcing the normal component of the incident electric field by constructive superposition. Thus, $\hat{\mathbf{E}}$ of the reflected light is phase shifted by ~90°. As the angle of incidence increases, the incident and reflected

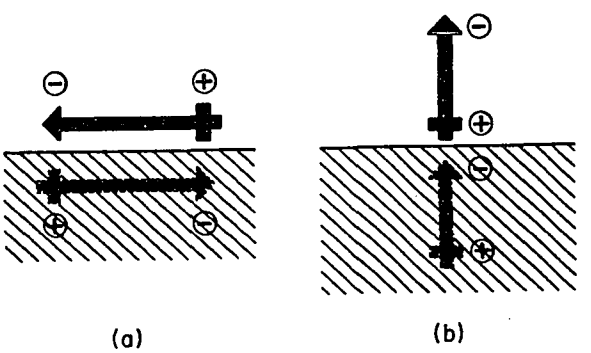

Figure 5. Orientation of the image dipole in a metal juxtaposed with the external electric field arising from the incident radiation for the component of radiation (a) parallel to, and (b) perpendicular to the metal surface.

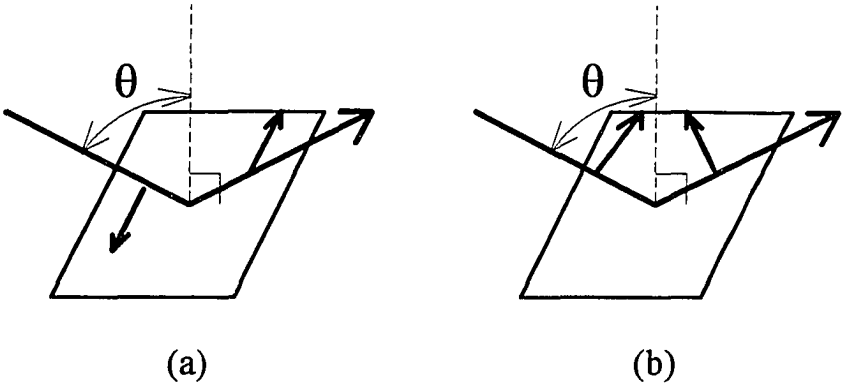

Figure 6. A representation of the phase change upon reflection for (a) perpendicular-polarized light, and (b) parallel-polarized light.

electric field vectors become virtually indistinguishable, corresponding to a phase shift approaching −180°. It should be noted that by convention, when the incident and reflected $\hat{\mathbf{E}}$ are antiparallel and equal in magnitude at the surface, the phase change is defined as 0° for parallel-polarized light and −180° for perpendicular-polarized light.[101]

Figure 7 shows the phase change δ as a function of angle of incidence for both polarizations. The perpendicular (s-polarized) component is phase shifted by ~180° for all angles of incidence. As a result of the superposition of the incident and reflected $\hat{\mathbf{E}}$ vectors, the MSEF at the surface will be effectively zero for this component. If the MSEF is negligibly small, then the absorbance spectrum resulting from interactions between the incident light and a thin film at a metal substrate will be virtually undetectable. On the other hand, the phase shift for the p-polarized (parallel) component of $\hat{\mathbf{E}}$ varies from nearly 0° at normal incidence to −180° at grazing incidence. At normal incidence, the MSEF will be small; but as δ approaches 90° for near-grazing angles, the MSEF for the parallel component at the surface increases to almost four times that of the incident radiation. Therefore, the absorbance by a thin film at a metal surface will be at a maximum at grazing angles of incidence with p-polarized light.

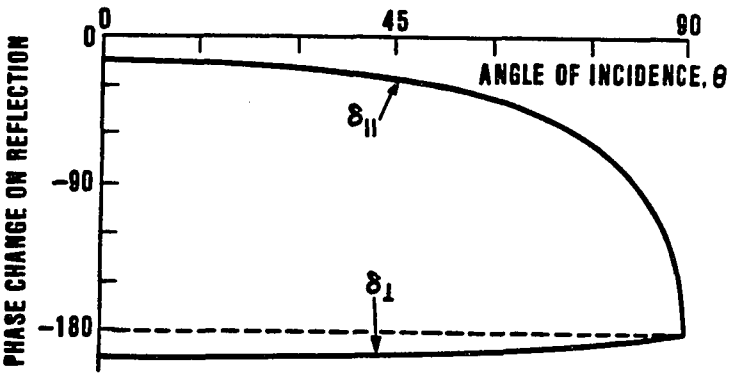

Figure 7. The phase change upon reflection as a function of angle of incidence for both polarizations of light. Reprinted with permission from R.G. Greenler *J. Chem. Phys.* **1966**, *44*, 310.

Calculations of the electric field intensity due to the superposition of the incident and reflected beams reveal, quantitatively, the effect of many of the experimental parameters upon a reflection spectrum. The boundary conditions imposed by electromagnetic theory define the MSEF of the standing wave at each phase boundary, the value of which is strongly dependent on the optical properties of the substrate, the angle of incidence, and the polarization of the incident light. To foster an understanding of the effects of these experimental parameters, it is instructive to examine the MSEF in a two-phase optical medium. Since there is little energy dissipation (absorption) in a thin film such as a monomolecular assembly, the attenuation of the MSEF by the film is relatively small and can be neglected. In other words, for monolayers and thin polymeric films, deductions for a two-phase system accurately represent those for a three-phase system. Values for MSEFs are generally expressed as the ratio of the MSEF in the j^{th} phase, $\langle E_j^2 \rangle$, to that of the incident plane wave in phase 1, $\langle E_1^{0t2} \rangle$. Expressions for relative MSEF in each phase of a three-phase medium are given in Section II. A

comparison of the results of MSEF calculations using different experimental parameters provides a means to select conditions for high detectability.

A plot of the MSEF at an air/Au interface at 2000 cm^{-1} is shown in Figure 8. As follows from the foregoing discussion of boundary conditions, this plot provides insights as to how the high reflectivity of a metal influences the detectability of a surface film. The optical constants for Au were interpolated from a previous study.[102] Figure 8 shows that the MSEF for E_x and E_y are negligibly small (<0.004) for all angles of incidence. In contrast, E_z slowly increases with θ_1, reaching a maximum of ~3.4 at 79°. Hence, as noted above, the conditions for high surface detectability at metals are large angles of incidence and p-polarized light.

It should also be noted that the anisotropy of the MSEF at a highly reflecting interface such as air/Au results in the selective excitation of vibrational modes that have a component of their transition dipole normal to the surface. This polarization dependence, commonly referred to as the IR surface selection rule,[28,103] can be exploited to predict the orientation of an adsorbed species. Limitations of such an orientational analysis for materials with a low IR reflectivity have recently been examined.[104]

To summarize, for the absorption of light of wavenumber ν by a molecule immobilized at an air-metal interface, three conditions must be met:

1. The molecule must have a non-zero transition dipole moment at ν.
2. The magnitude of the MSEF at the interface must be non-zero (and conditions for high detectability are large angles of incidence and p-polarized light).
3. The transition dipole moment must have a component oriented along the surface normal.

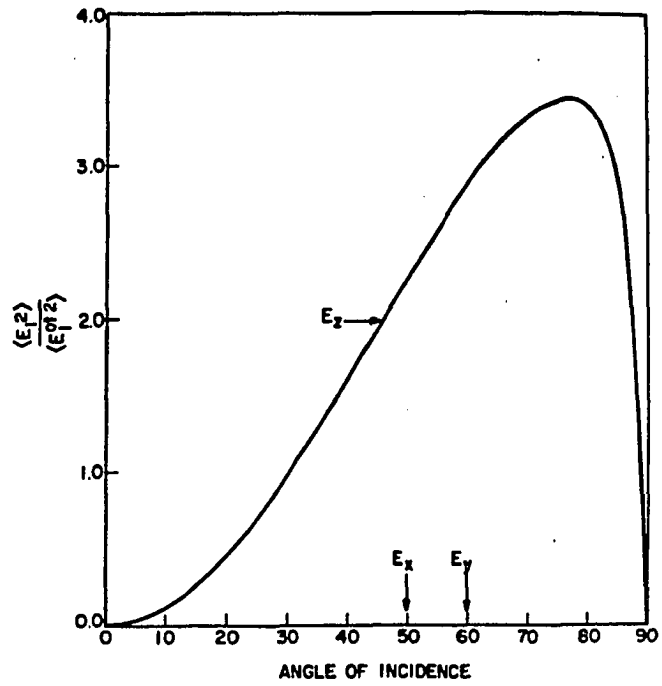

Figure 8. The mean square electric field at 2000 cm^{-1} as a function of angle of incidence and polarization at the air/Au interface. Reprinted with permission from M.D. Porter, et al. *Anal. Chem.* **1986**, *58*, 2461. Copyright 1986 American Chemical Society.

4. Conclusion

In this chapter, we have examined many of the principles of electromagnetic theory which govern IRRAS of a monolayer-coated interface—either in situ or ex situ. We have seen how reflectance and transmittance for a stratified medium may be calculated from the optical properties of the medium together with several experimental parameters.

In the main sections of this dissertation, these principles are applied to several problems in the study of in situ IRRAS. First, Section I applies the relationships between

transmittance (or reflectance) and optical properties of a medium to the determination of n and k as functions of frequency for several compounds used in later work. Then, Sections II and III apply calculations of MSEF and reflection spectra, respectively, to examining the effects of experimental parameters upon spectral sensitivity.

SECTION I. DETERMINATION OF OPTICAL FUNCTIONS FOR MATERIALS AND TECHNIQUES FOR INTERCONVERTING BETWEEN SPECTRA AND OPTICAL FUNCTIONS

A. INTRODUCTION

The optical functions n and k of a material are the properties that give rise to spectra. In our work with monolayer films, my co-workers and I use spectral information consisting of the IR peak positions, absorbance values, and band shapes to make inferences about the structure and composition of a film. Comparisons of peak intensities, positions, and widths between a reflection spectrum of an oriented film and a calculated spectrum for an analogous randomly oriented species are used to study monolayer properties. For the work described in this dissertation, expected reflection spectra are calculated for an in situ IRRAS arrangement to examine what kind of optical artifacts would arise in a spectrum of a monolayer film at an aqueous/metal interface. Before doing calculations of this type, one must experimentally determine values of the optical functions of the materials which affect the spectra, unless such values already appear in the literature.

In order to perform these types of calculations, I created, compiled, and tested a series of programs to interconvert between IR transmission or reflection spectra and the optical functions of frequency, n and k. If n and k are known for a substance, an IR spectrum can be calculated under almost any set of experimental conditions using the program RTCALC, followed by SPREP. If one desires to calculate n and k, then a spectrum of a substance (for example, a transmission spectrum of the material dispersed in a KBr disk) can be converted to optical functions using the program OPFXNS1, which uses a Kramers-Kronig integration algorithm. These three programs--RTCALC, SPREP, and OPFXNS1--form a "calculational cycle" around which a set of spectral data can be sent any number of times (within the limits of error imposed by the computations). To test the integrity and accuracy of the calculational cycle, I wrote a set of programs to generate

synthetic spectral profiles, consisting of CAUCHY, MakeCurv, and KtoN. The relationship between these programs is illustrated in Figure 1.

This Section discusses the creation, testing, and use of the programs in the cycle. Most of the programs are adapted from earlier versions written by D. L. Allara, M. D. Porter, and others; their groundwork is hereby acknowledged. In the next subsection, the theory and organization of these programs are discussed. Then, experimental methods used in this work are detailed. The following subsection describes work done to verify the operation of the programs. Finally, the last subsection presents *n* and *k* data obtained for several compounds that are important to the research of Porter and co-workers.

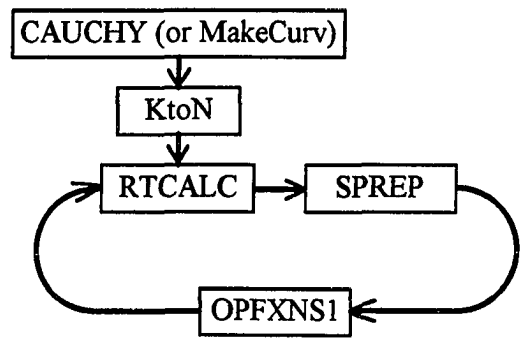

Figure 1. The calculational cycle of programs for interconverting spectra and optical functions.

B. CONSTRUCTION OF PROGRAMS

This section discusses the algorithms, architecture, and use of the computer programs for interconverting spectra and optical functions. The programs were written in FORTRAN; most were compiled using Microsoft FORTRAN Version 4.1 (Microsoft Corp.). Thus, a few extensions to the FORTRAN 77 standard are used; however, these affect only formatting and the way listing files are generated. Also, most of the programs call mathematical subroutines from the PORT3 Library (AT&T Bell Laboratories). Unfortunately, updates and support for this library are not readily available; however, routines from another library could be substituted effectively. Appendix 1 gives listing files which contain the source code—in addition to summary and compilation information—for each of the programs discussed herein.

1. The Program OPFXNS1 to Convert Spectra to Optical Functions

a. Kramers-Kronig integration

The program OPFXNS1 transforms an IR spectrum of a material into the optical functions of that material. Spectra used for input can be in any form, but two requisite conditions are that the sample can be represented by a stratified medium and that all except one phase in the medium can be represented by a constant complex refractive index $\hat{n}$ (i.e., one that is not a function of ν).

The principal algorithm used in the transformation is the Kramers-Kronig integration for interconverting k and n.[1,2,3,4,5,6,7] The relationship between the optical functions $n(\nu)$ and $k(\nu)$, given by the Kramers-Kronig dispersion relation, may be written

$$n_i = n_\infty + \frac{2}{\pi} \mathrm{P} \int_0^\infty \frac{\nu k(\nu)}{(\nu^2 - \nu_i^2)} \mathrm{d}\nu, \qquad (26)$$

where n_i is the value of $n(\nu)$ calculated at a particular frequency ν_i; n_∞ is the "zero-frequency" refractive index which holds for the material at a frequency far from any regions of absorption; and P indicates that the principal value of the integral be taken, because a singularity occurs in the integrand at $\nu=\nu_i$. Obviously, the integration indicated over all frequencies from zero to infinity cannot be performed in practice. Therefore, an approximation is made by performing the integration

$$n_i = \bar{n} + \frac{2}{\pi} \mathrm{P} \int_{\nu_a}^{\nu_b} \frac{\nu k(\nu)}{(\nu^2 - \nu_i^2)} \mathrm{d}\nu \qquad (27)$$

between frequency limits ν_a and ν_b, which are chosen to lie on the baseline and to bracket the spectral band(s) of interest. The baseline refractive index $\bar{n}$ is an approximation of n_∞. The methods used for approximating n_∞ are discussed in the experimental section.

b. Operation of the program

A flow chart illustrating the operation of OPFXNS1 is shown in Figure 2. The parts of the program most relevant to this presentation are the logic for the iterative calculations and the procedure for determining convergence; therefore, details of the input and output routines are omitted here. The first step to calculating n and k is to assume a certain sample thickness and to approximate k as being proportional to absorbance. For example, if a transmission spectrum is obtained from a pure film of thickness d, the approximation $k \approx 2.303 \cdot A/4\pi d\nu$ is made, where A is absorbance. The program has the option of setting negative absorbance values to zero. This option should not be used when spectra contain interference fringes, as the fringes oscillate naturally between positive and negative absorbance values even in the absence of intrinsic absorbance.

After calculating initial values of k, OPFXNS1 then enters an iterative loop that is repeated until the calculation has converged within a predetermined limit--or until a

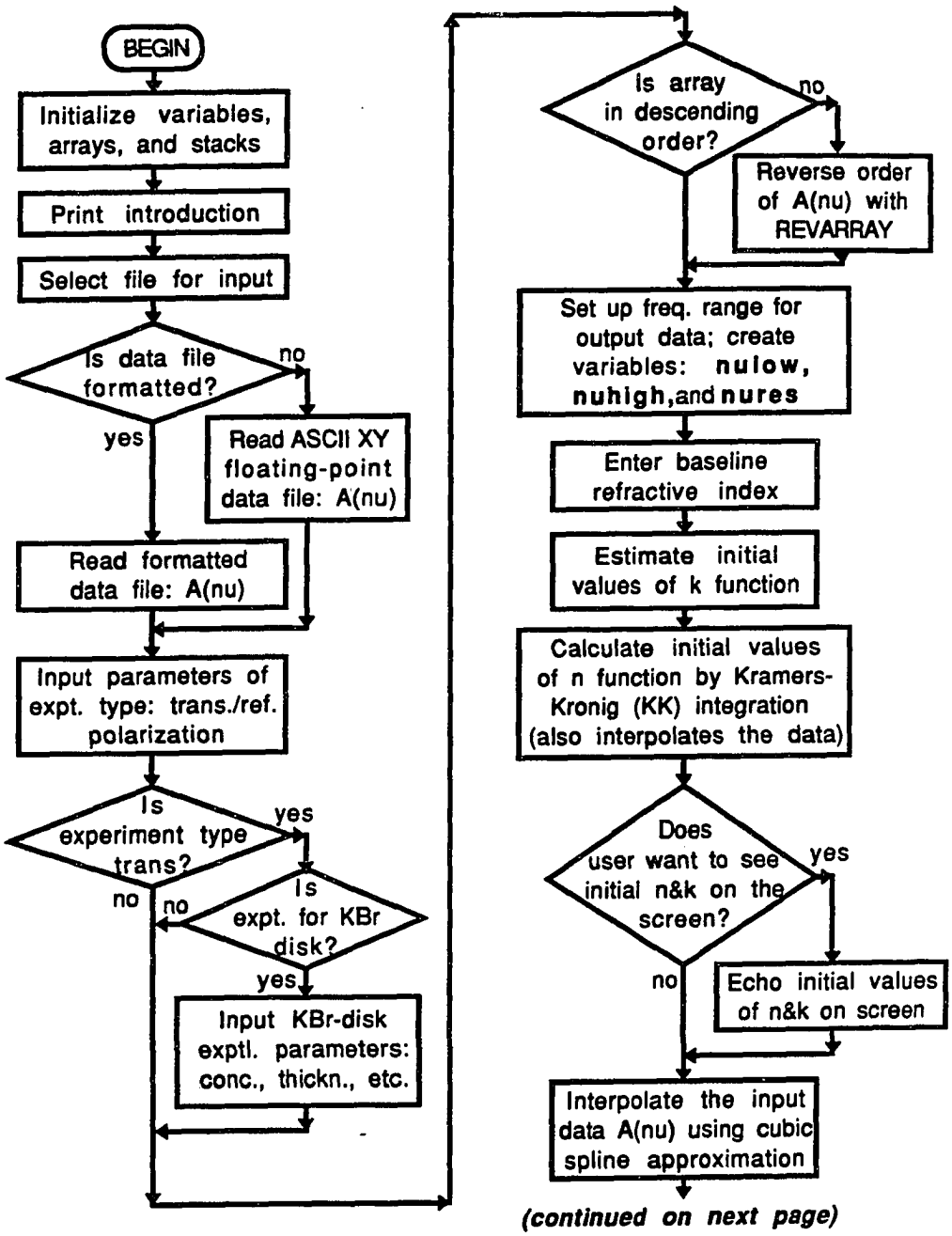

Figure 2. Flowchart of the Organization of the Program OPFXNS1.

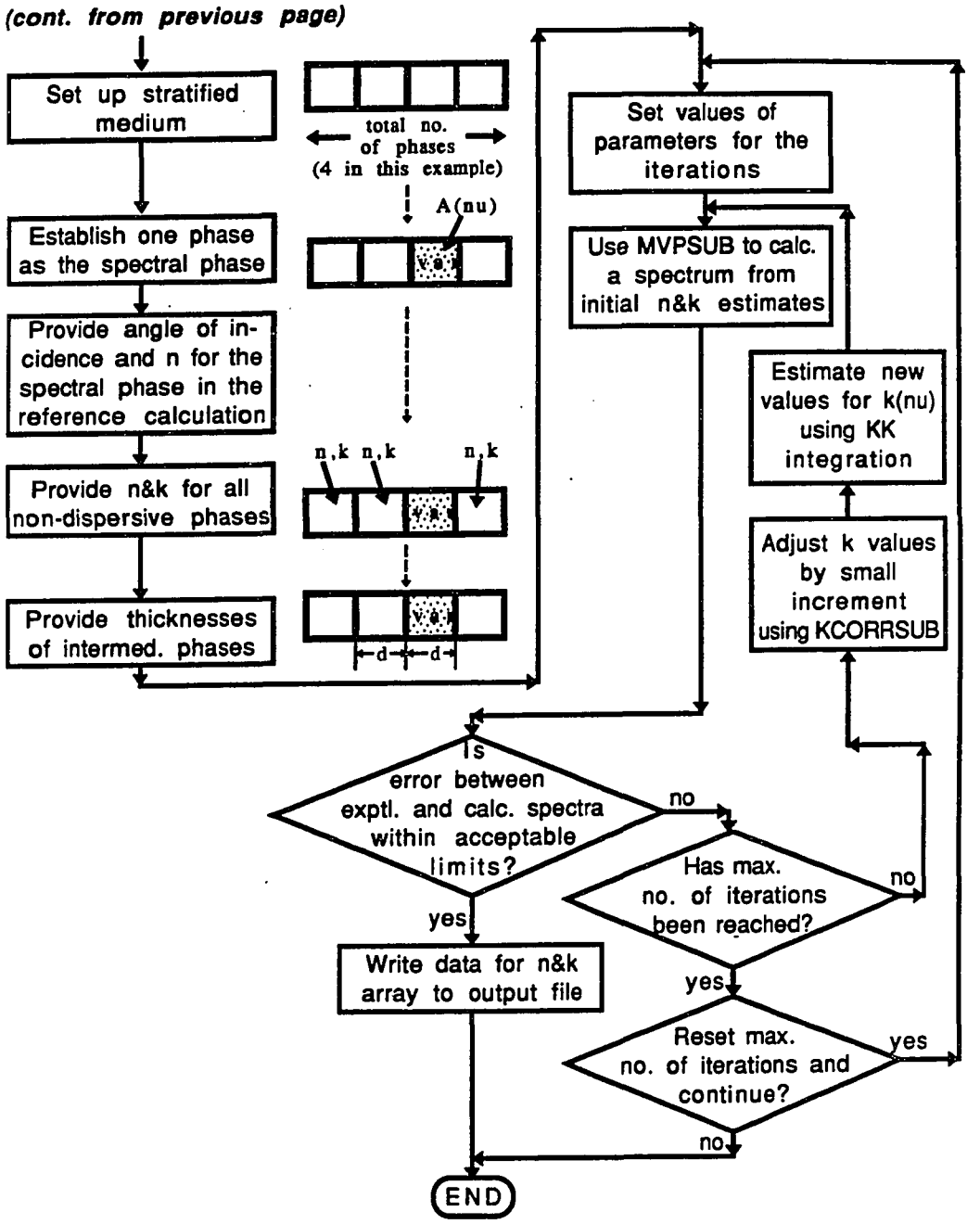

Figure 2. (continued)

maximum number of iterations, specified by the user, have been performed. In this loop, the Kramers-Kronig integration is applied within the external subroutine KKSUB2 to generate $n(\nu)$ from the array of $k(\nu)$. This subroutine also interpolates n and k to output them as functions of an evenly spaced array of ν values. The subroutine MVPSUB then generates an absorbance spectrum from the calculated n and k values using the same parameters that were input for the original experimental data. That subroutine calculates the boundary field strengths for the phases by a matrix method using the mean value theorem. Finally, the routine KCORRSUB compares the values of $A(\nu)$ calculated by MVPSUB with those in the original experimental data; if the error between the two is greater than a set limit ε at any value of ν, KCORRSUB adjusts k at each frequency by a small amount so as to reduce the error $|A_{exp}-A_{calc}|$. The loop then is repeated, beginning with the Kramers-Kronig integration. If the error is within ε at all ν, the final array of $\hat{n}(\nu)$ is output.

2. The Programs RTCALC and SPREP to Calculate Spectra

The program RTCALC calculates a spectrum for a material under a variety of conditions, using the optical functions of the material and the experimental parameters as input. This, in effect, is the converse of OPFXNS1. The output of RTCALC actually consists of calculated values of reflectance (R) and transmittance (T) as functions of frequency; an auxiliary program called SPREP converts these to a spectrum of the desired type (for example, reflectance-absorbance). This pair of programs is versatile; it allows calculation of a spectrum corresponding to an experiment consisting of a stratified medium of up to six phases. In contrast to OPFXNS1, RTCALC allows phases other than the spectral phase to have optical functions that vary with frequency.

The overall logic used by RTCALC is illustrated in Figure 3. One phase is chosen for which to generate spectra (i.e., it is not present as an absorbing phase in the reference

calculation). Any other phases, except the first, may have optical functions that vary with frequency. These variable phases are denoted by "var" in Figure 3. Sets of variable optical functions are input as formatted ASCII files; constant values are typed directly from the keyboard. The angle of incidence and the thicknesses (in angstroms) of all intermediate phases must be entered in order to fully define the stratified medium.

One important feature of the program which increases flexibility is the option of using separate sample and reference strata, which is offered to the user at the beginning of execution. If this option is used, R and T are calculated first for the stratified medium corresponding to the "sample" measurement. Then the strata are redefined and the "reference" R and T are calculated. This option is useful for modeling certain IRRAS arrangements where one of the phases may be present in the sample but not in the reference. If the separate-strata option is not used, the reference calculation is the same as that of the sample, except that the absorbing spectral phase is replaced by a non-absorbing phase of a specified constant refractive index (usually $n_{ref} = 1.00$, corresponding to air in ex situ IRRAS).

After the appropriate parameters have been entered into the program, RTCALC uses these parameters, optical constants, and optical functions to calculate sets of $R(\nu)$ and $T(\nu)$ for both the sample and the reference measurements. This program calculates boundary field strengths in a subroutine similar to the method used in OPFXNS1. After execution of RTCALC is complete, the program SPREP simply converts the R and T values into spectra by applying the function corresponding to the type of spectrum desired. For most of this work, reflectance-absorbance, given by equation 25, is the quantity that is calculated.

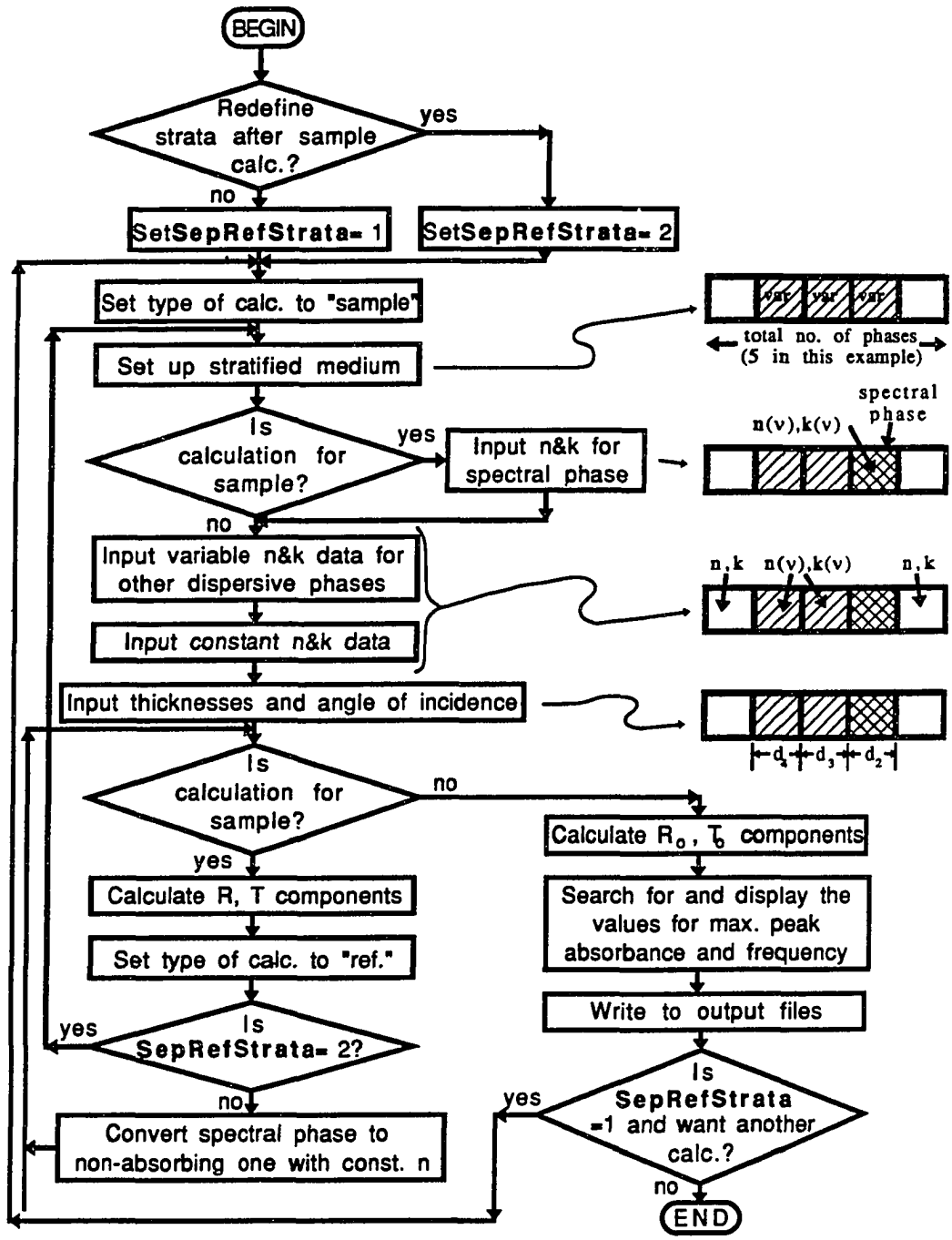

Figure 3. Flowchart of the Organization of the Program RTCALC.

3. Other Programs

Three other programs were written to test the integrity of the aforementioned three programs of the calculational cycle, as well as to provide capabilities of modeling the effects of experimental parameters upon bandshapes. These three programs are MakeCurv, CAUCHY, and KtoN. The first two programs generate synthetic profiles of absorptive index, $k(\nu)$; the third calculates the corresponding refractive index, $n(\nu)$ from a set of absorptive index values.

The IR spectrum from a set of j vibrational modes in a condensed phase may be modeled by setting the absorptive index of that phase equal to a Cauchy (i.e., Lorentzian) function, given by the equation

$$k(\nu) = \sum_{j=1} k_{\max,j}\left(1 + b_j^{-2}\left(\nu - \nu_0\right)^2\right)^{-1}, \qquad (28)$$

where $\nu_0=\nu_j$ at the band center and $2b$ is the full width at half-maximum of the band in cm^{-1}.[5] The program CAUCHY generates synthetic absorption profiles of up to nine peaks, each of which corresponds to a Cauchy function. Values of k_{max} and b and spacings between the bands can be set individually for each band. The output data are values of absorptive index as a function of wavenumber. Another program, MakeCurv, can create a synthetic $k(\nu)$ spectrum consisting of either Lorentzian or Gaussian profiles; however, the parameters controlling the peak height and width must be the same for all bands. These two programs are useful for generating model optical functions to determine how different experimental conditions may give rise to optical artifacts in a reflection spectrum, such as shifts in peak frequencies.

Before the $k(\nu)$ output of CAUCHY or MakeCurv can be used further, the corresponding $n(\nu)$ must be calculated. The program KtoN performs this task using the Kramers-Kronig integration in the same manner as the program OPFXNS1.

C. EXPERIMENTAL SECTION

1. Transmission IR Spectroscopy

Spectra were collected on a Nicolet 740 FTIR spectrometer with a cryogenic HgCdTe detector. All measurements used at least 128 scans co-added with Happ-Genzel apodization at 4-cm^{-1} nominal resolution zero-filled once to give better than 2-cm^{-1} resolution. Transmission spectra of polymer films were obtained by extending the films across the opening of a KBr pellet holder and holding them in place with a flexible magnetic retaining strip.

2. ATR Spectroscopy

Attenuated total reflection spectra of liquids were obtained using a Prism Liquid Cell (Harrick) containing a ZnSe prism set up for a 45° angle of incidence. In the calculations, the optical constants n=2.41 and k=0.0 were used for ZnSe. A wire-grid polarizer was placed in the beam before the cell so that the incident light was p-polarized. The liquids were used neat and the background spectrum was of dry nitrogen, taken with the same cell.

3. Approximation of the Zero-Frequency Refractive Index

In this work, the zero-frequency refractive index n_∞ was approximated by several methods, depending on the type of spectrum recorded. Hawranek et al. discussed how to choose n_∞ as part of a study on errors in IR spectroscopy.[5] For the alkanethiols, the value of the refractive index in the visible region was used. For D_2O, n_∞ was estimated to equal the refractive index of H_2O; this estimate was adjusted slightly by trial and error to attain convergence of the Kramers-Kronig integration. The baseline refractive index of the polymers studied was first estimated by noting the functional groups present and

combining their contributions, deduced from known refractive indices of related monomers. This initial estimate was refined by using the program FRINGE.AB.

The program FRINGE.AB, included in Appendix 1, is used to estimate thickness of a polymer film from a transmission spectrum of the film. This program generates synthetic interference fringes which are compared with the experimentally measured fringes in the IR transmission spectrum. In the calculation, the film is assumed to be a non-absorbing material with a constant refractive index which is approximately equal to n_∞ for the real film. The transmission spectrum of the non-absorbing analog is calculated from the Fresnel equations; since this analogous film is not intrinsically absorbing, the imaginary terms in the equations drop out, simplifying the calculation significantly. By adjusting both n and d for the film, the synthetic interference fringes are "tuned" until they overlap with the fringes in the experimental spectra, as determined visually. In this manner, both d and n_∞ for the actual film used can be estimated very closely. The program FRINGE.AB will run only within the commercial Spectra Calc software (Galactic Industries), with its Array Basic language built in.

4. Preparation of Unsupported Polymer Films

The polymer films which were used for spectroscopy were first prepared on glass; these were then delaminated and used as free-standing films. Glass microscope slides (3 in x 1 in) comprised the initial substrates—which were pretreated by an initial cleaning, drying, and rubbing the surface of the glass on a block of poly(tetrafluoroethylene) to ease the eventual removal of the polymer film. A solution of 5 - 20% of the polymer in a compatible solvent was flooded onto the surface with a Pasteur pipet. Spinning the slide at ~1000 rpm on a photoresist spinner (Headway Research Corp.) removed the excess solution and left a uniform film. The slides were then dried in air for ~1 h to remove the majority of solvent and annealed at ~100° for 12 h.

To delaminate the film, the slide was immersed in deionized water, which separated the polymer from the glass and caused the former to float to the surface. Sometimes it was necessary to run a knife blade around the edge of the slide before immersing it in order to cut any part of the film that may have wrapped around the edges. The delaminated films were removed from the water, suspended, and dried in an oven or at room temperature.

5. Reagents

All solvents were reagent grade and used as obtained. A Milli-Q purification system (Millipore) produced the deionized water. Of the polymers tested, poly(methyl methacrylate), poly(styrene/acrylonitrile), and poly(vinylidene chloride/acrylonitrile) were from Polysciences. The hexanethiol and dodecanethiol were supplied by Kodak. All other compounds for which optical functions were obtained were from Aldrich. All the aforementioned materials were used without further purification, except octadecanethiol, which was recrystallized twice from ethanol in the laboratory.

D. VERIFICATION OF OPERATION OF THE PROGRAMS FOR CALCULATIONS

1. Simulated Profiles

As mentioned above, the integrity of programs in the calculational cycle was tested, using both simulated and real spectral data. This section discusses the tests used for verification, beginning with the simulated data.

The test of the programs with simulated absorbance profiles for a hypothetical absorbing thin film followed the steps shown in Figure 1. First, a synthetic $k(\nu)$ spectrum consisting of two Lorentzian peaks was generated with the program CAUCHY. The parameters used for the spectrum were similar to those used in another study recently reported in the literature.[8] One peak, centered at 1700 cm^{-1}, had a maximum k of 0.00821 and FWHM of 60.6 cm^{-1}; for the other peak at 1400 cm^{-1}, k_{max} was 0.026 and FWHM was 39.4 cm^{-1}. The resulting sum of the two Cauchy functions is shown in Figure 4a.

From this initial $k(\nu)$ profile, $n(\nu)$ was calculated with KtoN, assuming $n_\infty = 1.5$. Then, a transmission spectrum (not shown) was calculated by modeling the absorbing material as a 30-μm-thick film suspended in air. The resulting absorbance spectrum was converted back to n and k using OPFXNS1. Figure 4b shows the resulting $k(\nu)$. The difference between the initial and final k functions (Figure 4c) is essentially random and $<<1\%$ of either k_{max} value, which verifies operation of the programs for the case of synthetic spectra.

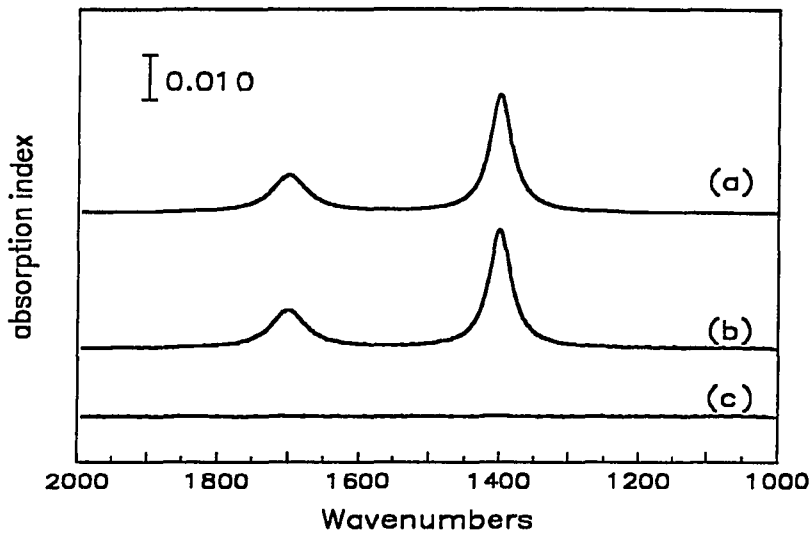

Figure 4. Synthetic $k(\nu)$ spectrum used for verification of the operation of programs in the calculational cycle. The Cauchy functions were calculated as described in the text: (a) initial $k(\nu)$ spectrum generated with CAUCHY; (b) spectrum resulting from converting the profile in (a) into an absorbance spectrum and back to an absorption index; (c) resulting error from subtracting (b)-(a).

2. Optical Constants of Water

Determination of the complex refractive index of water from experimental data and comparison with literature values provided further verification of the calculational cycle using spectra in the attenuated total reflectance (ATR) mode, rather than the simpler case of transmission. The experimentally determined optical functions for H_2O between 4000 and 1300 cm^{-1} are compared with literature results in Figure 5.[9] The experimental data were obtained from OPFXNS1, using as input an ATR spectrum of H_2O taken with p-polarized light, together with a baseline refractive index of $n_\infty = 1.31$. The experimental and literature data agree fairly well among both n and k except at the lower wavelengths; the reason for the disagreement in that region is that the input data to the n and k calculation did not include the intense band near 1000 cm^{-1}.

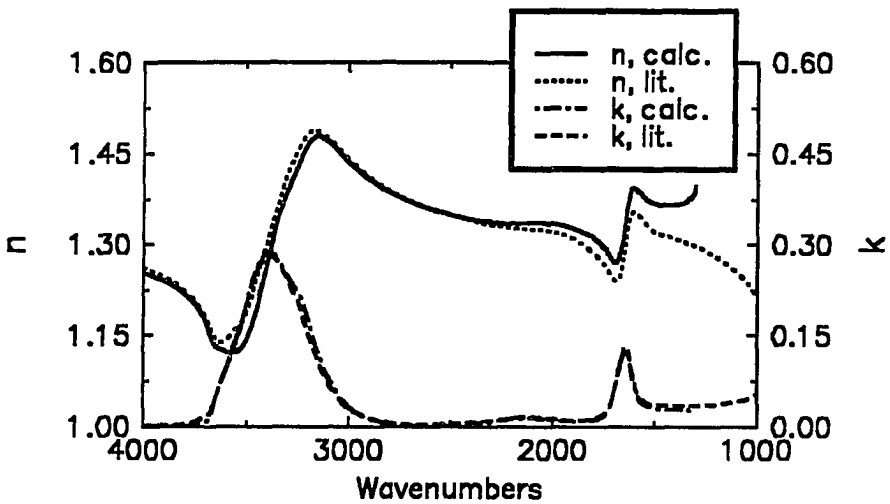

Figure 5. Comparison of optical functions of water between those calculated from ATR spectra and those from the literature.

3. Experimental and Calculated Reflection Spectra of Polymer Films

Since it was desired to use RTCALC to calculate reflection spectra under a variety of conditions, a test was made of the program's performance calculating a reflection spectrum taken using a semiconducting substrate. Surfaces of semiconductors are poorer reflectors than those of metals; thus, the former give rise more easily to optically induced distortions in band shapes.[10]

A spectrum of a 2.725-μm film of PMMA cast on glassy carbon, taken at 60° incidence using p-polarized light, is shown in the low-energy region in Figure 6 and in the high-energy region in Figure 7. The expected reflection spectrum corresponding to this experiment was calculated under the same conditions (60° incidence, etc.) using RTCALC and the optical functions of PMMA. These *n* and *k* values had been previously calculated from a transmission spectrum of a free-standing thin film of PMMA using OPFXNS1.

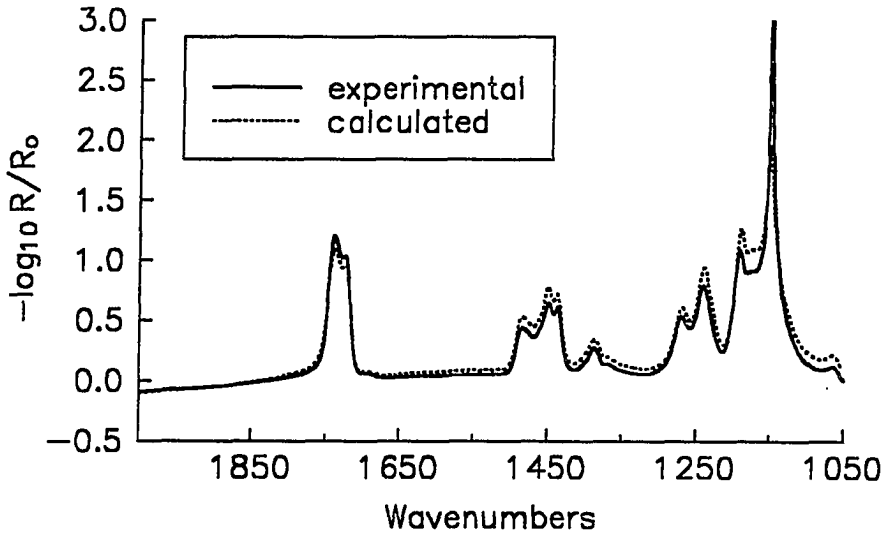

Figure 6. IR Reflection Spectra of PMMA on Glassy Carbon in the low-energy region.

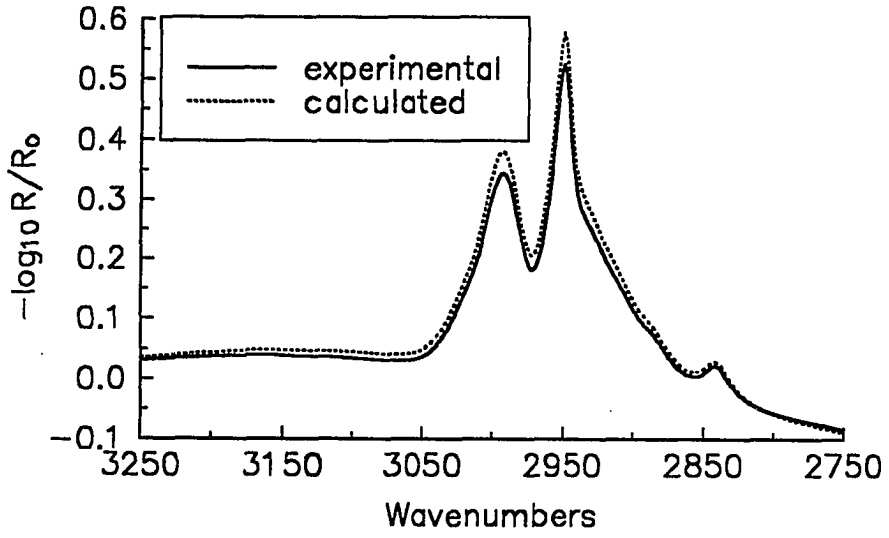

Figure 7. IR Reflection Spectra of PMMA on Glassy Carbon in the high-energy region.

Separate n and k calculations were done for the two frequency regions because of the limits on array sizes in OPFXNS1. The calculated spectrum shown in Figures 6 and 7 shows excellent agreement. The only peak absorbance differing by >10% between the two spectra is that for the band at ~1150 cm^{-1}. This discrepancy arises because of the narrowness and intensity of that band, along with the limited wavenumber resolution of the calculations. From the three efforts at verification listed above, we believe that a single round of the calculational cycle does not generally introduce errors of >10% in peak absorbances, provided that the correct experimental parameters and values of n_∞ are used in the calculations.

E. RESULTS OF CALCULATIONS OF OPTICAL FUNCTIONS

Spectra were recorded and thence optical functions n and k obtained for several compounds important for studies of in situ IRRAS and related techniques. The compounds for which data are presented are deuterium oxide; hexane-, dodecane-, and octadecane- thiols; eicosanoic acid; the homopolymer cellulose acetate; and the copolymers poly(styrene/acrylonitrile) and poly(vinylidene chloride/acrylonitrile). In this chapter, these n and k data are presented graphically; the same data appear in tabular form in Appendix 2 for the benefit of readers who may wish to enter them into a computer or use them for other calculations. The value of n_∞ used for the Kramers-Kronig integration for each compound appears in the corresponding figure legend.

Obtaining optical functions of D_2O was particularly important in developing the in situ technique for monolayer films. These values were used to examine the differences in optical effects between using D_2O and H_2O in the cell. The n and k values calculated for

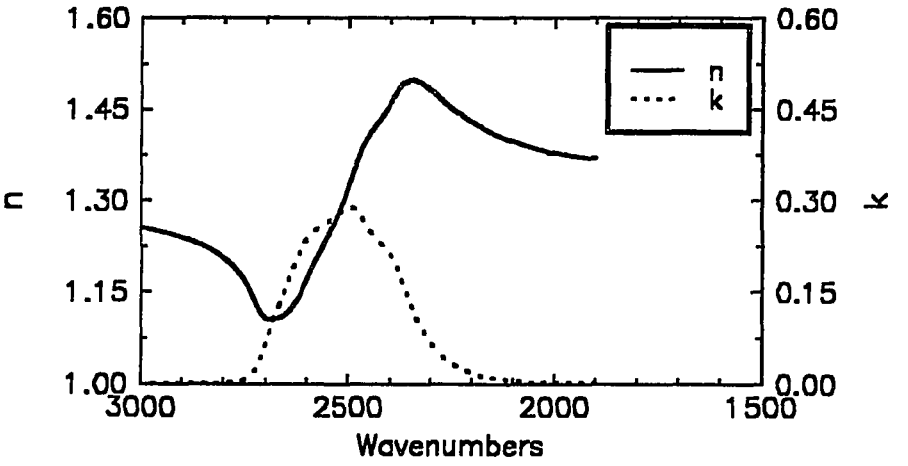

Figure 8. Optical functions (n and k as functions of frequency) for D_2O. The value of baseline refractive index used was $n_\infty = 1.31$.

D_2O are shown in Figure 8. Equivalent bands occur in the optical functions of water about 1000 cm^{-1} higher than they appear here.

The next several sets of data presented correspond to several compounds used as adsorbate precursors. Data for hexanethiol, $C_6H_{13}SH$, are given in Figure 9. Those for dodecanethiol, $C_{12}H_{25}SH$, are in Figure 10. Data were also generated for octadecanethiol, $C_{18}H_{37}SH$, shown in Figure 11. Since members of my research group originally used optical functions of eicosanoic acid, $C_{19}H_{39}COOH$, for calculating spectra of all long-chain alkanethiolate monolayers, the optical functions were obtained for that compound, too. These are shown in Figure 12. The first two compounds are liquids at room temperature and spectra of them were obtained by ATR. The last two are solids and were measured as KBr pellets by transmission.

The disparities between the values of k at the peak maxima of these compounds should be noted. For example, the maxima for $\nu_i(CH_2)$ at ~2920 cm^{-1} going from

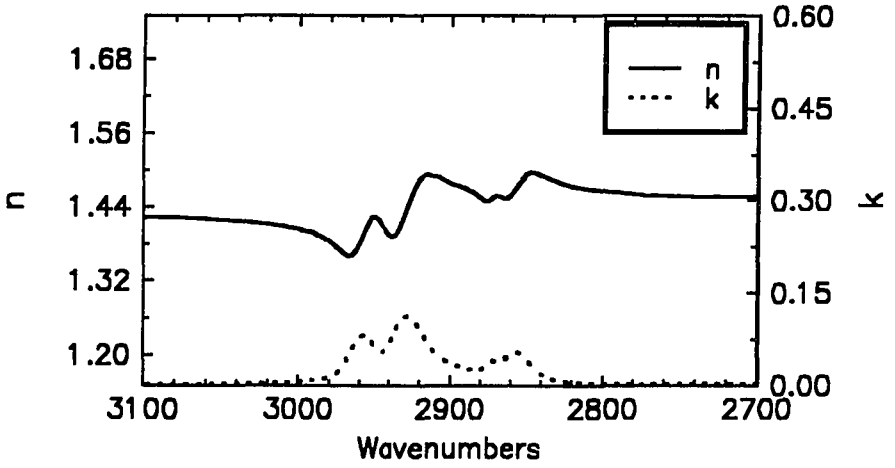

Figure 9. Optical functions as a function of frequency for hexanethiol. The value of baseline refractive index used was $n_\infty = 1.44$.

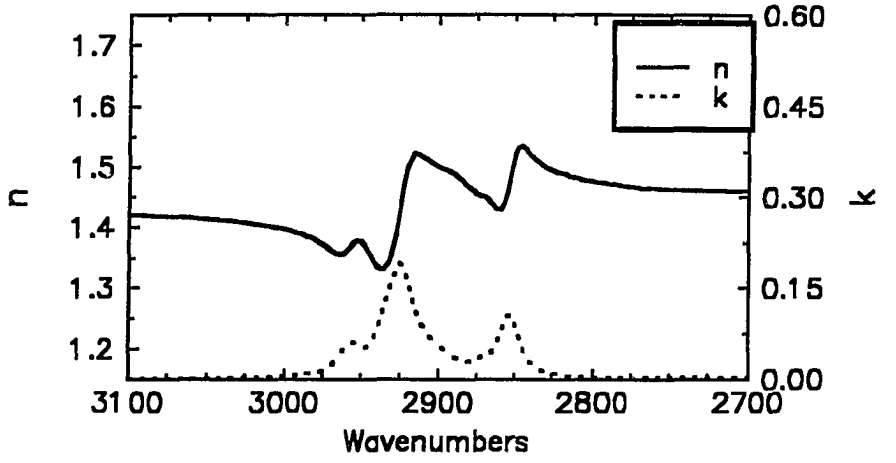

Figure 10. Optical functions as a function of frequency for dodecanethiol. The value of baseline refractive index used was $n_\infty = 1.44$.

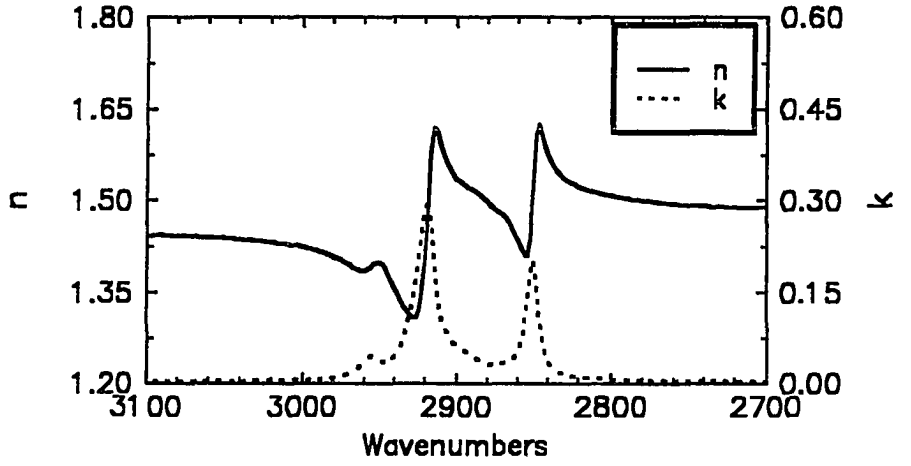

Figure 11. Optical functions as a function of frequency for octadecanethiol. The value of baseline refractive index used was $n_\infty = 1.465$.

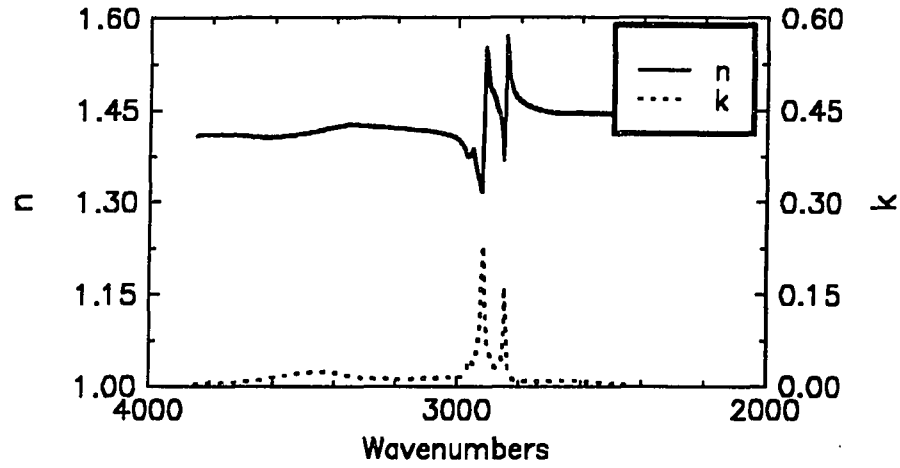

Figure 12. Optical functions as a function of frequency for eicosanoic acid. The value of baseline refractive index used was $n_\infty = 1.425$.

$C_6H_{13}SH$ to $C_{12}H_{25}SH$ to $C_{18}H_{37}SH$ increase from 0.114 to 0.192 to 0.302, with a change in ν_{peak} from 2927 to 2918 cm^{-1}. This is to be expected because of the change in the number of methylene groups, combined with changes in density and the degree of order in the bulk compounds at room temperature. More surprising is the change in the maxima of k for $\nu_a(CH_2)$ between $C_{18}H_{37}SH$ and $C_{19}H_{39}COOH$, from 0.302 to 0.229. The latter has one more CH_2 group and yet a lower k value. This difference is attributed to effects of the head group (acid or mercapto moiety) upon the local environment of the polymethylene chains.

Optical functions were also obtained for several polymers, which I desired to use as thin films to study the operation of the in situ cell before proceeding to study monolayer films. Since a major goal of this work was to study films in contact with water, polymers were chosen that would not swell or delaminate upon contact with aqueous solutions. Several polymers used for moisture barriers were candidates for these studies, including poly(styrene-co-acrylonitrile) poly(vinylidene chloride-co-acrylonitrile) [known

commercially as "Saran-F120"—a trademark of Dow Chemical], and poly(vinylidene fluoride). Spectra and optical functions were obtained for poly(styrene/acrylonitrile) and poly(vinylidene chloride/acrylonitrile), shown in Figures 13 and 14 respectively. In connection with another study on the hydrolysis of polymer films by S. M. Stole,[11] the optical functions for cellulose acetate were also generated, shown in Figure 15.

Some of the n and k data for polymers were used to calculate expected IRRA spectra using the in situ cell (not shown). Comparison of the calculated spectra with experimental spectra provided further confirmation of the effectiveness of the aforementioned programs for modeling the in situ cell. This comparison was not hindered by the surface selection rule, since the polymer films prepared by spin coating have essentially random orientation of the chains.

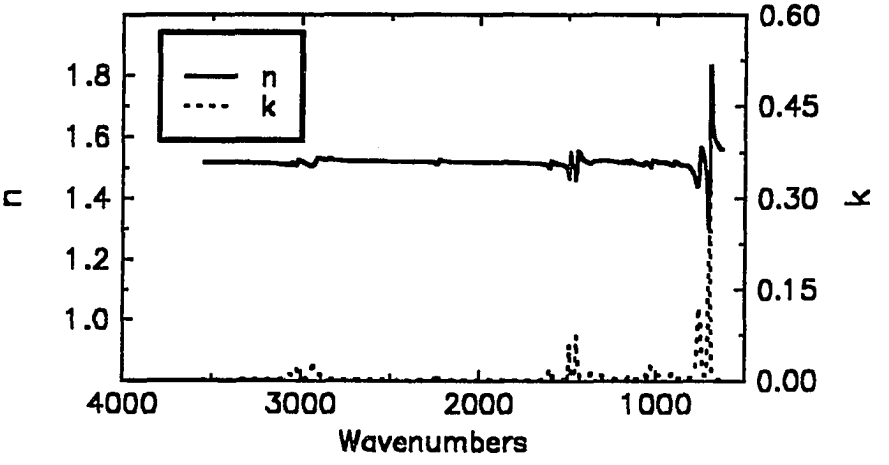

Figure 13. Optical functions as a function of frequency for poly(styrene/acrylonitrile). The value of baseline refractive index used was $n_\infty = 1.52$.

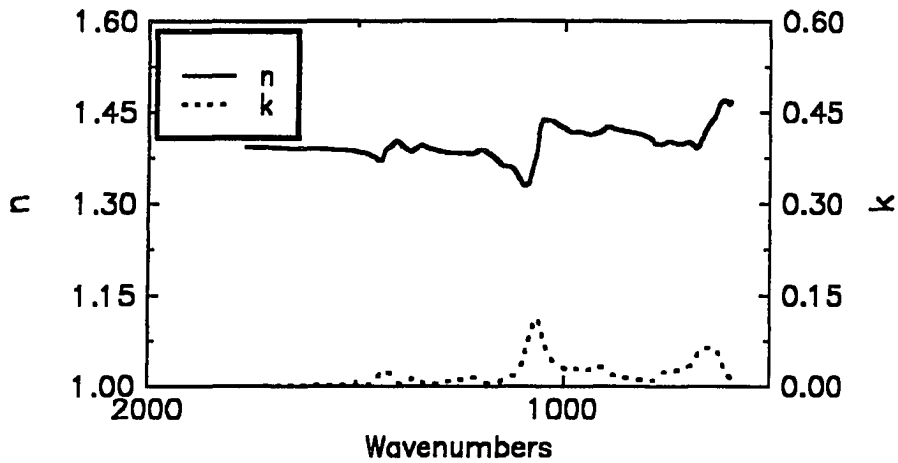

Figure 14. Optical functions as a function of frequency for poly(vinylidene chloride/acrylonitrile). The value of baseline refractive index used was $n_\infty = 1.40$.

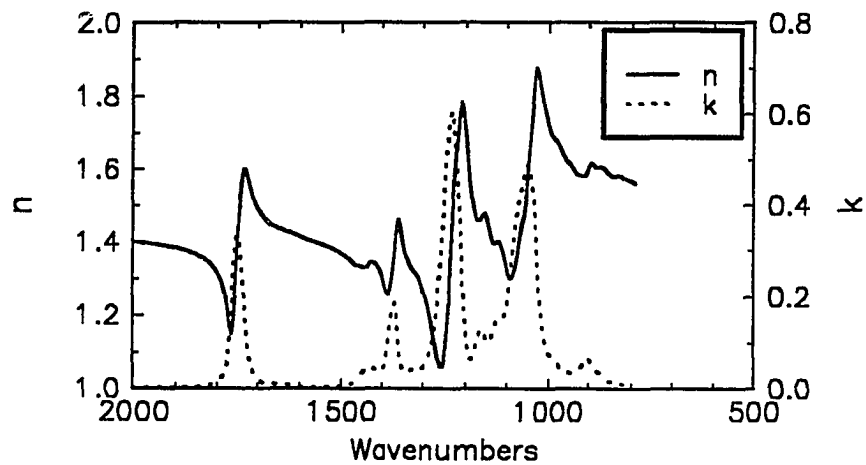

Figure 15. Optical functions as a function of frequency for cellulose acetate. The value of baseline refractive index used was $n_\infty = 1.44$.

F. CONCLUSIONS

This chapter has shown that use of the Fresnel equations, together with other elements of electromagnetic theory given in the previous section, facilitate the interconversion of optical functions with transmission or reflection spectra. Several computer programs to perform this interconversion have been developed and tested. The employment of these techniques has converted IR spectra of several liquids, polymers, and crystalline compounds into sets of n and k for those compounds which constitute useful reference data for future studies.

More specifically, the quantitative comparison of $k(\nu)$ for the $\nu(CH_2)$ modes of alkanethiols and of eicosanoic acid illustrate the difficulty of using values for one compound to represent those of another compound. The maxima of $k(\nu)$ differ significantly across the four compounds, even though the three alkanethiols are analogs differing only in chain length and even though eicosanoic acid has only one more methylene group than octadecanethiol.

REFERENCES

1. Fahrenfort, J. In *Infrared Spectroscopy and Molecular Structure*; Davies, M., Ed.; Elsevier: New York, 1963; Chapter 11.
2. Harrick, N.J. *Internal Reflection Spectroscopy;* Wiley: New York, 1973.
3. Jones, R.N.; Escolar, D.; Hawranek, J.P.; Neelakantan, P.; Young, R.P. *J. Mol. Structure* **1973**, *19*, 21-42.
4. Hawranek, J.P.; Neelakantan, P.; Young, R.P.; Jones, R.N. *Spectrochim. Acta* **1976**, *32A*, 85-98.
5. Hawranek, J.P.; Jones, R.N. *Spectrochim. Acta* **1976**, *32A*, 99-109.
6. Cameron, D.G.; Hawranek, J.P.; Neelakantan, P.; Young, R.P.; Jones, R.N. *Computer Programs for Infrared Spectroscopy*; N.R.C.C. Bulletin No. 16; National Research Council of Canada: Ottawa, 1977; Vol. 6.
7. Allara, D.L.; Baca, A.; Pryde, C.A. *Macromolecules* **1978**, *11*, 1215.
8. Graf, R.T.; Koenig, J.L.; Ishida, H. *Appl. Spectrosc.* **1985**, *39*, 405-408.
9. Downing, H.D.; Williams, D.J. *J. Geophys. Res.* **1975**, *80*, 1656.
10. Porter, M.D.; Bright, T.B.; Allara, D.L.; Kuwana, T. *Anal. Chem.* **1986**, *58*, 2461-2465.
11. Stole, S.M. Ph.D. Dissertation, Iowa State University, 1990.

SECTION II. CALCULATION OF MEAN SQUARE ELECTRIC FIELD VALUES FOR DETERMINING SUITABLE CONDITIONS FOR SPECTROSCOPY

A. INTRODUCTION

1. Statement of the Problem

This section addresses the technique of calculating mean square electric field (MSEF) values to model reflection spectroscopic experiments. The need to perform computer modeling of in situ IRRAS arose because of the difficulty of acquiring in situ spectra of an alkanethiolate monolayer film under a thin layer of an aqueous phase. Measurement of such spectra in the C–H stretching region (3000 ~ 2800 cm^{-1}) previously posed an experimental problem that had not been addressed. The difficulty of this measurement arises primarily from the overlap of the tail of the O–H stretching mode of H_2O with the C–H stretching modes of the monolayer. The nature of the problem can be seen by contrasting the physical details of an in situ measurement, shown in Figure 3 in the General Introduction, with those of an ex situ measurement, illustrated in Figure 1.

In the case of the ex situ measurement (i.e., a measurement where phase 1 is the nitrogen-purged chamber of a spectrometer, phase 2 is the monolayer, and phase 3 is the reflective metal), the dependence of surface detectability on the angle of incidence and polarization of the incoming light is well established.[1,2,3,4,5] This angular dependence results from the boundary conditions of the electromagnetic field at the surface, together with the effects of the free electrons of the metallic substrate. These factors result in near-zero values of the components E_x and E_y of the MSEF at the surface for all θ. On the other hand, E_z is enhanced, reaching large values at the surface at high θs, as noted in the theory chapter. Hence, from the standpoint of the MSEF, conditions for high detectability ex situ are large θs using p-polarized light.

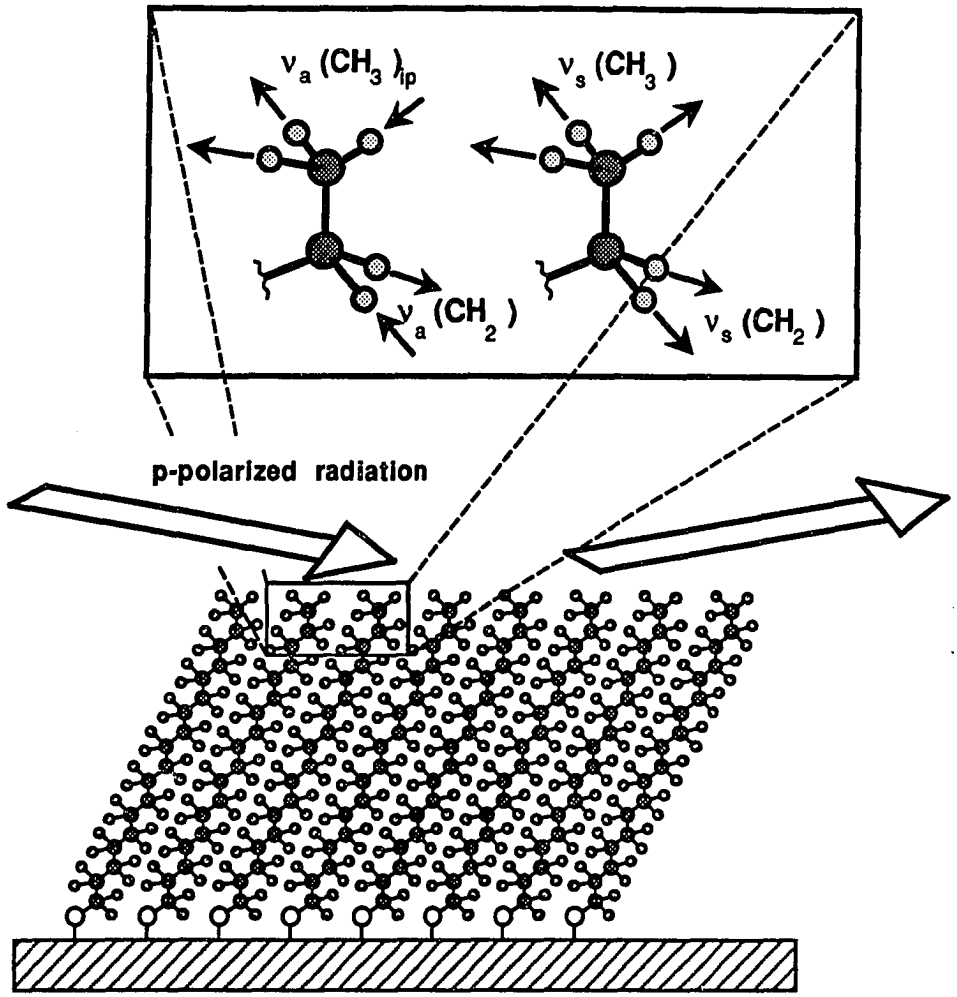

Figure 1. Schematic illustration of ex situ IRRAS of an octadecanethiolate film at Au. Descriptions of the modes shown are given in Table 1.

It is also important to note that the anisotropy of the surface MSEF results in the preferential excitation of vibrational modes with transition dipoles oriented along the surface normal. In Figure 1, all modes shown have a component of their transition dipoles perpendicular to the surface, since the monolayer chains are tilted ~30° from the surface

normal. The magnitudes of the normal components depend on the angle of the adsorbate chains from the surface normal.

The complication of the in situ measurements arises from the overlap of the tail of the O–H stretching mode of H_2O with the C–H stretching modes of the monolayer. This is shown by the respective plots of n and k for octadecanethiol and H_2O in Figures 2 and 3; peak positions and mode descriptions of the former are given in Table 1. In contrast to an ex situ measurement, the beam in an in situ measurement must propagate through a phase that has an $\hat{n}$ with a strong wavelength dependence and is orders of magnitude thicker than the monolayer. These factors, as will be shown, give rise to optically induced alterations of the strengths and shapes of an in situ spectrum that must be taken into account in developing a structural interpretation through comparisons with spectra from ex situ or transmission measurements.

Determining the magnitude of these distortions is particularly important for in situ studies of monolayers composed of long alkyl chains, since the C–H stretching modes provide a disclosure of the average local environment of the chains as well as their molecular orientation with respect to the substrate surface. Insights into the local environment are *qualitatively* inferred by the peak positions of ν_a (CH_2) and ν_s (CH_2), as evident from the differences in peak frequencies for representative liquid alkanethiols.[6] Orientational descriptions are developed by comparing the intensities of an observed spectrum with those calculated for an isotropic layer of similar packing density, taking into account the anisotropic nature of the surface MSEF.[7,8] The disclosures provided by these vibrational modes ex situ have played a key role in the development of the structural model of these films and will prove particularly useful as a starting point for comparison with results from in situ characterizations.

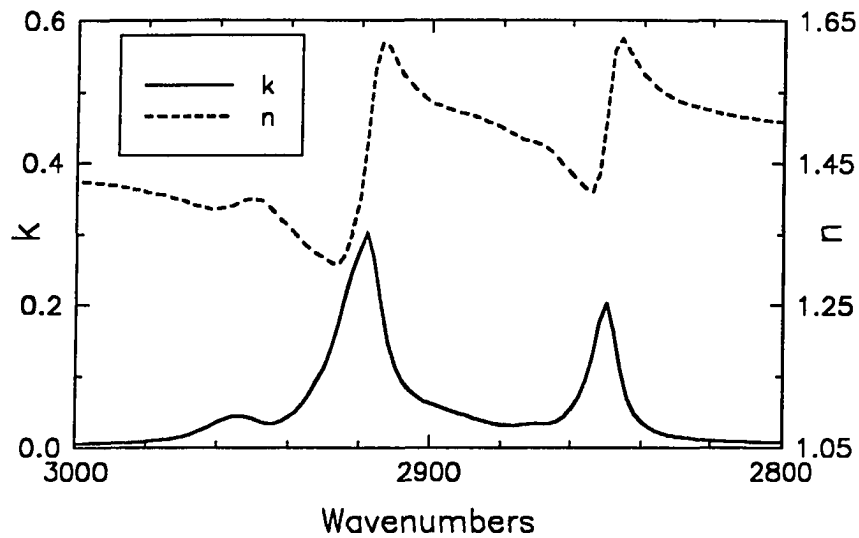

Figure 2. Optical indices n and k as a function of frequency in the C–H stretching region for $CH_3(CH_2)_{17}SH$.

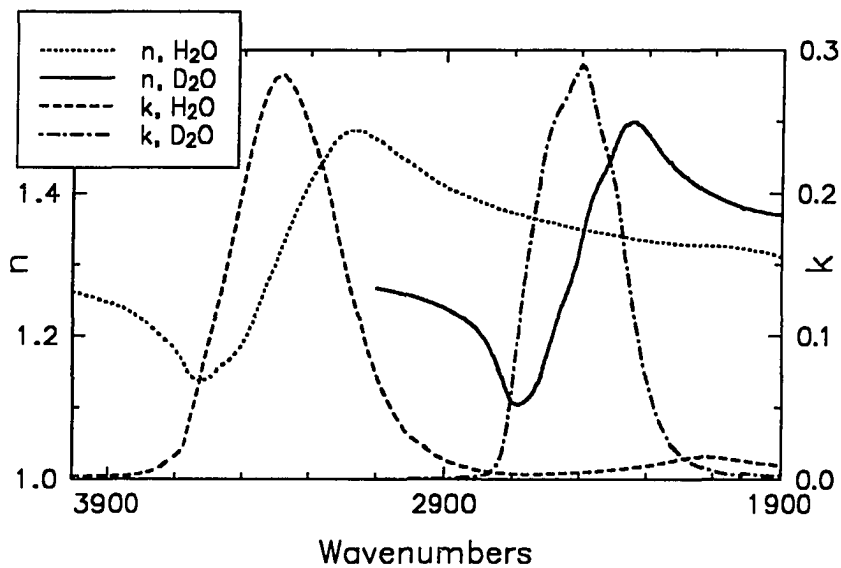

Figure 3. Optical indices n and k as a function of frequency for H_2O and D_2O.

Table 1. Predominant C–H stretching mode peak positions in solid octadecanethiol

	peak frequency,[a] cm^{-1}		
mode[b]	bulk material[c]	monolayer	Direction of transition dipole[d]
ν_a (CH_3, ip)	e	2965	⊥ to C–CH_3 bond in C–C–C catenary plane
ν_a (CH_3, op)	2956	f	⊥ to C–CH_3 bond and ⊥ to C–C–C catenary plane
ν_s (CH_3, FR)	g	2938	∥ to C–CH_3 bond
ν_a (CH_2)	2918	2917	⊥ to C–C–C catenary plane
ν_s (CH_3, FR)	g	2878	∥ to C–CH_3 bond
ν_s (CH_2)	2850	2850	∥ to C–C–C plane, bisecting H–C–H

[a]Peak positions are determined as the average for four independent spectra and are accurate to within 1 cm^{-1}. Data are from reference 8.

[b]ip = in-plane; op = out-of-plane

[c]Crystalline-state positions determined for $CH_3(CH_2)_{21}SH$ in KBr.

[d]From Snyder, R.G.; *J. Chem. Phys.* 1965, *42*, 1744.

[e]The ν_a(ip) is masked by the strong ν_a(op) in the crystalline- and liquid-state spectra.

[f]The position for ν_a(op) cannot be determined because of the low signal-to-noise ratio. This is a result of the orientation of this mode with respect to the surface.

[g]Both ν_s(FR) bands are masked by the $\nu_a(CH_2)$ band.

2. Our Approach: Calculate MSEF Values

This section describes results of mean square electric field (MSEF) calculations that elucidate the effects of solution-layer thickness, angle of incidence, solution composition (H_2O or D_2O), and the refractive indices of IR-transparent window materials (CaF_2 and Si) upon the observed spectrum. The following section includes calculations of reflectivity under different angles of incidence, together with experimental results to verify the calculations. Similar computational approaches have been used to devise strategies for the IRRAS of many other ex situ[7,9,10,11,12,13,14,15] and in situ[16,17,18,19] characterizations. My research adviser and I gave specific attention to the effects of the refractive indices of the solvent and the window material on the conditions yielding optimum surface detectability. Our analysis also facilitates a *qualitative* assessment of the underlying optical phenomena that influence the strengths and shapes of the in situ spectral bands. Development of structural descriptions of monolayer-coated liquid-solid interfaces based on comparisons to ex situ reflection and transmission spectra requires that such phenomena be accounted for.

B. CONSTRUCTION AND EXECUTION OF THE PROGRAM FOR CALCULATING MSEF

1. Parallel Slab Model Used for Electromagnetic Theory Calculations

For the purpose of calculations, the in situ cell was modeled as a stratified medium of optically isotropic phases that are separated by parallel, planar boundaries, as described in the theory chapter above. Figure 4 shows a model of four phases, which represent the cell window, liquid layer, monolayer film, and metal surface, respectively. Although the cell is best represented by four phases, calculations of MSEFs were performed using a three-phase model, in which the monolayer film is neglected, to simplify computation. Test calculations which included an organic monolayer in a four-phase model differed by negligible amounts from the results using the three-phase approximation.

In the three-phase approximation, the window and metal are considered semi-infinite and the distance (z) normal to the phase boundaries is measured from the phase 1/phase 2 boundary (Figure 4). The angle of incidence at the phase 1/phase 2 boundary, θ, is given with respect to the surface normal. The optical properties of each phase j are defined by the complex refractive index. Since the entry phase is transparent by definition, $k_1 = 0$ in all cases. Each intermediate phase is further defined by its thickness d_j.

2. Algorithms for Calculating MSEF

This section describes the algorithms and other details involved in calculations of MSEF. For assessing the sensitivity of IRRAS to a surface film, we are only interested in the value of $\hat{\mathbf{E}}$ at the metal surface; however, it is useful to calculate values as a function

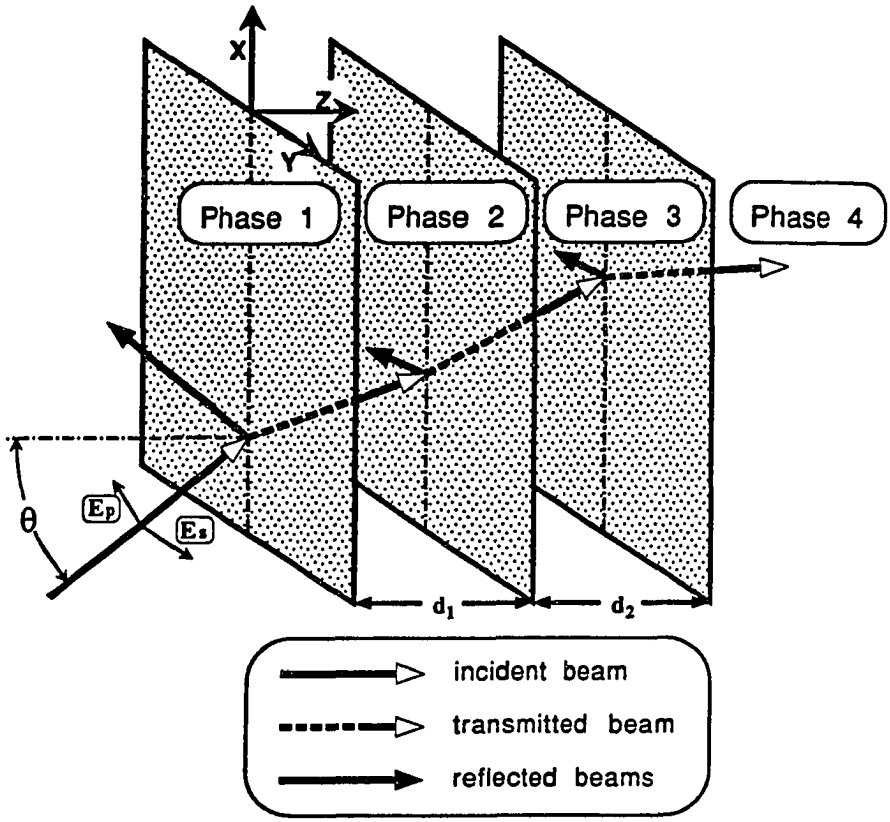

Figure 4. Model of four-phase stratified medium.

of position throughout the liquid phase and into the adjoining phases to understand the physical optics of the experiment.

The actual formulas used for MSEF are taken for the most part from an article published by Hansen in 1968 and from his subsequent review article in 1973.[20,21] The major difference between the two papers is the fact that the former defines $\hat{n} \equiv n + ik$ while the latter uses $\hat{n} \equiv n - ik$ to meet revised conventions of nomenclature. The former definition applies here. For the benefit of readers who may pursue these calculations in detail, several discrepancies between the two articles should be noted. There are several

errors in the 1968 work which were corrected in the later one. These errors include equations 6, 48, 67, and 68 and the definition of ξ_j near the beginning of the text. Also in the 1968 work, equation 61 is actually two equations that were printed together as one, and the x-axis of Figure 5 should be divided by 2.

Although the expressions for calculating MSEF are lengthy, they are worth presenting here to foster an understanding of the computer program THREEPHASE. Separate expressions apply for s-polarized (perpendicularly polarized) and for the x- and z- components arising from p-polarized (parallel polarized) radiation. The expressions for MSEF appear first for s-polarization and then for p-polarization below. Assuming that the system in question can be modeled by a three-phase approximation, values of MSEF in each phase as a function of distance normal to the phase boundary are given for s-polarized light, relative to the MSEF in the incident phase, by:

$$\frac{\langle E_{\perp 1}^2 \rangle}{\langle E_{\perp 1}^{0r2} \rangle} = (1+R_\perp) + 2R_\perp^{1/2} \cos\left[\delta_\perp^r - 4\pi\left(\frac{z}{\lambda}\right)\xi_1\right], \tag{29}$$

$$\frac{\langle E_{\perp 2}^2 \rangle}{\langle E_{\perp 1}^{0r2} \rangle} = \left| \exp\left[i\left(\frac{2\pi}{\lambda} n_1 \sin\theta_1 x - \omega t\right)\right] \left[\begin{array}{l} (1+r_\perp)\cos\left(\dfrac{2\pi\xi_2}{\lambda} z\right) \\ +i\dfrac{\xi_1\mu_2}{\xi_2\mu_1}(1-r_\perp)\sin\left(\dfrac{2\pi\xi_2}{\lambda} z\right) \end{array} \right] \right|^2, \tag{30}$$

and

$$\frac{\langle E_{\perp 3}^2 \rangle}{\langle E_{\perp 1}^{0r2} \rangle} = |t_{E\perp}|^2 \exp\left[-(4\pi/\lambda)\,\mathrm{Im}\,\xi_3 (z-h)\right]. \tag{31}$$

For p-polarized incident radiation, MSEF is given in the initial phase by:

$$\frac{\left\langle E_{\parallel 1x}^2 \right\rangle}{\left\langle E_{\parallel 1x}^{0t2} \right\rangle} = \cos^2\theta_1 \left\{ \left(1+R_{\parallel}\right) - 2R_{\parallel}^{1/2} \cos\left[\delta_{\parallel}^{r} - 4\pi\left(\frac{z}{\lambda}\right)\xi_1 \right] \right\} \tag{32}$$

and

$$\frac{\left\langle E_{\parallel 1z}^2 \right\rangle}{\left\langle E_{\parallel 1z}^{0t2} \right\rangle} = \sin^2\theta_1 \left\{ \left(1+R_{\parallel}\right) + 2R_{\parallel}^{1/2} \cos\left[\delta_{\parallel}^{r} - 4\pi\left(\frac{z}{\lambda}\right)\xi_1 \right] \right\}. \tag{33}$$

In the second, intermediate, phase, it is expressed by

$$\frac{\left\langle E_{\parallel 2x}^2 \right\rangle}{\left\langle E_{\parallel 1}^{0t2} \right\rangle} = \left| \exp\left[i\left(\frac{2\pi}{\lambda}\hat{n}_2 \sin\theta_2 x - \omega t \right) \right] \right| \left[\begin{array}{l} \cos\theta_1\left(1-r_{\parallel}\right)\cos\left(\dfrac{2\pi\xi_2}{\lambda}z\right) \\ +i\dfrac{\xi_2 n_1}{\hat{n}_2^2}\left(1+r_{\parallel}\right)\sin\left(\dfrac{2\pi\xi_2}{\lambda}z\right) \end{array} \right]^2 \tag{34}$$

and

$$\frac{\left\langle E_{\parallel 2z}^2 \right\rangle}{\left\langle E_{\parallel 1}^{0t2} \right\rangle} = \left| -\exp\left[i\left(\frac{2\pi}{\lambda}\hat{n}_2 \sin\theta_2 x - \omega t \right) \right] \right| \left[\begin{array}{l} \dfrac{\hat{n}_2 \sin\theta_2}{\hat{n}_2^2} n_1\left(1+r_{\parallel}\right)\cos\left(\dfrac{2\pi\xi_2}{\lambda}z\right) \\ +i\dfrac{\hat{n}_2 \sin\theta_2}{\xi_2}\cos\theta_1\left(1-r_{\parallel}\right)\sin\left(\dfrac{2\pi\xi_2}{\lambda}z\right) \end{array} \right]^2, \tag{35}$$

and in the third and final phase by

$$\frac{\left\langle E_{\parallel 3x}^2 \right\rangle}{\left\langle E_{\parallel 1}^{0t2} \right\rangle} = \left| \frac{\xi_3}{\hat{n}_3} t_{\parallel} \right|^2 \exp\left[-4\pi \mathrm{Im}\,\xi_3 \frac{(z-h)}{\lambda} \right] \tag{36}$$

and

$$\frac{\left\langle E_{\parallel 3z}^2 \right\rangle}{\left\langle E_{\parallel 1}^{0t2} \right\rangle} = \left| \frac{n_1 \sin\theta_1}{\hat{n}_3} t_{\parallel} \right|^2 \exp\left[-4\pi \mathrm{Im}\,\xi_3 \frac{(z-h)}{\lambda} \right]. \tag{37}$$

Note that in Equations 30, 34, and 35, the factors in parentheses which multiply i are real. Therefore, when the complex conjugate is taken of the right member of each equation, those factors drop out. It should also be noted that in a previous publication,[22] I erroneously placed "+" instead of "-" within the square brackets in equations 29, 32, and 33.

3. Architecture of the Program THREEPHASE

The FORTRAN program THREEPHASE calculated values of MSEF via Equations 29 through 37 on an IBM PC/AT microcomputer. A flow chart illustrating the logic of the program for calculating MSEF is shown in Figure 5. All of the parameters which define the optical properties of the stratified medium are input by the user. Although the first and third phases are theoretically semi-infinite, the user must, of course, provide limiting distance values in those phases to limit the calculation to the regions near phase 2. After obtaining the required parameters, THREEPHASE calculates values of the Fresnel coefficients and other intermediate variables. Then MSEF values are calculated as a function of the normalized-distance variable z, one phase at a time. The output consists of separate files for the x-, y-, and z-components of MSEF.

The source code for THREEPHASE appears in Appendix 1. The program is internally documented, so minute details of its architecture are not given here. Its operation was verified by calculating several two-phase cases (and combining two of these into a single, continuous phase during program execution) and comparing the results to calculations done by my research adviser using an older, two-phase program.

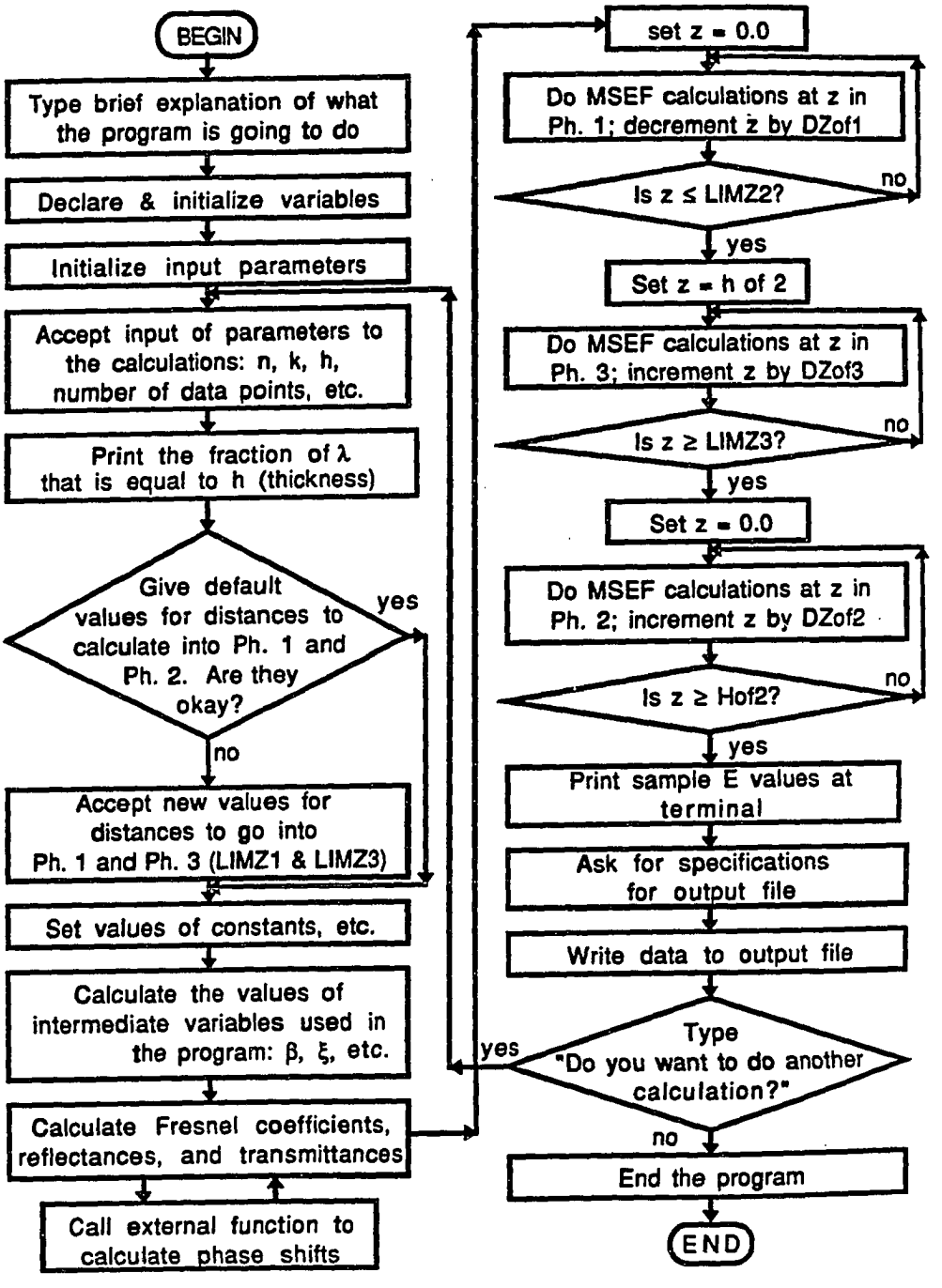

Figure 5. Flow chart of the operation of the THREEPHASE program for calculating MSEF values.

4. Input and Output Data

The values of n and k used for MSEF calculations are given in Table 2. Results are given with respect to the MSEF of the incident beam, $\langle E_1^{0t2} \rangle$. In designating relative MSEF, the superscript *0* refers to wave amplitude and *t* refers to transmission away from the incident phase and toward the final phase.[20]

Table 2. Values of optical functions n and k at 2920 cm^{-1}

Material	n	k	Reference
Si	3.42	0.0	23
CaF_2	1.40	0.0	23
D_2O	1.243	7.7×10^{-4}	this work
H_2O	1.415	0.016	24
Au	1.510	19.881	23

C. RESULTS AND DISCUSSION

1. Choices of Experimental Parameters for In Situ IRRAS

The design and construction of in situ IRRAS cells requires several choices about component materials and cell dimensions. As elucidated in many earlier studies,[7,25,26,27,28,29,30,31,32] however, the flexibility in selecting component materials is limited to the composition of the IR-transparent window and the thickness, d, of the contacting solution. Selection of solvent, supporting electrolyte, and electrode material is usually dictated by the chemical system being studied. Here, H_2O and D_2O are used as solvents and Au as a substrate because of my research group's interests in thiolate monolayers as models for probing aqueous-phase interfacial processes; testing with both H_2O and D_2O provides a means to assess the role of the $\hat{n}$ of the solvent (see Figure 3) as well as the utility of D_2O as an alternative to H_2O. Though many metals are well suited as substrate materials for the measurement, Au is used because of its ability to spontaneously adsorb a monolayer from dilute solutions of alkanethiols.[33,34,35,36,37,38,39,40,6,41,42,43] Nonetheless, the results for Au are readily translated to all other highly reflective metal surfaces (e.g. Pt, Ag, Al).

The choice of the window material represents a compromise based on insolubility, refractive index, and transmissivity of visible (for alignment purposes) and IR light—as is usual for in situ IRRAS experiments.[7,25,26,27,28,29,30,31,32] Two common window materials are CaF_2 and Si; these materials are insoluble in aqueous solutions, available in disc, hemispherical, and prismatic forms, and have quite different refractive indices (see Table 2). Use of hemispherical and prismatic window shapes minimizes reflection losses and facilitates the optimization of the measurement by attaining a high angle of incidence at the

solution/metal interface.[19] Only results from calculations and experiments with hemispherical or prismatic windows, both of which are treated identically by the physical optical model used, are presented in this dissertation. Much of the discussion will focus on measurements using CaF_2 windows, as they have proven easiest to use experimentally; however, results from a few interesting MSEF calculations using Si are presented for comparison.

2. Effect of Solution-Layer Thickness on Surface MSEF

To gain insights into the influence of the solution-layer thickness (*d*) and angle of incidence on in situ IRRAS measurements in the C–H stretching region, the standing wave patterns of the z-component of the MSEF for a three-phase isotropic system were calculated for a variety of conditions. The results are presented as the ratio of the MSEF in phase *i*, $\langle E_{i,z}^2 \rangle$, to the MSEF of the incident phase, $\langle E_1^{0/2} \rangle$. Examples of the standing wave patterns for a three-phase system composed of an IR transparent cell window, a thin liquid layer, and a gold electrode are given for D_2O in Figure 6 and for H_2O in Figure 7. In each figure, liquid-layer thicknesses (1.0 μm and 2.5 μm) and the cell window material (CaF_2 and Si) were varied. The angles of incidence at the cell-window/liquid interface (θ) are 60° at CaF_2/D_2O, 70° at CaF_2/H_2O, and 20° at both Si/H_2O and Si/D_2O; the differences in the incident angles with CaF_2 reflect the differences in the refractive indices of H_2O and D_2O (see below).

This set of results reveals several interesting features pertaining to light propagation in an in situ IRRAS measurement. For example, the four permutations of the two window materials and the two liquids reveal a seemingly unpredictable dependence of MSEF on *d*. At the metal surface, the MSEF decreases with *d* for CaF_2/H_2O but increases for CaF_2/D_2O, albeit for different incident angles between the two cases. On the other hand, for an Si window using 20° incidence, the MSEF at the metal surface increases

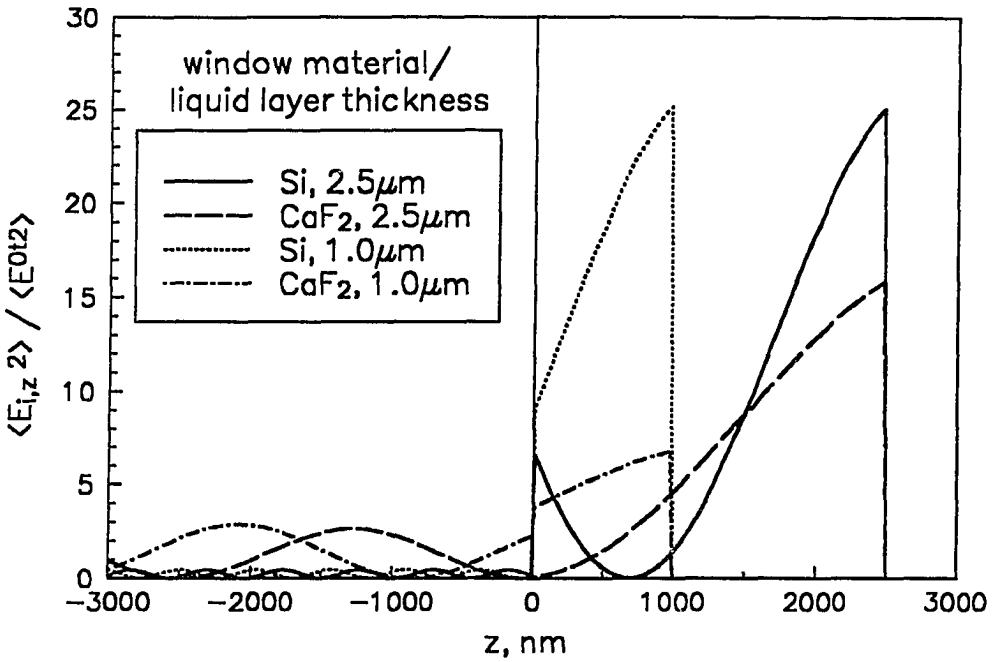

Figure 6. z-Component of MSEF at 2920 cm^{-1} in the in situ cell with different D_2O layer thicknesses using a Si window at 20° incidence or a CaF_2 window at 60°.

H_2O but remains constant for D_2O. Other differences between the four stratified media appear in the period of the standing wave within the window material, as well as in the discontinuity between the MSEF values at the phase 1/phase 2 interface.

These differences may be accounted for with classical electromagnetic theory. Let us begin with the disparity in the period of the standing waves in the two window materials. The period of a standing wave in a nonabsorbing phase is given by $z_p = (2\nu n_i \cos\phi)^{-1}$, where z_p represents the distance between adjacent nodes, ϕ is the angle of propagation measured from the z-axis, and the other terms have their usual meaning. Thus, z_p is inversely proportional to both $\cos\phi$ and n, which accounts for the differences in Si and CaF_2. The discontinuity of the z-component of MSEF across the window/liquid

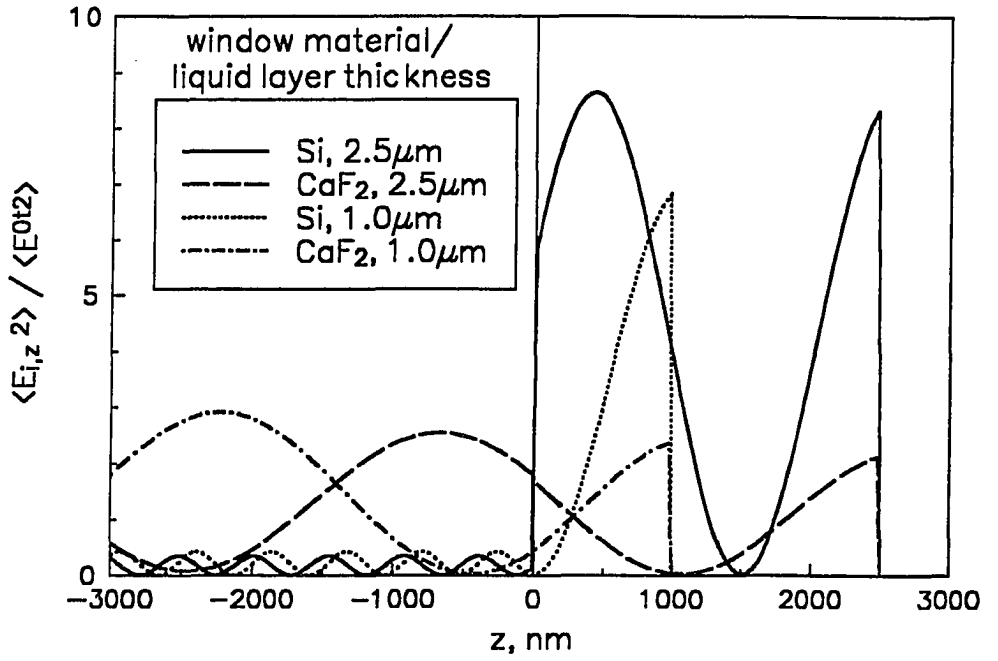

Figure 7. *z*-Component of MSEF at 2920 cm^{-1} in the in situ cell with different H_2O layer thicknesses using a Si window at 20° incidence or a CaF_2 window at 70°.

interface arises from the requirement that the normal component of the *magnetic* field vector be continuous across a phase boundary. From the relationships between the electric and magnetic vectors given by Maxwell's equations—together with the material equations—the ratio of the MSEF in the liquid phase to the MSEF in the window at the interface is given by n_1^4/n_2^4, where n_1 is the refractive index of the window and n_2 is the refractive index of the liquid.

The noted variations in Figures 6 and 7 of MSEF at the metal surface with *d*, however, turn out to be a complicated quasi-periodic function. The nature of this function, which is governed by the angle of propagation through the liquid phase and effects of multiple reflection at the window and metal surfaces, resembles that of the

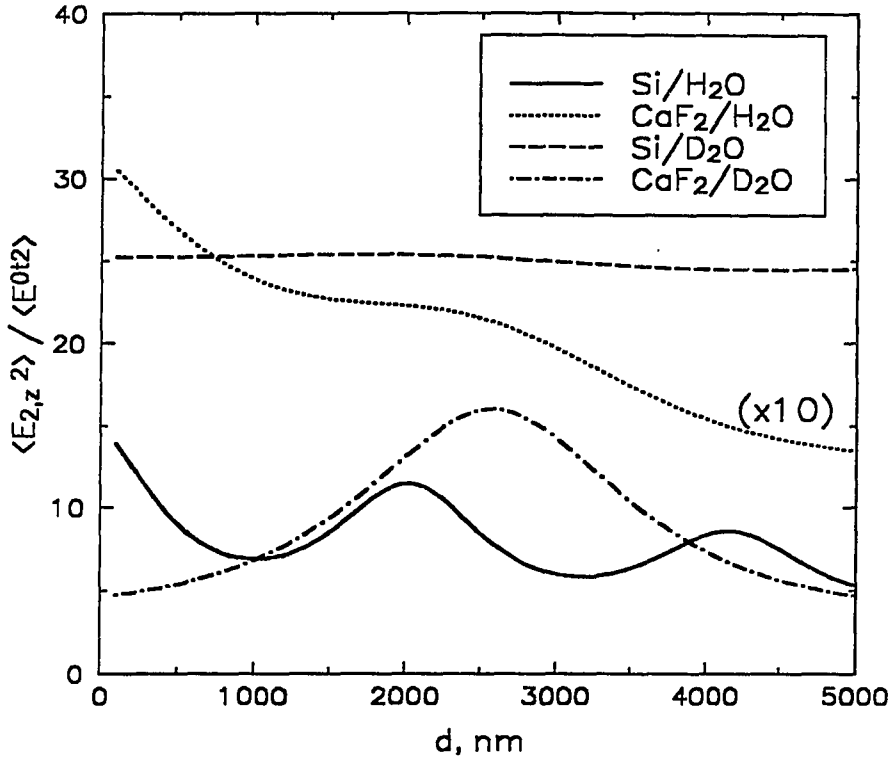

Figure 8. z-Component of MSEF at the Au surface in the in situ cell at 2920 cm^{-1} as a function of liquid-layer thickness. Angles of incidence correspond to Figures 6 and 7. The angles of propagation in the liquid layer corresponding to the respective window/liquid combinations are: Si/H_2O, 55.7°; CaF_2/H_2O, 68.4°; Si/D_2O, 70.2°; and CaF_2/D_2O, 77.3°. N.B.: In a previous publication,[44] the multiplier "(x5)" was incorrectly placed near the curve for Si/D_2O, when it should have designated the curve for CaF_2/H_2O, as the "(x10)" does here.

interference in a Fabry-Perot etalon.[17,18] Figure 8 shows the MSEF at the metal surface plotted as a function of d for the four different stratified media used in Figures 6 and 7. The local maxima in Figure 8 for Si/H_2O and CaF_2/D_2O correspond to thicknesses at which cavity resonance in the liquid lamina is maximized. The curves for Si/H_2O and CaF_2/H_2O are initially concave-downward while that for CaF_2/D_2O is concave-upward. This variation results not from the different materials used; rather it reflects the increase in

propagation angle (the refracted angle in the liquid) from ~56° for Si/H_2O to ~77° for CaF_2/D_2O. In this angular range the phase shift of p-polarized light reflected on a metal surface varies dramatically.[1] Coupled with multiple-reflection and superposition effects, this change in phase shift gives rise to the observed dependence. A similar situation has been found and described in more detail for in situ IRRAS measurements in the C–O stretching region (~2000 cm^{-1}).[17,18] This phase shift equals $\pi/2$ radians at ~70° incidence at the metal surface. This corresponds to the case for Si/D_2O in Figure 8 in which local resonant maxima and minima nearly disappear. Calculation of the variation of surface MSEF with thickness for the Si/D_2O system at different angles of incidence corresponding to propagation angles above and below 70° (not shown) verified the aforementioned dependence on propagation angle.

In spite of the dependence of surface MSEF on liquid-layer thickness, we have found practical difficulties in separating small adsorbate peaks from overwhelming and often broad liquid peaks whenever spectral bands overlap even slightly with solvent absorption. These difficulties are partly due to: (1) instrumental signal-to-noise limitations arising because solvent absorption reduces the total throughput of the FTIR while the detector-limited noise remains nearly constant; (2) fundamental physical optical effects caused by the dispersion of n; (3) difficulty in machining identical substrates; and (4) problems repositioning the plungers perfectly each time. Where the absorbance of the solvent is measurable, the thinnest liquid layer that is physically attainable is optimum, notwithstanding the results of MSEF calculations.

3. Effects of Angle of Incidence

To understand further the dependence of in situ IRRAS in the C–H stretching region on the experimental parameters, MSEFs at both 2920 cm^{-1} and 2850 cm^{-1} were calculated as a function of θ for several experimental conditions. Figure 9 shows results

of the calculations for the *z*-component of MSEF at the metal surface at 2920 cm^{-1} for cell configurations using Si and CaF_2 windows and H_2O and D_2O thicknesses of 1.0 μm. The plots at 2850 cm^{-1} (not shown) are comparable to those in Figure 9, although with slightly larger MSEFs using H_2O. This difference reflects the smaller value of k in D_2O compared to H_2O at 2850 cm^{-1}. Each of the plots shows that the MSEFs are zero at 0° incidence, increase with θ to a maximum value, and then return to zero, although the angles of the maxima differ. Maxima in the MSEF for Si occur for both liquids between 20° and 25°, and at ~60° for CaF_2/D_2O. In these three cases, the maxima occur just below the critical angles at each of the window/solution interfaces; the subsequent decrease in MSEF results from a decrease in the coupling of the evanescent wave with the metal surface.[45] The MSEF with CaF_2/H_2O reaches a maximum at ~67°; internal reflection does not occur, however, because at 2920 cm^{-1} the n of CaF_2 is less than that of H_2O.

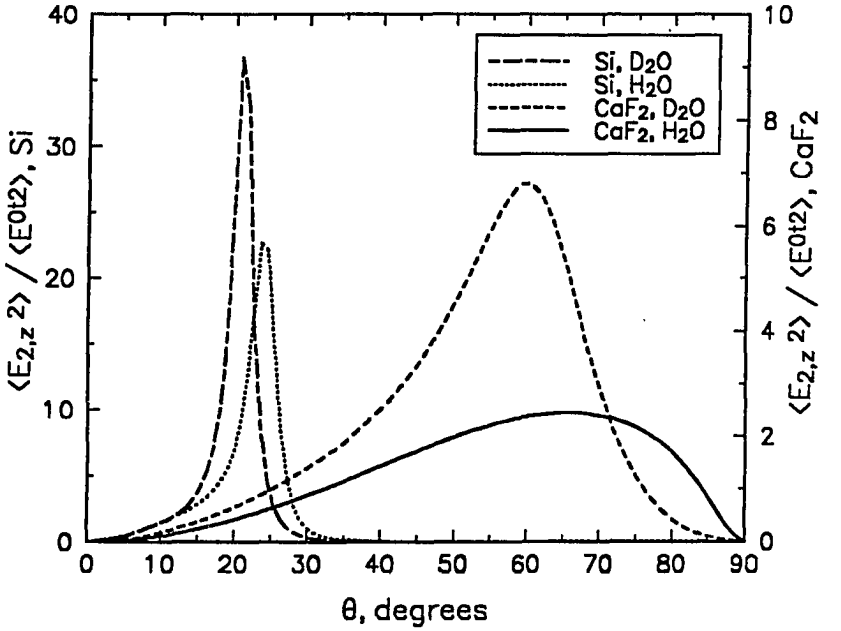

Figure 9. *z*-Component of MSEF at Au surface in in situ cell at 2920 cm^{-1} as a function of incident angle using an Si or CaF_2 window and a liquid layer of H_2O or D_2O with a thickness of 1.0 μm.

The plots in Figure 9 further show that the angular dependence of the MSEF is governed by the optical constants of the IR window. Specifically, the greater the difference between n of the window and n of the liquid, the narrower the angular range over which the MSEF exhibits a nonzero value. From an experimental standpoint, if windows of high n (e.g., Si, Ge) are used, θ must be more tightly controlled to yield a measurement with high surface detectability. As has recently been discussed,[19] it is also preferable to employ an incident beam with a small angular divergence. This insures that the rays of the incident beam strike the surface at the appropriate θ. Taken together, these plots indicate that a suitable θ for in situ IRRAS measurements in H_2O is ~20° for Si and ~70° for CaF_2.

The dependence of the MSEF on θ, however, is only one of many factors to consider in determining conditions for in situ IRRAS measurements with high surface detectability. In making such predictions, one must also examine the concomitant change in irradiated surface area of the sample. For a given incident beam size, the irradiated surface area increases as $1/\cos\theta$. Thus, the absorbance of a surface species increases as the product of the MSEF and $\sec\theta$. For ex situ measurements, the effect of irradiated surface area leads to an improvement in detection of slightly more than a factor of two, which occurs at a θ approximately 10° greater than that for the maximum MSEF.[46] The $\sec\theta$ advantage necessitates the use of an electrode with an extended surface area, however, which places a practical limitation upon the experimental measurement. The next section discusses the consequences of this $\sec\theta$ dependence—as well as other factors influencing the measurement which arise from the multilayer construction of the in situ cell.

D. CONCLUSIONS

This section has illustrated the usefulness of calculating mean square electric field values as a function of normalized distance to reveal some of the optical phenomena within our in situ cell. Values of MSEF in the liquid phase at the liquid/metal interface are a qualitative indicator of the effects of experimental parameters upon spectral sensitivity to an adsorbed monolayer film. For the angle of incidence—the parameter which is easiest to adjust experimentally—the calculations show that optimum sensitivity would be obtained at an incident angle of ~70° at the CaF_2/H_2O interface and ~20° at the Si/H_2O interface, based on consideration of MSEF alone. These results will be compared in the next section with calculated and experimental in situ IRRA spectra of a monolayer film.

REFERENCES

1. Greenler, R.G. *J. Chem. Phys.* **1966**, *44*, 310.
2. Greenler, R.G.; Rahn, R.R.; Schwartz, J.P. *J. Catal.* **1971**, *23*, 42.
3. Greenler, R.G. *J. Vac. Sci. Technol.* **1975**, *12*, 1410.
4. Golden, W.G. In *Fourier Transform Infrared Spectroscopy*; Ferraro, J.R.; Basile, L.J., Eds.; Academic Press: New York, 1985; Vol. 4., pp. 315-344.
5. Pritchard, J. In *Chemical Physics of Solids and their Surfaces*; London: The Chemical Society, 1978; Vol. 7; pp. 158-160.
6. Porter, M.D.; Bright, T.B.; Allara, D.L.; Chidsey, C.E.D. *J. Am. Chem. Soc.* **1987**, *109*, 3559.
7. Porter, M.D. *Anal. Chem.* **1988**, *60*, 1143A.
8. Allara, D.L.; Nuzzo, R. *Langmuir* **1985**, *1*, 52.
9. Allara, D.L.; Baca, A.; Pryde, C.A. *Macromolecules* **1978**, *11*, 1215.
10. Porter, M.D.; Karweik, D.; Kuwana, T.; Theis, W.; Norris, G.B.; Tiernan, T.O. *Appl. Spectrosc.* **1984**, *38*, 11.
11. Dluhy, R.A. *J. Phys. Chem.* **1986**, *90*, 1373.
12. Porter, M.D.; Bright, T.B.; Allara, D.L.; Kuwana, T. *Anal. Chem.* **1986**, *58*, 2461.
13. Mielczarski, J.A.; Yoon, R.H. *J. Phys. Chem.* **1989**, *93*, 2034.
14. Mielczarski, J.A.; Yoon, R.H. *Langmuir* **1991**, *7*, 101.
15. Yen, Y.-S.; Wong, J.S. *J. Phys. Chem.* **1989**, *93*, 7208.
16. Seki, H.; Kunimatsu, K.; Golden, W.G. *Appl. Spectrosc.* **1985**, *39*, 437.
17. Roe, D.K.; Sass, J.K.; Bethune, D.S.; Luntz, A.C. *J. Electroanal. Chem.* **1987**, *216*, 293.

18. Bethune, D.S.; Luntz, A.C.; Sass, J.K.; Roe, D.K. *Surface Science* **1988**, *197*, 44.

19. Faguy, P.W.; Fawcett, W.R. *Appl. Spectrosc.* **1990**, *44*, 1309.

20. Hansen, W.N. *J. Opt. Soc. Am.* **1968**, *58*, 380.

21. Hansen, W.N. In *Advances in Electrochemistry and Electrochemical Engineering*; Delahay, P.; Tobias, C.W., Eds.; Wiley: New York, 1973.

22. Stole, S.M.; Popenoe, D.D.; Porter, M.D. In *Electrochemical Interfaces: Modern Techniques for In-Situ Interface Characterization;* Abruña, H.D., Ed.; VCH: New York, 1991; pp 339-410.

23. *API Handbook*, 3rd ed.; Gray, D.E. Ed.; McGraw Hill: New York, 1972.

24. Downing, H.D.; Williams, D.J. *J. Geophys. Res.* **1975**, *80*, 1656.

25. Bewick, A.; Kunimatsu, K.; Pons, B.S. *Electrochim. Acta* **1980**, *25*, 465.

26. Russell, J.W.; Overend, J.; Scanlon, K.; Severson, M.; Bewick, A. *J. Phys. Chem.* **1982**, *86*, 3066.

27. Bewick, A.; Pons, B.S. In *Advances In Infrared and Raman Spectroscopy*; Clark, R.J.H.; Hester, R.E., Eds.; Wiley Heyden: London, 1985; Vol. 12, pp 1-63.

28. Foley, J.K.; Pons, B.S. *Anal. Chem.* **1985**, *57*, 945A.

29. Pons, B.S.; Foley, J.K.; Russell, J.; Severson, M. In *Modern Aspects of Electrochemistry*; No. 17; Bochris, J. O'M.; Conway, B.E. Eds.; Plenum: New York, 1986; p 223.

30. Ashley, K.; Pons, B.S. *Chem. Rev.* **1988,** *88*, 673.

31. C. Korzeniewski, and S. Pons, *Prog. Analyt. Spectrosc.* **1987,** *10*, 1.

32. Beden, B.; Lamy, C. In *Spectroelectrochemistry: Theory and Practice*; Gale, R.J., Ed.; Plenum Press: New York, 1988; 189.

33. Nuzzo, R.G.; Allara, D.L. *J. Am. Chem. Soc.* **1983,** *105*, 4481.

34. Troughton, E.B.; Bain, C.D.; Whitesides, G.M.; Nuzzo, R.G.; Allara, D.L.; Porter, M.D. *Langmuir* **1988**, *4*, 365.

35. Chidsey, C.E.D.; Loiacono, D.N. *Langmuir* **1990**, *6*, 682.

36. Thomas, R.C.; Sun, L.; Crooks, R.M.; Ricco, A.J. *Langmuir* **1991**, *7*, 620.

37. Bain, C.D.; Troughton, E.B.; Tao, Y.-T.; Evall, J.; Whitesides, G. M.; Nuzzo, R. *J. Am. Chem. Soc.* **1989**, *111*, 321-335.

38. Nuzzo, R.G ; Dubois, L.H.; Allara, D.L. *J. Am. Chem. Soc.* **1990**, *112*, 558.

39. Whitesides, G.M.; Laibinis, P.E. *Langmuir* **1990**, *6*, 87, and references therein.

40. Li, T.T.T.; Weaver, M.J. *J. Am. Chem. Soc.* **1984**, *106*, 6107.

41. Sabatani, E.; Rubenstein, I. *J. Phys. Chem.* **1987**, *91*, 6663.

42. Finklea, H.O.; Avery, S.; Lynch, M.; Furtsch, T. *Langmuir* **1987**, *3*, 409.

43. Widrig, C.A.; Chung, C.; Porter, M.D. *J. Electroanal. Chem.* **1991**, *310*, 335-59.

44. Popenoe, D.D.; Stole, S.M.; Porter, M.D. *Appl. Spectrosc.* **1992**, *46*, 79-87.

45. Harrick, N.J. *Internal Reflection Spectroscopy;* Wiley: New York, 1973.

46. Pritchard, J. In *Chemical Physics of Solids and their Surfaces*; London: The Chemical Society, 1978; Vol. 7; pp. 158-160.

SECTION III. IN SITU IRRAS OF AN OCTADECANETHIOLATE FILM AT GOLD

A. INTRODUCTION

The previous sections noted the difficulty of obtaining IRRA spectra of an alkanethiolate film in contact with a thin aqueous phase. One approach to alleviating that difficulty is to examine the physical optics of the measurement by modeling the cell as a stratified medium and calculating values of the mean square electric field (MSEF) arising in the cell under various experimental conditions. The preceding section used such calculations to predict conditions for obtaining high surface sensitivity to a monolayer film at an aqueous/metal interface.

Deductions from the modeling of the in situ IRRAS experiment led to the construction of an in situ IR cell that facilitates the interchange of sample and reference substrates. The mode of obtaining reflectance-absorbance spectra then reduces to that used during ex situ (film exposed to dry N_2) IRRAS which measures a spectrum for a monolayer with respect to that of a reference substrate. A preliminary interpretation of spectra obtained with an earlier version of the cell was published by Stole and Porter.[1]

This section extends the theoretical study of MSEF and addresses the development of the experimental technique of in situ IRRAS of such a system. It presents the details of the experimental method and an improved cell design, and will serve as a basis for the in situ studies of the structure and reactivity of organosulfur and related organic monolayers in Section IV and in the future. In order to account for the sec θ dependence of reflectance-absorbance and frequency-dependent effects that occur during in situ IRRAS, results of reflectivity calculations are described that are compared and contrasted with the MSEF calculations in the previous section. These calculations elucidate the effects of angle of incidence and solution composition (H_2O or D_2O) upon the observed spectrum. A monolayer of octadecanethiolate at gold is used as the test

interfacial structure. In several cases, the trends of the calculated results are confirmed by comparisons with experimentally measured spectra.

B. EXPERIMENTAL SECTION

1. Cell Design

A diagram of the in situ cell is shown in Figure 1. This cell allows the use of variable angles of incidence and an extremely thin ($\leq$ 1 μm) solution layer. The solution layer is sandwiched between an IR-transmitting window and a metal film that is deposited on a glass cylinder. The details of the front part of the cell were shown in Figure 3 of the General Introduction. The cell was machined from a 1.5-in.-d. (38.1-mm-d.) rod of Kel-F (3M Corp.) fluoropolymer resin with a length of 3.0 in. (76.2 mm). A 0.590-in. (15.0-mm) hole was drilled through the length of the cell to accept the plunger. The front region of the cell was hollowed out to a diameter of 1.0 in (25.4 mm) to function as a solution reservoir. Several nominally identical substrates were produced in the form of plungers by placing end-to-end cylindrical sections of brass and borosilicate glass. These core rods were 12 mm d. by ~2 in. (~50 mm) long. A jacket of Kel-F (12 mm i.d. by 16 mm o.d.) was fit over the composite cylinder by forcing it over the rods after heat expansion. The resulting plunger was turned down to a diameter that produced a snug fit in the cell and was then cut to a length of 3.625 in. (92.1 mm). In the back face of each brass end section, an indentation was drilled to mate with the screw on the rear retaining bracket. The glass rod protruded ~2 mm beyond the edge of the Kel-F to facilitate polishing.

A 25-mm-d. hemispherical window is held tightly against the front of the cell by a retaining bracket (not shown) and is sealed by an O-ring of Kalrez elastomer. The plunger is pushed forward and held against the front window via the rear retaining bracket . Two ports in the top of the cell allow filling and removing of solution. In this configuration, the thin solution overlayer is in contact only with inert Kel-F resin, Kalrez elastomer, the transmitting window, and the reflecting substrate surface.

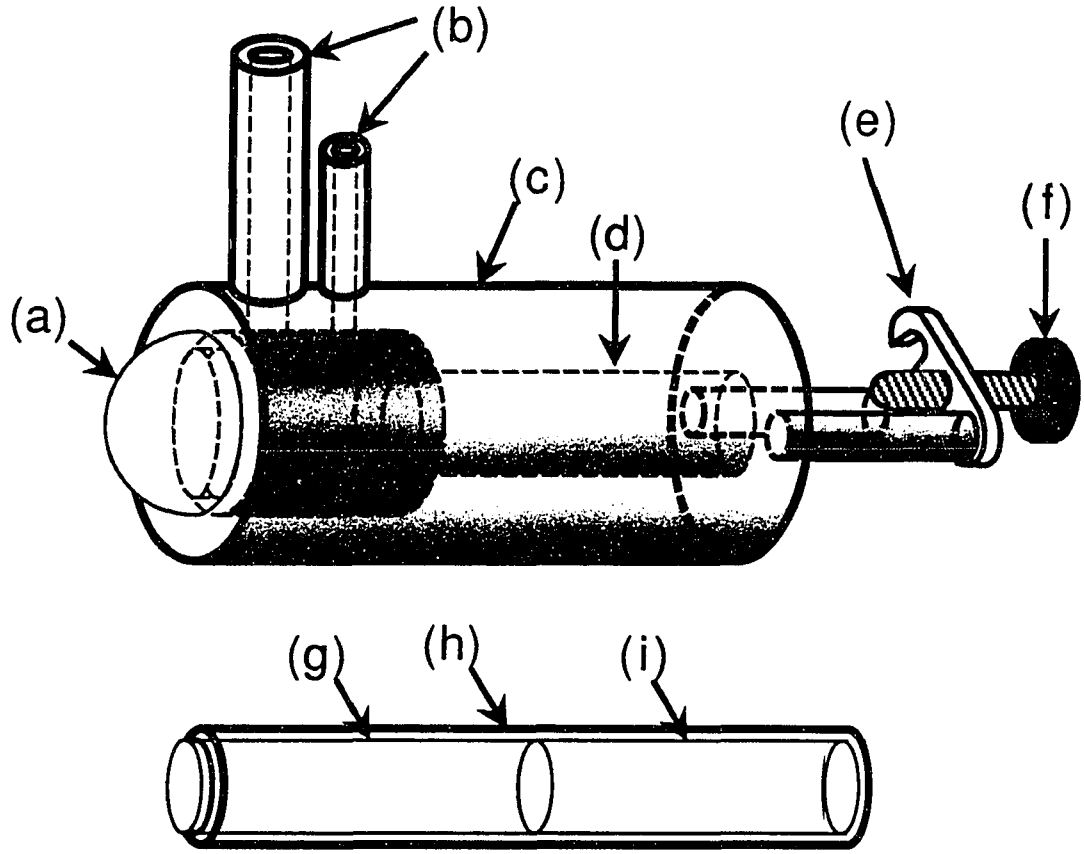

Figure 1. Schematic diagram of thin-layer in situ spectroelectrochemical cell for IRS: (a) hemispherical window (retaining bracket not shown), (b) ports for adding and removing solution, (c) Kel-F cell body, (d) barrel, (e) plunger retaining bracket, (f) retaining screw; and plunger consisting of (g) borosilicate glass core, (h) Kel-F jacket, and (i) brass core.

Metal films were evaporated onto the glass end of the plunger, which had been polished to a mirror-like finish, using a resistive vacuum deposition system (Edwards Temescal). These films consisted of ~10 nm adhesive layer of Cr and ~300 nm of Au. Deposition rates were between 1 nm/s and 5 nm/s. Another version of this cell has been constructed which can be used in electrochemical experiments, as shown in Figure 4 of the General Introduction.

2. Monolayer Film Preparation

Octadecanethiolate monolayer films were produced by immersing plungers coated with freshly evaporated Au films into ~ 1 mM ethanolic solutions of octadecanethiol for ~18 h. Upon removal from solution, the samples were rinsed with neat ethanol to remove residual material. Analysis of the monolayer films by external reflection IR spectroscopy at grazing incident angle indicated the films formed on the glass-supported Au are compositionally and structurally equivalent to those formed on Au on the more extensively studied polished silicon substrates.[2]

3. Instrumentation

Infrared spectroscopic measurements utilized an auxiliary bench of a Nicolet 740 FTIR spectrometer (Nicolet, Madison, WI) equipped with a narrow-band HgCdTe detector. The cell was mounted on an optical rail to facilitate alignment. A Focus Projection Accessory (Harrick Scientific, Ossining, NY) directed the radiation to and from the cell, as illustrated in Figure 2. Two peripheral plane mirrors, located on the cell mount, permitted alterations in the angle of incidence. A KRS-5 wire-grid polarizer (Cambridge Physical Sciences) selectively passed p-polarized light. Each in situ spectrum is the ratio of 2048 co-added scans of the sample and reference substrates collected at 4-cm^{-1} resolution and zero-filled once to yield 2-cm^{-1} resolution. For the ex situ spectra, 1024 scans were co-added, and the angle of incidence was 82°. A Happ-Genzel apodization function was applied during the Fourier transform process. Two nominally identical substrates were used for all spectra; one of the substrates was coated with a spontaneously assembled film formed from $CD_3(CD_2)_{17}SH$ and was used as the reference phase. The mean liquid-phase thickness was ~1000 nm, as estimated by observing Newton's rings under white light; however, the exact distribution of solution-layer

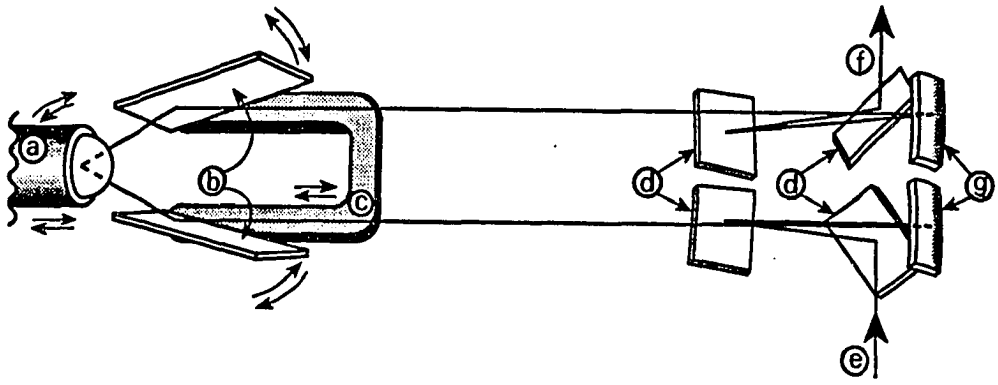

Figure 2. Illustration of optical beam path through cell assembly (a–c) and Focus Projection Accessory (d and g): (a) front of cell (which rotates and translates in the plane of propagation), (b) peripheral mirrors, (c) arm for peripheral mirrors (which translates parallel to optical axes), (d) plane mirrors, (e) incoming beam from interferometer, (f) outgoing beam to detector, and (g) concave mirrors to project focus.

thicknesses traversed by the IR beam is unknown. The uncertainty in the mean angle of incidence was ± 1°.

4. Reagents

D_2O (99.9 atom % D) was used as obtained from Aldrich. Octadecanethiol (Aldrich) was purified twice by recrystallization from ethanol. The analog of octadecanethiol having a fully deuterated alkyl chain, $CD_3(CD_2)_{17}SH$, was prepared following a previously described synthetic route[3] with $CD_3(CD_2)_{17}Br$ (99% D, Cambridge Isotopes) as the starting material. Briefly, $CD_3(CD_2)_{17}Br$ was treated with thiolacetic acid and sodium metal and refluxed in ethanol for 3 h. After cooling, conc. HCl was added to produce the thiol, which was recrystallized from ethanol. The purity of the product was confirmed by thin layer chromatography and transmission IR spectroscopy.

C. CALCULATIONS OF EXPECTED SPECTRA AT VARYING ANGLES OF INCIDENCE WITH D_2O AND H_2O

1. The Justification for Comparing Calculated Spectra with MSEF Calculations

To confirm the deductions made from the MSEF calculations performed in the previous section, reflection spectra were calculated using algorithms based on the Fresnel equations, as discussed in the theory section. These calculations, which include an organic monolayer film, use a four-phase model, as shown in Figure 4 of Section II. Similar approaches have been used to gain insights into in situ IRS measurements in the stretching region for adsorbed C–O.[4,5,6] The quantity which is both calculated and experimentally measured is the reflectance-absorbance for p-polarized light. It is given by $-\log R/R_0$, where R is the reflectance for the cell with an octadecanethiolate-coated substrate, and R_0 is that for either an uncoated substrate or one coated with octadecanethiolate-d_{37}. Details on the preparation and testing of the reference substrates have appeared elsewhere.[7] Literature values of n and k as a function of frequency were used for H_2O[8] and Au.[9]

2. Results of Calculated Spectra

This section presents the spectra calculated as a function of θ for a monolayer of octadecanethiolate at Au, compares their intensities and shapes with transmission and ex situ reflection spectra, and examines details of the beam propagation through the stratified medium of the cell. A spectrum of a monolayer film of octadecanethiolate at gold exposed to a nitrogen atmosphere (ex situ) is shown in Figure 3 for comparison with the in situ spectra presented below. Previous papers have discussed the features of this spectrum in detail.[10] Representative spectra from the calculations are shown in Figure 4 using a CaF_2 window and 1.0-μm thicknesses of D_2O (spectra a-d) and H_2O (spectra e-h); the angular dependences of $\nu_a(CH_2)$ and $\nu_s(CH_2)$, the two predominant bands in this spectral region,

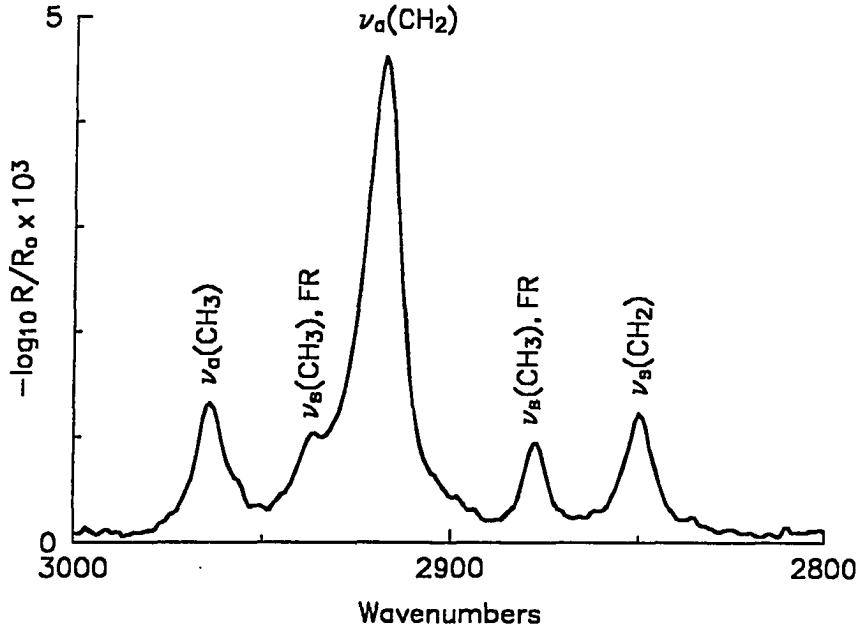

Figure 3. An ex situ IRRA spectrum of octadecanethiolate at gold in the C–H stretching region.

are summarized in Figure 5. The parameters for the calculations mimic the experimental conditions readily attainable with our in situ cell.

As shown collectively by Figures 4 and 5, the absorbances of $\nu_a(CH_2)$ and $\nu_s(CH_2)$ are negligibly small at normal incidence, reach maxima between 60° and 65° with D_2O and 80° and 85° with H_2O, and return to near-zero values as θ approaches 90°. In comparison with Figure 9 in Section II, the maxima with H_2O occur at θ's ~10° higher than the maxima of the corresponding MSEF plots; the maxima with D_2O, however, coincide with the maxima of the MSEF plots. The trends observed with H_2O are comparable with the detectability predictions which consider the coupling MSEF and irradiated surface area of the ex situ measurements. Such trends are also found with D_2O after considering the differences in the *n* of the two liquids. In the case of CaF_2/H_2O, the

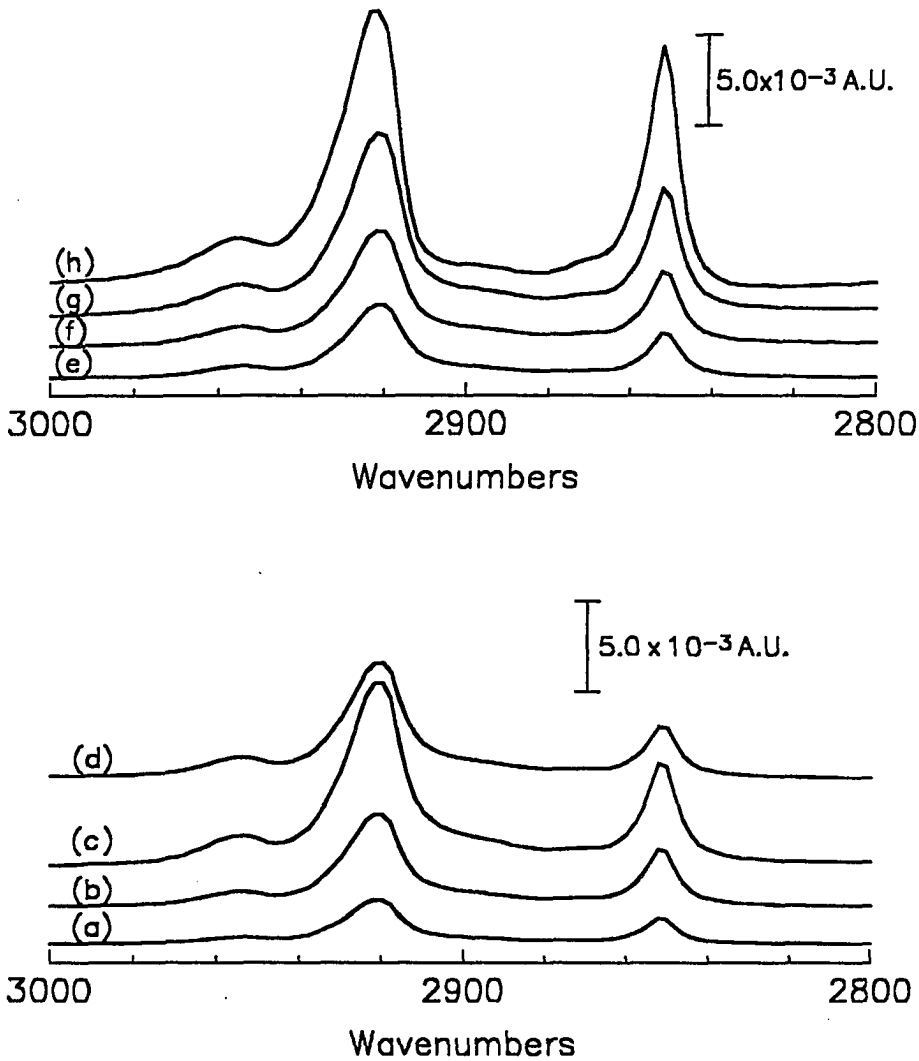

Figure 4. Calculated in situ spectra of $CH_3(CH_2)_{17}S/Au$ using a CaF_2 hemispherical window and D_2O and H_2O liquid layers. For D_2O, the angles of incidence are: (a) 40°, (b) 50°, (c) 60°, and (d) 70°. For H_2O the angles of incidence are: (e) 50°, (f) 60°, (g) 70°, and (h) 80°. Thicknesses used were 1.0 μm for D_2O and H_2O, and 2.8 nm for the thiolate film.

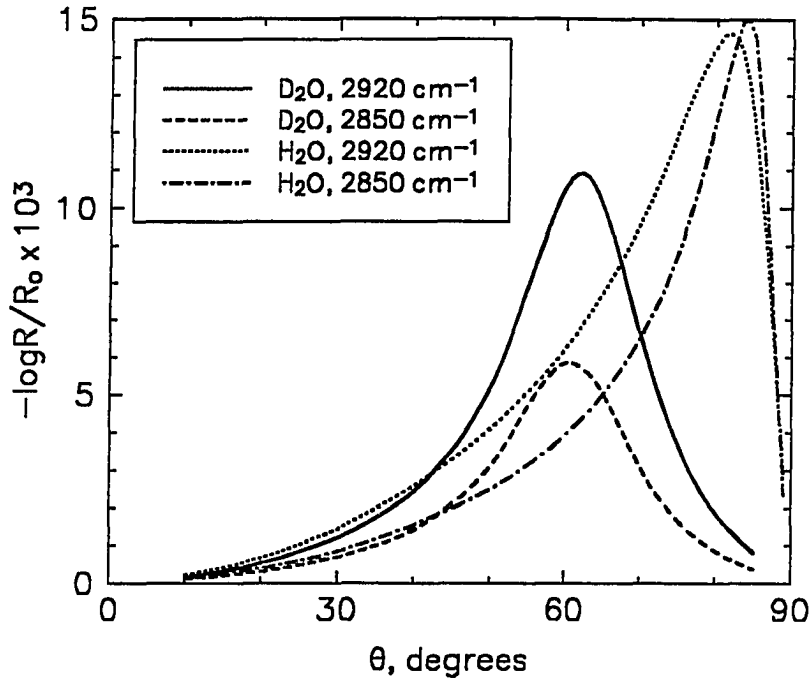

Figure 5. Reflectance-absorbance as a function of angle of incidence for the $\nu_a(CH_2)$ (2920 cm^{-1}) and $\nu_s(CH_2)$ (2850 cm^{-1}) peaks in the calculated in situ spectra in Figure 4: $\nu_a(CH_2)$ (—) and $\nu_s(CH_2)$ (- - -) using CaF_2 and D_2O; $\nu_a(CH_2)$ (· · ·) and $\nu_s(CH_2)$ (- · -) using CaF_2 and H_2O. The thickness of the liquid layer is 1.0 μm.

two media have comparable *n*'s, a case of index matching for which there is little difference between the incident and refracted angles at that interface. The two media that compose CaF_2/D_2O, however, have markedly different *n*'s, leading to larger refraction angles and, hence, large incident angles at D_2O/Au just below the CaF_2/D_2O critical angle.

There are additional effects of the propagation of the beam through the multilayer construction of the in situ cell that require examination. These include multiple-reflection and interference phenomena which, coupled with effects of the MSEF and irradiated

surface area, can lead to differences in band shapes and intensities relative to those obtained in both transmission and ex situ IRS measurements. Such differences become particularly apparent in a comparison of the data at the maxima of the angular dependence plot in Figure 5 with the ex situ spectrum in Figure 3. For example, at a θ of 60° at CaF_2/D_2O, the absorbance of $\nu_a(CH_2)$ is almost 1.9 times that of $\nu_s(CH_2)$, whereas the same comparison with the ex situ spectrum gives a value of ~1.5. Although it is difficult to identify and quantify the roles of all the possible contributors, as noted in the optical analysis of other IRS measurements,[11,12,13,14,15,16,17,18] the disparity at a θ of 60° results in part from the wavelength dependence of the reflectivity (R_{12}) of the incoming beam at CaF_2/D_2O, i.e., the phase 1/phase 2 interface. This component of the beam, in situations where k_2 is small or effectively constant, increases with the mismatch of the n's of phase 1/phase 2 (see Figure 3 in Section II). Thus, the relative contribution of R_{12} to the reflected intensity at 2850 cm^{-1} is greater than at 2920 cm^{-1}, resulting in an optically induced decrease in the relative absorbances of the two modes.

In contrast to CaF_2/D_2O, the effects of the multilayer cell construction at conditions of high detectability are reversed for measurements at CaF_2/H_2O. In this case, the relative absorbances of the two modes are comparable, which represents a diminution of the absorbance of $\nu_a(CH_2)$ relative to $\nu_s(CH_2)$. The diminution can also be understood through considerations of R_{12}. As is evident from the plot of the wavelength dependence of n of H_2O in Figure 5 in the General Introduction, R_{12} at 2920 cm^{-1} is greater than at 2850 cm^{-1}. This leads to a stronger contribution of R_{12} to the reflection spectrum at the higher energy mode, and a subsequent decrease in the absorbance of $\nu_a(CH_2)$ with respect to $\nu_s(CH_2)$.

In addition to R_{12}, the wavelength dependence of the reflectivity of the liquid/monolayer interface, the phase 2/phase 3 interface, can induce a distortion in the

monolayer spectrum. Such a distortion is observed in $\nu_a(CH_2)$ in Figure 4h, and leads to a shift in the absorbance maximum ~2 cm^{-1} higher in energy. This distortion results, in part, from the change in the mechanism for coupling light into the monolayer based on the *n*'s for both components. The lower *n* of D_2O in comparison to that of the monolayer precludes such a change.

Together, the above analyses point to the complexities of performing in situ IRS measurements in the C-H stretching region on monolayers under thin contacting layers of aqueous solutions. The next section presents the results of several experimental measurements, verifying the need for a detailed optical analysis of the measurement before developing structural descriptions from the in situ spectra relative to those from ex situ and transmission measurements.

D. EXPERIMENTAL RESULTS

Experimental spectra for an octadecanethiolate monolayer at Au were measured at several of the angles of incidence of the calculated spectra in Figure 5. The spectra are shown in Figures 6 and 7 with ~1-μm-thick layers of D_2O and H_2O, respectively; in both cases, a CaF_2 hemispherical window was used. It is important to note that the spectra were subjected to a fifth-order-polynomial baseline linearization (based on the selection of only five data points) to compensate for a broad residual solvent spectrum. Examples of uncorrected spectra and the corresponding polynomials are shown in Figures 6d and 7f. Their corresponding linearized spectra are shown in Figures 6b and 7c.

The residual solvent spectrum is attributed to difficulties in attaining an equivalent solution-layer thickness upon interchange of sample and reference substrates, although the imperfect surfaces of the substrates prevent a qualitative analysis. The positioning difficulties arise in part from the differences in the flatness of the two substrates, which lead to a non-uniform thickness of the contacting liquid. Also (not shown), both the magnitude and the distortion of the residual solvent spectrum increase with increasing θ. Such extensive distortion cannot be linearized with a fifth-order polynomial (see Figure 7e), which precludes measurements at large θ using the method of interchangeable sample and reference surfaces. This distortion will likely complicate polarization modulation measurements as well. The residual solvent spectrum observed using D_2O is usually smaller than that for H_2O (for θ values yielding equivalent surface sensitivity) because of the lower k values for D_2O in the C–H stretching region (see Figure 3 in Section II).

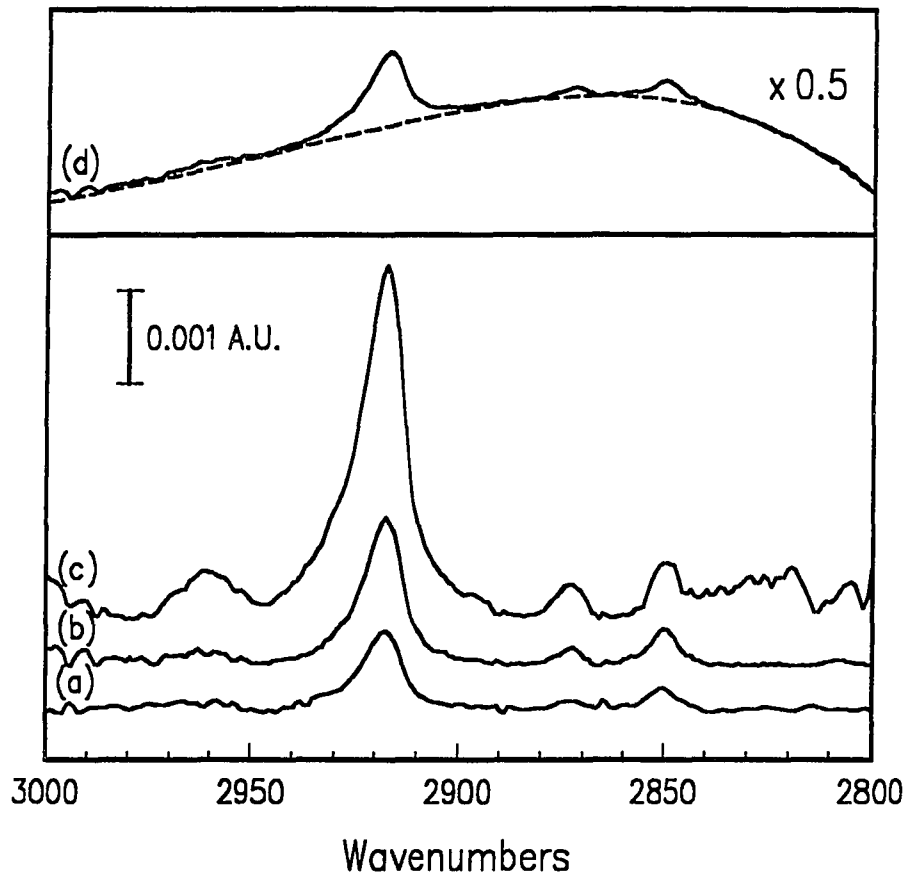

Figure 6. Experimental in situ spectra of $CH_3(CH_2)_{17}S/Au$, using a CaF_2 hemispherical window and ~1.0 μm thick layer of D_2O and angle of incidence at CaF_2/D_2O of (a) 40°, (b) 50°, (c) 60°. The spectrum at 50° without polynomial baseline correction (d) is shown for comparison. The dashed curve represents the fifth-order polynomial function that is subtracted from (d) to give (b).

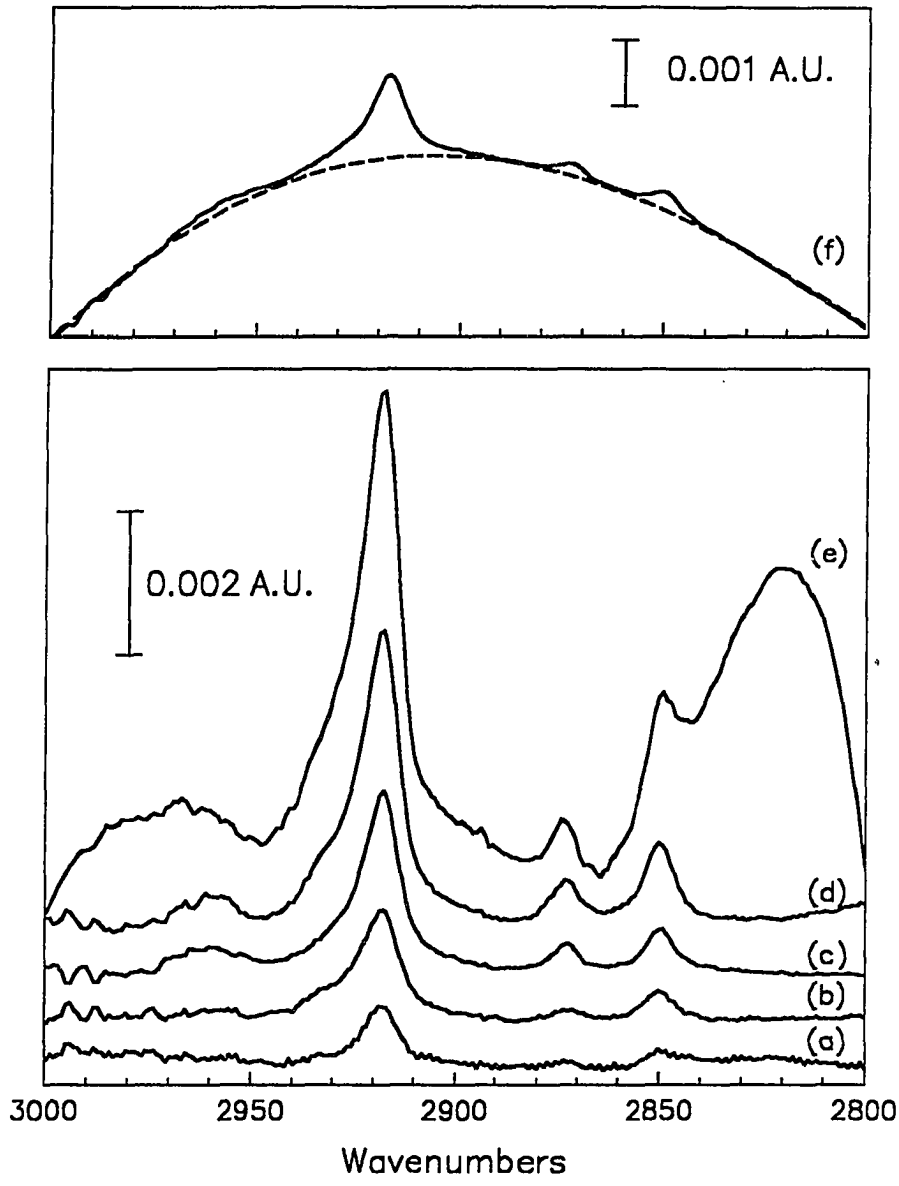

Figure 7. Experimental in situ spectra of $CH_3(CH_2)_{17}S/Au$, using a CaF_2 hemispherical window and ~1.0 μm thick layer of H_2O and angle of incidence at CaF_2/H_2O of (a) 40°, (b) 50°, (c) 60°, (d) 70°, (e) 80°. The spectrum at 60° without polynomial baseline correction (f) is shown for comparison. The dashed curve represents the fifth-order polynomial function that is subtracted from (f) to give (c).

The experimental spectra in Figures 6 and 7 confirm in general the trends found in the calculated spectra, though the absorbances differ because of chain orientation. With both contacting liquids, the absorbances of the observed modes increase over the θ's examined. The angular dependence of the disparity in the relative absorbances of the $\nu_a(CH_2)$ and $\nu_s(CH_2)$ modes is also observed. In addition, the shapes and peak positions of these modes in both sets of experimental spectra are comparable with those in the calculated spectra. The agreement qualitatively validates the use of the polynomial linearization. Such agreement also argues that any solvent-induced perturbation of the structure of the monolayer is confined to the chain terminus, an interpretation that is consistent with the crystalline-like packing of the alkyl chains[2,3,10,19,20,21,22,23,24,25,26,27] and an earlier discussion of the solvent-induced perturbation of methyl stretching modes.[1]

E. CONCLUSIONS

This section has demonstrated the possibility of obtaining in situ IRS spectra of organic monolayer films by the interchange of a coated and reference substrate. That approach, which represents an alternative to electrochemical and polarization techniques, was applied to the characterization of a spontaneously adsorbed monolayer of a long-chain thiolate at Au under H_2O and D_2O layers ~1μm in thickness. An optical analysis of the measurement revealed experimental conditions for high surface detectability as well as the presence of optical phenomena that give rise to alterations in band intensities and shapes. The experimentally measured spectra confirmed the predictions of the calculations. The next section presents an application of the in situ spectrochemical technique of my coworkers and mine to an alkanethiolate monolayer with an electrochemically reactive end group.

REFERENCES

1. Stole, S.M.; Porter, M.D. *Langmuir* **1990**, *6*, 1199.
2. Widrig, C.A.; Chung, C.; Porter, M.D. *J. Electroanal. Chem.* **1991**, *310*, 335-59.
3. Bain, C.D.; Troughton, E.B.; Tao, Y.-T.; Evall, J.; Whitesides, G. M.; Nuzzo, R. *J. Am. Chem. Soc.* **1989**, *111*, 321-335.
4. Roe, D.K.; Sass, J.K.; Bethune, D.S.; Luntz, A.C. *J. Electroanal. Chem.* **1987**, *216*, 293.
5. Bethune, D.S.; Luntz, A.C.; Sass, J.K.; Roe, D.K. *Surface Science* **1988**, *197*, 44.
6. Faguy, P.W.; Fawcett, W.R. *Appl. Spectrosc.* **1990**, *44*, 1309.
7. Walczak, M.M.; Chung, C.; Stole, S.M.; Widrig, C.A.; Porter, M.D. *J. Am. Chem. Soc.* **1991**, *113*, 2370.
8. Downing, H.D.; Williams, D.J. *J. Geophys. Res.* **1975**, *80*, 1656.
9. *API Handbook*, 3rd ed.; Gray, D.E. Ed.; McGraw Hill: New York, 1972.
10. Porter, M.D.; Bright, T.B.; Allara, D.L.; Chidsey, C.E.D. *J. Am. Chem. Soc.* **1987**, *109*, 3559.
11. Porter, M.D. *Anal. Chem.* **1988**, *60*, 1143A.
12. Allara, D.L.; Baca, A.; Pryde, C.A. *Macromolecules* **1978**, *11*, 1215.
13. Porter, M.D.; Karweik, D.; Kuwana, T.; Theis, W.; Norris, G.B.; Tiernan, T.O. *Appl. Spectrosc.* **1984**, *38*, 11.
14. Dluhy, R.A. *J. Phys. Chem.* **1986**, *90*, 1373
15. Porter, M.D.; Bright, T.B.; Allara, D.L.; Kuwana, T. *Anal. Chem.* **1986**, *58*, 2461.
16. Mielczarski, J.A.; Yoon, R.H. *J. Phys. Chem.* **1989**, *93*, 2034.
17. Mielczarski, J.A.; Yoon, R.H. *Langmuir* **1991**, *7*, 101.

18. Yen, Y.-S.; Wong, J.S. *J. Phys. Chem.* **1989**, *93*, 7208.

19. Nuzzo, R.G.; Allara, D.L. *J. Am. Chem. Soc.* **1983**, *105*, 4481.

20. Troughton, E.B.; Bain, C.D.; Whitesides, G.M.; Nuzzo, R.G.; Allara, D.L.; Porter, M.D. *Langmuir* **1988**, *4*, 365.

21. Chidsey, C.E.D.; Loiacono, D.N. *Langmuir* **1990**, *6*, 682.

22. Thomas, R.C.; Sun, L.; Crooks, R.M.; Ricco, A.J. *Langmuir* **1991**, *7*, 620.

23. Nuzzo, R.G ; Dubois, L.H.; Allara, D.L. *J. Am. Chem. Soc.* **1990**, *112*, 558.

24. Whitesides, G.M.; Laibinis, P.E. *Langmuir* **1990**, *6*, 87, and references therein.

25. Li, T.T.T.; Weaver, M.J. *J. Am. Chem. Soc.* **1984**, *106*, 6107.

26. Sabatani, E.; Rubenstein, I. *J. Phys. Chem.* **1987**, *91*, 6663.

27. Finklea, H.O.; Avery, S.; Lynch, M.; Furtsch, T. *Langmuir* **1987**, *3*, 409.

SECTION IV. PAPER: INFRARED SPECTROELECTROCHEMICAL CHARACTERIZATION OF FERROCENE-TERMINATED ALKANETHIOLATE MONOLAYERS AT GOLD

ABSTRACT

Cyclic voltammetry and in situ infrared reflection-absorption spectroscopy with electrochemical modulation were applied to the study of monolayers self-assembled from 11-mercaptoundecyl ferrocenecarboxylate ($FcCOOC_{11}SH$) at gold. Voltammetry was used to assess both the reactivity and stability of the surface film in various aqueous electrolytes. The results of these studies indicated that the ferrocenyl monolayers are relatively unstable at pH>2, except when perchlorate is the dominant anion present. A large change in double-layer capacitance observed upon oxidation of the ferrocenyl end group was attributed to the creation of cationic sites in the diffuse layer. Compositional and structural correlations between the monolayer and the redox chemistry of the ferrocenyl end group were probed using the in situ spectroscopic technique. The features observed in the differential spectra of the oxidized form of the film were ascribed to changes in the bond strengths of the adsorbate as a result of generation of a ferricinium ion. No detectable changes in orientation of the polymethylene chains as a function of applied voltage were observed. The spectral data also suggest that the redox chemistry leads to a reorientation of the water molecules in the region near the ferrocenyl end group. Vibrational mode assignments for $FcCOOC_{11}SH$, based on studies of several analogs with different alkoxy groups, are presented along with infrared spectra and band assignments for several isotopically labeled ferrocenyl esters (i.e., ethyl ferrocenecarboxylate, ethyl-d_5 ferrocenecarboxylate, and 2-(dimethylamino)-ethyl ferrocenecarboxylate).

A. INTRODUCTION

Monolayers of self-assembled organosulfur compounds at gold and other materials have become widely used as models of organic interfaces.[1,2] These monolayers have also opened new dimensions for studies of electron transfer at surfaces.[1,3,4,5] Insights into the distance dependence of electron transfer rates are emerging through the systematic variation of the chain length of the polymethylene spacer between the electrode surface and a redox couple (either in solution[3,6,7,8,9,10] or attached to the surface[4,11,12,13,14]). The effects of local environment on the thermodynamics of the redox reactions are being examined by "burying" the reactive moiety within the matrix of a longer chain monolayer.[15,16] End-group-derivatized monolayers have also proven useful in promoting redox processes that are slow at uncoated electrodes.[5,17]

In many of the above cases, it is vital to determine if a chemical transformation of a reactive moiety within the monolayer leads to a structural transformation of the monolayer. Dissociation reactions (e.g. ester hydrolysis) or redox chemistry may lead to a rearrangement of the polymethylene chain structure which may affect targeted performance. Chemical transformations may also lead to localized rearrangements of the double-layer structure at the interface. Surprisingly, few studies have appeared to date that have examined these issues.[11,15,18,19]

This paper presents and discusses the results of electrochemical and in situ infrared reflection-absorption spectroscopic (IRRAS) studies of a ferrocene-terminated monolayer formed by the chemisorption of 11-mercaptoundecyl ferrocenecarboxylate [$(\eta^5\text{-}C_5H_5)Fe(\eta^5\text{-}C_5H_4)COO(CH_2)_{11}SH$; abbreviated $FcCOOC_{11}SH$, where Fc denotes the ferrocenyl group] at gold. Previous studies showed that adsorption of alkanethiols at Au results in the loss of the mercapto hydrogen and formation of a gold

alkanethiolate.[20,21,22] Therefore, $FcCOOC_{11}SH$ is converted upon adsorption to the thiolate form, 11-sulfidoundecyl ferrocenecarboxylate (abbreviated $FcCOOC_{11}S$). The electrochemical studies assessed both the reactivity and stability of the surface film; the studies of stability helped identify suitable conditions for the IRRAS studies. The IRRAS studies, performed in an electrochemical modulation mode,[23,24,25,26,27] were conducted to probe for compositional and structural correlations of the monolayer with the redox chemistry of the ferrocenyl end group. Vibrational mode assignments, based on studies of a variety of isotopically labeled compounds, are also presented.

B. EXPERIMENTAL SECTION

1. Reagents

The synthesis of 2-(dimethylamino)-ethyl ferrocenecarboxylate (DEF) followed the procedure used for the preparation of ω-mercaptoalkyl ferrocenecarboxylates.[12] First, ferrocenecarboxylic acid (FcCOOH) was converted to its acyl chloride by reaction with oxalyl chloride. The resulting acyl chloride was dissolved in dichloromethane and reacted with a two-fold excess of 2-(dimethylamino)-ethanol. The solution was purged with nitrogen, sealed, and stirred for two days at 25°C. Unreacted starting materials were separated from the dichloromethane solution by three extractions into 0.1 M KOH. The orange organic layer was concentrated under reduced pressure to yield 1.62 g of purified DEF. The DEF gave the following physical data: ^{1}H NMR (300 MHz, $CDCl_3$): δ 2.45 (s, 6H, $N(CH_3)_2$); 2.66 (t, 2H, CH_2N); 4.20 (s, 5H, C_5H_5); 4.34 (t, 2H, CO_2CH_2); 4.38 (t, 2H, C_5H_4); 4.82 (t, 2H, C_5H_4). Melting range: 68° – 69°C. The synthesis of 11-sulfidoundecyl ferrocenecarboxylate followed a similar procedure, as described previously.[12]

Synthesis of two isotopically distinct forms of ethyl ferrocenecarboxylate, $FcCOOCH_2CH_3$ and $FcCOOCD_2CD_3$, was analogous to that of DEF, except that ethanol or ethanol-d_6 was used instead of 2-(dimethylamino)-ethanol. The products were purified by elution through a silica gel column with dichloromethane; the first colored fraction was collected in each case. The products were then characterized by IR spectroscopy (see below).

The oxidized (ferricinium) forms of $FcCOOCH_2CH_3$ and $FcCOOCD_2CD_3$ were made using a previously described method.[28] Briefly, 20 mg of each ester was dissolved

in 4 mL of ethyl ether and cooled in a dry ice/acetone bath. Ten drops of Br_2 were added which caused the immediate precipitation of the ferricinium salts. The products were collected by vacuum filtration and used without further purification. The oxidized form of the esters are reported to be ferricinium salts with a tetrabromoferrate(III) anion.[28]

Ferricinium triiodide was also synthesized using a previously described method.[28] Briefly, alcoholic solutions of I_2 and ferrocene (FcH) were mixed to form a black precipitate, which was recrystallized from acetone. Ferrocene was practical grade from Eastman; FcCOOH and 1,1'-ferrocenedicarboxylic acid ($Fc(COOH)_2$) were reagent grade from Aldrich. All other compounds were reagent grade. Deionized water was obtained from a Milli-Q purification system (Millipore). Acetonitrile (Fisher) was dried for 24 hr over molecular sieves (Fisher, type 4A) prior to use.

2. Electrochemistry

Electrochemical measurements were carried out in a conventional three-electrode cell, with a Pt-coil counter electrode and an Ag/AgCl (sat'd NaCl) reference electrode. An inert elastomer gasket defined the geometric area of the working electrode as 0.50 cm^2. The applied voltage was controlled by either a CV-27 potentiostat (Bioanalytical Systems) or a Princeton Applied Research Model 173 galvanostat/potentiostat and Model 175 universal programmer. Cyclic voltammograms were recorded on a Houston Instruments Omnigraphic 2000 xy-recorder. The pH of the $LiClO_4$ electrolyte solutions used for the electrochemical measurements was adjusted by addition of either $HClO_4$ or KOH. Monolayer films of $FcCOOC_{11}S$ used for the electrochemical studies were prepared on Au-coated silicon substrates, as described previously.[20]

3. Infrared Spectroscopy

IR spectra were acquired with a Nicolet 740 FT-IR spectrometer equipped with a narrow-band, liquid nitrogen-cooled HgCdTe detector. Transmission measurements

utilized 128 co-added scans of the solid materials dispersed in KBr. Reflection spectra of the monolayer films in a nitrogen atmosphere (i.e., ex situ spectra) used 1024 scans at 2 cm^{-1} resolution with p-polarized light incident at 80° from the surface normal. These measurements used films prepared analogously with those for the electrochemical studies. The background measurements for the ex situ reflection spectra used a monolayer film of octadecanethiolate-d_{37} on Au, the use and preparation of which are described elsewhere.[29]

Reflection spectroscopy of monolayer films in contact with electrolytic solution (i.e., spectra collected in situ) employed a Kel-F fluoropolymer cell that has been described earlier.[30] Measurements consisted of 2048 scans at 4 cm^{-1} resolution using p-polarized light incident on a CaF_2 hemispherical window at 59° from the surface normal. With D_2O as the solvent, the incident angle at the D_2O-metal interface is nominally 80°. The electrolytic solution used was either 1.0 M $HClO_4$ in H_2O or 1.0 M $DClO_4$ in D_2O.

Similar to our earlier designs, the working electrodes were constructed in "plunger" form from a stainless steel (SS) rod sheathed in Kel-F. The front faces of the rods were mechanically polished to a mirror finish using 0.25-μm diamond paste on an AB Rayvel pad (Buehler) and then coated with Au in a manner similar to that used for coating of the silicon substrates. The monolayer-coated Au surface served as the working electrode of the cell. For the background measurements of the absolute spectra in situ, the plunger was constructed with a core of glass rather than SS. A coil of Pt wire wrapped around the plunger formed the auxiliary electrode. An Ag/AgCl (sat'd KCl) reference electrode was also inserted in one of the cell ports. All voltages cited for the differential reflectance spectra are referenced to this electrode.

The in situ data were processed to remove net spectral features from both gaseous and liquid H_2O. The subtraction of liquid H_2O bands was necessary because of a gradual change in the thickness of the solution layer, which gave rise to relatively large distortions

in the baseline. A net spectrum of the solvent was calculated from one single-beam spectrum recorded at +0.20 V at the beginning and end of the experiment, and a fraction of this reference spectrum was subtracted from the differential spectra shown. This subtraction also removed most of the H_2O vapor lines in the spectra which resulted from a gradual improvement in purge over the duration of the experiment. We attribute the band at 1670 cm^{-1} (for example, in Figure 5 at +0.20 V) to a slight change in the shape of the solution layer, since it appeared only when a long time (>0.5 h) passed between acquisition of sample and background scans. This band could not be removed completely by the subtraction.

C. RESULTS AND DISCUSSION

The following sections describe the results of an electrochemical and an in situ infrared spectroelectrochemical characterization of a ferrocene-terminated thiolate monolayer at gold ($FcCOOC_{11}S/Au$). A primary goal of this study is to probe for alterations in the spatial arrangement of the monolayer that may result from the electrochemical generation of a ferricinium terminal group. The characterization is divided into two parts. First, electrochemical studies were performed to evaluate both the inherent reactivity and long-term stability of the monolayer. These studies also examined issues related to structural transformations (e.g., changes in the monolayer packing) which may occur upon generation of the ferricinium terminal group. Second, changes in the composition of the layer upon electrochemical transformations between the ferrocene and ferricinium forms of the end group were probed using in situ IRRAS. In these latter studies, band assignments were based on evidence provided from a series of isotopically labeled compounds.

1. Electrochemical Studies

Studies in aqueous solution have shown that ferricinium cations ($FeCp_2^+$) decompose through an exchange of cyclopentadienyl anions (Cp^-) with another nucleophile (e.g. OH^-, Cl^-, NO_3^-).[31,32] The rate of exchange increases with the donor strength of the nucleophile. The Cp^- can then reduce undissociated $FeCp_2^+$ to $FeCp_2$ in a follow-up reaction. As a result, cyclopentadienyl radicals are formed, which are lost through irreversible combination or hydrogen-abstraction reactions. Derivatives of $FeCp_2$ follow a similar decomposition path, though the rate is also dependent on the electron withdrawing/donating strengths of the substituents.[33] An earlier study reported on the

decomposition of ferrocenyl phenylacetic acid immobilized through a silane tether at the oxidized surface of a platinum electrode in acetonitrile solution;[34] the decomposition followed second-order reaction kinetics. We also presented evidence for the decomposition of the ferrocenyl monolayers formed by immobilization of ferrocenecarboxylic acid through esterification with a hydroxy-terminated alkanethiolate tether.[35] In the latter case, however, a clear delineation of the reaction kinetics was complicated by a parallel decomposition pathway through the hydrolytic cleavage of the polarized ester linkage.[36]

To delineate the most favorable conditions for studies by in situ IRRAS, the stability of the oxidized form of the ferrocenyl monolayers ($Fc^+COOC_{11}S$) was tested in several different electrolytes (e.g., sulfate, chloride, bromide, nitrate, and perchlorate). Electrochemical measurements of surface coverage were used to monitor the stability. The surface coverages, Γ_{Fc}, were determined according to equation 38

$$\Gamma_{Fc}=Q_{Fc}/nFA \qquad (38)$$

where Q_{Fc} is the charge passed for the electrolysis of the ferrocene sites, n is the number of electrons involved in the electron transfer process (n=1 for the ferrocene redox couple), F is the faraday, and A is the geometric surface area of the electrode. Values of Q_{Fc} were obtained by integration of the areas under cyclic voltammetric (CV) curves for sweeps between a lower limit of +0.20 V and an upper limit of +0.85 V, and were corrected for charging-current contributions. The lower voltage limit corresponds to the presence of the reduced form of $FcCOOC_{11}S$, and the upper limit to the oxidized form. For sulfate, chloride, bromide, and nitrate electrolytes (pH~6.5), the coverages decreased by more than 95% after 2-3 scans between the above voltage limits.[37] The half-life of the $Fc^+COOC_{11}S$ monolayers in the various electrolytes follows the donor strength dependence found in previously reported solution-phase studies (e.g. $Cl^- > Br^- > NO_3^- >$

SO_4^{2-}), indicating the mechanistic translation of the decomposition chemistry from the solution phase to the immobilized species.[32] A set of CV curves illustrating the decomposition of the ferrocenyl monolayers formed on annealed Au-coated mica substrates with a chloride-containing electrolyte were presented earlier.[35] The earlier study also provided clear evidence that the loss of electroactivity resulted from the loss of the ferrocenyl moiety and not the desorptive loss of the layer by cleavage of the Au-S bonds.

In contrast to the above findings, the loss of electroactivity was markedly less with perchlorate as the supporting electrolyte, as shown in Figures 1 and 2. The series of CV curves in Figures 1 and 2 were generated in 1.0 M $HClO_4$ and 0.1 M $LiClO_4$ (pH 4.0), respectively. The applied voltage (E_{app}) was held at either +0.20 V (Figures 1a and 2a) or +0.70 V (Figures 1b and 2b) between voltage scans separated by varied time intervals (for clarity, not all of the scans are shown). The 400 mV/s sweep rate was used to minimize possible perturbations induced by the voltammetric measurement. Figures 1a and 2a demonstrate the stability of the ferrocenyl layers in their reduced forms at both pH values, as shown by the essentially constant charge passed for both oxidation and reduction of the layer. The slight decrease in the oxidative and reductive charge after 100 min (~5%) is primarily a reflection of decomposition of the ferrocenyl moiety over the duration of the voltammetric measurement. The surface coverage of ferrocene, given as the average of 10 different electrodes, was $(4.7 \pm 0.6) \times 10^{-10}$ mol/cm^2, after correcting for surface roughness (roughness factor 1.2). This coverage agrees well with that predicted from packing-limitation considerations (4.5×10^{-10} mol/cm^2) based on treating the ferrocene group as a sphere with a 0.66-nm diameter.[12,38]

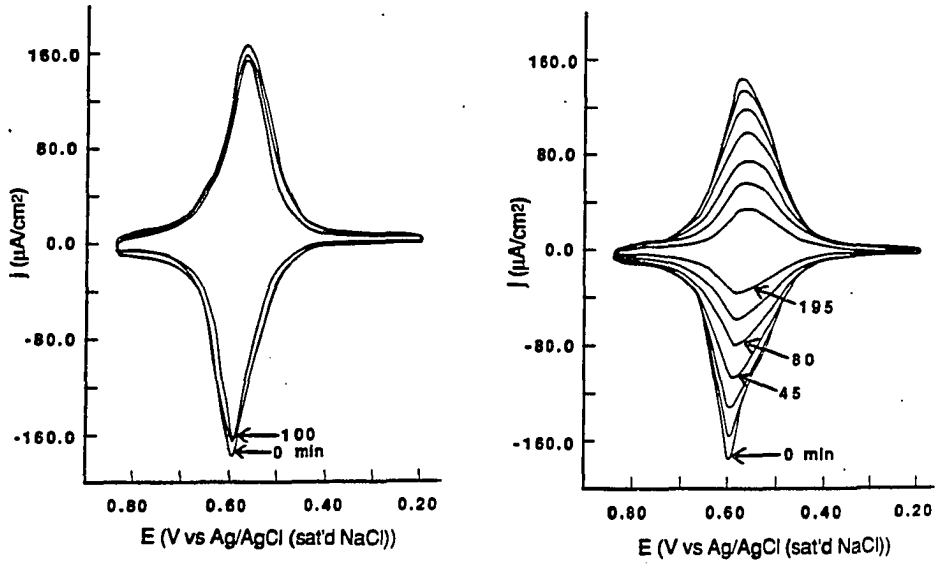

Figure 1. Cyclic voltammetric curves of $FcCOOC_{11}S/Au$ in 1.0 M $HClO_4$. Scans at a sweep rate of 400 mV/s were recorded sequentially after holding E_{app} for the noted time periods at: (a) +0.20 V and (b) +0.70 V.

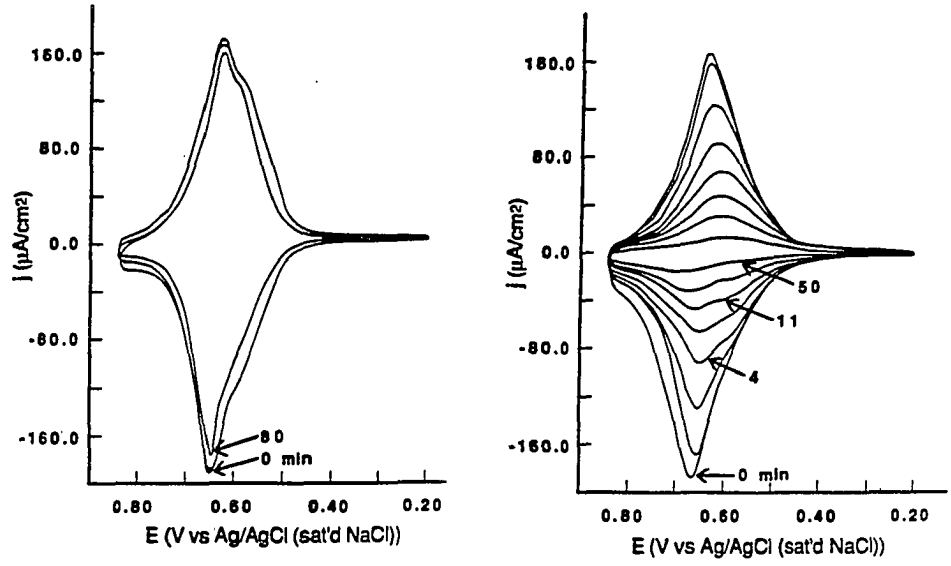

Figure 2. Cyclic voltammetric curves of $FcCOOC_{11}S/Au$ in 0.1 M $LiClO_4$ at pH = 4.0. Scans are collected analogously to Figure 1 by holding E_{app} at: (a) +0.20 V and (b) +0.70 V.

The average of the anodic and cathodic peak current voltages for these curves can be used to estimate the formal reduction potential, $E^{o'}$, for the ferrocenyl layers in both electrolyte solutions. Values of +0.58 V (1.0 M $HClO_4$) and +0.64 V (0.1 M $LiClO_4$, pH 4.0) were obtained, both of which are in qualitative agreement with previous results.[12,35] The positive shift in $E^{o'}$, observed upon altering the supporting electrolyte from 1.0 M $HClO_4$ to 0.1 M $LiClO_4$, is consistent with that expected for a ten-fold decrease in the solution ionic strength.[15]

To elucidate the effects of confining ferrocenecarboxylate within a monolayer structure on the relative stability of the oxidized and reduced ferrocene species, the $E^{o'}$ value for a solution analog of the monolayer-confined ferrocenecarboxylate—namely, 2-(dimethylamino)-ethyl ferrocenecarboxylate (DEF)—was compared to the $E^{o'}$ for the ferrocenyl monolayers in 1.0 M $HClO_4$. A CV curve recorded at bare Au (sweep rate = 50 mV/s) in 1.0 M $HClO_4$ containing 3.0 mM DEF (CV not shown) displayed features characteristic of a diffusional, reversible electrochemical process with a separation between the peak-current voltages of 60 mV and an $E^{o'}$ value of +0.48 V. The value of $E^{o'}$ is 0.10 V more negative than the value of +0.58 V obtained for the monolayer-confined ferrocenecarboxylate. This difference in the $E^{o'}$ values is likely a consequence of the decreased dielectric constant (ε) in the diffuse layer ($2 \leq \varepsilon \leq 10$) as compared to that of bulk solution (ε=78).[3,20] This conclusion is substantiated by the shift in $E^{o'}$ from +0.48 V to +0.60 V for 1.0 mM DEF when the electrolyte is changed from 0.1 M $HClO_4/H_2O$ to 0.1 M Et_4NClO_4/CH_3CN. Therefore, creation of cationic sites in the diffuse layer should be much less favorable than creation of cations in bulk solution. This has the effect of shifting $E^{o'}$ to more positive values.

Further examination of the curves shown in Figures 1a and 2a indicates that the double-layer capacitance changes significantly upon oxidation of the ferrocenyl layers. As is evident from the first scan shown in Figure 1a, the capacitance increases from 6.5 $\mu F/cm^2$ at +0.20 V to 15.6 $\mu F/cm^2$ at + 0.85 V. This increase in double-layer capacitance upon oxidation of the ferrocene moieties could result from either (1) a change in the orientation of the monolayer which produces a less ordered structure (more defect sites) or (2) an increase in the space-charge in the diffuse layer due to the creation of cationic sites. Because our in situ IRRAS analysis of these monolayers has indicated that minimal orientational changes occur upon oxidation (see below), we conclude that the second possibility is most likely. It is also evident from Figures 1b and 2b that the double-layer capacitance measured at +0.85 V decreases considerably as the amount of ferrocene in the monolayer decreases. This can be explained by a lower space-charge in the oxidized form of the partially decomposed layer relative to the full monolayer.

In contrast to the curves shown in Figures 1a and 2a, those in Figures 1b and 2b delineate clearly the relative instability of the oxidized ferrocenyl layers in both 1.0 M $HClO_4$ and 0.1 M $LiClO_4$, respectively. The curves show that the decomposition of the oxidized ferrocenyl layers as a function of time proceeds more rapidly at higher pH. For example, the curves in Figure 1b indicate that about 30% of the ferricinium in the oxidized layer has been lost after 50 min at pH 0, whereas in that same time period nearly all of the ferricinium has been lost at pH 4.0 (Figure 2b). At pH 6.5 (data not shown), the loss of ferricinium from the layer is essentially complete (>95%) within 20 min. This is in direct contrast to the much more rapid loss of ferricinium from the layer in the other electrolytes examined (see above). Apparently, the increase in decomposition rate at higher pH is primarily a result of increasing the hydroxide ion concentration in solution.[31] The progressive loss of ferricinium was confirmed by an ex situ IRRAS study of ferrocenyl

monolayers immersed in aqueous 0.1 M $LiClO_4$ (pH 4.0) solutions with E_{app} held at +0.70 V.

2. Infrared Spectroscopy

(a) General observations

Our presentation of the IR spectroscopic data begins with a brief summary of the spectroscopic properties of a monolayer of 11-sulfidoundecyl ferrocenecarboxylate ($FcCOOC_{11}S$) and its adsorbate precursor 11-mercaptoundecyl ferrocenecarboxylate ($FcCOOC_{11}SH$) together with peak assignments for the latter. We recently described some of the spectroscopic features of $FcCOOC_{11}S$ as part of an effort that used the ferrocenyl redox centers of these monolayers as probes of coverage at the gold surface.[35] This section, along with the Appendix, expands on that earlier discussion, providing a basis for the interpretation of the in situ IRRAS findings.

The monolayer of $FcCOOC_{11}S$ and its adsorbate precursor are compared across the low-frequency (2050–1050 cm^{-1}) region in Figure 3 and the high-frequency (3200–2700 cm^{-1}) region in Figure 4. Table 4 contains band assignments and peak frequencies for both spectra. The adsorbate precursor is dispersed in a KBr disk and the monolayer is assembled at a Au film deposited on an SS plunger. The absorbances of the methylene modes of $FcCOOC_{11}S$/Au (Figure 4b) are consistent with the formation of a single molecular layer of the adsorbate.

Careful analysis of changes in IR peak positions between different states of the ferrocenyl monolayer offers a possibility of understanding the various changes in adsorbate structure and environment between the states. Our analysis begins with comparison between the monolayer exposed to N_2 and the adsorbate precursor (i.e. crystalline $FcCOOC_{11}SH$). Most of the bands observed do not change in peak position or relative intensity between the spectra of these two states. We previously attributed the higher

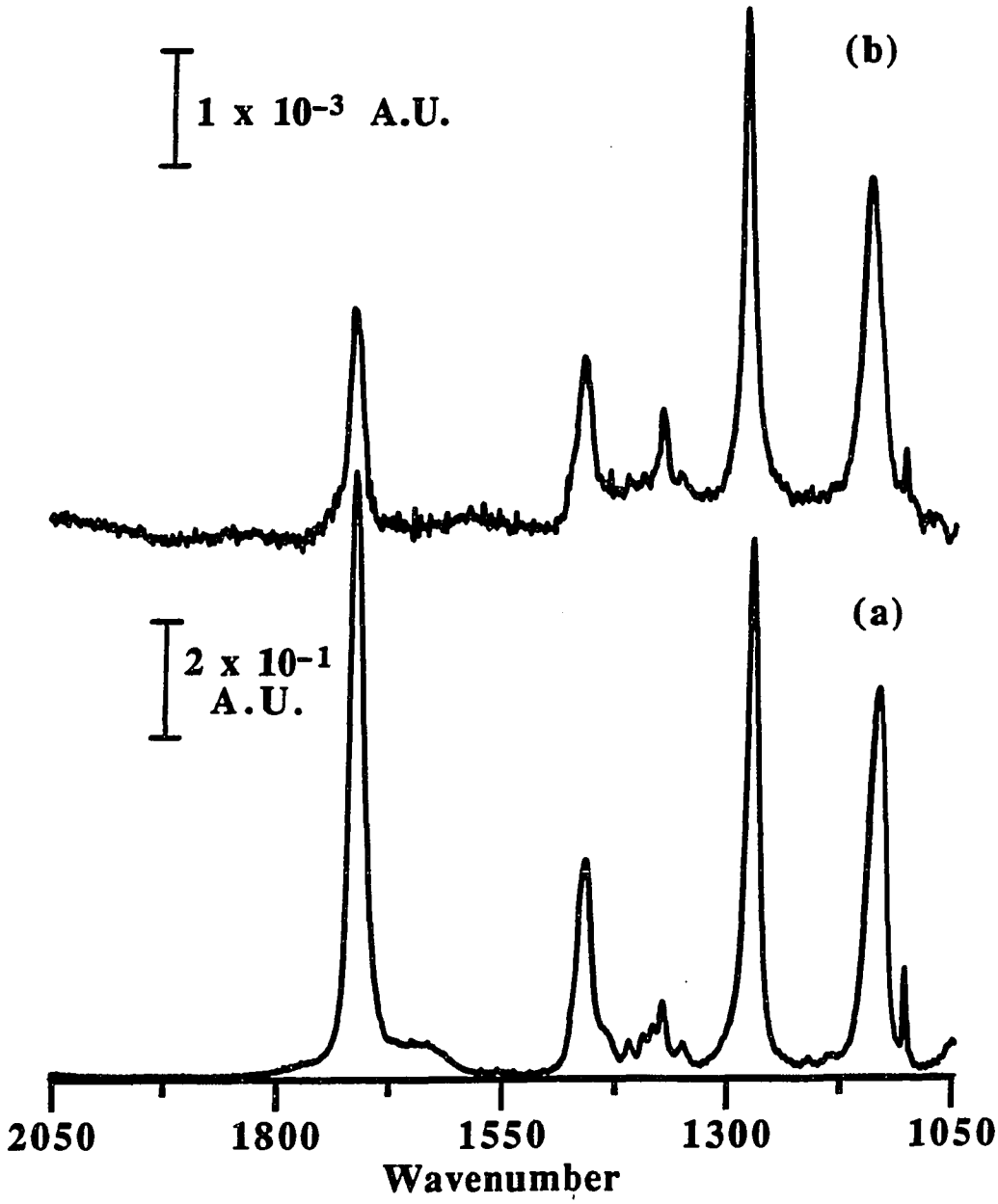

Figure 3. Infrared spectra in the low-frequency region of: (a) crystalline $FcCOOC_{11}SH$ measured in transmission mode, and (b) a monolayer of $FcCOOC_{11}S$ at Au.

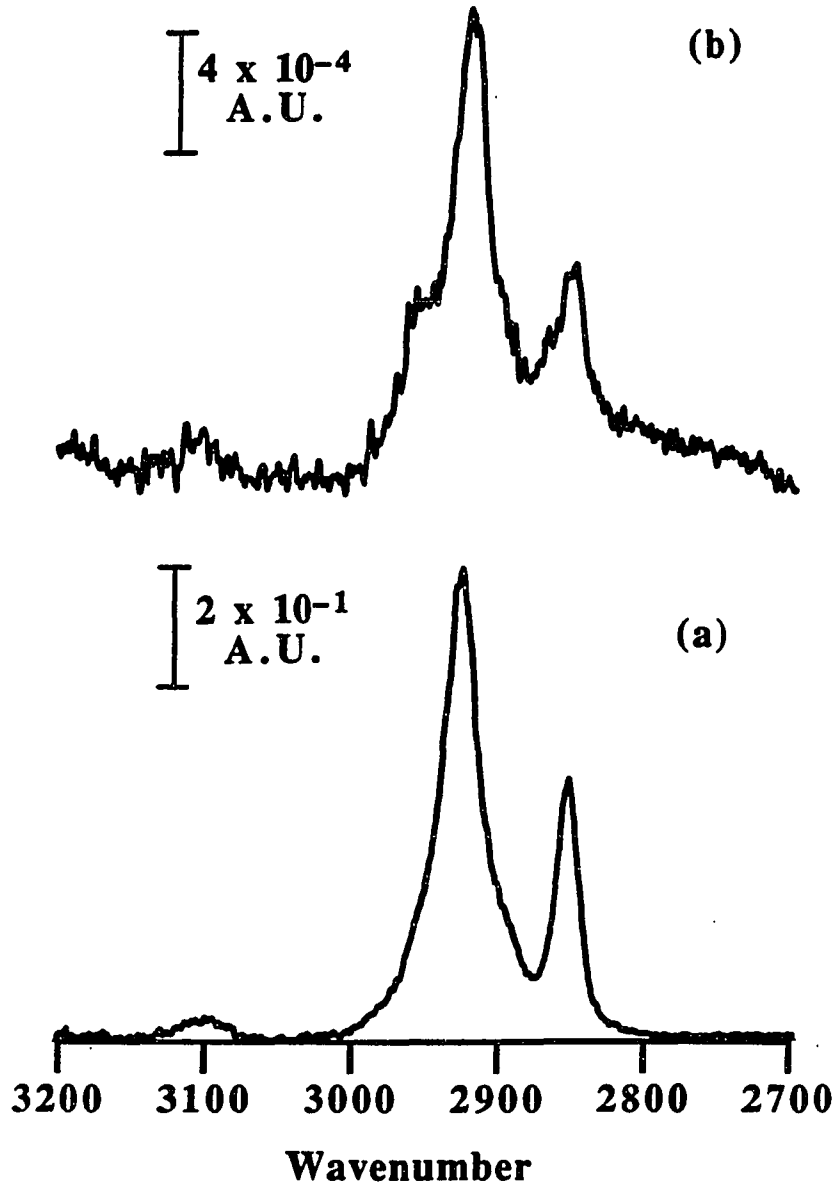

Figure 4. Infrared spectra in the high-frequency region of: (a) crystalline $FcCOOC_{11}SH$, and (b) a monolayer of $FcCOOC_{11}S$ at Au.

Table 4. Mode assignments and peak frequencies[a] (cm^{-1}) of the IR spectra of 11-mercaptoundecyl ferrocenecarboxylate in KBr and as a monolayer at a gold electrode

		monolayer at gold			
			in situ (1.0M $HClO_4$)[b]		
mode	in KBr	ex situ	+0.2 V	+0.7 V	0.7V/0.2V
ν(C–H)Fc	3098	~3105	n.o.	n.o.	3112
$\nu_a(CH_2)$	2926	2923	2921	2923	2929
$\nu_s(CH_2)$	2853	2853	2852	2853	2858
ν(C=O)[c]	1713	1714	1718 (sh) 1732	1731	1729
$\delta(CH_2)$ overlapping with Fc-C=O mode	1460	1463	1461	1464	1459
Fc ring mode	1411	1411	n.o.	n.o.	n.o.
Fc ring mode	1395	1396	n.o.	n.o.	n.o.
$\omega(CH_2$-O)	1385(sh)	n.o.	n.o.	n.o.	n.o.
δ(C–H)Fc (subst. ring)	1374	1375	1374	1376	1371, 1378
δ(C–H)Fc (subst. ring)	1351	1355	1349	1349	
ν(C–C(=O)–O)	1276	1283	1283	1290	1293, 1265
ν(O–C–C)	1137	1147	obs. by ClO_4^-	obs. by ClO_4^-	1174
γ(C–H)Fc	1107	1107			

[a]Abbreviations—n.o.: not observed; obs.: obscured by another mode; sh.: shoulder.

[b]Columns marked "+0.2 V" and "+0.7 V" correspond to absolute spectra of the monolayer relative to a non-absorbing reference film (see text). The peak positions for the differential spectrum at +0.70 V relative to +0.20 V are given in the final column.

[c]Determined from in situ data using 1.0M $DClO_4$ in D_2O.

energy shift of the two ester C–O modes upon film formation to neighbor interactions.[35] The ν(C=O) band does not change peak position; but its relative intensity decreases upon formation of the monolayer. We ascribe this to the orientation of the carbonyl group in the monolayer, combined with the IR "surface selection rule".[39,40] Since the packing density of the adsorbate is limited by the size of Fc, both the Fc–C bond and the chain axis are likely to be nearly normal to the surface. The C=O transition dipole makes an angle of ~120° with respect to the Fc–C bond and would therefore be oriented perpendicular to the chain axis, assuming that the polymethylene chains adopt an all-trans conformation. Thus, the C=O transition dipole is oriented close to the surface parallel. This results in a decrease in the absorbance of ν(C=O) relative to the other prominent modes in this region. For example, the two ester C–O modes, being delocalized across several bonds, are oriented nearly parallel to the chain axis and do not exhibit this relative decrease in intensity.

(b) In situ studies

The major objective of this study was examination of changes in the ferrocenyl layer in contact with an aqueous interface as a result of electrochemically induced transformations. This section presents the results of such an examination using IR spectroelectrochemistry. The spectral data are presented in the form of differential reflectance-absorbance spectra. In this mode, a reflectance spectrum $[R_0(\bar{\nu})]$ of the electrode is scanned at a base voltage (+0.20 V in this work). The applied voltage is then stepped to and held at a selected value while another spectrum $[R(\bar{\nu})]$ is scanned. The resulting "single beam" spectra for the two voltages are combined to give a differential spectrum as reflectance-absorbance $[-\log(R(\bar{\nu})/R_0(\bar{\nu}))]$.

Differential spectra of a monolayer of $FcCOOC_{11}S$ at Au in contact with 1.0 M $HClO_4$ are shown in Figures 5 and 6. Spectral bands observed are summarized in Table 1. Spectral changes occurring with changes in E_{app} were largely reversible; however, a few peaks grew in or diminished with time in some of the trials, even when E_{app} was held constant. For this reason, the data in Figures 5 and 6 were collected in quasi-random order. In addition to the differential spectra, "absolute" spectra were also measured of $FcCOOC_{11}S$ at Au in situ relative to a reference monolayer of perdeuterated alkanethiolate to elucidate bands that do not depend on E_{app}. The absolute spectra (not shown) are also summarized in Table 1.

Several notable features arise with increasing E_{app} across the low-frequency region of the differential spectra (Figure 5). First, the ν(C=O) band displays a derivative shape, showing an net increase in absorbance and a shift to higher frequency (1732 cm^{-1}). Next, there is a net decrease in absorbance with E_{app} at 1460 cm^{-1}, giving rise to a negative band. Four bands appear to grow in with E_{app} in the range 1350-1400 cm^{-1}, although only slightly above the noise. The band which is at 1280 cm^{-1} ex situ shows a dramatic change which is intermediate between splitting and a derivative form. There is an increase in absorbance at 1293 cm^{-1} and a smaller increase at 1265 cm^{-1}, while absorbance at 1280 cm^{-1} decreases slightly. The band at ~ 1150 cm^{-1} seems to undergo a derivative-like change, but is obscured by the cutoff of the CaF_2 window in the same region. Somewhat obscured by the ν(C=O) band in the differential spectra is a broader feature showing a net decrease at ~1660 cm^{-1}. We attribute the latter to changes in the concentration and/or orientation of H_2O molecules in the diffuse layer. This is distinct from the band at 1670 cm^{-1} noted in Figure 5 at +0.20 V, which is a function of time, but not of E_{app} (see Experimental Section).

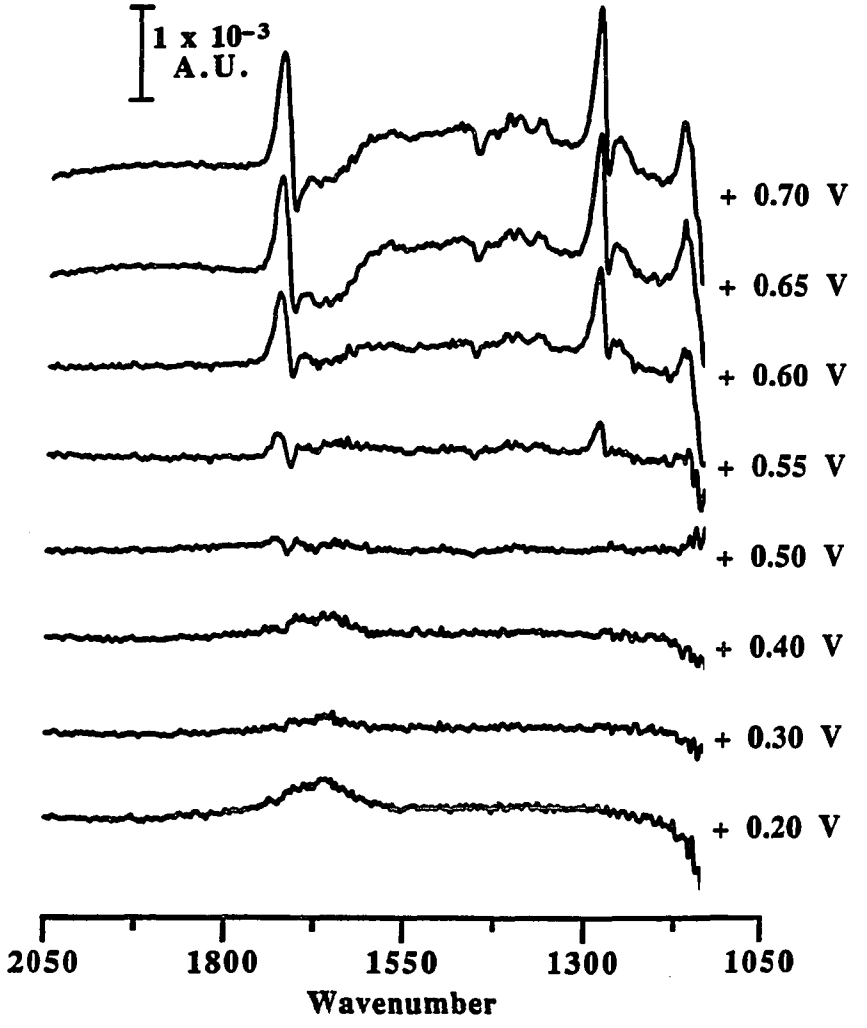

Figure 5. Differential spectra of a monolayer of $FcCOOC_{11}S$/Au in 1.0M $HClO_4$ in the low-frequency region as a function of E_{app}, which was stepped in the temporal order: +0.20, +0.60, +0.40, +0.55, +0.30, +0.70, +0.50, +0.20, and +0.65 V. All spectra were calculated relative to R_0 representing the penultimate scan at +0.20 V. The spectrum shown for +0.20 V, for example, represents the ratio of the first scan to the penultimate scan.

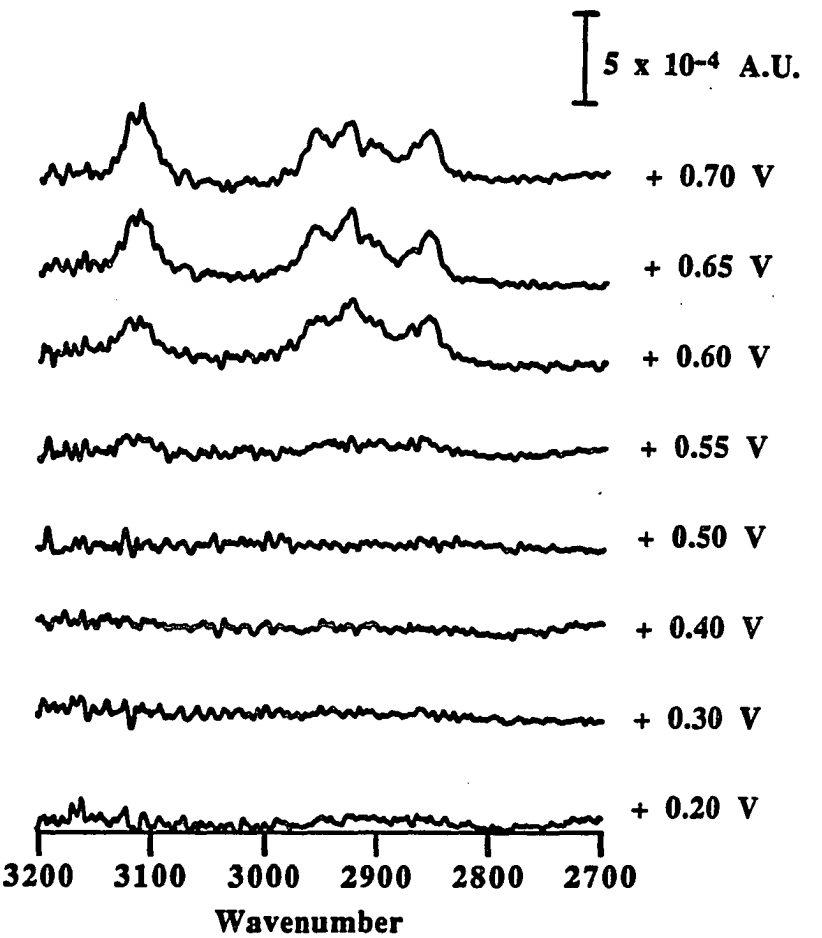

Figure 6. Differential spectra of a monolayer of $FcCOOC_{11}S$/Au in the high-frequency region. The conditions and the actual electrode and film used are the same as Figure 5.

Discerning the factors responsible for each of the effects noted in the differential spectra requires an analogical model of how $FcCOOC_{11}S$ would behave in a less ordered state upon oxidation. To this end, we studied the effect of oxidation upon IR spectra for two analogs of $FcCOOC_{11}S$—namely, ethyl ferrocenecarboxylate containing either a normal or a perdeuterated ethyl group ($FcCOOCH_2CH_3$ and $FcCOOCD_2CD_3$, respectively). These two isotopic forms of this analog were also used to aid IR band assignments.

Transmission IR spectra of the reduced and oxidized forms of these ethyl esters are shown in Figure 7 The peak positions and band assignments are given in Table 5 in the Appendix. Numerous peak shifts and changes in relative intensity occur upon oxidation, although very few bands actually appear or disappear. Of particular importance are the changes in the three major ester bands. The ν(C=O) band at 1695 cm^{-1} and the ν(C-(C=O)-O) band at 1277 cm^{-1} in $FcCOOCH_2CH_3$ shift to higher energy by 25 and 5 cm^{-1}, respectively, upon oxidation of Fc. These shifts agree with trends found for *para*-substituted methyl benzoates. For example, from methyl 4-methylbenzoate to methyl 4-nitrobenzoate, ν(C=O) shifts from 1715 to 1730 cm^{-1} and the stronger of two bands assigned to the ν(C-(C=O)-O) band shifts from 1272 to 1278 cm^{-1}.[41] Oxidation of the Fc group in $FcCOOCH_2CH_3$ should withdraw electron density from the ester group in a manner similar to an increase in the electron-withdrawing character of the *para*-substituent in the benzoates, because decreasing the electron density of the ring carbon attached to the carbonyl group increases the strength of both C-O bonds.

Oxidation shifts the third C-O band at 1134 cm^{-1} in $FcCOOCH_2CH_3$ to higher energy, but its intensity decreases relative to the other C-O bands. Again, this change agrees with the *para*-effect of the substituents on methyl benzoates, where the $-NO_2$ substituent shifts this band from 1110 to 1116 cm^{-1} and reduces its extinction coefficient

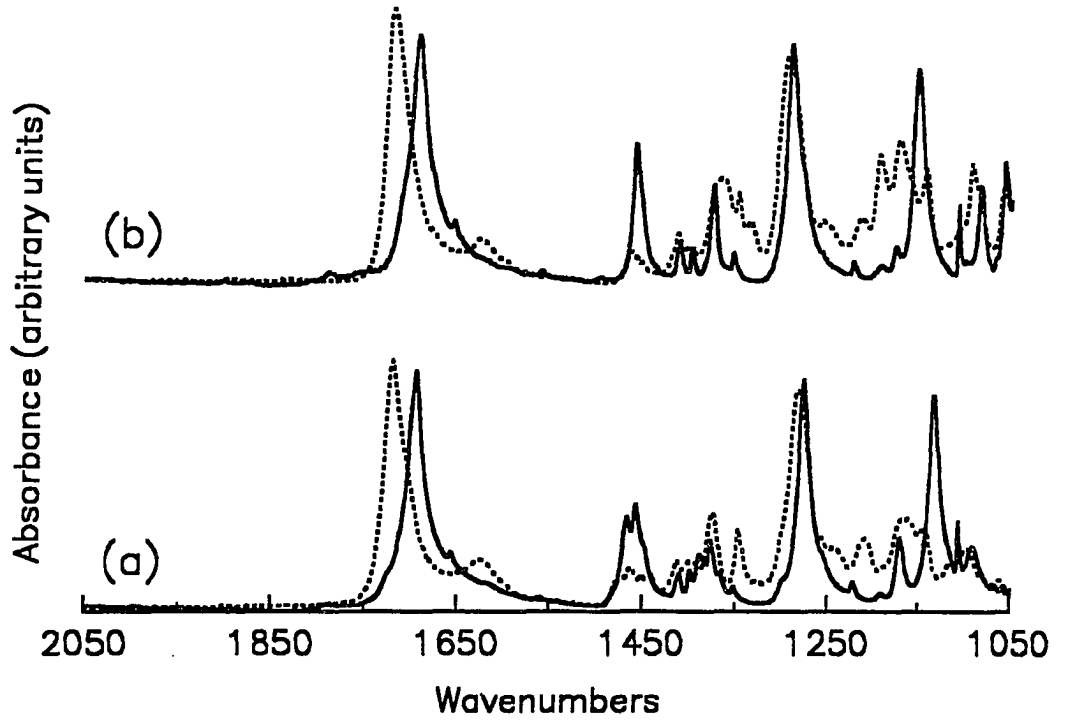

Figure 7. Transmission spectra of bulk forms of ethyl ferrocenecarboxylate in the low-frequency region: (a) $FcCOOCH_2CH_3$ in reduced (—) and oxidized (· · ·) forms; (b) $FcCOOCD_2CD_3$ in reduced (—) and oxidized (· · ·) forms.

relative to the $-CH_3$ substituent. In addition, a second, weaker, band appears at a frequency lower than the original mode.

Oxidation also greatly reduces the intensity of the band due to the substituted ring of Fc at ~1460 cm^{-1}. This is seen most clearly in the $FcCOOCD_2CD_3$ spectra in which there is no overlap by the $\delta(CH_2)$ band. All of the changes observed upon oxidation of the ethyl ferrocenecarboxylates are echoed in the differential spectra of $FcCOOC_{11}S$, as noted below.

Comparing the ex situ spectra of $FcCOOC_{11}S$/Au (Figure 3b) with the absolute in situ spectrum of the reduced monolayer (Table 4) shows a shift of ν(C=O) from 1714 to 1738 cm^{-1}. Since this region is strongly affected by the ν(O–H) of solvent H_2O, we also

acquired differential spectra (not shown) of $FcCOOC_{11}S$/Au in contact with 1.0 M $DClO_4$ in D_2O in order to remove overlap of the solvent and monolayer peak frequencies. Several effects of E_{app} become apparent as a result. In the absolute spectrum at +0.20 V, ν(C=O) is a strong band at 1732 cm^{-1} with an unresolved shoulder at ~1718 cm^{-1}. The absolute spectrum at +0.70 V for the oxidized film exhibits a two-fold increase in the magnitude of ν(C=O) with a maximum at 1731 cm^{-1} and disappearance of the shoulder. In the differential spectrum at +0.70 V, the derivative-shaped band has its peak at 1729 cm^{-1} and its trough at 1710 cm^{-1}. Apparently, immersion of the film into electrolyte affects the environment of the C=O group. The presence of the shoulder at 1714 cm^{-1} in the reduced form indicates that a portion of the C=O groups in situ are in an environment similar to that ex situ; the remaining C=O groups give rise to the 1732-cm^{-1} peak. The shift of absorbance of some of the C=O groups to higher energy may be due to a change in the resonance between the aromatic ring and the carbonyl group as a result of interactions between the Fc group and the electrolyte. Other possible causes of this shift are discussed below in connection with oxidation of the monolayer.

Upon oxidation of the monolayer, the lower-energy shoulder of ν(C=O) decreases and the component at higher energy increases in absorbance. The absolute spectra in deuterated electrolyte show that the component of ν(C=O) at 1732 cm^{-1} does not shift in frequency. This shift of the remaining C=O groups from 1714 to 1732 cm^{-1} could be due to four possible kinds of interactions involving either the O or C atom of the carbonyl group: (1) solvent may partition into the monolayer upon oxidation and hydrogen bond with the oxygens; (2) positively charged ferricinium may interact with oxygens in adjacent chains; (3) perchlorate ion may partition into the oxidized monolayer and interact with oxygens; and (4) the ferricinium group may inductively withdraw electron density from the carbon. The first two possibilities can be ruled out because such effects would lead to a

decrease in the ν(C=O) frequency. Of the remaining possibilities, (4) is most likely, since the bulk ethyl analogs also exhibit a shift of ν(C=O) to higher frequency upon oxidation. This explains the decrease in the 1714-cm^{-1} component of ν(C=O) and an increase in the 1732-cm^{-1} component, but it is as yet unclear why the carbonyls that absorb at 1732 cm^{-1} in the reduced state do not shift to even higher frequency upon oxidation.

Another change occurring upon oxidation is the decrease in intensity of the 1460-cm^{-1} band. No detectable frequency shift occurs, as evident from the lack of a derivative-like band in any of the differential spectra. Since this band has contributions from both the alkyl chain and the Fc ester group, this decrease could be due either to changes in the orientation of one or both of the regions of the molecule or to electronic changes in the Fc ester group. Most likely, the latter is responsible, since the relative absorbance of the 1460-cm^{-1} peak of both forms of ethyl ferrocenecarboxylate decreases significantly upon oxidation.

One other effect observed in the differential spectra is the splitting of the ester mode at 1280 cm^{-1}. This is also consistent with the spectra of reduced and oxidized forms of $FcCOOCH_2CH_3$, in which the band at 1277 cm^{-1} shifts to 1283 cm^{-1} upon oxidation and a shoulder grows in at 1244 cm^{-1}.

There are also several changes with E_{app} in the spectra in the high frequency region (Figure 6). At voltages near and greater than $E^{o'}$, six bands grow in which correspond to C–H stretches. A band at 2929 and a doublet at 2872 and 2858 cm^{-1} correspond to the usual positions for disordered polymethylene chains and a fourth (at 3112 cm^{-1}) corresponds to $\nu(C–H)_{Fc}$; however, the band at 2959 cm^{-1} coincides with the usual frequency of $\nu_a(CH_3)$ and an additional band appears at 2909 cm^{-1}. Several forms of evidence suggest that the latter two ν(C–H) bands are due to the α-methylene group (adjacent to the ester oxygen). It has been reported that the bands of methylene groups

adjacent to an oxygen atom are approximately 7 cm^{-1} higher than in alkanes.[42] Also, an additional band at ~2910 cm^{-1} often appears in terminal alcohols and their esters which does not seem to result from a shift in one of the ν(C–H) bands which are observed in alkanes. For example, bands have been observed in ethyl propanoate at 2946, 2912, and 2886 cm^{-1}.[43] The shifts of $\nu(CH_2)$ to higher frequencies can be explained in terms of strengthening of the C–H bond by the adjacent electronegative oxygen, even in the reduced form of $FcCOOC_{11}S$. Since the film is in its oxidized form when these bands are observed, we would expect an additional strengthening of the α-C–H bonds due to the inductive electron-withdrawing effect of the ferricinium group which is coupled by resonance to the carbonyl group. Our bulk spectrum of DEF also shows $\nu(CH_2)$ at frequencies higher than normal (Table 5 in Appendix), which we ascribe to the effect of the ester and the amine nitrogen. The bulk and monolayer spectra of $FcCOOC_{11}S$ show shoulders on the $\nu(CH_2)$ modes which also correspond to the α-methylene group. Therefore, we attribute the changes observed in the high-energy region between the reduced and oxidized forms to the effect of the added positive charge in Fc and not to changes in orientation of the polymethylene spacer.

A control experiment similar to the differential spectroscopy described above—but in the absence of an electroactive Fc end group—was performed in order to detect any effects of E_{app} upon monolayers without electroactive end groups. A monolayer of 1-dodecanethiolate at Au ($C_{12}S$/Au) was chosen as a non-electroactive analog because its length is similar to that of $FcCOOC_{11}S$. Differential spectra were obtained under conditions identical to those described for $FcCOOC_{11}S$/Au above, although the coverage of the latter is less than that of the alkanethiolate film.[35] The in situ spectra of $C_{12}S$/Au were also ratioed to a spectrum of a perdeuterated octadecanethiolate film in order to obtain absolute IRRA spectra. The absolute spectra revealed four bands corresponding to

the four major ν(C-H) bands normally observed for alkanethiolate monolayers on Au, thus verifying the presence of the monolayer. Differential spectra of $C_{12}S$/Au showed no voltage dependent absorbances in the high or low frequency regions. On the other hand, surface enhanced Raman spectroscopic studies of alkanethiolate monolayers at a liquid/solid interface have showed changes in chain orientation as a function of E_{app}, but those studies used a much rougher surface.[44]

Interestingly, the spectra of $C_{12}S$/Au show no evidence of the broad band at 1600 - 1750 cm^{-1}, which appears as a negative absorbance at the higher values of E_{app} in the differential spectrum of $FcCOOC_{11}S$/Au (Figure 5). Thus, that feature results from a monolayer of charged species and not from an increase in E_{app}. This confirms the assertion noted above that the broad band results from dipoles of H_2O lining up along the interface due to the array of charged sites in the oxidized form of the monolayer film.

D. CONCLUSION

A detailed study of the effects of E_{app} upon the structure and stability of a ferrocenyl monolayer at a gold/aqueous perchloric acid interface has been performed. Electrochemical studies of the ferrocenyl monolayers were performed to: (1) identify the conditions (e.g., aqueous electrolyte composition, pH) under which the monolayer was most stable in both its oxidized and reduced forms, (2) obtain average measurements of Γ_{Fc} and $E^{o'}$, and (3) probe for changes in double-layer capacitance which may indicate changes in monolayer structure upon oxidation. The results of these studies suggested that the ferrocenyl monolayers are highly unstable at pH>2, except when perchlorate is the dominant anion present . Both the surface coverage of $FcCOOC_{11}S$ ($(4.7 \pm 0.6) \times 10^{-10}$ mol/cm^2) and $E^{o'}$ (+0.58 V) determined from the CV curves in 1.0 M $HClO_4$ were in agreement with previously published results.[12,35] In addition, a large change in double-layer capacitance was observed upon oxidation of the ferrocenyl end group. This effect, which may result from either the creation of cationic sites in the diffuse layer or from changes in the orientation of the polymethylene spacer chains, was then further examined using in situ IRRAS.

The results of the electrochemical studies facilitated a thorough study of the effects of E_{app} on the structure and composition of the monolayer using IRRAS. The in situ IRRAS studies provided no evidence for change in the orientation of the polymethylene spacer chains upon oxidation of the ferrocene end group; rather, the features observed in the differential spectra of the film arise from changes in the bond strengths of the adsorbate as a result of generation of a ferricinium ion. All of the spectral features due to the ferrocenyl monolayer appeared to be reversible with respect to E_{app}. These IRRAS results can be used as a framework for further studies of ferrocenyl monolayers and similar

adsorbate systems; such experiments are planned. Efforts to address the extent of counter ion incorporation using spectroscopically accessible moieties are being devised. The latter effort may also benefit from characterization using piezoelectric mass balances.[11,45,46]

E. APPENDIX—DETERMINATION OF BAND ASSIGNMENTS FOR 11-MERCAPTOUNDECYL FERROCENECARBOXYLATE

A detailed description of the assignment of IR spectral bands of $FcCOOC_{11}SH$ and the ancillary data used to develop the assignments are presented in this section. Briefly, the spectral features observed for this compound arise from the ferrocenyl, ester, and polymethylene functional groups; however, the interactions and linkages between these groups—along with the increase in the number of observed spectral modes of ferrocene because of the loss of $\mathbf{D}_{5d}$ symmetry upon derivatization of the Fc group—complicate the interpretation. Previous studies have assigned many of the IR bands of ferrocene (FcH)[47,48] and its acyl derivatives.[49,50,51] A detailed assignment of peak positions for ferrocenecarboxylic acid or its derivatives has not, to our knowledge, appeared in the literature. We have used spectra of numerous compounds related to $FcCOOC_{11}SH$ (e.g. isotopically labeled esters of ferrocenecarboxylic acid, FcCOOH) to aid the mode assignments.

To delineate the mode assignments for the substituted ferrocene group and those of the acyl group, IR spectra (not shown) of related compounds—such as FcH; FcCOOH; 1,1'-ferrocenedicarboxylic acid ($Fc(COOH)_2$); and ferricinium triiodide ($Fc^+I_3^-$)—were compared. Two isotopic forms of ethyl ferrocenecarboxylate, $FcCOOCH_2CH_3$ and $FcCOOCD_2CD_3$, were also used to aid assignments of those groups, along with that of the α-methylene group. Spectra of the ferricinium forms of these ethyl esters were also taken for comparison with spectra of the oxidized form of the monolayer. Band assignments for the acyl, alkoxy, and methylene groups were aided further by the bulk spectrum of DEF, the compound used to probe the solution electrochemical behavior of ferrocenecarboxylate esters. Frequencies and mode assignments for transmission spectra

of DEF and the ethyl esters are given in Table 2; those of the other compounds are available in the literature.

Assignment of most of the strong peaks of $FcCOOC_{11}SH$—including all peaks in the region 3200-2700 cm^{-1}—was straightforward, following literature precedents.[52] Assignment of the modes in the 1500-1350 cm^{-1} range of the esters, however, proved more difficult as a result of delocalized, as well as coupled, vibrations.

The medium-to-strong band at ~1460 cm^{-1} is present in all forms of ferrocenecarboxylate esters examined. Previous studies with alkanethiolate monolayers place the methylene scissoring mode, $\delta(CH_2)$, in this region.[53] However, several observations imply the possible contributions of other modes to this region. First, the absorbances of the 1460-cm^{-1} mode relative to the three ester-group modes are comparable between $FcCOOC_{11}SH$ and DEF, even though these compounds differ by nine methylene groups and the longer-chain ester shows relatively much stronger $\nu(CH_2)$ modes. Second, the two acid derivatives of ferrocene show a band in this region that is approximately one-half as strong as $\nu(C=O)$. In $Fc(COOH)_2$, this band appears at 1491 cm^{-1}, whereas in FcCOOH (which is the more similar of these two acids to our ester derivatives) it falls at 1476 cm^{-1}. This band likely includes a coupled vibration involving both the ring and the acyl group, since short-chain alkanoic acids and FcH show no bands in this region. On the other hand, benzoic acid, which should exhibit analogous resonance between an aromatic ring and a carboxyl group, has two medium-intensity bands in this region. We postulate that this delocalized mode present in the ferrocenyl acids shifts to lower frequency in the esters and overlaps with the $\delta(CH_2)$. The strongest evidence for our assertion comes from the ethyl esters. In $FcCOOCH_2CH_3$, the band in question is a doublet with peak frequencies at 1467 and 1459 cm^{-1}; but in $FcCOOCD_2CD_3$, the band at 1459 cm^{-1} remains while the higher-frequency band disappears, having been shifted to

Table 2. Mode assignments and peak frequencies[a] (cm^{-1}) of the transmission IR spectra of ferrocenecarboxylate esters dispersed in KBr

		$FcCOOCH_2CH_3$		$FcCOOCD_2CD_3$	
mode	DEF	reduced	oxidized	reduced	oxidized
ν(C-H), Fc	multiplet at 3116-3069	3112, 3085	~3100 obs. by $\nu_a(CH_3)$	3112, 3086	3095, 3015
$\nu_a(CH_2)$, adj. N	2972	-	-	-	-
$\nu_a(CH_2)$, adj. O	2946	2940	2931	-	-
$\nu_s(CH_2)$, adj. O	2856	2875?	2864?	-	-
$\nu_a(CH_3)$	2821	2984, 2963	obs.by Fc	-	-
$\nu_s(CH_2)$, adj. N	2789	-	-	-	-
$\nu_s(CH_3)$	2774	2893?	2903?	-	-
	2723				
ν(C-D)	-	-	-	(7 bands in 2300-2100 range)	
ν(C=O)	1710 v.s. 1702 v.s.	1695 v.s.	1721 v.s.	1693 v.s.	1721 v.s.
	1662	1657	1627	1654	1626
$\delta(CH_2)$	1462[b]	1467	1464	-	-
Fc-C=O mode	1462[b]	1457	obs. by $\delta(CH_2)$	1459	1462

[a]Abbreviations: adj.: refers to the group adjacent to the given atom; n.o.: not observed; obs.: obscured by a another mode; sh.: shoulder; v.s.: very strong band

[b]These modes are superimposed.

Table 2. (continued)

		$FcCOOCH_2CH_3$		$FcCOOCD_2CD_3$	
mode	DEF	reduced	oxidized	reduced	oxidized
$\delta_a(CH_3)$	n.o.	sh.	n.o.	-	-
Fc ring mode	1412	1411	1413	1411	1413
Fc ring mode	1397	1397	1398	1397	1400
$\delta_s(CH_3) + \omega(CH_2\text{-}O)$	1385 (sh)	1388	n.o.	-	-
$\delta(C\text{–}H)_{Fc}$ (subst. ring)	1376	1376	1375	1375	1366?
mixed $\omega(CH_2\text{-}O)$ & $\delta_s(CH_3)$	sh.	sh.	sh.	-	-
$\delta(C\text{–}H)_{Fc}$ (subst. ring)	1351	1351	1347	1352	1348
$\nu(C\text{–}C(=O)\text{–}O)$	1275 v.s.	1277 v.s.	1283 v.s.	1290 v.s.	1294 v.s.
	1220	1222	1209	1222	1214
	1205	1191	sh. ~1190	1192	1194
$\nu(O\text{–}C\text{–}C)$ (minor)	sh.	1171	1168	1176	1172
$\nu(O\text{–}C\text{–}C)$	1138 v.s.	1134 v.s.	1144, 1119	1153 v.s.	1144
$\gamma(C\text{–}H)_{Fc}$	1105	1107	sh.	1108	sh.
ethyl group mixed mode	sh.	1092	1099	-	-
$\delta(CD_2)$	-	-	-	1084	1094
$\omega(CH_2)$?	1061	n.o.	n.o.	-	-
$\delta s(CD_3)$	-	-	-	1057	1059
$\omega(CD_2\text{-}O)$	-	-	-	1047	1047
	1031	1034	1035	1033	1030
$\delta_\perp(C\text{-}H)Fc$	999	1002	1004	1000	1002

1084 cm^{-1} by deuteration. Clearly, in $FcCOOCH_2CH_3$, $\delta(CH_2)$ is at 1467 cm^{-1} and the 1459-cm^{-1} mode is due to ferrocenecarboxylate. In addition, the $\delta_a(CH_3)$ mode may overlap with the aforementioned modes in the case of DEF.[52]

Moving to other bands in this region of the spectrum, the only peak present in $FcCOOC_{11}SH$ which is absent in DEF and the ethyl esters is the shoulder at ~1440 cm^{-1}. This is attributed to $\delta(CH_2)$ for the methylene group adjacent to sulfur.[52] It is present as a shoulder in condensed-phase spectra of most primary thiols, but not in secondary thiols.[54]

Next, there is a characteristic quintet at 1412-1351 cm^{-1} which is almost identical between $FcCOOC_{11}SH$ and DEF; the 1411-cm^{-1} peak is slightly stronger in the amine. The strong similarity between the two compounds rules out predominant contributions of the methylene groups to these peaks, since the number of methylene groups per molecule differs greatly between the two analogs. The peak at 1412 cm^{-1} probably corresponds to one or more of the coincidentally degenerate normal modes of unsubstituted Fc at 1408 cm^{-1}.[47]

One of the remaining five peaks probably corresponds to $\omega(CH_2)$ adjacent to the ester group. This mode has been reported in studies of many alkyl esters to be ~1380 cm^{-1}—higher in frequency and stronger than $\omega(CH_2)$ within an alkyl chain.[52] Thus, this mode is assigned to the shoulder at 1385 cm^{-1}, which varies among the ester analogs and is absent in $FcCOOCD_2CD_3$. In contrast, others reported the $\omega(CH_2)$ in butyl esters at 1350 cm^{-1}.[55] Acyl ferrocenes also absorb weakly at 1376 and ~1350 cm^{-1},[51] so we attribute both of these bands in $FcCOOC_{11}SH$ to the substituted ring. This agrees with considerations based on group theory, which prescribes that the single peak at 1408 cm^{-1} in Fc should be split into several resulting peaks upon substitution of one ring by the ester group—partly because it is coincidentally degenerate in Fc, corresponding to both a $\mathbf{E_{1u}}$ and an $\mathbf{A_{2u}}$ mode, and partly because the $\mathbf{D_{5d}}$ symmetry of Fc is broken upon substitution.

ACKNOWLEDGEMENTS

M.D.P. gratefully acknowledges the support of a Dow Corning Assistant Professorship. DDP acknowledges a BP America Graduate Fellowship in Analytical Chemistry. The authors thank Dr. Chinkap Chung for synthesizing the 11-mercaptoundecyl ferrocenecarboxylate. Ames Laboratory is operated for the U.S. Department of Energy by Iowa State University under Contract No. W-7405-eng-82.

REFERENCES AND NOTES

1. Whitesides, G.M.; Laibinis, P.E. *Langmuir* **1990**, *6*, 87-96, and references therein.
2. Ulman, A. An Introduction to Ultra-Thin Organic Films From Langmuir-Blodgett to Self-Assembly; Academic Press: San Diego, 1991.
3. Porter, M.D.; Bright, T.B.; Allara, D.L.; Chidsey, C.E.D. *J. Am. Chem. Soc.* **1987**, *109*, 3559-68.
4. Li, T.-T.; Weaver, M.J. *J. Am. Chem. Soc.* **1984**, *106*, 6107-08.
5. Tarlov, M.J.; Bowden, E.F. *J. Am. Chem. Soc.* **1991**, *113*, 1847-49.
6. Finklea, H.O.; Avery, S.; Lynch, M.; Furtsch, T. *Langmuir* **1987**, *3*, 409-13.
7. Finklea, H.O.; Snider, D.A.; Fedyk, J. *Langmuir* **1990**, *6*, 371-76.
8. Sabatani, E.; Rubenstein, I.; Maoz, R.; Sagiv, J. *J. Electroanal. Chem.* **1987**, *219*, 365-71.
9. Sabatani, E.; Rubenstein, I. *J. Phys. Chem.* **1987**, *91*, 6663-69.
10. Rubenstein, I.; Steinberg, S.; Tor, Y.; Shanzer, A.; Sagiv, J. *Nature* **1988**, *332*, 426-29.
11. De Long, H.C.; Donohue, J.J.; Buttry, D.A. *Langmuir* **1991**, *7*, 2196-2202.
12. Chidsey, C.E.D.; Bertozzi, C.R.; Putvinski, T.M.; Mujsce, A.M. *J. Am. Chem. Soc.* **1990**, *112*, 4301-36.
13. Li, T.-T.; Liu, H.-Y. Weaver, M.J. *J. Am. Chem. Soc.* **1984**, *106*, 1233-39.
14. Finklea, H.O.; Hanshew, D.D. *J. Am. Chem. Soc.* **1992**, *114*, 3173-81.
15. Rowe, G.K.; Creager, S.E. *Langmuir* **1991**, *7*, 2307-12.
16. Creager, S.E.; Rowe, G.K. *Anal. Chim. Acta* **1991**, *246*, 233-39.

17. Kunitake, M; Akiyoshi, K.; Kawatana, K.; Nakashima, N; Manabe O. *J. Electroanal. Chem.* **1980**, *292*, 277-80.

18. Corrigan, D.S.; Weaver, M.J. *Langmuir* **1988**, *4*, 599-606.

19. Sasaki, T.; Bae, I.T.; Scherson, D.A.; Bravo, B.G.; Soriaga, M.P. *Langmuir* **1990**, *6*, 1234-37.

20. Widrig, C.A.; Chinkap, C.; Porter, M.D. *J. Electroanal. Chem.* **1991**, *310*, 335-59.

21. Bryant, M.A.; Pemberton, J.E. *J. Am. Chem. Soc.* **1991**, *113*, 8284-93.

22. Bain, C.D.; Biebuyck, H.A.; Whitesides, G.M. *Langmuir* **1989**, *5*, 723-27.

23. Bewick, A.; Pons, B.S. In *Advances In Infrared and Raman Spectroscopy*, vol. 12; Clark, R.J.H.; Hester, R.E. Wiley Heyden: London, 1985; pp. 1-63.

24. Korzeniewski, C.; Pons, S. *Prog. Analyt. Spectrosc.* **1987**, *10*, 1.

25. Beden, B.; Lamy, C. In *Spectroelectrochemistry: Theory and Practice*; Gale, R.J., Ed.; Plenum Press: New York, 1988; pp 189-261.

26. Ashley, K.; Pons, B.S. *Chem. Rev.* **1988**, *88*, 673-95.

27. Stole, S.M.; Popenoe, D.D.; Porter, M.D. In *Electrochemical Interfaces: Modern Techniques for In-Situ Interface Characterization;* Abruña, H.D., Ed.; VCH: New York, 1991; pp 339-410.

28. Nesmeyanov, A.N.; Yur'eva, R.B.; Materikova, R.B.; Getnarski, B.Y. *Izv. Akad. Nauk SSSR, Ser. Khim.* **1965**, *(4)*, 731-33.

29. Walczak, M.M.; Chung, C.; Stole, S.M.; Widrig, C.A.; Porter, M.D. *J. Am. Chem. Soc.*, **1991**, *113*, 2370-78.

30. Popenoe, D.D.; Stole, S.M.; Porter, M.D. *Appl. Spectrosc.* **1992**, *46*, 79-87.

31. Prins, R.; Korswagen, A.R.; Kortbeek, A.G.T.G. *J. Organometal. Chem.* **1972**, *39*, 335-44.

32. Holecek, J.; Handlír, K.; Klikorka, J.; Dinh Bang, N. *Collection Czechoslov. Chem. Commun.* **1979**, *44*, 1379-87.

33. Szentrimay, R.; Yeh, P.; Kuwana, T. In *Electrochemical Studies of Biological Systems;* Sawyer, D.T., Ed.; American Chemical Society: Washington, D.C., 1977; pp 143-69.

34. Lenhard, J.R.; Murray, R.W. *J. Am. Chem. Soc.* **1978**, *100*, 7870-75.

35. Walczak, M.M.; Popenoe, D.D.; Deinhammer, R.S.; Lamp, B.D.; Chung, C.; Porter, M.D. *Langmuir* **1991**, *7*, 2687-93.

36. Deinhammer, R.S., unpublished results.

37. Values of Γ_{Fc} obtained by integration of the areas under the CV i-E curves obtained in these electrolytes for the first voltage scan are approximately 1.5-2 times larger than the coverage expected based on theoretical considerations of a 0.66-nm limiting diameter for the ferrocene groups ($\Gamma_{theoretical}$=4.5 x 10-10. mol/cm^2). This result is consistent with the decomposition mechanism proposed by Prins et al., discussed above, in which cyclopentadienyl anions released upon decomposition can reduce undissociated $FeCp_2^+$ to $FeCp_2$, thereby increasing the apparent charge required to fully oxidize the monolayer.

38. Seiler, P.; Dunitz, J.D. *Acta Crystallogr.* **1979**, *B35*, 1068-74.

39. Pearce, H.A.; Sheppard, N. *Surf. Sci.* **1976**, *59*, 205-17.

40. Porter, M.D. *Anal. Chem.* **1988**, *60*, 1143A-49A.

41. Katritzky, A.R.; Lagowski, J.M.; Beard, J.A.T. *Spectrochim. Acta* **1960**, *16*, 964-78.

42. Wiberley, S.E.; Bunce, S.C.; Bauer, W.H. *Anal. Chem.* **1960**, *32*, 217-21.

43. Pozefsky, A.; Coggeshall, N.D. *Anal. Chem.* **1951**, *23*, 1611-19.

44. Pemberton, J., private communication.

45. Shimazu, K.; Yagi, I.; Sato, Y.; Uosaki, K. *Langmuir* **1992**, *8*, 1385-87.

46. Buttry, D.A., private communication.

47. Fritz, H.P. In *Advances In Organometallic Chemistry,* Vol. 1; Stone, F.G.A.; West, R., Eds; Academic Press: New York, 1964; pp 240-316.

48. Adams, D.M. Metal-Ligand and Related Vibrations: A Critical Survey of the Infrared and Raman Spectra of Metallic and Organometallic Compounds; St. Martin's Press: New York, 1968; pp 189-234.

49. Nesmeyanov, A.N.; Kazitsyna, L.A.; Lokshin, B.U.; Kritskaya, I.I. *Dokl. Akad. Nauk SSSR* **1957**, *117*, 433-36.

50. Kazitsyna, L.A.; Lokshin, B.U.; Nesmeyanov, A.N. *Dokl. Akad. Nauk SSSR* **1959**, *127*, 333-35.

51. Rubalcava, H.E.; Thomson, J.B. *Spectrochim. Acta* **1962**, *18*, 449-59.

52. Colthup, N.B.; Daly, L.H.; Wiberley, S.E. *Introduction to Infrared and Raman Spectroscopy,* 3rd ed.; Academic Press: San Diego, 1990; pp 215-33.

53. Nuzzo, R.G.; Dubois, L.H.; Allara, D.L. *J. Am. Chem. Soc.* **1990**, *112*, 558-69.

54. Pouchert, C.J. *The Aldrich Library of Infrared Spectra,* 3rd ed.; Aldrich Chemical: Milwaukee, 1981.

55. Katritzky, A.R.; Lagowski, J.M.; Beard, J.A.T. *Spectrochim. Acta* **1960**, *16*, 954-63.

SECTION V. PAPER: SYNTHESIS AND CHARACTERIZATION OF A MONOLAYER OF ALKANETHIOLATE DERIVATIZED WITH FLAVIN

ABSTRACT

This paper describes a novel electrochemically active monolayer of an alkanethiolate derivatized with a flavin, formed by self-assembly from ethanolic solutions of 11,11'-dithiobisundecanoic acid, bis[2-(7,8-dimethyl-10-isoalloxazino)ethyl] ester. The method of synthesizing the adsorbate precursor is included. Films formed from this compound display the rapid and pH-dependent electrochemical behavior typical of immobilized flavins; however, the films are quite stable and display coverages up to $\sim 3 \times 10^{-10}$ mol/cm^2. This paper contrasts the electrochemical behavior of the flavin alkanethiolate monolayer with other types of immobilized flavins. IR reflection-absorption spectra of the film, which is a candidate for future in situ spectroscopic studies, are presented and compared with transmission spectra of bulk analogs. Potential applications of the flavin alkanethiolate film as a probe of interfacial properties and as a binding site for proteins are discussed.

A. INTRODUCTION

Monolayer films self-assembled at gold from alkanethiols have become widely used as model surfaces. Alkanethiols have been shown to adsorb oxidatively at Au with loss of a proton to form the corresponding alkanethiolate.[1,2,3] Adsorption from a solution of dialkyl disulfides can also form alkanethiolate monolayers.[4] Often, these monolayers are constructed with groups at the distal end that undergo reversible electron or proton transfer. Such systems offer probes for measuring interfacial pH, changes in interfacial capacitance, the translation of reactivity of a species from solution to the surface, and many other important properties.

At the same time, considerable work in recent years has emphasized immobilization of flavins at electrode surfaces, and the chemistry of flavins themselves continues to be actively studied.[5] Immobilization of the isoalloxazine moiety may provide a useful way to bind—or facilitate electron transfer of—proteins at surfaces, since most biological redox-active molecules by themselves do not interact well with electrode surfaces. Several recent reports describe the covalent bonding of isoalloxazine derivatives to a gold surface using a silane[6] or thiourea[7,8,9] linkage. In addition, flavin adenine dinucleotide (FAD) has been immobilized at glassy carbon via several types of covalent linkages to the adenine group.[10,11,12,13] Binding of flavins may also lead to new forms of artificial enzymes and molecular catalysis, an achievement already reached in aqueous solutions.[14] In addition, binding a flavin to a surface also promises new opportunities for understanding the reactivity of flavins themselves, especially their acid-base and redox behavior.

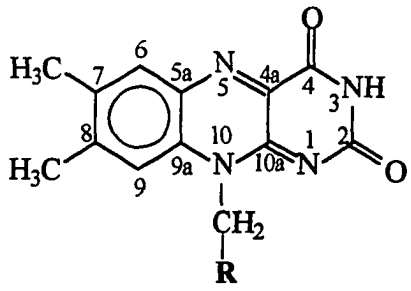

1: R = [–$CH_2OOC(CH_2)_{10}S]_2$;
11,11'-dithiobisundecanoic acid, bis[2-(7,8-dimethyl-10-isoalloxazino)ethyl] ester.[15]

2: R = –$CH_2OOC(CH_2)_{10}S$/Au;
monolayer film of 11-sulfidoundecanoic acid, 2-(7,8-dimethyl-10-isoalloxazino)ethyl ester, at gold.

3: R = –CH_2OH;
7,8-dimethyl-10-(2'-hydroxyethyl)-isoalloxazine.

4: R = –COH;
7,8-dimethyl-10-formylmethylisoalloxazine.

5: R= –H;
lumiflavin.

6: R= –$CH_2OOC(CH_2)_{10}CH_3$;
dodecanoic acid, 2-(7,8-dimethyl-10-isoalloxazino)ethyl ester.

Scheme I. Structure of flavin derivatives.[16]

These developments in studies of both flavins and self-assembled monolayers point to the opportunities enabled by tethering a flavin coenzyme to a metal surface via an alkanethiolate linkage. I report here the first example of a monolayer film of an alkanethiolate derivatized with 7,8-dimethylisoalloxazine. This film self-assembles at Au from solutions of **1** in ethanol, as shown in Scheme I. Adsorption of the symmetrical disulfide **1** forms the corresponding thiolate, **2**, at gold.

My research group is interested in using the isoalloxazine moiety as a probe of liquid-solid interfaces and of alkanethiolate films themselves. The flavin moiety, because of its polycyclic aromatic nature and the presence of several heteroatoms, is detectable by many techniques, including voltammetry, fluorescence spectroscopy, IR spectroscopy, Raman spectroscopy, and visible absorbance spectroscopy (or the naked eye in some cases). Because of its detectability, redox properties, and ability to exchange protons, a flavin-derivatized monolayer can elucidate differences in pKa and other properties between immobilized and solution species.

In addition to its prospects as a model interface, a flavin-derivatized alkanethiolate monolayer presages new understanding of the electrochemical behavior of flavins themselves. This is important because this flavin monolayer, unlike other alkanethiolate monolayer systems heretofore, carries a physiologically occurring redox group. By incorporating the flavin derivative together with an methyl-terminated alkanethiolate co-adsorbate, we can vary the packing of flavin groups as well as varying the flavin-metal surface separation. This kind of mixed monolayer system offers a way to manipulate the parallel stacking of the isoalloxazine groups and to determine the effects of association between isoalloxazines upon electrochemical behavior.

This paper presents the details of the synthesis of **1** and a preliminary study of the system using electrochemistry and IR reflection-absorption spectroscopy (IRRAS), providing a foundation for later studies of mixed monolayers containing **2**. Cyclic and differential pulse voltammetries are used to examine the coverage, stability, reversibility, and pH dependence of redox potential of the films. IRRAS verifies the formation of the monolayer and reveals the degree of order of the films. The reflection spectra of **2** are compared with transmission spectra of bulk **1**, **3**, and **6**.

B. EXPERIMENTAL SECTION

1. Synthesis of the flavin-derivatized adsorbate precursor

This section outlines the synthesis of **1**. The synthetic route is convergent; one branch (Scheme II) consists of the conversion of riboflavin to **3** and the other branch (Scheme III) produces the disulfide diacid derivative which is esterified with **3** to yield **1**. I begin by presenting the synthesis of the disulfide diacid.

a. 11-Mercaptoundecanoic acid

Synthesis of the disulfide diacid intermediate (Scheme III) began with 13.26 g (50.0 mmol) of 11-bromoundecanoic acid, which was dissolved in 50 mL of 95% ethanol. A boiling chip and 4.18 g (55.0 mmol) thiourea were added, and the mixture was allowed to reflux for 15 h (only ~3 h was necessary for complete reaction as determined from TLC). The reaction mixture was cooled to 0°C. The isothiuronium salt did not precipitate out, so it must have hydrolyzed due to the presence of H_2O. Nonetheless, a solution of 4.8 g (120 mmol) NaOH in 45 mL H_2O was added to the solution to hydrolyze any isothiuronium ion remaining. This produced a thick white precipitate of the thiolate-carboxylate salt. The mixture was heated under an N_2 blanket, causing the precipitate to dissolve. The faint pink solution was refluxed for 3 h after which the volume was reduced to 50 mL by rotary evaporation. Next, the viscous solution was vacuum filtered. The flask and filter were rinsed with 25 mL H_2O, which was added to the filtrate.

The mercaptoacid was separated by gradual acidification with 25 mL (200 mmol H^+) of 4.0 M H_2SO_4. A thick white precipitate formed and floated to the top of the solution. The suspension was cooled and the precipitate collected by vacuum filtration. The product was rinsed with H_2O and ether only, since ethanol dissolved it easily.

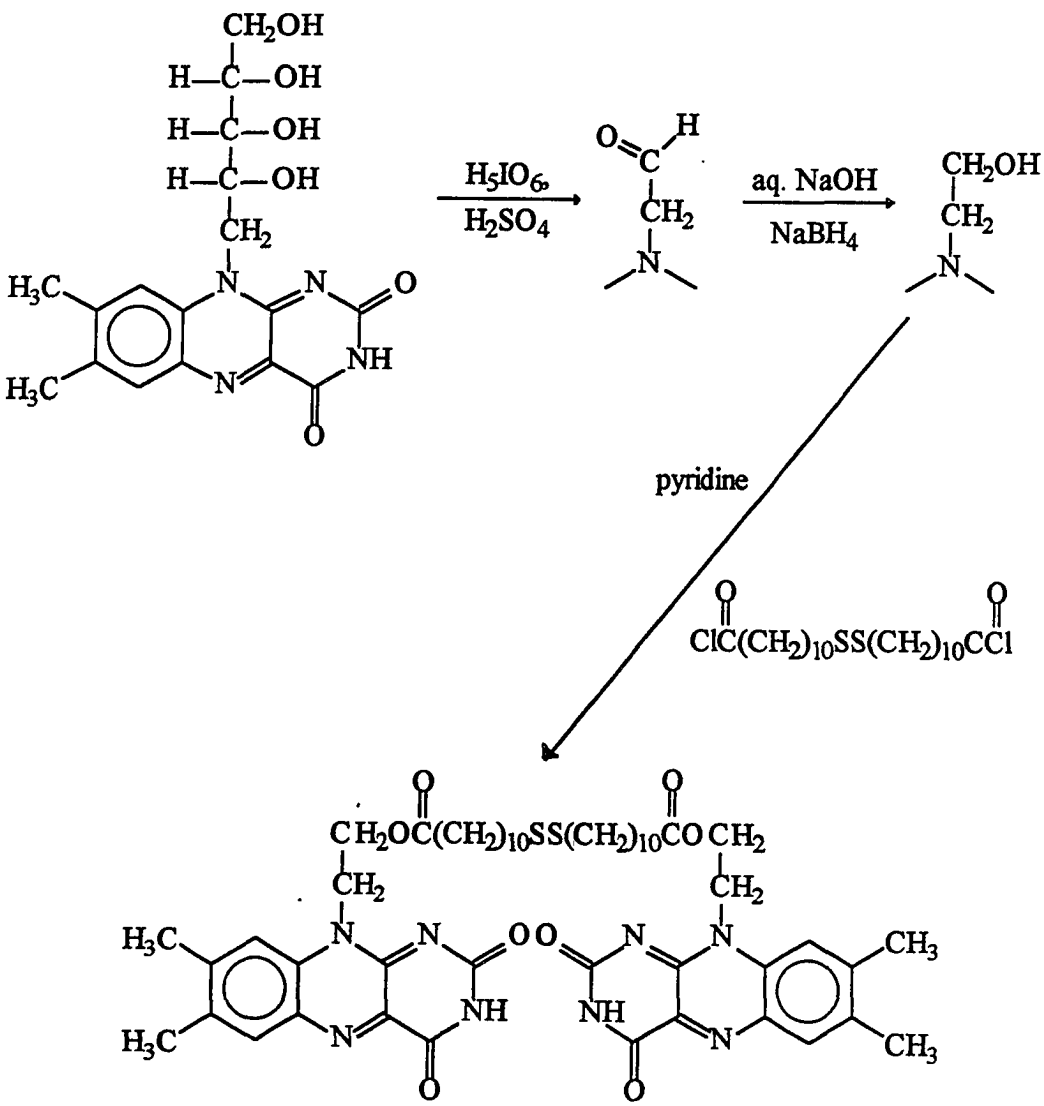

Scheme II. Synthesis of 11,11'-dithiobisundecanoic acid, bis[2-(7,8-dimethyl-10-isoalloxazino)ethyl] ester (1) from riboflavin.

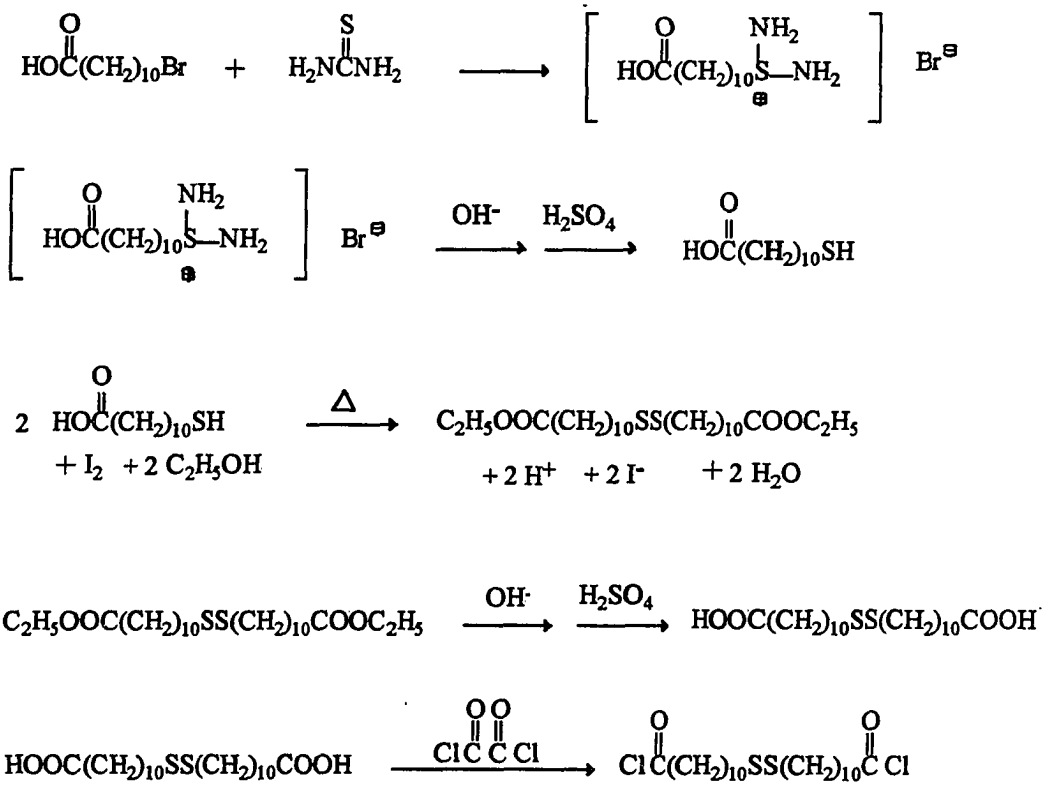

Scheme III. Synthesis of the intermediate 11,11'-dithiobisundecanoyl chloride.

b. 11,11'-Dithiobisundecanoic acid, diethyl ester

To oxidize the thiol from the preceding step to a disulfide (Scheme III), 12.06 g of the crude mercaptoacid was added to 200 mL of boiling ethanol and stirred to dissolve. Vacuum filtration removed the small amount of undissolved solid, which was discarded. The clear solution was titrated with 0.1 M ethanolic I_2. During the later part of the titration, the solution was heated and stirred for ~30 s after each addition. After 160 mL I_2 had been added, a faint yellow color persisted. (That volume of iodine corresponds to only 7.0 g of $HOOC(CH_2)_{10}SH$, indicating that the thiol had already oxidized considerably prior to beginning the titration.) The volume of the titration solution was

reduced by rotary evaporation to ~30 mL. Most of the product precipitated out, and excess I_2 also appeared as distinct violet crystals. Analysis of the product by NMR indicated that the acid groups had esterified with ethanol during the titration, generating 11,11'-dithiobisundecanoic acid, diethyl ester.

The crude disulfide diester precipitate was purified by extraction and recrystallization. In the extraction step, ether was added to the residue from the previous titration and warmed to dissolve the solid. The orange-brown solution and several ether rinses, yielding a total vol. of ~100 mL, were transferred to a 250-mL separatory funnel. Water-soluble compounds (e.g., HI) were removed with three extractions—one each of 20 mL of 10% NaCl in 0.5 M H_2SO_4, 20 mL of 10% NaCl in H_2O, and 10 mL H_2O. The first two extractions yielded three phases, and only the bottommost phase was removed and discarded each time. In the third extraction, the top (organic phase) was removed, dried over 10 g anhydrous sodium sulfate, and filtered. The solvent was removed by rotary evaporation. The 7.50 g of crude product (15.3 mmol, 71% yield from $HOOC(CH_2)_{10}Br$).

Of the crude disulfide diester, 4.70 g was recrystallized from 20 mL of hot CH_3CN. After filtering, more CH_3CN was added to the filtrate to avoid solidification upon cooling, since the differential solubility with respect to temperature is very high for this system. The resulting crystals were collected by filtration and rinsed with 75 mL CH_3CN and 50 mL MeOH—both at −10°C. The crystals, while still damp, were recrystallized from CH_3CN again, this time without filtering. After rinsing and drying, 2.86 g of recrystallized disulfide diester was obtained.

c. 11,11'-Dithiobisundecanoic acid

The disulfide diester was base-hydrolyzed to the corresponding diacid (Scheme III). A solution of 2.4 g (60 mmol) of NaOH in 25 mL H_2O was added to 2.4 g (4.9

mmol) of disulfide diester in a round-bottomed flask. The mixture was allowed to reflux for 12 h and then quenched in cold H_2O to make 200 mL total volume. Cooling the solution caused a thick white precipitate to form, so the suspension was heated, stirred until everything dissolved, and then vacuum filtered. To the warm solution, 15 mL of 4.0 M H_2SO_4 (120 mmol H^+) was added, producing a thick white precipitate. The precipitate was collected, rinsed with H_2O and ether, and partially air dried.

The disulfide diacid was recrystallized from 25 mL boiling EtOH, with filtration of the hot solution. The crystalline product was rinsed with EtOH at –10°C and ice-cold ether, followed by vacuum drying. The net mass of 11,11'-dithiobisundecanoic acid obtained was 0.88 g (2.0 mmol, 41% yield from the disulfide diester).

d. 7,8-Dimethyl-10-formylmethylisoalloxazine

The first step of the flavin chemistry involved oxidative cleavage of riboflavin to remove the ribityl group and yield the aldehyde 7,8-dimethyl-10-formylmethylisoalloxazine (**4**) (Scheme II), following a procedure from the literature.[17] Briefly, 28.7 g (76 mmol) riboflavin was oxidized with 63 g of H_5IO_6 to produce 19.6 g of **4** (69.0 mmol, 91% yield).

e. 7,8-Dimethyl-10-(2'-hydroxyethyl)-isoalloxazine

The flavin aldehyde **4** was reduced to the analogous flavin alcohol, 7,8-dimethyl-10-(2'-hydroxyethyl)-isoalloxazine (**3**), using sodium borohydride (Scheme II), again following a published procedure.[17] Reduction of 15.3 g of **4** with 2.0 g $NaBH_4$ yielded 12.10 g of **3** (42.3 mmol, 79% yield from the aldehyde).

f. 11,11'-Dithiobisundecanoyl chloride

Immediately before esterification of **3** with 11,11'-dithiobisundecanoic acid, the latter was converted to the corresponding diacyl halide, 11,11'-dithiobisundecanoyl

chloride (Scheme III). In this step, 10 mL of heptanes and 0.87 mL of oxalyl chloride (1.27 g, 10 mmol) were added to 0.435 g of 11,11'-dithiobisundecanoic acid (1.0 mmol). The mixture was stirred at room temperature for 1 h and heated slowly until all of the acid dissolved (~20 min). The solution was allowed to cool and then vacuum filtered; rinses of the flask with more heptanes were added to the solution.

The volume (initially ~25 mL) of this solution was reduced to ~5 mL by rotary evaporation to remove excess oxalyl chloride. Heptanes (25 mL) was added again to the residue and the evaporation process repeated. The final product, which was thick, oily, and faintly yellow, was used directly in the next step.

g. Flavin disulfide

To the acyl chloride from the last step, 20 mL pyridine was added, which caused some of the former to precipitate out as a white solid. Next, 0.764 g of **3** (2.68 mmol) was added (Scheme II), giving a mixture that appeared green and orange. After the mixture was refluxed for 2.5 h, a sample of the reaction mixture was tested by TLC on silica gel plates with a solvent mixture of 7:2:1 1-butanol, chloroform, and glacial acetic acid. Comparison of the reaction mixture with pure **3** suggested that two esters had been partially formed (i.e., the mono- and di-esters). The mixture was refluxed 2.5 h more and tested again to show that more of the **3** had reacted. However, after an additional 10 h reflux, TLC revealed no further change.

After the 15-h refluxing, the reaction mixture cooled slightly for 2 min and then was vacuum-filtered. Material began to precipitate immediately in the filtrate as it cooled further, but no subsequent filtration was done. The volume of the suspension resulting from the filtration was reduced by rotary evaporation to remove almost all pyridine. Methanol (~20 mL) was added and then removed by evaporation. The product in the round-bottomed flask was a dark gum.

The flavin ester residue was recrystallized by dissolving in 80 mL boiling ethanol and vacuum filtering. The filtrate was set aside for 9 h in the dark. At that point, much orange precipitate had settled at the bottom of the orange-green fluorescent liquid. The supernatant was decanted off, reduced in volume by ~75% to produce more crystals, and recombined with the original precipitate. The solid product was collected and rinsed twice with ethanol at –10°C and twice with ether at 0°C. After drying by drawing air through for 15 min, 0.20 g of crystals were obtained (0.21 mmol, 21 % yield from the disulfide diacid if we assume that only the diester **1** was formed).

h. Chromatographic separation of esters

Because the final esterification step was an equilibrium process, it was necessary to purify the product by liquid chromatography in order to obtain only the diester. The best solvent system for separation of flavin esters (out of nine systems tested) was found to be a mixture of 1-butanol, chloroform, and glacial acetic acid in a volume ratio of 7:2:1 (this was used to test the products by TLC during the esterification). The ester was purified by flash chromatography of the recrystallized product, using silica gel (230-400 mesh) as the stationary phase. The second colored band was collected and this fraction was evaporated almost to dryness.

The residue from the chromatographic fraction, which contained some dissolved silica gel and residual acetic acid, was suspended in water to remove the acetic acid and recollected by vacuum filtration. After air was passed over the residue to remove water, the flavin diester was recrystallized in hot ethanol, with filtration to separate the silica gel.

i. Analysis of the intermediates and final product

The stable intermediates and final product in the synthesis of **1** were analyzed by mass spectrometry and melting point determination. The results of these tests are shown

in Table 1. In addition, ^{1}H NMR spectroscopy was used to verify the identity of most of the intermediates.

2. Preparation of films

Monolayer films used for both electrochemical and spectroscopic studies were prepared on Au-coated silicon substrates, as described previously.[1] Immersion times in the ethanolic solutions (~0.1 mM) were typically 24 h. Attempts to assemble films on Au from saturated solutions of **1** in water or aqueous buffer resulted in very poor coverages and reproducibility. All solutions, films, and stock bottles of **1** were shielded from light except during use.

Table 1. Characterization of intermediates and final product in the synthetic scheme.

			Mass spectrum		
Compound	Mol. formula	Mol wt.	Type[a]	m/z of parent	Melting range, °C[b]
11-mercaptoundecanoic acid	$C_{11}H_{22}O_2S$	218.36	E.I.	218.1	~45
11,11'-dithiobisundecanoic acid, diethyl ester	$C_{26}H_{50}O_4S_2$	490.7	E.I.	490	43.5-44.5
11,11'-dithiobisundecanoic acid	$C_{22}H_{42}O_4S_2$	434.71	E.I.	434.2	92-94
flavin aldehyde, **4**	$C_{14}H_{12}N_4O_3 \cdot H_2O$	284.3	C.I. (-)	284.1	275-77 (dec)
flavin alcohol, **3**	$C_{14}H_{14}N_4O_3$	286.3	C.I. (-)	286.2	310-12 (dec)
flavin disulfide, **1**	$C_{50}H_{66}O_8N_8S_2$	971.2	FAB	971	~230 (dec)

[a]Mass spectrometry was done using electron ionization (E.I.) negative-ion ionization (C.I.), or fast atom bombardment (FAB) with 3-nitrobenzyl alcohol as a matrix.

[b]Abbreviation: dec—decomposes upon melting.

3. Electrochemistry

Electrochemical measurements were carried out in a conventional three-electrode cell, with a Pt-coil counter electrode and an Ag/AgCl (sat. KCl) reference electrode. An inert elastomer gasket defined the geometric area of the working electrode as 1.33 cm^2. The cell was purged with Ultra High Purity grade Ar (Air Products) which passed through a gettering furnace (Centorr Associates). Cyclic voltammetric measurements utilized a CV-27 potentiostat (Bioanalytical Systems), whereas differential pulse voltammetry employed a Princeton Applied Research Model 174A polarographic analyzer. The output was recorded in both cases on a Houston Instruments Omnigraphic 2000 xy-recorder. All electrochemical measurements were made in aqueous buffers at 22 ± 2°C. Voltammetry at pH ≤ 8 utilized McIlvaine buffers adjusted to 1.0 M constant ionic strength.[18] Measurements at pH > 8 used a universal buffer system[19] containing borate, citrate, and phosphate with 0.1 M KCl added. Before each measurement, the solution was purged with dry Ar for 10 min and for at least 5 min the working electrode was either held at a potential ~100 mV positive of $E^{0'}$ for the flavin redox couple or scanned between oxidized and reduced forms.

4. IR spectroscopy

IR spectra were acquired with a Nicolet 740 FT-IR spectrometer equipped with a narrow-band, liquid nitrogen-cooled HgCdTe detector. Transmission measurements utilized 128 co-added scans of the solid materials dispersed in KBr or Fluorolube. Reflection spectra of the monolayer films used 1024 scans at 2 cm^{-1} resolution with p-polarized light incident at 80° from the surface normal. The background measurements for the reflection spectra used a monolayer film of octadecanethiolate-d_{37} on Au, the use and preparation of which are described elsewhere.[29]

5. Reagents

Decanethiol-d_{21} was synthesized from 1-bromodecane-d_{21} (Cambridge Isotopes) using a method from the literature for a related thiol.[20] The product was purified by fractional distillation and its identity confirmed by transmission IR spectroscopy. All other compounds were reagent grade. Deionized water was obtained from a Milli-Q purification system (Millipore).

C. RESULTS AND DISCUSSION

1. Mode of Flavin Attachment

This section presents and discusses examination of monolayers of 11-sulfidoundecanoic acid, 2-(7,8-dimethyl-10-isoalloxazino)ethyl ester at gold (**2**) with electrochemistry and IRRAS. In this study, we chose to attach the side chain to the 10-position of isoalloxazine for several reasons. This locus of attachment provided a relatively easy synthetic route, part of which had already been worked out, from the readily accessible riboflavin. Moreover, we did not expect this mode of attachment to alter significantly the reactivity and IR spectra of the isoalloxazine moiety from what is observed in riboflavin, FMN, and FAD—at least not through any intramolecular interactions. In all of these flavins the 10-ethyl group separates the isoalloxazine moiety from the side chain. The disulfide form of the adsorbate precursor was used instead of a thiol to avoid autooxidation of the thiol group by the flavin. Previous studies show that flavins in solution generally can oxidize thiols to the corresponding disulfides.[21]

Although some workers[6] have suggested that immobilization of flavins via the 8α methyl group offers the most promise for binding apoflavoproteins, many exceptions exist. For example, reaction rates of L-lactate oxidase, glucose oxidase and putrescine oxidase containing flavocoenzyme modified at the 8α position indicate that the 8α methyl group is buried within the apoprotein in these enzymes.[22] Also, one important issue in the biochemistry of flavins currently is the identification of types of riboflavin binding protein (RBP), which is present in trace amounts in plasma. Some types of RBP may contain heme, and binding of the protein at the surface of an electrode modified with **2** may offer additional means of characterizing the RBP. Experiments to bind and extract RBP from

tissue using flavins derivatized at N_{10} suggest that such proteins might also bind to **2**.[23] This is just one example of a possible application of **2** in bioanalytical chemistry.

2. Electrochemical Studies

a. Cyclic voltammetry and stability of films

Studies with cyclic and differential pulse voltammetry revealed the electrochemical response of the flavin film. Figure 1 shows a cyclic voltammogram (CV) of a film of **2** in pH 6.0 buffer scanned at 100 mV/s between 0 and -600 mV vs. Ag/AgCl, KCl(sat.) This scan was recorded after repeated scans had reached a steady state. The CV displays single current peaks at E_c = -350 mV and E_a = -290 mV—where E_c is the voltage of the current peak in the cathodic sweep, and E_c is the corresponding voltage in the anodic sweep. Here ΔE_p, which is defined as the separation between E_c and E_a, is 60 mV. The cathodic and anodic charge densities are Q_c/A = 53.4 $\mu C/cm^2$ and Q_a/A = 53.3 $\mu C/cm^2$. The corresponding coverage is $\Gamma = 2.77 \times 10^{-10}$ mol/cm^2, calculated from the average of cathodic and anodic charges. The shape of the anodic and cathodic waves are indicative of electron transfer with a surface-confined species. Also, the capacitance of the film appears not to change between the oxidized and reduced forms.

The monolayer was stable in both its oxidized and reduced forms; repetitive scanning at 100 mV/s at pH = 8.1 for 2.0 h resulted in a loss of coverage less than 15%, even in the presence of normal artificial room light. This observed stability is not surprising, since even films of FAD adsorbed on graphite displayed such stability.[24] We attribute the minor decrease in coverage observed to desorption of some physisorbed flavin molecules as a result of repeated cycling. Most of this decrease occurred in the first few minutes of scanning.

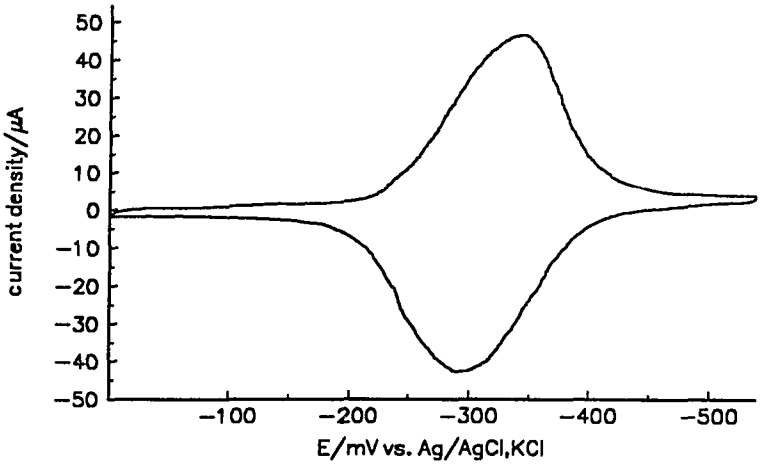

Figure 1. Cyclic voltammogram of film formed from **1**, scanned in pH 6.0 buffer at 25°C.

b. Adventitious oxidation of reduced species

Acquisition of a CV like that in Figure 1 with a fairly flat baseline required extensive purging of the cell with Ar to remove O_2, combined with either repetitive scanning across the redox region of the monolayer or holding the electrode voltage in the region of reduced flavin (this is usually done holding the applied voltage at -450 mV at pH $\approx$ 6), as noted in the Experimental Section. Without such treatment for > 10 min, CVs are obtained with $Q_c >> Q_a$, ostensibly due to catalytic reduction of O_2 by the flavin film in its reduced state.

c. Coverage

Coverages (Γ) of films of **2** measured from the peak area of CVs varied, but values up to $\Gamma = 3.2 \times 10^{-10}$ mol/cm^2 were obtained. For comparison, measurements of a molecular model of 7,8-dimethylisoalloxazine give areas of 1.04 nm^2/molecule if the molecules are placed flat on a surface (with their rings parallel to the surface) or 0.43

nm^2/molecule if they are closest packed while standing on their long edge. Those areas, calculated based on the van der Waals radii of the molecule, correspond to theoretical maximum coverages of 1.60 x 10^{-10} mol/cm^2 in the flat-lying orientation and 3.86 x 10^{-10} mol/cm^2 in the upright orientation. These values imply that the flavin groups in **2** are packed side-by-side with their rings nearly normal—and their long axes nearly parallel—to the surface of the monolayer; their size is probably the factor that limits Γ. Our experimental Γ values are somewhat less than the value of 3.86 x 10^{-10} mol/cm^2 predicted for a side-by-side orientation probably because the large, bulky adsorbate precursor has difficulty packing with the degree of order typical of methyl-terminated alkanethiolate monolayers and because the ester group introduces some steric hindrance into the adsorbate.

d. Dependence of voltammetry on scan rate

To study the scan-rate dependence of the peak current density, cyclic voltammograms of a film of **2** were scanned in pH 5.69 buffer at scan rates varying from 5 to 500 mV/s to see the relationship between dV/dt and the current density (i/A) values of the cathodic and anodic peaks. Plots of log(i/A) vs. log(dV/dt) were linear in this range and exhibited a slope of 0.985 for the cathodic wave and 0.955 for the anodic wave. The occurrence of such a linear relationship with slope ≈ 1.0 implies that the faradaic current from these peaks is due exclusively to a surface-bound redox species. The potentials of cathodic and anodic peaks were E_c = -340 ± 10 mV and E_a = -290 ± 10 mV throughout this range of scan rates, indicating that electron-transfer is kinetically reversible in this time scale.

e. Variation of redox potential with pH

The electrochemical behavior of **2** varies with pH. At pH > 6, two peaks appear in the CVs in both cathodic and anodic directions. At pH < 8, the peaks at more negative

voltages predominate over the other two; but at pH > 8.5 the pair of peaks at less negative voltages predominates. The use of differential pulse voltammetry helped clear up the dependence of the peak voltages E_p on pH. Figure 2 illustrates DPVs obtained for a film at pH 6.0 and 8.1.

The dependence of the number and voltages of the DPV current peaks on pH is illustrated in Figure 3. The differential pulse technique gives a single current peak for each redox wave, the voltage of which is approximately equal to $E^{0'}$ and to the average of E_c and E_a measured from CVs. As Figure 3 shows, the peak voltages at low pH appear collinear with the set of peaks at more negative voltages at higher pH (we refer to these collectively as "Set 1"). A linear least squares fit of those points yields a slope of -60.5 mV/pH and a y-intercept of 26.4 mV. In contrast, the E values of the less-negative peaks ("Set 2"), which occur only at high pH, do not seem to have a linear relationship. The E values of Set 2 seem to merge with Set 1 asymptotically at pH ≈ 6. At pH > 9 the two sets of peaks have a fairly constant separation in peak voltage (E_p) with increasing pH; however, we did not measure DPVs or CVs at pH > 11 to avoid base-catalyzed hydrolysis

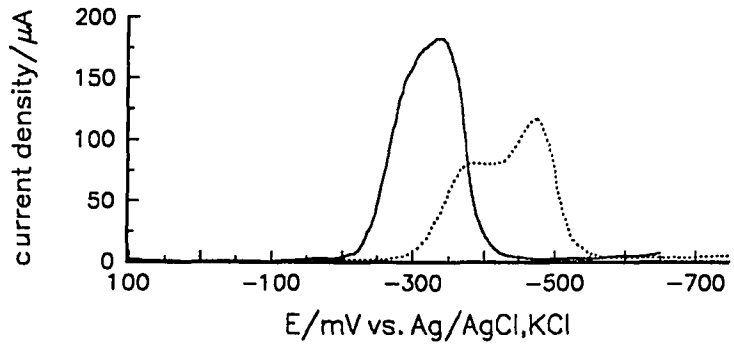

Figure 2. Differential pulse voltammograms of the flavin films in pH 6.0 (—) and 8.1 (· · ·). DPVs were scanned at 2 mV/s with a pulse amplitude of 10 mV.

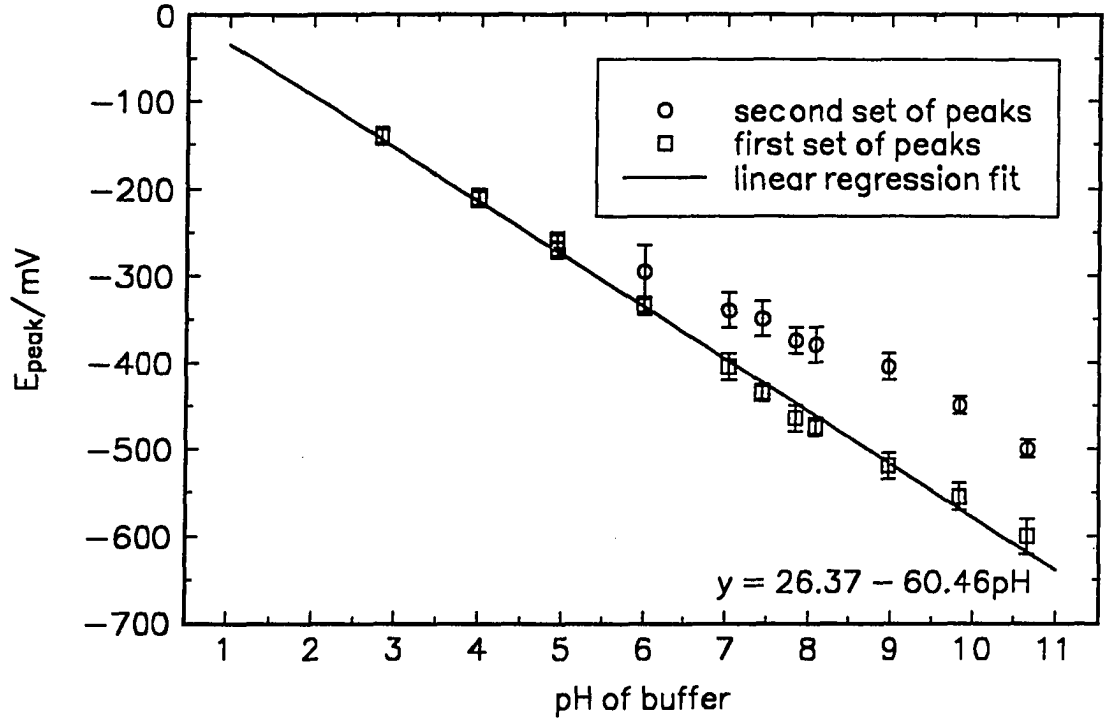

Figure 3. Variation of peak potential with pH, determined from differential pulse voltammetry. The error bars represent the uncertainty in visually determining peak potentials from the often overlapping peaks. The straight line is a least squares fit to the first set (Set 1) of peaks.

of the ester linkage in the monolayer. The behavior of this film with pH is similar to that of FAD multilayers adsorbed on graphite;[24] but the FAD degraded at pH ≥ 9.0, in contrast to monolayers of **2** which are stable at least up to pH ≈ 11. Our results are in stark contrast to those reported for a flavin immobilized via the 8-methyl group.[6] In that study, only one set of peaks was seen; those peaks appear to correspond to Set 2 here.

We attribute the emergence of Set 2 of voltammetric peaks at higher pH to an increase in the stability of the semiquinone intermediate. This effect is complicated by the multiple equilibria between neutral and anionic forms of the flavin in its three redox states,

shown in Scheme IV (at the pH values used in our work, the cationic forms of the flavin are insignificant).[5,24] Indeed, equilibrium calculations for the related molecule FMN have shown that the relative concentration of flavosemiquinone in the presence of both the flavoquinone and the flavohydroquinone form is greatest in the approximate region $8 \leq pH \leq 9.5$.[5] This phenomenon appears to translate to the surface, as indicated by the presence of two peaks with approximately equal peak currents in the CVs and DPVs in this intermediate pH range.

Although it is difficult to resolve the two DPV peaks observed in the range $6 \leq pH \leq 8$, Set 2 of peaks may correspond to the pH dependence of E_p previously observed for the flavin tethered via the 8-methyl group.[6] In that study, the plot of E_p vs. pH displayed a linear region with slope -40 mV/pH at intermediate pH (between pH 6.3 and 10.6) and a region with slope -56 mV/pH above pH 10.6. The peaks at high pH, corresponding to Set 1 in this study, were not observed. Their absence suggests that the semiquinone intermediate, which is stable for films of **2** at higher pH values, is not stable for the 8-methyl-derivatized flavin, possibly due to effects of the side chain upon the electronic structure of the isoalloxazine rings. If this is the case, **2** may be a more suitable candidate for subsequent studies of association of the flavosemiquinone with the fully reduced or oxidized species.

f. Mixed monolayers of 2 with a methyl-terminated alkanethiolate

In a preliminary study to examine any effects which may result from the vacant space between alkyl chains or the close packing of isoalloxazines in films of **2**, we produced mixed monolayers of the flavin thiolate with a methyl-terminated thiolate. The adsorbate precursor used to fill in the spaces was decanethiol-d_{21}. The chain length of

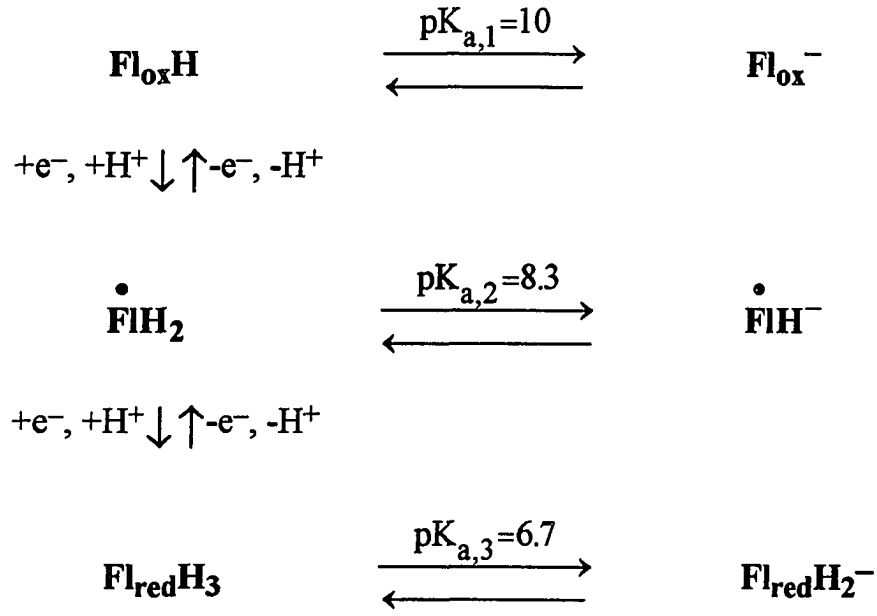

Scheme IV. Equilibria between various forms of flavins. The cationic forms, present at very low pH, are omitted for brevity. Here $\mathbf{Fl_{ox}H}$ represents the oxidized form of 7,8-dimethylisoalloxazine with a side chain at the 10 position. Adapted from Reference 5.

nine methylene units was used because it is approximately the same length as the straight-chain portion of **2**, and the deuterated form of the thiol was used to distinguish IRRAS bands of **2** from those of the interspersed alkanethiolate chains. The mixed monolayers were produced by taking previously adsorbed films of **2** and immersing them in $C_{10}D_{21}SH$ solutions for 3 h. This *decreased* the coverage of flavin-derivatized chains by one-half to one-third, as determined from peak areas of the CVs. Immersion of the films in the $C_{10}D_{21}SH$ solution for only 0.5 h resulted in a proportionally smaller decrease in coverage. Thus, the alkanethiol effectively displaced the flavin-derivatized chains, a result somewhat in contrast to a similar study using ferrocene-derivatized thiolate monolayers.[20]

In the study of the ferrocenyl monolayers, an alkanethiol appeared to displace only those ferrocene-derivatized chains in defect sites; even after long immersion times, the displacing thiol solution did not reduce the coverage of the original adsorbate by more than one-half. The cause of this disparity between the two systems is not known. Although I expected the $C_{10}D_{21}SH$ to "fill in the gaps" between the alkyl chains in the original monolayer, IRRAS of the mixed monolayer (not shown) indicated that the alkyl chains were still quite disordered after this treatment. This phenomenon suggests that the $C_{10}D_{21}SH$ adsorbed and displaced **2** only in distinct regions in the original monolayer, thereby reducing the coverage of flavin groups but not increasing the order of the chains to which they are attached.

It is important to note that immersion of films of **2** into thiol solutions probably results in gradual oxidation of the dissolved thiol. As discussed above, flavins generally can oxidize thiols to disulfides. If any O_2 is present, it will subsequently and quickly reoxidize the dihydroflavin. Since I made no attempt to exclude O_2 from the solutions of $C_{10}D_{21}SH$, I assume that the disulfide $(C_{10}D_{21}S)_2$ is the species that interacts with the surface.

The partial displacement of **2** by $C_{10}D_{21}S$/Au in the mixed monolayer affected the peak potentials of the CVs slightly at pH 6.0, relative to their positions in Figure 1. In a mixed layer containing ~30% of full coverage, E_c = -350 mV and E_a = -330 mV. These values indicate that association between flavin groups may affect electron transfer and the stability of the flavosemiquinone, although further study of this matter is needed. Surprisingly, ΔE_p is only 20 mV for this mixed film—much less than the 60 mV observed for the full monolayer of **2**. In addition, ΔE_p increases with scan rate; for example, at dV/dt = 800 mV/s, I observed ΔE_p = 60 mV. This value suggests that the rate of electron transfer is less in the mixed monolayer than in the full monolayer of **2**.

3. IR Studies

a. Spectra for bulk and monolayer forms of the flavin compound

This subsection presents the IR spectra, which potentially give considerable information about the structure, orientation, and degree of order of the film. Figure 4a shows an IRRA spectrum of **2** in the low-energy region and Figure 5a in the high-energy region. The absorbances observed are consistent with the formation of a monomolecular film. For comparison, Figures 4d and 5d contain a spectrum of **1** as a Fluorolube mull and Figures 4b and 5b a spectrum of **3**, the precursor of **1**. Also, spectra are shown in Figures 4c and 5c of compound **6**, an analog of **1** having a methyl group in place of the disulfide group. Oddly, the monolayer spectrum resembles the crystalline form of **3** more than it resembles **1**. We attribute this to inhomogeneous broadening arising from the inability of **1** to form ordered crystals due to the long dialkyl disulfide chain (see below). On the other hand, both crystalline **3** and monolayers of **2** can form ordered condensed phases in which the isoalloxazine rings can arrange themselves side by side.

b. Band assignments and discussion of spectral features

Many of the bands due to the flavin group can be assigned easily, based on earlier work in which the normal modes for lumiflavin (**5**) were calculated and determined experimentally.[25,26] In this section, I present probable assignments for most of the bands observed in the low-frequency region in the spectrum of **2** (Figure 4a). The observed frequencies and band assignments are summarized in Table 2 for **2**, **3**, and **6**. At the same time, I discuss some of the features particular to the monolayer-bound form of this type of isoalloxazine derivative and make some inferences about the degree of order in the film.

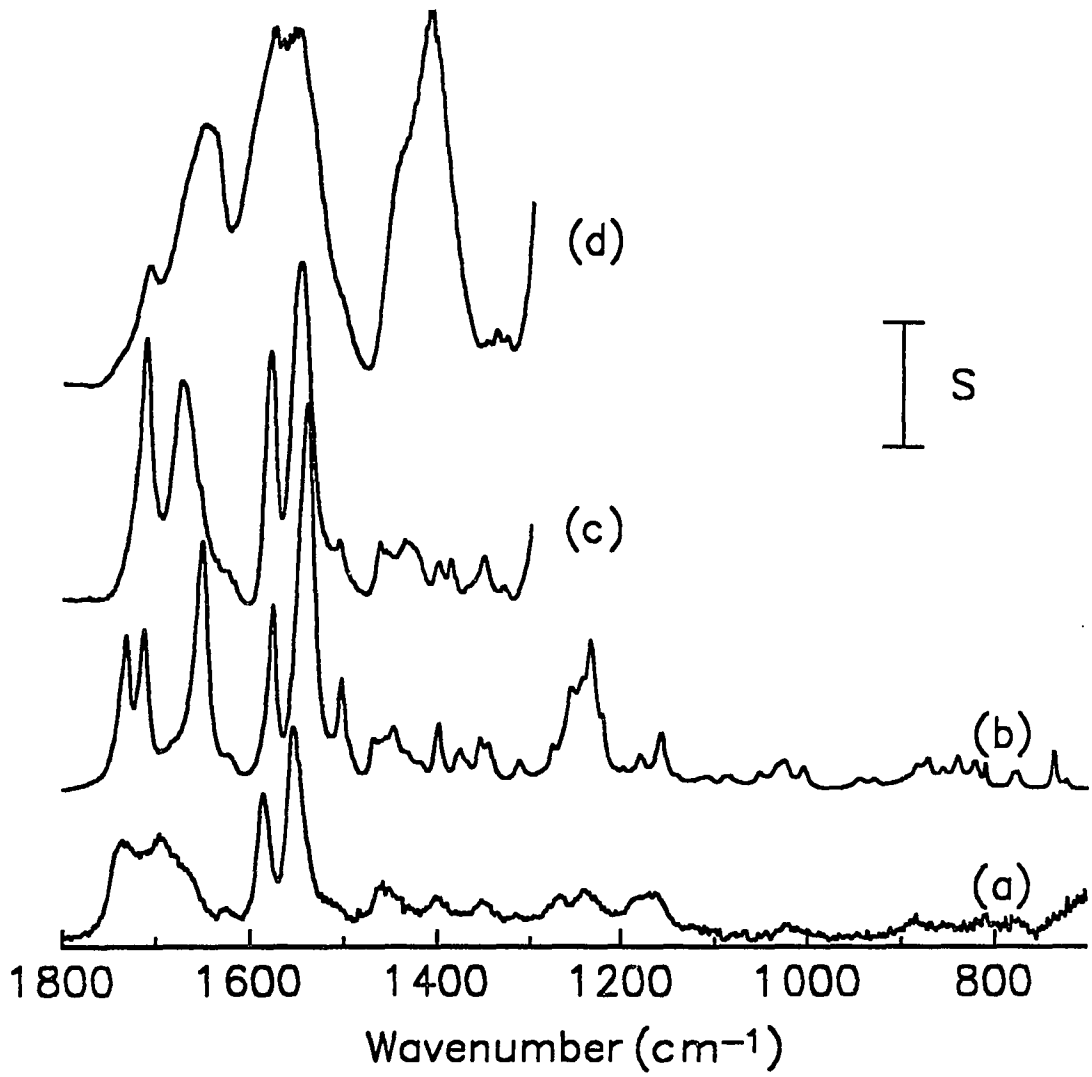

Figure 4. (a) IRRA spectrum in the low energy region of a monolayer of **2** at Au (S = 2.0 x 10^{-4} A.U.); and transmission spectra in the low energy region of: (b) bulk flavin dodecanoate ester **6** as a KBr pellet (S = 0.4 A.U.); (c) bulk flavin alcohol analog **3** as a mull with Fluorolube (S = 0.2 A.U.); (d) adsorbate precursor **1** as a Fluorolube mull (S = 0.4 A.U.). Spectra c and d are cut off below 1300 cm^{-1} because Fluorolube absorbs strongly in that region.

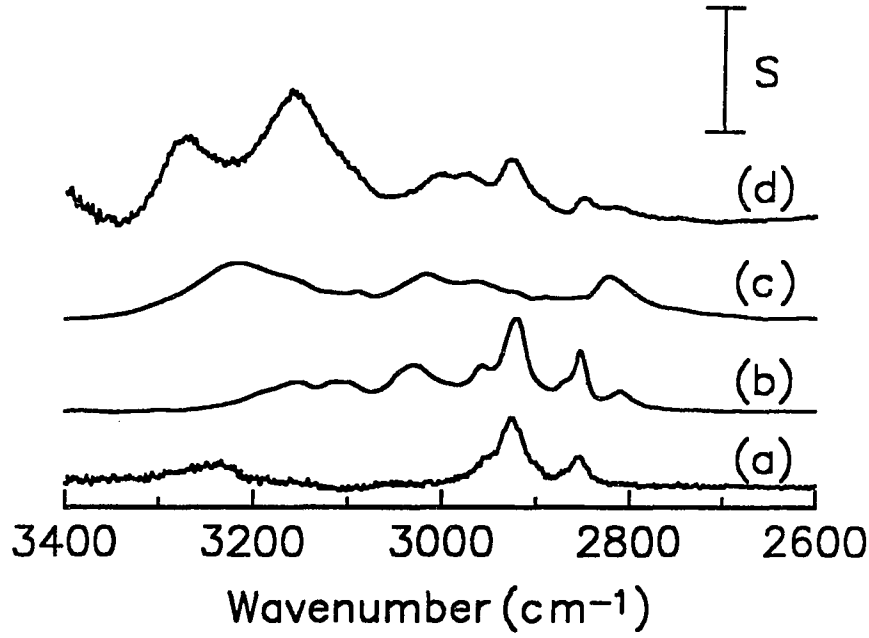

Figure 5. (a) IRRA spectrum in the high energy region of a monolayer of **2** at Au (S = 2.0 x 10^{-4} A.U.); and transmission spectra in the high energy region of: (b) bulk flavin dodecanoate ester **6** as a KBr pellet (S = 0.4 A.U.); (c) bulk flavin alcohol analog **3** as a mull with Fluorolube (S = 0.2 A.U.); (d) adsorbate precursor **1** as a Fluorolube mull (S = 0.2 A.U.). Samples measured are the same as Figure 4.

Table 2. Peak positions[a] and mode assignments[b] for IR spectra of **2** and its analogs in the range of 1800 - 1000 cm^{-1}.

	observed frequency (cm^{-1})[c]		
mode assignments	monolayer, **2**	dodecanoate, **6**	alcohol, **3**
ν(C=O), ester	1737	1732	-
$\nu(C_4{=}O)$	~1715[d]	1714	1712
$\nu(C_2{=}O)$	1697	1651	1673
$\nu(C_{4a}C_{9a})$	1626	sh. ~1625	1626
ν(C=N), in phase	1587	1577	1579
ν(C=N), out of phase	1554	1539	1548
$\nu(C_{4a}N_5C_{5a})$	sh. ~1515	1503	1505
$\delta(CH_2)$	sh. ~1470	1469	-
xylene ring	1461	1448	1453, 1464
δ(OH)	-	-	1435
$\nu_a(N_1C_2N_3)$	1401	1400	1401
	-	1376	1386
pyrazine ring breathing mode	1352	1454	1350
pyrazine ring stretch	1315	1313	1330
ν(C-(C=O)-O), skeletal vibration or $\omega(CH_2O)$	sh. ~ 1280, 1267	1255	1287, 1276
$\nu(C_2N_3C_4)$, coupled with δ(NH)	1242	1235	1247
ν(C-O-C)	sh. ~ 1182	1179	-
pyrazine ring stretch	1161	1157	1174, 1153
$\nu(CH_2\text{-}O)$	-	-	1049
$\nu_s(N_1C_2N_3)$	1023	1027	1029

[a]Peak positions for **2** represent the average from measurements of 8 films. The assignments for **3** were determined from a spectrum in KBr.

[b]Mode assignments are adapted from references 25, 26, 27, and 28. Most of the vibrations, especially of the isoalloxazine ring, involve many atoms. The vibrations of the atoms listed are the primary contributors to the given bands.

[c]Abbreviation: sh.—shoulder

[d]This band is not well resolved.

Starting at the high-energy end of Figure 4a, the carbonyl stretching frequencies appear first. These overlap and are quite broad. By comparison with the bulk spectra of **3** and other flavin compounds, we would expect three ν(C=O) bands—one for the ester linkage around 1740 cm^{-1} and two corresponding mostly to the vibrations of C_4=O and C_2=O at ~1700 and ~1650 cm^{-1}, respectively. In **2**, ν(C=O) for the ester appears at 1737 cm^{-1}, but only one other band appears clearly. I attribute the 1697-cm^{-1} peak to the mode that is due mostly to C_2=O, which appears at 1673 cm^{-1} in the spectrum of **3** (Figure 4c). This band shifts to higher energy because the end group of the monolayer is restricted so that hydrogen bonds cannot easily form between the C_2=O or C_4=O group in one molecule and the N_3–H in another. Previous evidence that tetraacetylriboflavin in dilute chloroform solution exhibits the same three respective carbonyl modes at 1745, 1717, and 1694 cm^{-1} supports our assertion.[26] The remaining carbonyl mode, which is due mostly to C_4=O, probably lies between the bands at 1737 and 1697 cm^{-1} in Figure 4a, since I sometimes observe a small band in the region 1712-1720 cm^{-1}, slightly above the noise. The ν(C_4=O) mode appears at 1712 cm^{-1} in crystalline **3** (Figure 4c). Next, there is a small band at 1626 cm^{-1}. Previous normal mode calculations assign this band to the xylene ring, mostly to the C_{4a}–C_{9a} bond.[25]

The most characteristic spectral signature of flavins is the pair of modes assigned mostly to the two C=N bonds. Figure 4a shows these modes for **2** at 1587 and 1554 cm^{-1}, close to the values observed for crystalline **5**[26] but at higher energy by 8 and 6 cm^{-1} than the values for **3** (Figure 4c). These bands appeared in the same region, and with nearly the same resolution and relative intensities, in spectra of all other analogous flavin compounds we tested. The only exception was the bulk spectra of **1**, discussed below.

Several less-intense peaks appear in Figure 4a between 1500 and 1000 cm^{-1}. Most of these are attributed to various delocalized vibrations of the isoalloxazine ring

system; these correlate well with band assignments of spectra of other flavins.[25,26] A group of overlapping bands appears with a maximum at 1461 cm^{-1}. This group may be due to vibrations involving mostly the xylene ring; however, the $\delta(CH_2)$ mode probably is included as a high-energy shoulder here. The band at 1401 cm^{-1} is attributed to the mode involving N_1–C_2–N_3 bonds. The 1352-cm^{-1} band is probably due to a breathing-like mode of the central pyrazine ring. Next, two unresolved bands appear at 1267 and 1242 cm^{-1}. I attribute the former to an ester mode, possibly overlapping with the wag of the α-CH_2 group of the ester or a ring mode of isoalloxazine. The 1242-cm^{-1} band arises mostly from stretching of the C_2–N_3–C_4 bonds, coupled with the N_3–H bend (analogous to the so-called "amide II" band). The broad band with a peak at 1161 cm^{-1} probably contains a stretching mode of the pyrazine ring. In addition, I place the other ester mode at the high-energy side of this band; in fact, I see another peak at ~1183 cm^{-1} in other spectra of **2** that I attribute to the ester. This variation in the appearance of that peak suggests that the average orientation of ester groups with respect to the surface may vary from film to film. The weak band at 1023 cm^{-1} probably arises from the mode involving the N_1–C_2–N_3 bonds.

I have not attempted a detailed analysis of the high-frequency region of the spectrum in Figure 5a. At ~ 3250 cm^{-1} is a band corresponding to $\nu(N_3$–H). The most important observation here is that the bands corresponding to the C–H stretching modes are significantly higher in energy compared to methyl-terminated alkanethiolates at Au.[29] In Figure 5a, $\nu_a(CH_2)$ appears at 2926 cm^{-1} and $\nu_s(CH_2)$ at 2853 cm^{-1}. These frequencies suggest that the alkyl chains in the films of **2** are very disordered, in contrast to the higher degree of order apparent in the end group. Taken together, Figures 4a and 5a suggest a structure of **2** in which the end groups are fairly tightly packed, although with some disorder; but the underlying alkyl chains are much more disordered.

c. The IR spectrum of the bulk adsorbate precursor

The differences between the spectrum of the monolayer of **2** in Figure 4a and that of the bulk adsorbate precursor **1** in Figure 4c are quite startling. The bulk compound shows only a few broad bands in the low-energy region: a shoulder at 1710 cm^{-1}, a band at 1650 cm^{-1}, a strong doublet at 1578 and 1553 cm^{-1}, and a strong band at 1412 cm^{-1}. The first two bands probably correspond the C=O modes of the flavin; the larger of the two has probably been shifted and intensified because intermolecular hydrogen bonding is possible in the bulk. Certainly, the doublet is due to the ubiquitous C=N modes. However, the origin of the mode at 1412 cm^{-1} is quite perplexing. This frequency corresponds to that usually observed for $\delta(CH_2)$ adjacent to a carbonyl group (as in the ester group of **1**), but the band is unusually strong and not observed at all in the monolayer spectrum. The transmission spectra of **1** measured for a KBr pellet or a Fluorolube mull were qualitatively equivalent. The only major difference was that the bands at 1710 and 1650 cm^{-1} were relatively more intense in the Fluorolube spectrum. The breadth of all the bands in the spectrum of Figure 4c implies a great amount of disorder in the solid state; probably **1** precipitated out of solution as a glassy solid during recrystallization.

For comparison, I synthesized and measured a KBr-pellet spectrum of **6**, an analog of **1** differing only by substitution of the disulfide linkage by a methyl group, and by the fact that it is not a dimer. The bulk spectrum of **6** in Figure 4b appears very similar to that of its precursor **3** shown in Figure 4c; only minor peak shifts—and changes in peaks that would be expected from the esterification—distinguish the two spectra. We believe that the linkage of two flavin groups by a long chain in solid **1** results in tangling of the disulfide chains and a large amount of disorder in the solid. On the other hand, the smaller molecules of **6** can pack in a more ordered fashion in a crystal. The positions of the C–H stretching bands in the bulk spectrum of **6** confirm this hypothesis. In the high-energy

region, $\nu_a(CH_2)$ falls at 2921 and $\nu_s(CH_2)$ at 2852 cm^{-1}; the lower energy of $\nu_a(CH_2)$ relative to Figure 5a indicates that the polymethylene chains of **6** are in a more crystalline environment than those of **1**.

d. Orientation of flavin group

I have not been able to make many decisive conclusions about the orientation of the flavin group in **2** on the basis of the IR spectra. The fact that most of the modes expected from the isoalloxazine group appear in the spectrum indicates that the rings are not parallel to the surface. However, the disparity between the spectra of the monolayer and its adsorbate precursor precludes a detailed orientational analysis. A few pieces of evidence suggest that the long axis of the isoalloxazine group lies nearly parallel to the surface. The band at ~1505 cm^{-1}, which appears in bulk spectra of **3**, **5**, and **6**, is absent (or possibly a weak shoulder) in the spectrum of **2**. This band has been assigned primarily to a stretching mode of C_{4a}–N_5–C_{5a} with a transition dipole nearly parallel to the long axis of the ring system.[25] On the other hand, the band at 1626 cm^{-1} which is due mostly to stretching of the C_{4a}–C_{9a} bond, is relatively stronger in the spectrum of **2** than in spectra of the bulk analogs. Both these findings are consistent with the isoalloxazine oriented with its long axis nearly parallel to the surface. Such an orientation is consistent with the electrochemically determined coverage of the monolayer (see part 2a above).

D. CONCLUSION

This section has demonstrated that a monolayer at Au constructed by derivatizing an alkanethiolate chain with a flavin via position 10 of 7,8-dimethylisoalloxazine exhibits remarkable stability and reversible electron transfer. The electrochemical behavior of this film shows that rapid electron transfer can occur between a flavin and a gold electrode surface even though the isoalloxazine ring system is not in direct contact with the gold. Further studies are needed with mixed monolayer systems incorporating a flavin to further elucidate the kinetics and mechanism of electron transfer. Preliminary studies in our laboratory also show that interaction with numerous inorganic and organic species (e.g., Ca^{2+} and dissolved aromatic acids) affects the electrochemical behavior of bound flavin, similar to effects seen previously in solution. This introduces the possibility of applying **2** as a sensor for one of those species.

This flavin monolayer is also a suitable candidate for future studies using in situ IR spectroelectrochemistry. Measurement of IR spectra of **2** in contact with buffer as a function of applied voltage may elucidate the role of intermolecular association upon the relative stabilities of the flavoquinone, flavosemiquinone, and flavohydroquinone species.

The stability of this flavin monolayer and the accessibility of the flavin groups to species in a contacting solution portend the application of this system in biochemistry as well. Future applications of this monolayer system may include the binding and electroanalysis of riboflavin binding protein—or binding of an apoflavoenzyme, followed by application of the resulting immobilized holoenzyme as a bioanalytical microsensor.

ACKNOWLEDGMENTS

The author expresses gratitude to Professor Alan Schwabacher for discussions and valuable advice concerning the design and synthesis of **1**. The assistance of Jan Beane in obtaining the mass spectra is acknowledged. For the FAB measurements, mass spectral determinations were made at the Midwest Center for Mass Spectrometry with partial support by the National Science Foundation, Biology Division (Grant No. DIR9017262). Ames Laboratory is operated for the U.S. Department of Energy by Iowa State University under Contract No. W-7405-eng-82.

REFERENCES AND NOTES

1. Widrig, C.A.; Chinkap, C.; Porter, M.D. *J. Electroanal. Chem.* **1991**, *310*, 335-59.
2. Bryant, M.A.; Pemberton, J.E. *J. Am. Chem. Soc.* **1991**, *113*, 8284-93.
3. Bain, C.D.; Biebuyck, H.A.; Whitesides, G.M. *Langmuir* **1989**, *5*, 723-27.
4. Troughton, E.B.; Bain, C.D.; Whitesides, G.M.; Nuzzo, R.G.; Allara, D.L.; Porter, M.D. *Langmuir* **1988**, *4*, 365.
5. *Chemistry and Biochemistry of Flavin Enzymes*, Vol I; Müller, F., Ed.; Boca Raton: CRC Press, 1991; Chapter 1.
6. Durfor, C.N.; Yenser, B.A.; Bowers, M.L. *J. Electroanal. Chem.* **1988**, *244*, 287-300.
7. Edwards, T.R.G.; Gani, D. *Tetrahedron* **1990**, *46*, 935-956.
8. Edwards, T.R.G.; Cunnane, V.J.; Parsons, R.; Gani, D.*J. Chem. Soc., Chem. Commun.* **1989**, *(15)*, 1041-1043.
9. Mallik, B.; Gani, D. *J. Electroanal. Chem.* **1992**, *326*, 37-49.
10. Miyawaki, O.; Wingard, L.B.Jr. *Biochim. et Biophys. Acta* **1985**, *838*, 60-68.
11. Miyawaki, O.; Wingard, L.B.Jr. *Biotechnol. Bioeng.* **1984**, *26*, 1364-1371.
12. Wingard, L.B.Jr.; Narasimhan, K.; Miyawaki, O. *Flavins Flavoproteins, Proc. Int. Symp., 8th* Bray, R.C.; Engel, P.C.; Mayhew, S.G., Eds.; de Gruyter: Berlin, 1984; pp 893-896.
13. Narasimhan, K.; Wingard, L.B.Jr. *J. Mol. Catal.* **1986**, *34*, 253-273.
14. See for example Ye, H.; Tong, W.; D' Souza, V.T. *J. Am. Chem. Soc.* **1992**, *114*, 5470-5472.
15. The systematic name for this compound is: undecanoic acid, 11,11'-dithiobis-, bis[2-(3,4-dihydro-7,8-dimethyl-2,4-dioxobenzo[g]pteridin-10(2H)-yl) ethyl]ester.

16. The structural drawing is flipped upside down, relative to its traditional presentation, to illustrate more accurately its probable orientation in the monolayer film.

17. Fall, H.H.; Petering, H.G. *J. Am. Chem. Soc.* **1956**, *78*, 377-380.

18. Elving, P.J.; Markowitz, J.M.; Rosenthal, I. *Anal. Chem.* **1956**, *28*, 1179-1180.

19. Perrin, D.D. *Buffers for pH and Metal Ion Control* Chapman and Hall: London, 1974; p.156.

20. Chidsey, C.E.D.; Bertozzi, C.R.; Putvinski, T.M.; Mujsce, A.M. *J. Am. Chem. Soc.* **1990**, *112*, 4301-4306.

21. Gibian, M.J.; Winkelman, D.V. *Tetrahedron Lett.* **1969**, *(44)*, 3901-3904.

22. Schopfer, L.M.; Massey, V.; Claiborne, A. in *Flavins and Flavoproteins* Massey, V.; Williams, C.H., Eds.; New York: Elsevier/North-Holland, 1982; pp 102-105.

23. Merrill, A.H.; Shapira, G.; McCormick, D.B. in *Flavins and Flavoproteins* Massey, V.; Williams, C.H., Eds.; New York: Elsevier/North-Holland, 1982; pp 508-513.

24. Gorton, L.; Johansson, G. *J. Electroanal. Chem. Interfacial Electrochem.* **1980**, *113*, 151-158.

25. Abe, M.; Kyogoku, Y.; Kitagawa, T.; Kawano, K.; Ohishi, N.; Takai-Suzuki, A.; Yagi, K. *Spectrochim. Acta, Part A*, **1986**, *42A*, 1059-68.

26. Abe, M.; Kyogoku, Y. *Spectrochim. Acta, Part A*, **1987**, *43A*, 1027-37.

27. Colthup, N.B.; Daly, L.H.; Wiberley, S.E. *Introduction to Infrared and Raman Spectroscopy*, 3rd ed.; Academic Press: San Diego, 1990; pp 215-33.

28. Popenoe, D.D.; Deinhammer, R.S.; Porter, M.D. Accepted for publication in *Langmuir*.

29. Porter, M.D.; Bright, T.B.; Allara, D.L.; Chidsey, C.E.D. *J. Am. Chem. Soc.* **1987**, *109*, 3559.

GENERAL CONCLUSIONS

This work has provided several important developments to the field of in situ IR spectroscopy. An analysis of the conditions of an IRRAS experiment using classical electromagnetic theory and calculations of MSEF has resulted in development of a suitable cell and conditions for IRRAS of an alkanethiolate film at an aqueous/metal interface. Tests of this cell by obtaining spectra of an octadecanethiolate film at the H_2O/Au and D_2O/Au interfaces have verified some of the conclusions from the model calculations and have helped identify the origin of several optical artifacts in the spectra.

In addition to the study of requisite conditions for high surface detectability, this dissertation has presented the application of the above spectroscopic technique to study an electrochemically active monolayer film. The study of the ferrocene-derivatized monolayer shows that oxidation and re-reduction of the film do not lead to detectable changes in orientation of the adsorbate. The preliminary study of an alkanethiolate film derivatized with isoalloxazine presages the use of that system for probing other types of electrochemically induced transformations in monolayer films.

Finally, the outlook for future developments and applications of our in situ technique warrants some comments. One of the major future applications of self-assembled monolayer films appears to be in microelectronics, where they may be used passively (as capacitors, insulators, etc.) or actively (if derivatized with moieties bearing faradaic, electrically conductive, or photochemical response). As new films and applications are developed, in situ IRSEC with and without electrochemical modulation will prove valuable for probing the structure and reactivity of the films.

In situ IRRAS also holds promise for new applications in biomedical and biotechnological fields. It may be applied, for example, to the study of natural or synthetic

bilayer membranes. As the work on the flavin-derivatized monolayer suggests, in situ IRRAS combined with other techniques may lead to new types of chemically modified electrodes for analysis of physiologically relevant species. All of these considerations pose a bright future for in situ IR techniques.

LITERATURE CITED

1. Nuzzo, R.G.; Allara, D.L. *J. Am. Chem. Soc.* **1983,** *105*, 4481.
2. Troughton, E.B.; Bain, C.D.; Whitesides, G.M.; Nuzzo, R.G.; Allara, D.L.; Porter, M.D. *Langmuir* **1988,** *4*, 365.
3. Chidsey, C.E.D.; Loiacono, D.N. *Langmuir* **1990,** *6*, 682.
4. Thomas, R.C.; Sun, L.; Crooks, R.M.; Ricco, A.J. *Langmuir* **1991,** *7*, 620.
5. Bain, C.D.; Troughton, E.B.; Tao, Y.-T.; Evall, J.; Whitesides, G. M.; Nuzzo, R. *J. Am. Chem. Soc.* **1989,** *111*, 321-335.
6. Nuzzo, R.G ; Dubois, L.H.; Allara, D.L. *J. Am. Chem. Soc.* **1990,** *112*, 558.
7. Whitesides, G.M.; Laibinis, P.E. *Langmuir* **1990,** *6*, 87, and references therein.
8. Li, T.T.T.; Weaver, M.J. *J. Am. Chem. Soc.* **1984,** *106*, 6107.
9. Porter, M.D.; Bright, T.B.; Allara, D.L.; Chidsey, C.E.D. *J. Am. Chem. Soc.* **1987,** *109*, 3559.
10. Sabatani, E.; Rubenstein, I. *J. Phys. Chem.* **1987,** *91*, 6663.
11. Finklea, H.O.; Avery, S.; Lynch, M.; Furtsch, T. *Langmuir* **1987,** *3*, 409.
12. Widrig, C.A.; Chung, C.; Porter, M.D. *J. Electroanal. Chem.* **1991,** *310*, 335-59.
13. Bryant, M.A.; Pemberton, J.E. *J. Am. Chem. Soc.* **1991,** *113*, 8284-93.
14. Bain, C.D.; Biebuyck, H.A.; Whitesides, G.M. *Langmuir* **1989,** *5*, 723-27.
15. Stefely, J.; Markowitz, M.A.; Regen, S.L. *J. Am. Chem. Soc.* **1988,** *110*, 7463.
16. Bunding-Lee, K.A. *Langmuir* **1990,** *6*, 709.
17. Chidsey, C.E.D.; Bertozzi, C.R.; Putvinski, T.M.; Mujsce, A.M. *J. Am. Chem. Soc.* **1990,** *112*, 4301.

18. DeLong, H.C.; Buttry, D.A. *Langmuir* **1990**, *6*, 1319.

19. Alves, C.A.; Smith, E.L.; Porter, M.D. *J. Am. Chem. Soc.* **1992**, *114*, 1222-1227, and references therein.

20. Bewick, A.; Kunimatsu, K.; Pons, B.S. *Electrochim. Acta* **1980**, *25*, 465.

21. Russell, J.W.; Overend, J.; Scanlon, K.; Severson, M.; Bewick, A. *J. Phys. Chem.* **1982**, *86*, 3066.

22. Bewick, A.; Pons, B.S. In *Advances In Infrared and Raman Spectroscopy*; Clark, R.J.H.; Hester, R.E., Eds.; Wiley Heyden: London, 1985; Vol. 12, pp 1-63.

23. Foley, J.K.; Pons, B.S. *Anal. Chem.* **1985**, *57*, 945A.

24. Pons, B.S.; Foley, J.K.; Russell, J.; Severson, M. In *Modern Aspects of Electrochemistry*; No. 17; Bochris, J. O'M.; Conway, B.E. Eds.; Plenum: New York, 1986; p 223.

25. Ashley, K.; Pons, B.S. *Chem. Rev.* **1988**, *88*, 673.

26. C. Korzeniewski, and S. Pons, *Prog. Analyt. Spectrosc.* **1987**, *10*, 1.

27. Beden, B.; Lamy, C. In *Spectroelectrochemistry: Theory and Practice*; Gale, R.J., Ed.; Plenum Press: New York, 1988; 189.

28. Porter, M.D. *Anal. Chem.* **1988**, *60*, 1143A.

29. Seki, H.; Kunimatsu, K.; Golden, W.G. *Appl. Spectrosc.* **1985**, *39*, 437.

30. Stole, S.M.; Popenoe, D.D.; Porter, M.D. In *Electrochemical Interfaces: Modern Techniques for In-Situ Interface Characterization;* Abruña, H.D., Ed.; VCH: New York, 1991; pp 339-410.

31. Popenoe, D.D.; Stole, S.M.; Porter, M.D. *Appl. Spectrosc.* **1992**, *46*, 79-87.

32. Popenoe, D.D.; Deinhammer, R.S.; Porter, M.D. Accepted for publication in *Langmuir*.

33. Stole, S.M. Ph.D. Dissertation, Iowa State University, 1990.

34. Rajeshwar, K.; Lezna, R.O.; de Tacconi, N.R. *Anal. Chem.* **1992**, *64*, 429A-441A.

35. Hamnett, A.; Christensen, P.A.; Higgins, S.J. *Port. Electrochim. Acta* **1989**, *7*, 591-617.

36. Ong, Ward, Davies, Bain submitted as a Communication to the Editor, *J. Am. Chem. Soc.*, 1992.

37. Roth, J.D.; Weaver, M.J. *J. Electroanal. Chem. Interfacial Electrochem.*, **1991**, *307*, 119-137.

38. Roth, J.D.; Weaver, M.J. *Anal. Chem.* **1991**, *63*, 1603-1606.

39. Jiang, Z.; Xiang, Y.; Wang, J. *J. Electroanal. Chem. Interfacial Electrochem.* **1991**, *316*, 199-209.

40. Parry, D.B., The University of Utah, 1989, 203pp. Chair: Joel M. Harris; Diss. Abstracts No. DA9014321.

41. Faguy, P.W.; Fawcett, W.R. *Appl. Spectrosc.* **1990**, *44*, 1309-1316.

42. Chang, S.C.; Weaver, M.J. *Surf. Sci.* **1990**, *230*, 222-236.

43. Chang, S.C.; Weaver, M.J. *J. Phys. Chem.* **1990**, *94*, 5905-5102.

44. Chang, S.C.; Weaver, M.J. *J. Electroanal. Chem. Interfacial Electrochem.* **1990**, *285*, 263-272.

45. Jiang, X.; Chang, S.C.; Weaver, M.J. *J. Phys. Chem.* **1991**, *95*, 7453-7459.

46. Chang, S.C.; Weaver, M.J. *J. Phys. Chem.* **1991**, *95*, 5391-5400.

47. Roth, J.D.; Weaver, M.J. *Langmuir* **1992**, *8*, 1451-1458.

48. Yau, S.L.; Gao, X.; Chang, S.C.; Schardt, B.C.; Weaver, M.J. *J. Am. Chem. Soc.* **1991**, *113*, 6049-6056.

49. Bae, I.T.; Xing, X.; Liu, C.C.; Yeager, E. *J. Electroanal. Chem. Interfacial Electrochem.* **1990**, *284*, 335-349.

50. Bae, I.T.; Yeager, E.; Xiang, X.; Liu, C.C. *J. Electroanal. Chem. Interfacial Electrochem.* **1991**, *309*, 131-145.

51. Christensen, P.A.; Hamnett, A.; Muir, A.V.G.; Freeman, N.A. *J. Electroanal. Chem. Interfacial Electrochem.* **1990**, *288*, 197-215.

52. Huang, H.; Fierro, C.; Scherson, D.; Yeager, E. *Langmuir* **1991**, *7*, 1154-1157.

53. Bae, I.T.; Sasaki, T.; Scherson, D.A. *J. Electroanal. Chem. Interfacial Electrochem.* **1991**, *297*, 185-195.

54. Anderson, M.R.; Huang, J. *J. Electroanal. Chem. Interfacial Electrochem.* **1991**, *318*, 335-347.

55. Gutierrez, C.; Caram, J.A.; Beden, B. *J. Electroanal. Chem. Interfacial Electrochem.* **1991**, *305*, 289-299.

56. McQuillan, J. *Chemistry in New Zealand*, June 1990, 61-64.

57. Kunimatsu, K. *Ber. Bunsen-Ges. Phys. Chem.* **1990**, *94*, 1025-1030.

58. Pham, M.C.; Moslih, J.; Simon, M.; Lacaze, P.C. *J. Electroanal. Chem. Interfacial Electrochem.* **1990**, *282*, 287-294.

59. Zippel, E.; Kellner, R.; Breiter, M.W. *J. Electroanal. Chem. Interfacial Electrochem.* **1990**, *289*, 297-298.

60. Olivi, P.; Bulhoes, L.O.S.; Beden, B.; Hahn, F.; Leger, J.M.; Lamy, C. *Port. Electrochim. Acta* **1991**, *9*, 279-82.

61. Christensen, P.; Paliteiro, C.; and Hamnett, A. *Port. Electrochim. Acta* **1991**, *9*, 275-278.

62. Sun, S; Yang, D.; Tian, Z. *Prog. Nat. Sci.* **1991**, *1*, 48-54.

63. Talonen, P.; Rastas, J.; Leppinen, J. *Surf. Interface Anal.* **1991**, *17*, 669-674.

64. Sasaki, T.; Bae, I.T.; Scherson, D.A.; Bravo,B.G.; Soriaga, M.P. *Langmuir* **1990**, *6*, 1234-1237.

65. Bothwell, M.E.; Soriaga, M.P. *J. Electroanal. Chem. Interfacial Electrochem.* **1990**, *295*, 123-138.

66. Bae, I.T.; Huang, H.; Yeager, E.B.; Scherson, D.A. *Langmuir* **1991**, *7*, 1558-1562.

67. Sariciftci, N.S.; Mehring, M.; and Neugebauer, H. *Synth. Met.* **1991**, *43*, 2971-2974.

68. You, J.; Wu, H *Chin. Chem. Lett.* **1991**, *2*, 55-56.

69. Datta, M.; Datta, A. *J. Phys. Chem.* **1990**, *94*, 8203-8207.

70. Datta, M.; Datta, A. *J. Chem. Soc., Chem. Commun.* **1991**, 33-4.

71. Neugebauer, H.; Moser, A.; Strecha, P.; Neckel, A. *J. Electroanal. Chem. Interfacial Electrochem.* **1990**, *137*, 1472-1475; and Tschinkel, W.; Neugebauer, H.; Neckel, A. *J. Electroanal. Chem. Interfacial Electrochem.* **1990**, *137*, 1475-1480.

72. Peter, L.M.; Blackwood, D.J.; Pons, S. *J. Electroanal. Chem. Interfacial Electrochem.* **1990**, *294*, 111-121.

73. Bewick, A.; Kalaji, M.; Larramona, G. *J. Electroanal. Chem. Interfacial Electrochem.*, **1991**, *318*, 207-221.

74. Habib, M.A.; Maheswari, S.P. *J. Electroanal. Chem. Interfacial Electrochem.* **1991**, *138*, 2029-2031.

75. Huang, H.; Zhao, M.; Xing, X.; Bae, I.T.; Scherson, D. *J. Electroanal. Chem. Interfacial Electrochem.* **1990**, *293*, 279-284.

76. Mandal, K.C.; Ozanam, F.; Chazalviel, J.N. *Appl. Phys. Lett.* **1990**, *57*, 2788-90.

77. Rao, A.V.; Ozanam, F.; Chazalviel, J.N. *J. Electron Spectrosc. Relat. Phenom.* **1990**, *54-55*, 1215-1218.

78. Rao, A.V.; Ozanam, F.; Chazalviel, J.N. *J. Electrochem. Soc.* **1991**, *138*, 153-159.

79. Christensen, P.A.; Hamnett, A. *Electrochim. Acta* **1991**, *36*, 1263-86.

80. Novak, P.; Vielstich, W. *DECHEMA Monogr.* **1990**, *121*, 311-321.

81. Novak, P.; Rasch, B.; Vielstich, W. *J. Electrochem. Soc.* **1991**, *138*, 3300-3304.

82. Novak, P.; Vielstich, W. *Mater. Sci. Forum* (Mater. Sci. High Technol.: MASHTEC '90, Pt. 2) 1990, *62-64*, 471-472.

83. Cattaneo, E.; Rasch, B.; Vielstich, W. *J. Appl. Electrochem.* **1991**, *21*, 885-894.

84. Rasch, B.; Cattaneo, E.; Novak, P.; Vielstich, W. *Electrochim. Acta* **1991**, *36*, 1397-1402.

85. Rasch, B.; Novak, P.; Vielstich, W. *Synth. Met.* **1991**, *43*, 2963-2966.

86. Pham, M.C.; Moslih, J. *Synth. Met.* **1990**, *39*, 109-115.

87. Pham, M.C.; Moslih, J.; Lacaze, P.C. *J. Electroanal. Chem. Interfacial Electrochem.* **1991**, *303*, 297-305.

88. Pham, M.C.; Moslih, J. *J. Electroanal. Chem. Interfacial Electrochem.* **1991**, *310*, 255-268.

89. Pham, M.C.; Moskih, J.; Chauveau, F.; Lacaze, P.C. *J. Appl. Electrochem.* **1991**, *21*, 902-909.

90. Pham, M.C.; Aeiyach, S.; Moslih, J.; Soubiran, P.; Lacaze, P.C. *J. Electroanal. Chem. Interfacial Electrochem.* **1990**, *277*, 327-336.

91. Pham, M.C.; Moslih, J.; Lacaze, P.C. *Bull. Soc. Chim. Fr.* **1990**, 32-37.

92. Zhou, Z. *Wuli Huaxue Xuebao* **1990**, *6*, 470-473.

93. Sariciftci, N.S.; Kuzmany, H.; Neugebauer, H.; Neckel, A. *J. Chem. Phys.* **1990**, *92*, 4530-4539.

94. Seeger, D.; Kowalchyk, W.; Korzeniewski, C. *Langmuir* **1990**, *6*, 1527-1534.

95. Hansen, W.N. *J. Opt. Soc. Am.* **1968**, *58*, 380.

96. McIntyre, J.D.E. In *Advances In Electrochemistry and Electrochemical Engineering*; Delahay, P.; Tobias, C.W., Eds.; Wiley: New York, 1973.

97. Allara, D.L.; Baca, A.; and Pryde, C.A. *Macromolecules* **1978**, *11*, 1215.

98. Hansen, W.N. In *Advances In Electrochemistry and Electrochemical Engineering*; Delahay, P.; Tobias, C.W., Eds.; Wiley: New York, 1973.

99. Heavens, O.S. *Optical Properties of Thin Solid Films*; Dover: New York, 1965.

100. Stern, F. In *Solid State Physics, Advances In Research and Applications*; Seitz, F.; and Turnbull, D., Eds.; Academic Press: New York, 1963; Vol. 15.

101. Jenkins, F.A., and White, H.A. *Fundamentals of Optics*, 3rd ed.; McGraw Hill: New York, 1957.

102. *CRC Handbook of Chemistry and Physics*; Weast, R.C., Ed.; CRC Press: Cleveland, OH, 1973.

103. Pearce, H.A., and Sheppard, N., *Surf. Sci.* **1976**, *59*, 205-17.

104. Porter, M.D.; Bright, T.B.; Allara, D.L.; Kuwana, T. *Anal. Chem.* **1986**, *58*, 2461-2465.

GLOSSARY OF TERMS AND ABBREVIATIONS

α	absorption coefficient in spectroscopy
A	absorbance; surface area
A.U.	absorbance units
ATR	attenuated total reflectance infrared spectroscopy
δ	designation of a bending vibrational mode; phase change in radians
d	thickness of a material or of a layer
$\hat{\varepsilon}$	complex dielectric constant
ε	real dielectric constant
E	magnitude of the electric field
E_{app}	value of applied voltage at the working electrode in an electrochemical cell
E_a, E_c	voltage corresponding to the peak current in voltammetry for the anodic and cathodic sweeps, respectively
$E^{0'}$	electrochemical redox potential corresponding to a reaction at the working electrode
ΔE_p	voltage difference between two current peaks in voltammetry
FWHM	full-width at half-maximum of a spectral band or voltammetric peak
γ	designates a bending vibrational mode out of the plane of an aromatic ring
Γ	surface coverage of an adsorbate
i	magnitude of the electric current
IR	infrared

IRRAS	infrared reflectance-absorbance spectroscopy
IRSEC	infrared spectroelectrochemistry
k	absorptive index (imaginary part of $\hat{n}$)
λ	wavelength
ν	wavenumber (cm^{-1})
$\hat{n}$	complex refractive index
n	refractive index (real part of $\hat{n}$)
n_∞	zero-frequency or baseline refractive index
Q	magnitude of the electric charge
θ	angle of a vector with respect to the surface normal
r	complex value of reflectivity; pertaining to reflection
R	reflectance (a real quantity)
RA	reflectance-absorbance
SS	stainless steel
T	transmittance (a real quantity)
t	complex value of transmissivity; pertaining to transmission
ω	designates a wagging vibrational mode
ξ	refractive coefficient (defined in text)
z	normalized distance from a surface or from the phase 1/phase 2 boundary in a stratified medium

APPENDIX 1. SOURCE LISTINGS OF COMPUTER PROGRAMS

1. Program for Calculating Mean Square Electric Fields

a. THREEPHASE


```
Line#  Source Line          Microsoft FORTRAN Optimizing Compiler Version 4.10

   1  C
   2  C                        T H R E E P H A S E
   3  C                        ===================
   4  C   ... a program to calculate electric field values in a three-phase
   5  C                           stratified medium.
   6  C
   7  C  IBM PC-AT VERSION FOR MICROSOFT FORTRAN!
   8  $DEBUG
   9  $NOFLOATCALLS
  10  $TITLE:'THREEPHASE'
  11  C
  12  C                                INTRODUCTION
  13  C                  This program calculates relative values of the cartesian
  14  C       components (x-, y-, and z-components) of the mean square electric
  15  C       field (MSEF) for a three phase stratified medium used in an external
  16  C       reflection experiment.  The calculations depend on the wavelength
  17  C       and angle of incidence of the radiation used as well as on the op-
  18  C       tical properties of the three phases used (i.e. the complex refrac-
  19  C       tive index "n-caret".  The relative MSEF values are calculated as a
  20  C       function of z (distance along the axis normal to the phase bounda-
  21  C       ries) at a fixed interval throughout Phase 2.  The calculation is
  22  C       also carried out a certain distance into Phase 1 (the incident
  23  C       phase) and into Phase 3, which distances can be set by the user.
  24  C                  The calculations of MSEF require one first to determine
  25  C       the complex Fresnel coefficients of reflection and transmission,
  26  C       as well as some other intermediate constants.  Most of the formulas
  27  C       used in this program come originally from:
  28  C         Wilford N. Hansen, "J. Opt. Soc. Am.", vol. 58, no.3, 1968,
  29  C         pp. 380-90
  30  C       In this reference, Hansen used the convention for the complex
  31  C       refractive index: "n-caret" = n + ik.
  32  C       Some corrections to the equations were obtained from:
  33  C         W. N. Hansen, Internal Reflection Spectroscopy in Electrochemistry,
  34  C         in vol. 9 of "Advances in Electrochemistry and Electrochemical
  35  C         Engineering," New York: John Wiley & Sons, 1973.
  36  C       The latter reference uses the convention: "n-caret" = n - ik,
  37  C       which is NOT used in this program.  Thus, many of the complex values
  38  C       derived in the latter paper must be replcaed by their complex con-
  39  C       jugates in order to agree with this program.  In general, variable
  40  C       names in this program are designed to resemble as much as possible
  41  C       the variables used in Hansen's papers.
  42  C
  43  C                SOURCE CODE FOR THE PROGRAM
  44  C
  45        PROGRAM THREEPHASE
  46  C
  47  C  Allocation of storage for arrays.
  48  C       The arrays for the MSEF (abbreviated "E") are named using the fol-
  49  C       lowing conventions:
  50  C                Phases: 1, 2, 3; Cartesian coordinates: x, y, z
  51  C                Perpendicular polarization = PRP
  52  C                Parallel polarization = PLL
  53        DIMENSION EPRP1Y(500), EPLL1X(500), EPLL1Z(500),
```

```
 Line#  Source Line          Microsoft FORTRAN Optimizing Compiler Version 4.10

    54       &           EPRP2Y(500), EPLL2X(500), EPLL2Z(500),
    55       &           EPRP3Y(200), EPLL3X(200), EPLL3Z(200)
#   56  C    The abscissae for the E values for the three phases are, respectively
    57        DIMENSION Z of 1(500), Z of 2(500), Z of 3(200)
    58
    59        INTRINSIC CMPLX, CABS, CONJG, CSQRT, CCOS, CSIN
    60        EXTERNAL ASCOUT
    61
    62  C                TYPE DECLARATIONS FOR VARIABLES USED IN THE PROGRAM
    63  C
    64  C       The refractive indices of each phase:
    65        REAL RFRIN1, N of 2, AK of 2, N of 3, AK of 3
    66        COMPLEX CREF 2, CREF 3
    67  C       Complex Fresnel coefficients of reflection and transmission:
    68        COMPLEX rPLL, rPRP, tPLL, tPRP
    69  C       Fresnel coefficients for the two interfaces:
    70        COMPLEX rPRP12, rPRP23, tPRP12, tPRP23,
    71       &        rPLL12, rPLL23, tPLL12, tPLL23
    72  C       Other complex variables
    73        COMPLEX CI, XI of 2, XI of 3, BETA 2
    74        COMPLEX cFCTRA, cFCTRB, cFCTRC, cFCTRD, cFCTRE
    75  C       Auxiliary variables:
    76        CHARACTER RESP, FILENAME*40
    77        LOGICAL FIRSTPASS
    78  C       Minimum value of z in Phase 1:
    79        REAL LIMZ 1
    80  C       Maximum value of z in Phase 3:
    81        REAL LIMZ 3
    82  C       Number of data points used in each phase:
    83        INTEGER NDAT 1, NDAT 2, NDAT 3
    84  C  Other variables whose type declarations are implicit:
    85  C       Phase changes (lower-case "delta"):
    86  C               DLTPLR is delta for parallel component upon reflection
    87  C               DLTPRR is delta for perpendicular component upon reflection
    88  C       Incident radiation:
    89  C               THT1 is the angle of incidence in radians
    90  C               THT1 DG is the angle of incidence in degrees
    91  C               WAVEL is the wavelength of radiation in Angstroms (A)
    92  C               WAVEN is the frequency of radiation in wavenumbers
    93  C               XI of 1 is a factor defined by Hansen.   It is real.
    94  C  Other parameters:
    95  C       Distance between points on z-axis used in calculation:
    96  C               DZ of 1, DZ of 2, DZ of 3
    97  C       Thickness of Phase 2: H of 2
    98  C       Real reflectance values (capital "R"):
    99  C               RRPLL, RRPRP
   100  C       Temporary variables used in calculations:
   101  C               FCTRA(n) where (n) is one of the following:
   102  C                  1A, 1B, 1C, 3A, 3B, 3C
   103
   104  C  Set initial values of constants and variables:
   105       PARAMETER (PI = 3.1415927)
   106       PARAMETER (CI = (0,1))
```

```
Line#  Source Line          Microsoft FORTRAN Optimizing Compiler Version 4.10

  107  C  Initialize all the array variables by setting them equal to zero:
  108        DATA EPRP1Y/500*0.0/, EPLL1X/500*0.0/, EPLL1Z/500*0.0/
  109        DATA EPRP2Y/500*0.0/, EPLL2X/500*0.0/, EPLL1Z/500*0.0/
  110        DATA EPRP3Y/200*0.0/, EPLL3X/200*0.0/, EPLL3Z/200*0.0/
  111        DATA Z of 1/500*0.0/, Z of 2/500*0.0/, Z of 3/200*0.0/
  112        DATA FIRSTPASS/.TRUE./
  113
  114  C  Begin the interactive part of the program.
  115  C                          DOCUMENTATION
  116        WRITE (*,'(A)') ' This is the program THREEPHASE, which calculates
  117       & relative values of the'
  118        WRITE (*,'(A)') ' cartesian components of MSEF for a three-phase
  119       & stratified medium. You must'
  120        WRITE (*,'(A)') ' provide values of the optical properties and oth
  121       &er experimental parameters.'
  122        WRITE (*, 410) 'The stratified medium is defined thus:'
  123     410 FORMAT ('0', A)
  124        WRITE (*, 420) '    Incident beam ---> PHASE1/PHASE2/PHASE3'
  125     420 FORMAT ('0', A)
  126        WRITE (*, 430) 'Phase 1 is assumed to be non-absorbing (k=0).'
  127     430 FORMAT ('0', A)
  128
  129  C                          INPUT USER DEFINED DATA
  130
  131  C  If the user decides to re-run the program, it will return to here.
  132     510 IF (FIRSTPASS) THEN
  133    WRITE (*,'(A)') ' '
  134    WRITE (*,'(A)') ' Enter the optical properties (include decimal
  135         & points).'
  136    GO TO 550
  137        ELSE
  138    WRITE (*, 520) ' The optical constants you have entered are:'
  139     520    FORMAT ('0', A)
  140    WRITE (*, 530) RFRIN1, N of 2, AK of 2, N of 3, AK of 3
  141     530    FORMAT (1X, 'N1= ', F5.2, ' N2= ', F5.2, ' K2= ', F6.3,
  142        &         ' N3= ', F5.2, ' K3= ', F6.3)
  143    WRITE (*, '(A\)') ' Are these values okay (type "y"or "n")? '
  144    READ (*,'(A1)') RESP
  145    IF ((RESP.EQ.'y') .OR. (RESP.EQ.'Y')) GO TO 600
  146        END IF
  147     550 WRITE (*,'(A\)') ' Enter n for Phase 1:'
  148        READ (*,'(F5.3)') RFRIN1
  149        WRITE (*,'(A\)') ' Enter n,k for Phase 2 (with comma):'
  150        READ (*, 570) N of 2, AK of 2
  151     570 FORMAT (BN, 2(F6.3))
  152        WRITE (*,'(A\)') ' Enter n,k for Phase 3 (with comma):'
  153        READ (*, 580) N of 3, AK of 3
  154     580 FORMAT (BN, 2(F6.3))
  155     600 IF (FIRSTPASS) THEN
  156    WRITE (*,'(A)') ' '
  157    WRITE (*,'(A)') ' Please provide some other parameters (include
  158         & decimal points).'
  159    GO TO 680
```

Line# Source Line Microsoft FORTRAN Optimizing Compiler Version 4.10

```
160         ELSE
161       WRITE (*, 620) ' Other parameters you have entered are'
162        620    FORMAT ('0', A)
163       WRITE (*, 650) H of 2, THT1 DG
164        650    FORMAT (1X, 'Thickness of Phase 2 = ', F7.0, 'A.',
165           &           2X, 'Angle of incidence = ', F4.1, ' degrees.')
166       WRITE (*, 660) WAVEN
167        660    FORMAT (1X, 'Frequency in wavenumbers = ', F7.1,
168           &   ', which is equivalent to a wavelength of ')
169       WRITE (*, 670) WAVEL/10000.0
170        670    FORMAT (1X, F7.3, ' microns.')
171       WRITE (*,'(A\)') ' Are these values okay (type "y" or "n")? '
172       READ (*, '(A1)') RESP
173       IF ((RESP.EQ.'y') .OR. (RESP.EQ.'Y')) GO TO 750
174         END IF
175        680 WRITE (*,'(A\)') ' What is the thickness of Phase 2 in A? '
176         READ (*, '(F8.1)') H of 2
177         WRITE (*,'(A\)') ' What is the frequency of incident radiation in
178        & wavenumbers? '
179         READ (*, '(F8.2)') WAVEN
180       C  Calculate the wavelength in angstroms:
181         WAVEL = 1.00E+08 / WAVEN
182         WRITE (*,'(A\)') ' What is the angle of incidence in degrees? '
183         READ (*, '(F5.2)') THT1 DG
184         WRITE (*, 700) H of 2 / WAVEL
185        700 FORMAT (1X, 'The thickness of Phase 2 in units of wavelengths',
186           & ' is: ', F8.3, '.')
187        750 IF (FIRSTPASS) GO TO 800
188         WRITE (*, 760) ' The parameters that control the iterations are se
189           &t as follows: '
190        760 FORMAT ('0', A)
191         WRITE (*, 770) LIMZ 1, LIMZ 3
192        770 FORMAT (1X, ' The calculation will go ', F8.0,
193           & ' A into Phase 1 and ', F7.0, ' A into Phase 3.')
194         WRITE (*,'(A)') ' The number of data points that will be generated
195           & in each phase is '
196         WRITE (*, 780) NDAT 1, NDAT 2, NDAT 3
197        780 FORMAT (1X, I3, ' points in Phase 1, ', I3,
198           & ' in Phase 2, and ', I3, ' in Phase 3.')
199         WRITE (*,'(A\)') ' Are these okay (type "y" or "n")? '
200         READ (*,'(A1)') RESP
201         IF ((RESP.EQ.'y') .OR. (RESP.EQ.'Y')) GO TO 1010
202        800 WRITE (*,'(A)') ' '
203         WRITE (*,'(A)') ' How far do you want the calculation to go into P
204           &hase 1 (in Angstroms)?'
205         READ (*, '(F9.1)') LIMZ 1
206         WRITE (*,'(A)') ' How far do you want to proceed into Phase 3?'
207         WRITE (*, 870) 0.1*WAVEL
208        870 FORMAT (1X, 'A recommended value is ', F7.1,
209           & 'A, or 1/10 of the wavelength:')
210         READ (*, '(F8.1)') LIMZ 3
211         WRITE (*,'(A)') ' The maximum number of data points is 500 in eac
212           &h of Phase 1 and Phase 2,'
```

Line# Source Line Microsoft FORTRAN Optimizing Compiler Version 4.10

```
      WRITE (*,'(A)') ' and 200 in Phase 3.  Enter the number of data
     &points to be used in'
      WRITE (*,'(A)') ' each phase.  Please type integers with no decima
     &l points, separated by'
      WRITE (*,'(A)') ' spaces or commas.'
      WRITE (*, '(A\)') ' Phase 1, Phase 2, Phase 3: '
      READ (*, 890) NDAT 1, NDAT 2, NDAT 3
  890 FORMAT (BN, 3I4)
#     C  If the user-set parameters have been entered for the first time, run throug
      C  the entry routine to allow the user to confirm or change them.
 1000 IF (FIRSTPASS) THEN
      FIRSTPASS = .FALSE.
      GO TO 510
      END IF
 1010 WRITE (*,'(A)') ' All user-set parameters have been confirmed.'
      PAUSE 'Type "CONTINUE<ret>" to proceed'

      C  Manipulation of the user-set parameters:
      CREF 2 = CMPLX (N of 2, AK of 2)
      CREF 3 = CMPLX (N of 3, AK of 3)
      THT1 = 2*PI*THT1 DG/360
      DZ of 1 = LIMZ 1/(NDAT 1 - 1)
      DZ of 2 = H of 2/(NDAT 2 - 1)
      DZ of 3 = LIMZ 3/(NDAT 3 - 1)

      C  Calculation of the intermediate coefficients XI and BETA:
      XI of 1 = SQRT(RFRIN1**2*(1-(SIN(THT1))**2))
      XI of 2 = CSQRT(CREF 2**2 - RFRIN1**2*(SIN(THT1))**2)
      XI of 3 = CSQRT(CREF 3**2 - RFRIN1**2*(SIN(THT1))**2)
      BETA 2  = 2*PI*H of 2/WAVEL* XI of 2

      C  Calculation of the complex Fresnel coefficients of reflection and
      C  transmission -- PERPENDICULAR polarization:
      rPRP12 = (XI of 1 - XI of 2)/(XI of 1 + XI of 2)
      rPRP23 = (XI of 2 - XI of 3)/(XI of 2 + XI of 3)
      rPRP = (rPRP12 + rPRP23*exp(2*CI*BETA 2))/
     &     (1 + rPRP12*rPRP23*exp(2*CI*BETA 2))
      tPRP12 = 2*XI of 1/(XI of 1 + XI of 2)
      tPRP23 = 2*XI of 2/(XI of 2 + XI of 3)
      tPRP = (tPRP12*tPRP23*exp(CI*BETA 2))/
     &    (1 + rPRP12*rPRP23*exp(2*CI*BETA 2))
      C  Fresnel coefficients -- PARALLEL polarization:
      rPLL12 = (CREF 2**2 * XI of 1 - RFRIN1**2 * XI of 2)/
     &         (CREF 2**2 * XI of 1 + RFRIN1**2 * XI of 2)
      rPLL23 = (CREF 3**2 * XI of 2 - CREF 2**2 * XI of 3)/
     &         (CREF 3**2 * XI of 2 + CREF 2**2 * XI of 3)
      rPLL = (rPLL12 + rPLL23*exp(2*CI*BETA 2))/
     &     (1 + rPLL12*rPLL23*exp(2*CI*BETA 2))
      tPLL12 = (2*RFRIN1*CREF 2*XI of 1)/
     &         (CREF 2**2 * XI of 1 + RFRIN1**2 * XI of 2)
      tPLL23 = (2*CREF 2*CREF 3*XI of 2)/
     &         (CREF 3**2 * XI of 2 + CREF 2**2 * XI of 3)
      tPLL = (tPLL12*tPLL23*exp(CI*BETA 2))/
```

Line# Source Line Microsoft FORTRAN Optimizing Compiler Version 4.10

```
      &    (1 + rPLL12*rPLL23*exp(2*CI*BETA 2))
C            Note that the complex Fresnel coefficient of reflection used in
C         all MSEF calculations is "t-subscript 'parallel'". This is equal to
C         "t-subscript 'H-parallel'" and was used in the calculations in
C         Hansen's 1973 review.  In his 1968 article he used a different
C         coefficient, "t-subscript 'E-parallel'", which is not used here.

C  Calculation of reflectivities:
       RRPRP = CABS(rPRP * CONJG(rPRP))
       RRPLL = CABS(rPLL * CONJG(rPLL))

C  Calculation of phase changes on reflection:
       DLTPRR = ARG(rPRP)
       DLTPLR = ARG(rPLL)
C         The function ARG finds the argument of a complex number and is
C         defined at the end of the program.)
       WRITE (*,'(A)') ' The phase changes on reflection are:'
       WRITE (*, 1200) DLTPRR/PI, DLTPLR/PI
 1200 FORMAT (6X, F4.2, ' X pi for perpendicular and ',
      &             F4.2, ' X pi for parallel polarization.')

C                          MSEF CALCULATIONS
C  Phase 1, PERPENDICULAR (y-component)
       Z = 0.0
       ADDND1 = 1.0 + RRPRP
       RPRSQROOT = SQRT(RRPRP)
       DO 1510 I=1, NDAT 1
EPRP1Y(I) = ADDND1 +
      &       2.0*RPRSQROOT*COS(DLTPRR - 4.0*PI*XI of 1*Z/WAVEL)
Z of 1(I) = Z
Z = Z - DZ of 1
 1510 CONTINUE
C  Phase 1, PARALLEL (x- and z-components)
       Z = 0.0
       FCTR1A = (COS(THT1))**2
       ADDND1 = 1.0 + RRPLL
       FCTR1B = 2.0*SQRT(RRPLL)
       FCTR1C = (SIN(THT1))**2
       DO 1540 I=1, NDAT 1
EPLL1X(I) = FCTR1A *
      &       (ADDND1 - FCTR1B*COS(DLTPLR - 4.0*PI*XI of 1*Z/WAVEL))
EPLL1Z(I) = FCTR1C *
      &       (ADDND1 + FCTR1B*COS(DLTPLR - 4.0*PI*XI of 1*Z/WAVEL))
Z = Z - DZ of 1
 1540 CONTINUE
C
C  Phase 3, PERPENDICULAR (y-component)
       Z = H of 2
       FCTR3A = CABS(tPRP*CONJG(tPRP))
       FCTR3B = -4.0*PI*AIMAG(XI of 3)/WAVEL
       DO 1610 I=1, NDAT 3
EPRP3Y(I) = FCTR3A * exp(FCTR3B*(Z - H of 2))
Z of 3(I) = Z
```

Line# Source Line Microsoft FORTRAN Optimizing Compiler Version 4.10

```
 319  Z = Z + DZ of 3
 320   1610 CONTINUE
 321  C  Phase 3, PARALLEL (x- and z-components)
 322        Z = H of 2
 323        FCTR3A = CABS((XI of 3*tPLL/CREF 3)*CONJG(XI of 3*tPLL/CREF 3))
 324  C        [The factor FCTR3B remains as above.]
 325        FCTR3C = CABS((RFRIN1*SIN(THT1)*tPLL/CREF 3)
 326       &         * CONJG(RFRIN1*SIN(THT1)*tPLL/CREF 3))
 327        DO 1640 I=1, NDAT 3
 328  EPLL3X(I) = FCTR3A * exp(FCTR3B*(Z - H of 2))
 329  EPLL3Z(I) = FCTR3C * exp(FCTR3B*(Z - H of 2))
 330  Z = Z + DZ of 3
 331   1640 CONTINUE
 332  C
 333  C Phase 2, PERPENDICULAR (y-component):
 334        Z = 0.0
 335        cFCTRA = 1.0 + rPRP
 336        cFCTRB = CI*(XI of 1/XI of 2) * (1.0 - rPRP)
 337        cFCTRC = 2.0 * PI * XI of 2/ WAVEL
 338        DO 1710 I=1, NDAT 2
 339  EPRP2Y(I) = CABS( (cFCTRA * CCOS(cFCTRC*Z)
 340       &                    + cFCTRB * CSIN(cFCTRC*Z) ) *
 341       &               (CONJG(cFCTRA * CCOS(cFCTRC*Z)
 342       &                    + cFCTRB * CSIN(cFCTRC*Z))) )
 343  Z of 2(I) = Z
 344  Z = Z + DZ of 2
 345   1710 CONTINUE
 346  C  Phase 2, PARALLEL (x- and z- components)
 347        Z = 0.0
 348        cFCTRA = COS(THT1) * (1.0 - rPLL)
 349        cFCTRB = (CI * XI of 2 * RFRIN1 / CREF 2**2) * (1.0 + rPLL)
 350        cFCTRC = (RFRIN1**2 / CREF 2**2) * SIN(THT1) * (1.0 + rPLL)
 351        cFCTRD = CI * (RFRIN1*SIN(THT1)/XI of 2) * COS(THT1)*(1.0 - rPLL)
 352        cFCTRE = 2.0 * PI * XI of 2 / WAVEL
 353        DO 1750 I=1, NDAT 2
 354  EPLL2X(I) = CABS( (cFCTRA * CCOS(cFCTRE*Z)
 355       &                + cFCTRB * CSIN(cFCTRE*Z)) *
 356       &           (CONJG(cFCTRA * CCOS(cFCTRE*Z)
 357       &                + cFCTRB * CSIN(cFCTRE*Z))) )
 358  EPLL2Z(I) = CABS( (cFCTRC * CCOS(cFCTRE*Z)
 359       &                + cFCTRD * CSIN(cFCTRE*Z)) *
 360       &           (CONJG(cFCTRC * CCOS(cFCTRE*Z)
 361       &                + cFCTRD * CSIN(cFCTRE*Z))) )
 362  Z = Z + DZ of 2
 363   1750 CONTINUE
 364  C  This is the end of the MSEF calculations.
 365        WRITE (*,'(1X, A)') 'The MSEF calculations are complete.'
 366
 367  C                          WRITING THE DATA TO FILES
 368  C  A summary of the results is printed at the keyboard.
 369        WRITE (*, 2010)
 370   2010 FORMAT ('0', 'MSEF values at the Phase 1/Phase 2 interface:')
 371        WRITE (*, 2020)
```

Line# Source Line Microsoft FORTRAN Optimizing Compiler Version 4.10

```
 372   2020 FORMAT (1X, 14X, 'E(Y)', 4X, 'E(X)', 4X, 'E(Z)')
 373        WRITE (*, 2030) EPRP1Y(1), EPLL1X(1), EPLL1Z(1)
 374   2030 FORMAT (4X, ' Phase 1:', 3(1X, F7.4))
 375        WRITE (*, 2040) EPRP2Y(1), EPLL2X(1), EPLL2Z(1)
 376   2040 FORMAT (4X, ' Phase 2:', 3(1X, F7.4))
 377        WRITE (*, 2050) H of 2
 378   2050 FORMAT ('0', 'MSEF values at the Phase 2/Phase 3 interface (Z=',
 379       &        F7.1, ' A):')
 380        WRITE (*, 2060)
 381   2060 FORMAT (1X, 14X, 'E(Y)', 4X, 'E(X)', 4X, 'E(Z)')
 382        WRITE (*, 2070) EPRP2Y(NDAT 2), EPLL2X(NDAT 2), EPLL2Z(NDAT 2)
 383   2070 FORMAT (4X, ' Phase 2:', 3(1X, F7.4))
 384        WRITE (*, 2080) EPRP3Y(1), EPLL3X(1), EPLL3Z(1)
 385   2080 FORMAT (4X, ' Phase 3:', 3(1X, F7.4))
 386        WRITE (*, '(A)') ' '
 387
 388   C  The data can now be written to files.
 389        WRITE (*, '(1X,A)') 'Do you want to print all the MSEF values to a
 390       & single file with headings'
 391        WRITE (*, '(A\)') ' (type "y" or "n")? '
 392        READ (*, '(A1)') RESP
 393        IF (.NOT.((RESP.EQ.'y') .OR. (RESP.EQ.'Y'))) GO TO 2500
 394        WRITE (*, '(A\)') ' What is the name of the output file? '
 395        READ (*, '(A40)') FILENAME
 396        OPEN (3, FILE=FILENAME, STATUS='new')
 397   C  Write a heading on the output file:
 398        WRITE (3,2180)'MSEF values for a three-phase stratified medium'
 399    2180 FORMAT (A)
 400        WRITE (3, 2200) THT1 DG
 401    2200 FORMAT ('Angle of incidence=', F4.1, ' degrees.')
 402    2210 FORMAT (4X, A)
 403        WRITE (3,2210) 'Note: columns 5-7 contain E values for a value of
 404       & Z midway between the'
 405        WRITE (3,2210) 'Z value given in the same row and the Z value in
 406       & the following row.'
 407   C  Write the data to the output file:
 408    2220 FORMAT (A)
 409        WRITE (3, 2220) 'Phase 1:'
 410    2230 FORMAT (5X, 'Z', 2(6X, 'E(Y)', 4X, 'E(X)', 4X, 'E(Z)'))
 411        WRITE (3, 2230)
#412   C       Format statements for a full and partial row of data are, respectively:
 413    2240 FORMAT (SP, F9.1, S, 3(1X, F7.4), 2X, 3(1X, F7.4))
 414    2250 FORMAT (SP, F9.1, S, 3(1X, F7.4))
 415        DO 2260 I=NDAT 1, 1, -2
 416   IF (I .GE. 2) THEN
 417     WRITE (3, 2240) Z of 1(I), EPRP1Y(I), EPLL1X(I), EPLL1Z(I),
 418       &                      EPRP1Y(I-1), EPLL1X(I-1), EPLL1Z(I-1)
 419   ELSE
 420     WRITE (3, 2250) Z of 1(I), EPRP1Y(I), EPLL1X(I), EPLL1Z(I)
 421   END IF
 422    2260 CONTINUE
 423
 424        WRITE (3, 2220) 'Phase 2:'
```

```
THREEPHASE                                                    PAGE   9
                                                              07-15-92
                                                              11:45:08

 Line#  Source Line          Microsoft FORTRAN Optimizing Compiler Version 4.10

   425        WRITE (3, 2230)
   426        DO 2300 I=1, NDAT 2, +2
   427   IF ((NDAT 2-I) .GE. 1) THEN
   428     WRITE (3, 2240) Z of 2(I), EPRP2Y(I), EPLL2X(I), EPLL2Z(I),
   429       &                    EPRP2Y(I+1), EPLL2X(I+1), EPLL2Z(I+1)
   430   ELSE
   431     WRITE (3, 2250) Z of 2(I), EPRP2Y(I), EPLL2X(I), EPLL2Z(I)
   432   END IF
   433    2300 CONTINUE
   434
   435        WRITE (3, 2220) 'Phase 3:'
   436        WRITE (3, 2230)
   437        DO 2360 I=1, NDAT 3, +2
   438   IF ((NDAT 3-I) .GE. 1) THEN
   439     WRITE (3, 2240) Z of 3(I), EPRP3Y(I), EPLL3X(I), EPLL3Z(I),
   440       &                    EPRP3Y(I+1), EPLL3X(I+1), EPLL3Z(I+1)
   441   ELSE
   442     WRITE (3, 2250) Z of 3(I), EPRP3Y(I), EPLL3X(I), EPLL3Z(I)
   443   END IF
   444    2360 CONTINUE
   445
   446        CLOSE (3)
   447        WRITE (*, 2400) FILENAME
   448    2400 FORMAT ('0', 'The program has written the data to ', A, '.')
   449
 # 450    2500      WRITE (*,'(A\)') ' Do you want to create files to be read by Spec
   451       &traCalc (type "y" or "n")? '
   452        READ (*,'(A)') RESP
   453        IF ((RESP .EQ. 'y') .OR. (RESP .EQ. 'Y'))
   454       &   CALL ASCOUT ( NDAT1,  NDAT2,  NDAT3, EPRP1Y, EPLL1X, EPLL1Z,
   455       &                EPRP2Y, EPLL2X, EPLL2Z, EPRP3Y, EPLL3X, EPLL3Z,
   456       &                Z of 1, Z of 2, Z of 3)
   457   C  [The above statement calls the external subroutine "ASCII_XY OUT",
   458   C  which must be separately compiled and linked to this program.]
   459
   460   C  Allow the user to repeat the calculation:
   461        WRITE (*, '(A\)') ' Do you want to perform another calculation (ty
   462       &pe "y" or "n")? '
   463        READ (*, '(A1)') RESP
   464        IF ((RESP .EQ. 'y') .OR. (RESP .EQ. 'Y')) GO TO 510
   465   C
   466        END


main  Local Symbols

Name                      Class   Type            Size   Offset

WAVEN . . . . . local   REAL*4             4    0002
RPRP. . . . . local   COMPLEX*8            8    0006
TPRP. . . . . local   COMPLEX*8            8    000e
I . . . . . local   INTEGER*4              4    0016
ADDND1. . . . . local   REAL*4            4    001a
```

Microsoft FORTRAN Optimizing Compiler Version 4.10

main Local Symbols

Name	Class	Type	Size	Offset
RRPLL	local	REAL*4	4	001e
BETA2	local	COMPLEX*8	8	0022
HOF2.	local	REAL*4	4	002a
DLTPLR.	local	REAL*4	4	002e
CREF2	local	COMPLEX*8	8	0032
CREF3	local	COMPLEX*8	8	003a
AKOF2	local	REAL*4	4	0042
AKOF3	local	REAL*4	4	0046
NOF2.	local	REAL*4	4	004a
RRPRP	local	REAL*4	4	004e
NOF3.	local	REAL*4	4	0052
DLTPRR.	local	REAL*4	4	0056
NDAT1	local	INTEGER*4	4	005a
NDAT2	local	INTEGER*4	4	005e
Z	local	REAL*4	4	0062
NDAT3	local	INTEGER*4	4	0066
RPLL12.	local	COMPLEX*8	8	006a
TPLL12.	local	COMPLEX*8	8	0072
RPLL23.	local	COMPLEX*8	8	007a
FCTR1A.	local	REAL*4	4	0082
THT1.	local	REAL*4	4	0086
TPLL23.	local	COMPLEX*8	8	008a
FCTR1B.	local	REAL*4	4	0092
FCTR3A.	local	REAL*4	4	0096
FCTR1C.	local	REAL*4	4	009a
FCTR3B.	local	REAL*4	4	009e
DZOF1	local	REAL*4	4	00a2
FCTR3C.	local	REAL*4	4	00a6
DZOF2	local	REAL*4	4	00aa
DZOF3	local	REAL*4	4	00ae
XIOF1	local	REAL*4	4	00b2
RPRP12.	local	COMPLEX*8	8	00b6
XIOF2	local	COMPLEX*8	8	00be
XIOF3	local	COMPLEX*8	8	00c6
TPRP12.	local	COMPLEX*8	8	00ce
RPRP23.	local	COMPLEX*8	8	00d6
RPRSQR.	local	REAL*4	4	00de
TPRP23.	local	COMPLEX*8	8	00e2
THT1DG.	local	REAL*4	4	00ea
LIMZ1	local	REAL*4	4	00ee
LIMZ3	local	REAL*4	4	00f2
FILENA.	local	CHAR*40	40	00f6
RFRIN1.	local	REAL*4	4	011e
CFCTRA.	local	COMPLEX*8	8	0122
CFCTRB.	local	COMPLEX*8	8	012a
CFCTRC.	local	COMPLEX*8	8	0132
CFCTRD.	local	COMPLEX*8	8	013a
CFCTRE.	local	COMPLEX*8	8	0142

Microsoft FORTRAN Optimizing Compiler Version 4.10

main Local Symbols

Name	Class	Type	Size	Offset
EPLL2Z.	local	REAL*4	2000	014a
EPRP1Y.	local	REAL*4	2000	081a
RESP.	local	CHAR*1	1	091a
RPLL.	local	COMPLEX*8	8	091c
TPLL.	local	COMPLEX*8	8	0924
WAVEL	local	REAL*4	4	092c
EPLL1X.	local	REAL*4	2000	0fea
EPLL1Z.	local	REAL*4	2000	17ba
EPRP2Y.	local	REAL*4	2000	1f8a
EPLL2X.	local	REAL*4	2000	275a
EPRP3Y.	local	REAL*4	800	2f2a
EPLL3X.	local	REAL*4	800	324a
EPLL3Z.	local	REAL*4	800	356a
ZOF1.	local	REAL*4	2000	388a
ZOF2.	local	REAL*4	2000	405a
ZOF3.	local	REAL*4	800	482a
FIRSTP.	local	LOGICAL*4	4	4b4a

Symbolic Constant	Type	Value
PI.	REAL*4	3.1415927E+000
CI.	COMPLEX*8	(0.0000000E+000, 1.0000000E+000)

```
  467  C
  468  $SUBTITLE:'ARG'
  469  $PAGE
```

```
THREEPHASE                                                    PAGE  12
ARG                                                           07-15-92
                                                              11:45:08

 Line#  Source Line          Microsoft FORTRAN Optimizing Compiler Version 4.10

   470  C  Define the function to calculate the argument of a complex number.
   471  C        If the complex variable is represented as a vector in Cartesian
   472  C        coordinates, the function ARG returns the angle between the real axis
   473  C        and the vector, where -PI/2 <= ARG <= PI/2.
   474         REAL FUNCTION ARG(r)
   475         COMPLEX r
   476         PI=3.1415927
   477         ARG = 0.0
   478  C        (The function will be set arbitrarily to zero if it is undefined.)
   479         IF (REAL(r) .EQ. 0.0) THEN
   480   IF (AIMAG(r) .GT. 0.0) ARG = PI/2.0
   481   IF (AIMAG(r) .LT. 0.0) ARG = -PI/2.0
   482   IF (AIMAG(r) .EQ. 0.0) THEN
   483     WRITE (*, 3020) 'UNDEFINED PHASE CHANGE DETECTED!'
   484    3020      FORMAT ('0', A)
   485   END IF
   486         ELSE
   487  C        (in the case where REAL(r) <> 0,)
   488   ARG = ATAN(AIMAG(r)/REAL(r))
   489   IF (REAL(r) .LT. 0.0) ARG = ARG + PI
   490         END IF
   491         RETURN
   492         END


ARG  Local Symbols

Name                      Class   Type            Size   Offset

ARG . . . . . param                               0006
R . . . . . param                                 0008
PI. . . . . local   REAL*4              4         0930


Global Symbols

Name                      Class   Type            Size   Offset

ARG . . . . . FFUNCT  REAL*4            ***       2f96
ASCOUT. . . . . extern  ***             ***        ***
main. . . . . FSUBRT  ***               ***       0072

Code size = 3171 (12657)
Data size = 500c (20492)
Bss size  = 0934 (2356)

No errors detected
```

b. Subroutine ASCII_XYOUT

```
                                                                PAGE   1
                                                                07-15-92
                                                                11:42:06

Line#  Source Line          Microsoft FORTRAN Optimizing Compiler Version 4.10

    1  C                       A S C I I _ X Y O U T    SUBROUTINE
    2  C                       ================================
    3
    4        SUBROUTINE ASCOUT (N1, N2, N3, Y1, X1, Z1,
    5       &                   Y2, X2, Z2, Y3, X3, Z3,
    6       &                   ZAXIS1, ZAXIS2, ZAXIS3)
    7
    8  $DEBUG
    9  $NOFLOATCALLS
   10  $TITLE:'ASCII_XY OUT'
   11  C  Written in Microsoft FORTRAN for use on an IBM PC-AT.
   12
   13  C               This subroutine will create 3 files containing the MSEF
   14  C        values so that the program SpectraCalc can read them and plot
   15  C        them.  The files are in "ASCII_XY" format.  In each, the first
   16  C        line contains the x-label and y-label.    Subsequent lines contain
   17  C        ASCII representations of data in 2 columns to be read by the
   18  C        translator.  The first column contains values of distance along
   19  C        the z-axis.  Either the y-, x-, or z-component of the MSEF is
   20  C        given in the second column, and the file is named correspondingly.
   21  C        ly.  Data for Phases 1, 2, and 3 are combined in each file.
   22  C               The main program can be compiled separately and combined
   23  C        with this subroutine at linking time.  This subroutine is in-
   24  C        tended to be combined with the FORTRAN source code program
   25  C        THREEPHASE.
   26
   27  C  Allocation of storage for arrays:
   28        DIMENSION Y1(500), X1(500), Z1(500), Y2(500), X2(500), Z2(500),
   29       &          Y3(200), X3(200), Z3(200)
   30        DIMENSION ZAXIS1(500), ZAXIS2(500), ZAXIS3(200)
   31  C  Type declarations for variables:
   32        INTEGER N1, N2, N3
   33        CHARACTER PREFIX*7, CMPNT*1, SUFFIX*4, YFILE*12, XFILE*12,
   34       &          ZFILE*12
   35        CHARACTER*1 RESP
   36  C  Format statements for writing to the screen:
   37     41 FORMAT (1X, A)
   38     42 FORMAT ('0', A)
   39     43 FORMAT (1X, A\)
   40  C  Documentation
   41        WRITE (*,42) 'The program will now write ASCII_XY files which can
   42       & be translated by'
   43        WRITE (*,41) 'SpectraCalc.  Three files will be created, called:'
   44        WRITE (*,41) '     *Y.PRN,     *X.PRN,     and  *Z.PRN'
   45        WRITE (*,41) 'where "*" is a string of seven characters that you
   46       &provide.'
   47        WRITE (*, 4080) N1, N2, N3
   48   4080 FORMAT(1X,'The numbers of data points are: ',2(I3,', '),I3,'.')
   49  C  Create the three file names:
   50   4100 WRITE (*,43) 'What is the filename root (type 7 characters)?'
   51        READ (*,'(A7)') PREFIX
   52  $NOTSTRICT
   53  C  [Use concatenation of substrings to generate similar filenames.]
```

Line# Source Line Microsoft FORTRAN Optimizing Compiler Version 4.10

```
   54        SUFFIX = '.PRN'
   55
   56        CMPNT = 'Y'
   57        YFILE(1:7) = PREFIX
   58        YFILE(8:8) = CMPNT
   59        YFILE(9:12) = SUFFIX
   60
   61        CMPNT = 'X'
   62        XFILE(1:7) = PREFIX
   63        XFILE(8:8) = CMPNT
   64        XFILE(9:12) = SUFFIX
   65
   66        CMPNT = 'Z'
   67        ZFILE(1:7) = PREFIX
   68        ZFILE(8:8) = CMPNT
   69        ZFILE(9:12) = SUFFIX
   70
   71  C  Confirmation of names:
   72        WRITE (*,42) 'The program will create the files:'
   73        WRITE (*, 4200) YFILE, XFILE, ZFILE
   74   4200 FORMAT (8X, A12, ', ', A12, ', and ', A12, '.')
   75        WRITE (*,43) 'Are these okay (type "y" or "n")? '
   76        READ (*, '(A)') RESP
   77        IF (.NOT. ((RESP.EQ.'y') .OR. (RESP.EQ.'Y'))) GO TO 4100
   78
   79  C                          WRITE THE DATA TO FILES
   80
   81   4300 FORMAT (SP, F9.1, ',', S, F7.4)
   82
   83        OPEN (11, FILE=YFILE, STATUS='NEW')
   84        WRITE (11, '(A)') 'ANGSTROMS, MSEF'
   85        DO 4320 I=N1, 1, -1
   86  WRITE (11, 4300) ZAXIS1(I), Y1(I)
   87   4320 CONTINUE
   88  C        [Skip the first and last points in Phase 2.]
   89        DO 4340 I=2, N2-1, +1
   90  WRITE (11, 4300) ZAXIS2(I), Y2(I)
   91   4340 CONTINUE
   92        DO 4360 I=1, N3, +1
   93  WRITE (11, 4300) ZAXIS3(I), Y3(I)
   94   4360 CONTINUE
   95        CLOSE(11)
   96        WRITE (*, 42) 'The file for the y-component has been completed.'
   97
   98        OPEN (12, FILE=XFILE, STATUS='NEW')
   99        WRITE (12, '(A)') 'ANGSTROMS, MSEF'
  100        DO 4420 I=N1, 1, -1
  101  WRITE (12, 4300) ZAXIS1(I), X1(I)
  102   4420 CONTINUE
  103  C        [Skip the first and last points in Phase 2.]
  104        DO 4440 I=2, N2-1, +1
  105  WRITE (12, 4300) ZAXIS2(I), X2(I)
  106   4440 CONTINUE
```

```
ASCII_XY OUT                                                    PAGE   3
                                                                07-15-92
                                                                11:42:06

 Line#  Source Line          Microsoft FORTRAN Optimizing Compiler Version 4.10

   107        DO 4460 I=1, N3, +1
   108   WRITE (12, 4300) ZAXIS3(I), X3(I)
   109    4460 CONTINUE
   110        CLOSE(12)
   111        WRITE (*, 41) 'The file for the x-component has been completed.'
   112
   113
   114        OPEN (13, FILE=ZFILE, STATUS='NEW')
   115        WRITE (13, '(A)') 'ANGSTROMS, MSEF'
   116        DO 4520 I=N1, 1, -1
   117   WRITE (13, 4300) ZAXIS1(I), Z1(I)
   118    4520 CONTINUE
   119   C        [Skip the first and last points in Phase 2.]
   120        DO 4540 I=2, N2-1, +1
   121   WRITE (13, 4300) ZAXIS2(I), Z2(I)
   122    4540 CONTINUE
   123        DO 4560 I=1, N3, +1
   124   WRITE (13, 4300) ZAXIS3(I), Z3(I)
   125    4560 CONTINUE
   126        CLOSE(13)
   127        WRITE (*, 41) 'The file for the z-component has been completed.'
   128
   129        WRITE (*,'(A)') ' '
   130        RETURN
   131
   132        END


ASCOUT  Local Symbols

Name                    Class   Type            Size   Offset

ZAXIS3. . . . . . . . . param                           0006
ZAXIS2. . . . . . . . . param                           000a
ZAXIS1. . . . . . . . . param                           000e
Z3. . . . . . . . . . . param                           0012
X3. . . . . . . . . . . param                           0016
Y3. . . . . . . . . . . param                           001a
Z2. . . . . . . . . . . param                           001e
X2. . . . . . . . . . . param                           0022
Y2. . . . . . . . . . . param                           0026
Z1. . . . . . . . . . . param                           002a
X1. . . . . . . . . . . param                           002e
Y1. . . . . . . . . . . param                           0032
N3. . . . . . . . . . . param                           0036
N2. . . . . . . . . . . param                           003a
N1. . . . . . . . . . . param                           003e
CMPNT . . . . . . . . . local   CHAR*1           1      0002
I . . . . . . . . . . . local   INTEGER*4        4      0004
PREFIX. . . . . . . . . local   CHAR*7           7      0008
SUFFIX. . . . . . . . . local   CHAR*4           4      0010
XFILE . . . . . . . . . local   CHAR*12         12      0014
YFILE . . . . . . . . . local   CHAR*12         12      0020
```

Microsoft FORTRAN Optimizing Compiler Version 4.10

ASCOUT Local Symbols

Name	Class	Type	Size	Offset
RESP.	local	CHAR*1	1	002c
ZFILE	local	CHAR*12	12	002e

Global Symbols

Name	Class	Type	Size	Offset
ASCOUT.	FSUBRT	***	***	003c

Code size = 0baf (2991)
Data size = 0380 (896)
Bss size = 003a (58)

No errors detected

2. Programs for Calculating Optical Functions (n and k) of Materials

a. OPFXNS1

```
                                                                PAGE   1
                                                                07-15-92
                                                                11:46:45

 Line#  Source Line          Microsoft FORTRAN Optimizing Compiler Version 4.10

     1  $storage:2
     2  $large
     3  $pagesize:58
     4  $linesize:86
     5  $title:'OPFXNS1'
     6  $debug
     7        PROGRAM OPFXNS1
     8  C                              OPTICAL FUNCTIONS 1
     9  C                              ===================
    10
    11  C       This is a program to calculate n,k's  from transmission experi-
    12  C ments using the Kramers-Kronig analysis.  Thicknesses are input in
    13  C Angstroms from the default input device.  Spectral data is input from
    14  C Unit 09.  This program was revised for use on an IBM PC/AT in
    15  C January and March 1989.  It is a modified version of OPTCON2.FOR.
    16  C Subroutine KKSUB2 has been separated into file KKSUB2.FOR.
    17  C Also, LABLER and ASCOUT have been combined into OPF_IO.FOR.
    18  C These three modules should be compiled separately and linked
    19  C together, along with P3FRAME.
    20
    21        dimension aexp(2000),a(2000),nu(2000),an(2000),ak(2000),
    22       &          dStrata(6), adata(2000), nuin(2000)
    23
    24  C Data type declarations:
    25        character title*70, FILNAM*12, outfil*12, ANSWER, IMORE,
    26       &          BELL*1
    27        integer varph, nrphzs, ifrmt
    28  C       VARPH is the ordinate of the variable phase (film) in the
    29  C       stratified medium having NRPHZS phases total.
    30        real nSpPhRef, dFilm, dFilmAng, dAngst
    31  C       nSpPhRef is the value in the reference calculation of the
    32  C       real refractive index of the phase containing the spectrum
    33  C       of interest.
    34  C       The variable dFilmAng is the film thickness in angstroms.
    35  C       dStrata is an array containing the thickness of each phase.
    36  C               Frequency data variables:
    37        real nu, nuhigh, nuin, nulow, nures
    38        real a, adata, aexp, ak, an, aninf
    39        complex n(6)
    40  C       Array N contains the complex refractive index of each phase.
    41        logical*4 ikbr, itrans, NoNegA
    42  C       Logical variables such as IKBR and ITRANS are given 4-byte ad-
    43  C       dresses to prevent the compiler from putting non-char. variables
    44  C       at odd addresses in the common block, which would result in
    45  C       an error.
#   46        integer ChkErr                                                FXN
    47
#   48  C Data storage address commands (names in CAPS are labeled common blocks)
    49        common/MVPCOM/nrphzs, varph, ikbr, nSpPhRef, thetr1, n, dStrata
    50        common/KCORRCOM/beta,rstep,epsilon,imax, NoNegA
    51        common/TRANS/ipol,itrans
    52  C       Common stack KKCOM was eliminated when subroutine kkSub2 was
    53  C       separated from the program.
```

```
 Line#  Source Line          Microsoft FORTRAN Optimizing Compiler Version 4.10

    54
    55  C  Data storage address command (Common block CSTAK contains space
    56  C  for the PORT3 modules CSPDI and CSPIN to use.  This is converted from
#   57  C  double-precision type to real type by the EQUIVALENCE statement below.):
    58         COMMON/CSTAK/DSTAK
    59         double precision DSTAK(6000)
    60         real RSTAK(12000)
    61         equivalence (DSTAK(1), RSTAK(1))
    62
    63         external kkSub2, mvpsub, kcorrsub, pc, revarray, cspin,
    64        &         labler, ascout, istkin, chkerr
#   65  C The above units are subroutines declared within this program or from PORT3.
    66  C
    67         data pi/3.14159/
    68         ikbr = .FALSE.
    69         itrans = .FALSE.
    70         NoNegA = .FALSE.
    71         outfil = 'XXXXXXXX.XXX'
    72         bell = '\a'C
    73
    74  C Beginning of the executable statements
    75         write(*,*) ' This is the program OPFXNS1, written in Microsoft'
    76         write(*,*) ' FORTRAN to calculate optical functions (n and k) from
    77        & spectral data.'
    78         write(*,*) ' For headed files, the data must be input in ASCII'
    79         write(*,*) ' two-column format compatible with the specification'
    80         write(*,*) ' (2(F10.5)).  The first line of input must be a'
    81         write(*,*) ' heading and the second the number of data points.'
    82         write(*,*) ' All real numbers provided by the user must have an EX
    83        &PLICIT DECIMAL POINT.'
    84         write(*,*) ' This program was updated from OPTCON5 in March 1989.'
    85         write(*,*) ' '
    86
    87  C  The PORT3 library subprogram ISTKIN initializes the dynamic storage
    88  C  stack to create enough space for subprograms CSPDI and CSPIN to
    89  C  differentiate 2000 points containing single precision real data.  The
    90  C  parameter ITYPE = 3 represents real numbers.
    91         CALL ISTKIN(12000, 3)
    92  C  The call above initializes the dynamic stack for any and all calls to
    93  C  PORT3 subprograms in the main program or subroutines.
    94
    95  C Global FORMAT statement to be used for prompting user input:
    96      5 format (1X, A\)
    97
    98  C                 INPUT OF DATA FROM FILES
    99  C                 ------------------------
   100  C Option to convert an input data file from floating point to fixed
   101  C notation:
   102         write(*,*) ' The subroutine LABLER will read ASCII_XY files from
   103        &SpectraCalc and convert'
   104         write(*,*) ' them to files with a heading.'
   105         write(*,5) 'Do you want to use the labeler (type "y" or "n")? '
   106         read(*, '(A1)') answer
```

Line# Source Line Microsoft FORTRAN Optimizing Compiler Version 4.10

```
  107        if((answer .EQ. 'y')  .OR.  (answer .EQ. 'Y')) then
  108          write(*,*) ' '
  109          CALL LABLER(outfil)
  110          write(*,*) ' '
  111          write (*, 20) outfil
  112       20   format (' Do you want to use the file ', A12, '(type "y" or "n")
  113         &? ')
  114          read (*, '(A1)') answer
  115          if((answer .EQ. 'y')  .OR.  (answer .EQ. 'Y')) then
  116            filnam = outfil
  117            GO TO 70
  118          end if
  119        end if
  120       50 write(*,5) 'What is the name of the input file? '
  121          read (*, '(A12)') FILNAM
  122       70 OPEN(09, file= FILNAM, status='old')
  123  C
  124       75 write(*,*) ' Is file (1) floating type [from SpectraCalc],'
  125          write(*,*) ' or (2) fixed pt. with heading [from LABELER],'
  126          write(*,5) 'Type "1" or "2":'
  127          read(*, '(I1)') ifrmt
  128  C
  129          write(*,*)' Should I set all negative abs. data equal to zero?'
  130          write(*,5) '(type "y" or "n"): '
  131          read(*, '(A1)') answer
  132          if ((answer .EQ. 'y') .OR. (answer .EQ. 'Y'))  NoNegA = .TRUE.
  133
  134          if (ifrmt .EQ. 1) then
  135  C         (Read a floating point, not decimal-formatted, file)
  136           write(*,5) 'Do you want to skip the first line ("y" or "n")?:'
  137           read(*,'(A1)') answer
  138           if ((answer .EQ. 'y') .OR. (answer .EQ. 'Y')) read(09,*)
  139           DO 100 j=1, 2000
  140             read (09, *, END = 110) nu(j),adata(j)
  141  C            (The program reads in data unformatted)
  142  C          (The program sets negative exptl. absorbance values equal to
  143  C          zero:)
  144             if ((adata(j).lt.0) .AND. (NoNegA)) adata(j) = 0
  145             nuin(j)=nu(j)
  146             npin = j
  147     100   CONTINUE
  148     110   CLOSE(9)
  149           write (*, 120) npin
  150     120   format (1X, 'This program has read', 1X, I4, 1X,
  151        &          'data points from the file.')
  152  C
  153         elseif (ifrmt .EQ. 2) then
  154  C         (Read a fixed point headed file)
  155           read(09, 130) title
  156     130   FORMAT (A70)
  157           write (*,'(A)') ' The heading on the top of the file is:'
  158           write (*, '(6X, A70)') title
  159           write (*,*) ' '
```

Line# Source Line Microsoft FORTRAN Optimizing Compiler Version 4.10

```
 160    145   read(09,'(I4)') npin
 161          write (*,160) npin
 162    160   FORMAT(1X,'The number of data points in the input file = ',I4)
 163          write(*,*) ' '
 164          DO 190 j=1,npin
 165            read (09,170) nu(j),adata(j)
 166    170     format(2f10.5)
 167  C         (The program sets negative exptl. absorbance values equal to
 168  C         zero:)
 169            if ((adata(j).lt.0) .AND. (NoNegA))   adata(j) = 0
 170           nuin(j)=nu(j)
 171    190   CONTINUE
 172          CLOSE(9)
 173  C
 174        elseif ((ifrmt .NE. 1) .AND. (ifrmt .NE. 2)) then
 175          write(*,*) ' You have not entered a valid choice.'
 176          GO TO 75
 177  C
 178        end if
 179
 180  C                ESTABLISHING USER-INPUT PARAMETERS
 181  C
 182     200 write(*,5) 'Are these transm. or refl. data ("T" or "R")? '
 183        read (*, '(A1)') answer
 184        if ( (answer .NE. 'T') .AND. (answer .NE. 't')
 185       &.AND.(answer .NE. 'R') .AND. (answer .NE. 'r') ) GO TO 200
 186        if ( (answer.EQ.'T').OR.(answer.EQ.'t') ) itrans = .TRUE.
 187        if (.NOT. (itrans)) then
 188          write(*, 5) 'Is the polarization (1)s  or (2)p (type 1 or 2): '
 189          read(*,'(bn,i1)') ipol
 190        end if
 191
 192  C If the calculation is for a KBr pellet set dFilm equal to an
 193  c equivalent thickness for a film of pure bulk material which
 194  c would give the same absorbance neglecting real index
 195  c effects on the spectra.
 196  C    Equivalent thickness of KBr pellet =
 197  C                 Conc. of       Measured thickness of pellet
 198  C                 material   X   ____________________________
 199  C                 in pellet      Molar density of pure material
 200        if (.NOT. (itrans) ) GO TO 245
 201  C  The user inputs the parameters for KBr pellet spectral data:
 202     220 write(*,5) ' Is input for KBr disk? (type "y" or "n"):'
 203        read(*,'(A1)') answer
 204        if((answer .EQ. 'y')  .OR.  (answer .EQ. 'Y')) IKBR = .TRUE.
 205        if (IKBR) then
 206          write(*,5) ' What is the thickness of disk (cm)? '
 207          read(*,'(f9.7)') ddisk
 208          write(*,5) ' What is the density of pure material (g/cm3)? '
 209          read(*,'(f5.3)') rho
 210          write(*,5) ' The weight conc. of disk (mg sample/mg disk)? '
 211          read(*,'(f8.5)') wconc
 212          dFilm= (wconc*2.75/rho) * ddisk
```

Line# Source Line Microsoft FORTRAN Optimizing Compiler Version 4.10

```
 213          dFilmAng= dFilm * 1.0e08
 214          write (*, 230) dFilmAng
 215   230    format(2x,'The equivalent disk thickness (angstroms)= ',f9.2)
 216        else
 217  C          (Input film thickness for transmission spectral data:)
 218          write(*,5) ' What is the thickness of film (angstroms)? '
 219          read (*, 240) dFilmAng
 220    240   format(f9.1)
 221          dFilm= dFilmAng * 1.0e-08
 222        end if
 223
 224  C     nu must be entered in increasing order for input into kkSub2.
 225    245 if (nu(2).lt.nu(1)) then
 226          write(*,*) ' The input points were in decreasing freq. order.'
 227          write(*,*) ' Therefore, the subroutine REVARRAY has been called
 228       &to reverse their order.'
 229          CALL REVARRAY (nu,npin)
 230          CALL REVARRAY (adata,npin)
 231          CALL REVARRAY (nuin, npin)
 232        endif
 233
 234        write (*,*) ' '
 235    260 format(f7.2)
 236        write(*,5) 'Supply lower freq. limit nu in final data set: '
 237        read(*,260) nulow
 238        write(*,5) 'Supply upper freq. limit nu in final data set: '
 239        read(*,260) nuhigh
 240        write(*,5) 'Input resolution in cm-1 of final nu set: '
 241        read(*,420) nures
 242    420 format(f5.2)
 243        write(*,*) ' OPFXNS1 must have a zero-freq. n value for the phase
 244       &of interest.'
 245        write(*,5)'Input a value of n out of the integration range: '
 246        read(*,430) aninf
 247  C       The value ANINF goes into the function call to kkSub2.
 248    430 format(f7.5)
 249
 250  C                          ESTIMATE n AND k
 251  C                          ----------------
 252  C
 253  c  The following is a guess at the effective depth of penetration of
 254  c  light for a reflection experiment.  It gives a rough initial
 255  c  guess for k as though the experiment were transmission through
 256  c  a film of thickness equal to the penetration depth:
 257        if (.NOT. (itrans)) dFilm= 1.0 * 1.0e-04
 258        write(*,*) ' Initial estimates of k have been calculated.'
 259        beta= 4.0 * pi * dFilm/2.303
 260        write(*, 440)
 261     440 format (10X, 'WAVENUMBER',2X, 'ABSORBANCE',2X, 'CALCULATED K')
 262     450 do 500 j=1,npin
 263           ak(j) = adata(j) / (beta*nu(j))
 264  C          (Note that ak can be negative.)
 265           if (j.eq.1.or.j.eq.npin) then
```

Line# Source Line Microsoft FORTRAN Optimizing Compiler Version 4.10

```
 460      write(*,470) nu(j), adata(j), ak(j)
 470      format(10X, F6.1, 6X, F8.5, 4X, F8.5)
        end if
 500  CONTINUE

      np= npin
      write(*,*) ' The subroutine kkSub2 has been called.'
      CALL kkSub2 (nu, ak, np, nulow, nuhigh, nures, aninf, an)
      write(*,*) BELL
      write(*,*)' Do you want to see the first set of calculated n and
     &k values on the screen? '
      write(*,5) '      Type "y" or "n": '
      read (*, '(A1)') answer
      if ((answer.EQ.'Y') .OR. (answer.EQ.'y')) then
        write(*,*) ' The program''s first guesses at n and k are:'
        do 515 j=1,np
          write(*,510) nu(j),an(j),ak(j)
  510     format (2x, 3f10.5)
C         (The following command interrupts scrolling:)
          if ( (mod(j, 22)) .EQ. 0 ) PAUSE
  515   CONTINUE
        write(*,*) ' '
      end if

C               INTERPOLATE EXPERIMENTAL ABSORBANCE DATA
C               ----------------------------------------

      write(*,*) ' PORT3 subprogram CSPIN has been called to interpolate
     & points.'
      ifrmt = ChkErr(nuin, adata, npin, nu, aexp, np)
      if (ifrmt .NE. 0) then
        write (*, 525) ifrmt
  525   format (1X, 'ERROR ', I2, ' DETECTED IN PORT3 CSPIN SUBR.')
        GO TO 1500
      end if
      CALL cspin (nuin, adata, npin, nu, aexp, np)
C  The PORT3 subprogram CSPIN interpolates at requested points
C  in given input data using a cubic spline approximation.  There
C  are NPIN input data points defined by the arrays nuIN and ADATA.
C  The NP values of the abscissa for interpolated points are input
C  as nu.  The module returns only the array AEXP containing
C  interpolated absorbance values.

C                         SET UP THE STRATA
C                         -----------------
C       (for KBr:)
      if(ikbr) then
        nrphzs=3
        varph=2
        nSpPhRef=1.52
        thetr1=0.0
        n(1)=cmplx(1.0,0.0)
        n(3)=cmplx(1.0,0.0)
```

Line# Source Line Microsoft FORTRAN Optimizing Compiler Version 4.10

```
 319          dStrata(2)=dFilm
 320          GO TO 675
 321        endif
 322
 323  C       (For a reflection or regular transmission experiment:)
 324        write(*,5) ' Input the total number of phases: '
 325        read(*,'(bn,i1)') nrphzs
 326        write(*,5) ' Which phase has variable n,k (1=entry)? '
 327        read(*,'(bn,i1)') varph
 328        write(*,5) ' What is the real n value of the spectral phase for th
 329       &e reference calc.? '
 330        READ(*,550) nSpPhRef
 331     550 FORMAT(F6.3)
 332        write(*,5) ' What is the angle of incidence (degs)? '
 333        READ(*,560) THETA1
 334     560 FORMAT(F5.2)
 335        THETR1=(PI/180.0)*THETA1
 336
 337     580 format(1X, A)
 338        write(*,580)
 339        write(*,580) 'Specify values of n and k for the phases in which'
 340        write(*,580) 'they are constants.  Phase 1 is the entry phase.'
 341        write(*,580) 'Enter the values as real numbers, separated by'
 342        write(*,580) 'commas: (n,k):'
 343        DO 600 layer=1, nrphzs
 344          IF (.NOT.(layer.EQ.varph)) then
 345            write(*,590) layer
 346     590    format(2x, 'Phase number ', i1,': '\)
 347            read(*,595) N(layer)
 348     595    format(2F6.3)
 349          end if
 350     600 CONTINUE
 351        if(nrphzs.gt.3) then
 352     610   write(*,620)
 353     620   format(2x, 'Input the thickness (Angstroms) of each phase:')
 354           DO 670 layer=2, nrphzs-1
 355             write(*,590) layer
 356             if(layer.eq.varph) then
 357               dStrata(layer)=dFilm
 358             else
 359               read(*,630) dAngst
 360     630       format(f9.1)
 361               dStrata(layer)=dAngst*(1.0e-08)
 362             end if
 363     670   CONTINUE
 364         else
 365           dStrata(2) = dFilm
 366  C          If there are only three phases, the middle one will be the
 367  C          film of interest.
 368        end if
 369
 370  C  Input the parameters needed by KCORRSUB:
 371    675 write(*,*) ' What is the solution accuracy limit for convergence?'
```

Line# Source Line Microsoft FORTRAN Optimizing Compiler Version 4.10

```
372         write(*,*) ' (This is the maximum difference between exptl. and'
373         write(*,5) ' calculated values of abs. in the final result.): '
374         read(*, 680) epsilon
375      680 format(f8.6)
376         write(*,5) 'Enter the iteration rate parameter in the range 0.0 -
377        &1.0 (typically 0.7): '
378         read(*, 690) rstep
379      690 format(f5.3)
380         write(*,5)'What is the maximum number of iterations to try? '
381         read(*,'(bn,i2)') imax
382
383         write(*,*) ' The subroutine MVPSUB has been called.'
384         CALL mvpsub(nu, an, ak, np, a)
385         write(*,*) BELL
386
387   C                 CALCULATE n AND k VALUES BY ITERATION:
388   C                 ______________________________________
389         lstep=0
390         write(*,*) ' '
391      750  write(*,*) ' The subroutine KCORRSUB has been called. '
392         CALL kcorrsub(nu,ak,a,aexp,np,latep,*900,*1000)
393   C  KCORRSUB has two conditional returns. One of them, to line 900, is
394   C  used if the most recent calc. n and k agree with expt. within allowed
395   C  error.  The other, to line 1000, obtains if the maximum allowed num-
396   C  ber of iterations have been performed.  In lieu of these two, a
397   C  normal return continues execution at line 800.
398      800 write (*,*) BELL, BELL
399         write(*,*) ' The subroutine kkSub2 has been called. '
400         CALL kkSub2 (nu, ak, np, nulow, nuhigh, nures, aninf, an)
401         write (*,*) BELL
402         write(*,*) ' The subroutine MVPSUB has been called. '
403         CALL mvpsub(nu,an,ak,np,a)
404         GO TO 750
405   C                          END OF CALCS
406   C                          ____________
407
408   C  If calculations are completed, write the data to the output
409   C  file:
410      900  write(*,*) ' Solution convergence has been attained.'
411         write(*,*) ' Do you want to create (1) a headed three-column file'
412         write(*,*) ' or (2) separate files for SpectraCalc?'
413         write(*,5) 'Type "1" or "2":'
414         read (*,'(I1)') ifrmt
415         if (ifrmt .EQ. 1) then
416      910   write(*,5) ' What is the name of the output file? '
417            read (*, '(A12)') FILNAM
418            OPEN (10, file= FILNAM, status='new')
419            write(10, 130) title
420            write(10,'(i4)')np
421            do 950 j=1,np
422              write(10,920) nu(j),an(j),ak(j)
423      920     format(f8.2,2f8.5)
424      950   continue
```

Line# Source Line Microsoft FORTRAN Optimizing Compiler Version 4.10

```
 425  C
 426        elseif (ifrmt .EQ. 2) then
 427   CALL ASCOUT (nu, an, ak, np)
 428  C
 429        elseif ((ifrmt .NE. 1) .AND. (ifrmt .NE. 2)) then
 430          write (*,*) ' You have not entered a valid answer.'
 431          write (*,*)
 432          GO TO 900
 433  C
 434        end if
 435  C  Echo the values of the first and last points written at the screen:
 436        write (*, '(A)') ' The first and last points written to the output
 437       & have these values: '
 438        write (*,960) nu(1), an(1), ak(1)
 439        write (*,960) nu(np), an(np), ak(np)
 440   960  format(2x,'nu= ',f8.2,2x,'n= ',f8.5,2x,'k= ',f8.5)
 441        GO TO 1500
 442
 443  C  Print a message if convergence has not been attained in the initially
 444  C  specified number of iterations.
 445   1000 write(*,*) ' The maximum number of iterations has been exceeded.'
 446        write(*,5) ' Do you wish more iterations? (type "y" or "n"): '
 447        read(*, '(A1)') imore
 448        if((imore .EQ. 'y')  .OR.  (imore .EQ. 'Y')) then
 449          lstep=0
 450          GO TO 675
 451        end if
 452  C
 453   1500 STOP
 454        END
```

main Local Symbols

Name	Class	Type	Size	Offset
A	local	REAL*4	8000	0000
DANGST	local	REAL*4	4	0002
IFRMT	local	INTEGER*2	2	0006
TITLE	local	CHAR*70	70	0008
NUHIGH	local	REAL*4	4	004e
LSTEP	local	INTEGER*2	2	0052
J	local	INTEGER*2	2	0054
NURES	local	REAL*4	4	0056
ANSWER	local	CHAR*1	1	005a
OUTFIL	local	CHAR*12	12	005c
NULOW	local	REAL*4	4	0068
NP	local	INTEGER*2	2	006c
BELL	local	CHAR*1	1	006e
THETA1	local	REAL*4	4	0070
RHO	local	REAL*4	4	0074
ANINF	local	REAL*4	4	0078
DFILM	local	REAL*4	4	007c

Microsoft FORTRAN Optimizing Compiler Version 4.10

main Local Symbols

Name	Class	Type	Size	Offset
DFILMA.	local	REAL*4	4	0080
DDISK	local	REAL*4	4	0084
NPIN.	local	INTEGER*2	2	0088
FILNAM.	local	CHAR*12	12	008a
WCONC	local	REAL*4	4	0096
IMORE	local	CHAR*1	1	009a
LAYER	local	INTEGER*2	2	009c
PI.	local	REAL*4	4	0c50
AK.	local	REAL*4	8000	1f40
AN.	local	REAL*4	8000	3e80
ADATA	local	REAL*4	8000	5dc0
NU.	local	REAL*4	8000	7d00
AEXP.	local	REAL*4	8000	9c40
NUIN.	local	REAL*4	8000	bb80
DSTRAT.	MVPCOM	REAL*4	24	0040
VARPH	MVPCOM	INTEGER*2	2	0002
NRPHZS.	MVPCOM	INTEGER*2	2	0000
NSPPHR.	MVPCOM	REAL*4	4	0008
N	MVPCOM	COMPLEX*8	48	0010
IKBR.	MVPCOM	LOGICAL*4	4	0004
ITRANS.	TRANS	LOGICAL*4	4	0002
NONEGA.	KCORRC	LOGICAL*4	4	000e
THETR1.	MVPCOM	REAL*4	4	000c
BETA.	KCORRC	REAL*4	4	0000
RSTEP	KCORRC	REAL*4	4	0004
EPSILO.	KCORRC	REAL*4	4	0008
IMAX.	KCORRC	INTEGER*2	2	000c
IPOL.	TRANS	INTEGER*2	2	0000
DSTAK	CSTAK	REAL*8	48000	0000
RSTAK	CSTAK	REAL*4	48000	0000

```
                                    --SUBLIST--
C
C
      INTEGER FUNCTION ChkErr(XIN, YIN, lstptin, xout, yout, lstptout)
C
      real xin(*), yin(*), xout(*), yout(*)
      integer lstptin, lstptout
C
      ChkErr = 0
C
      if (lstptout .LT. 1) chkerr = 1
      if (lstptin .LT. 4) chkerr = 2
      do 1620 j = 1, lstptin - 1
        if (xin(j) .GE. xin(j+1)) chkerr = 3
1620  continue
      do 1630 j = 1, lstptout
        if ((xout(j) .LE. xin(1)) .OR. (xout(j) .GT. xin(lstptin)))
     &        chkerr = 4
```

```
OPFXNS1                                                          PAGE  11
                                                                 07-15-92
                                                                 11:46:45

 Line#  Source Line          Microsoft FORTRAN Optimizing Compiler Version 4.10

   472   1630 continue
   473   1690 return
   474        end
***** opfxns1.for(474) : warning F4202: CHKERR : formal argument YIN : never used
***** opfxns1.for(474) : warning F4202: CHKERR : formal argument YOUT : never used


CHKERR  Local Symbols

Name                      Class   Type              Size   Offset

LSTPTO. . . . . . . . . . param                            0006
YOUT. . . . . . . . . . . param                            000a
XOUT. . . . . . . . . . . param                            000e
LSTPTI. . . . . . . . . . param                            0012
YIN . . . . . . . . . . . param                            0016
XIN . . . . . . . . . . . param                            001a
CHKERR. . . . . . . . . . param                            fffe
J . . . . . . . . . . . . local   INTEGER*2           2     009e

   475
   476  $subtitle:'MVPSUB'
   477  $page
```

Line# Source Line Microsoft FORTRAN Optimizing Compiler Version 4.10

```
      subroutine mvpsub(nu,an,ak,np,absp)
C  This subroutine computes values of reflectivity and
C  transmissivity for a multilayer stack of absorbing films.
C  PHASE varph, to be specified, has variable optical constants to
C  provide band shape calculations.
C  The parameters passed in a call to this subroutine are
C    INPUT>
C       nu:  array of freq. as abscissa.
C       AN: array of real refr. index n as a function of nu.
C       AK: array of complex refr. "  k "  "     "    "  ".
C       NP: number of pts. input as arrays A, AN, and AK.
C    <OUTPUT
C       ABSP: array of calc. absorbance for the given polarization.
C       (The above variable becomes a(j) in KCORRSUB.)
C  PHASES 2 THRU nrphzs-1 ARE OF VARIABLE THICKNESS.  TRANSMISSION
C  ONLY CALCULATED FOR CASES WHERE K(nrphzs)=0.0.  BASELINE R AND T ARE
C  CALCULATED FOR K(varph)=0 AND N(varph)=nSpPhRef, TO BE SUPPLIED AS
C  INPUT.  THE CALCULATION IS DONE IN A SUBROUTINE, fields, BY A
C  MATRIX METHOD WHICH CALCULATES THE BOUNDARY FIELD STRENGTHS.
C  THE TOTAL NUMBER OF PHASES, nrphzs, MUST BE SPECIFIED
C  AND CANNOT EXCEED THE SIZE SPECIFIED BY THE DIMENSION STATEMENTS.
c  When KBr pellet spectra are calculated set IKBR=true so
c  that N(varph) = nSpPhRef.
      DIMENSION dStrata(6), nu(2000), absp(2000), an(2000), ak(2000)

C Data type declarations:
      LOGICAL ikbr*4, itrans*4
      REAL nSpPhRef, nu, OvrFlo
      COMPLEX N(6), Nvarph(2000), UFS(6,6), UBS(6,6),
     & UFP(6,6), UBP(6,6), I, A(6)
      CHARACTER TITLE*70
      INTEGER varph, SplRefFlag
      PARAMETER (OvrFlo = 99.999)

C  Data storage address commands
      common/MVPCOM/nrphzs, varph, ikbr, nSpPhRef, thetr1, n, dStrata
      common/TRANS/ipol,itrans
      EXTERNAL fields
      PI=3.1415926
      I=CMPLX(0.0,1.0)
C  I equals the square root of -1.
C  Begin the executable statements (one large DO loop):
  410 DO 600 J=1,NP
        nvarph(j)=cmplx(an(j),ak(j))
        SplRefFlag=0
C  For a KBr pellet real n is replaced by nSpPhRef = n(KBr).
        if(ikbr) then
          N(varph) = CMPLX(nSpPhRef,AIMAG(Nvarph(J)))
        else
          n(varph) = nvarph(j)
        end if

  420   CALL FIELDS(nrphzs,THETR1,N, dStrata, nu(j),
```

Line# Source Line Microsoft FORTRAN Optimizing Compiler Version 4.10

```
      &              UFS,UBS,UFP,UBP,A)
         ZRS= (UBS(1,2)/UFS(1,2))*CONJG(UBS(1,2)/UFS(1,2))
         ZRP= (UBP(1,2)/UFP(1,2))*CONJG(UBP(1,2)/UFP(1,2))
         IF (AIMAG(N(nrphzs)).GT.0) GO TO 450
C        UFS (nrphzs,nrphzs-1) = 1.0
C        UFP (nrphzs,nrphzs-1) = 1.0
         S = (N(nrphzs)*A(nrphzs))/(N(1)*A(1))
         ZTS = S*(1.0/UFS(1,2))*CONJG(1.0/UFS(1,2))
         ZTP = S*(1.0/UFP(1,2))*CONJG(1.0/UFP(1,2))
 450     IF (SplRefFlag .EQ. 0) then
C          (Do the calculation with the absorbing sample present.)
 560       RP = ZRP
           RS = ZRS
           IF (.NOT.(AIMAG(N(nrphzs)) .GT. 0)) then
             TP = ZTP
             TS = ZTS
           end if
           SplRefFlag = 1
           N(varph) = CMPLX(nSpPhRef,0.0)
           GO TO 420
C          (i.e. go back and calculate fields for the reference spectrum)
         else
C          (Assign variables for the reference spectrum.)
           RP0 = ZRP
           RS0 = ZRS
           if (RP0 .GT. 0) then
             ARP = -ALOG10(RP/RP0)
           else
             ARP = OvrFlo
           end if
           if ( .NOT. (itrans) ) then
             if (ipol.eq.1) then
               if (RS0 .GT. 0) then
                 ARS = -ALOG10(RS/RS0)
               else
                 ARS = OvrFlo
               end if
               absp(j) = ars
             else
               absp(j) = arp
             end if
           else
C            (Calculate transmittance results.)
 480         IF (AIMAG(N(nrphzs)) .GT. 0) GO TO 600
             TP0 = ZTP
             TS0 = ZTS
             ATP = -ALOG10(TP/TP0)
             ats = -alog10(ts/ts0)
             if (itrans) absp(j) = atp
           end if
         end if
 600   CONTINUE
1000   RETURN
```

Line# Source Line Microsoft FORTRAN Optimizing Compiler Version 4.10

584 END

MVPSUB Local Symbols

Name	Class	Type	Size	Offset
ABSP.	param			0006
NP.	param			000a
AK.	param			000e
AN.	param			0012
NU.	param			0016
NVARPH.	local	COMPLEX*8	16000	0000
ZTS	local	REAL*4	4	00a0
I	local	COMPLEX*8	8	00a4
J	local	INTEGER*2	2	00ac
SPLREF.	local	INTEGER*2	2	00ae
RPO	local	REAL*4	4	00b0
S	local	REAL*4	4	00b4
TPO	local	REAL*4	4	00b8
RSO	local	REAL*4	4	00bc
TSO	local	REAL*4	4	00c0
PI.	local	REAL*4	4	00c4
RP.	local	REAL*4	4	00c8
ARP	local	REAL*4	4	00cc
TP.	local	REAL*4	4	00d0
ATP	local	REAL*4	4	00d4
RS.	local	REAL*4	4	00d8
ARS	local	REAL*4	4	00dc
TS.	local	REAL*4	4	00e0
ATS	local	REAL*4	4	00e4
ZRP	local	REAL*4	4	00e8
ZTP	local	REAL*4	4	00ec
ZRS	local	REAL*4	4	00f0
UBP	local	COMPLEX*8	288	3e80
UBS	local	COMPLEX*8	288	3fa0
UFP	local	COMPLEX*8	288	40c0
UFS	local	COMPLEX*8	288	41e0
A	local	COMPLEX*8	48	dd6d
DSTRAT.	MVPCOM	REAL*4	24	0040
IKBR.	MVPCOM	LOGICAL*4	4	0004
ITRANS.	TRANS	LOGICAL*4	4	0002
NSPPHR.	MVPCOM	REAL*4	4	0008
N	MVPCOM	COMPLEX*8	48	0010
VARPH	MVPCOM	INTEGER*2	2	0002
NRPHZS.	MVPCOM	INTEGER*2	2	0000
THETR1.	MVPCOM	REAL*4	4	000c
IPOL.	TRANS	INTEGER*2	2	0000

Symbolic Constant	Type	Value
OVRFLO.	REAL*4	9.9999001E+001

```
  585
  586  $subtitle:'FIELDS'
  587  $page
```

Line# Source Line Microsoft FORTRAN Optimizing Compiler Version 4.10

```
588        SUBROUTINE FIELDS (nrphzs,THETR1,N,dStrata, nu,
589       &                   UFS,UBS,UFP,UBP,A)
590   C
591        DIMENSION dStrata(6)
592   C
593        COMPLEX N(6),TFS(6),TFP(6),RFS(6),RFP(6),UFS(6,6),UBS(6,6),
594       1      UFP(6,6),UBP(6,6),A(6),DELTA,ZCD,I
595        real nu
596        PI=3.1415926
597        I=CMPLX(0.0,1.0)
598        UFS(nrphzs,nrphzs-1) = 1.0
599        UFP(nrphzs,nrphzs-1) = 1.0
600        UBS(nrphzs,nrphzs-1) = 0.0
601        UBP(nrphzs,nrphzs-1) = 0.0
602   C
603        DO 100 LCOUNT=1, nrphzs
604          L = (nrphzs+1)-LCOUNT
605          A(L) = (((N(L))**2)-(N(1)**2)*((SIN(THETR1))**2))**0.5/N(L)
606          IF (L .EQ. nrphzs) GO TO 100
607          IF (L .EQ. 1) GO TO 50
608          ZCD = nu*dStrata(L)*N(L)*A(L)
609          ZID = AIMAG(ZCD)
610          ZRD = REAL(ZCD)
611          ZRD = ZRD-AINT(ZRD)
612          DELTA = 2*PI*CMPLX(ZRD,ZID)
613       50 RFS(L) = (N(L)*A(L)-N(L+1)*A(L+1))/(N(L)*A(L)+N(L+1)*A(L+1))
614          RFP(L) = (N(L+1)*A(L)-N(L)*A(L+1))/(N(L+1)*A(L)+N(L)*A(L+1))
615          TFS(L) = (2*N(L)*A(L))/(N(L)*A(L)+N(L+1)*A(L+1))
616          TFP(L) = (2*N(L)*A(L))/(N(L)*A(L+1)+N(L+1)*A(L))
617          UFS(L,L+1) = (1.0/TFS(L))*(UFS(L+1,L)+RFS(L)*UBS(L+1,L))
618          UBS(L,L+1) = (1.0/TFS(L))*(RFS(L)*UFS(L+1,L)+UBS(L+1,L))
619          UFP(L,L+1) = (1.0/TFP(L))*(UFP(L+1,L)+RFP(L)*UBP(L+1,L))
620          UBP(L,L+1) = (1.0/TFP(L))*(RFP(L)*UFP(L+1,L)+UBP(L+1,L))
621          IF (L .EQ. 1) GO TO 100
622          UFS(L,L-1) = CEXP(-I*DELTA)*UFS(L,L+1)
623          UBS(L,L-1) = CEXP(I*DELTA)*UBS(L,L+1)
624          UFP(L,L-1) = CEXP(-I*DELTA)*UFP(L,L+1)
625          UBP(L,L-1) = CEXP(I*DELTA)*UBP(L,L+1)
626      100 CONTINUE
627          RETURN
628          END
```

FIELDS Local Symbols

Name	Class	Type	Size	Offset
A	param			0006
UBP	param			000a
UFP	param			000e
UBS	param			0012
UFS	param			0016
NU.	param			001a

FIELDS Local Symbols

Name	Class	Type	Size	Offset
DSTRAT.	param			001e
N	param			0022
THETR1.	param			0026
NRPHZS.	param			002a
I	local	COMPLEX*8	8	00f4
L	local	INTEGER*2	2	00fc
LCOUNT.	local	INTEGER*2	2	00fe
PI.	local	REAL*4	4	0100
ZCD	local	COMPLEX*8	8	0104
ZID	local	REAL*4	4	010c
DELTA	local	COMPLEX*8	8	0110
ZRD	local	REAL*4	4	0118
RFP	local	COMPLEX*8	48	4300
TFP	local	COMPLEX*8	48	4330
RFS	local	COMPLEX*8	48	4360
TFS	local	COMPLEX*8	48	4390

```
629
630  $subtitle:'KKCORRSUB'
631  $page
```

Line# Source Line Microsoft FORTRAN Optimizing Compiler Version 4.10

```
      SUBROUTINE kcorrsub(nu,k,a,aexp,np,lstep,*,*)

C  This routine calculates new k's for continued attempts to find
C  true n,k values from experimental spectra.
C  The algorithm for transmission spectra:
C                ABS(EXP)-ABS(LAST)= DELTA A
C                (DELTA A)*2.303/4*PI*D*WAVENO =DELTA K
C                K(NEW)=K(LAST) + DELTA K*rstep
c  rstep is chosen to avoid overshoot and oscillations around the
c  solutions.  Usually rstep=0.7
c  The k(new) is used to calculate n(new) and then the fresnel
C  equations are used to check the fit to experimental
C  transmission curves.
C  THE ALGORITHM FOR REFLECTION:
C               (?)
      DIMENSION A(2000),AEXP(2000),nu(2000)
C  Data type declarations:
      logical itrans*4, NoNegA*4
      real k(2000)
      real nu
      integer iconv
C       iconv is a flag that remains = 0 is a sol'n has converged.
C     a in the parameter passing list is actually the array a(j).
C  Data storage declarations:
      common/KCORRCOM/beta,rstep,epsilon,imax, NoNegA
      common/TRANS/ipol, itrans

C  Begin the executable statements:
      write(*,*) ' KKCORRSUB determines points for which the calculated
     &absorbance values'
      write(*,*) ' differ from exptl. ones by more than the error parame
     &ter you entered.'
      write(*,250)
  250 format (10x,'The points with errors > epsilon are:')
      write(*,260)
  260 format(10x,'wavenumber',2x,'(aexp-acalc)',2x,'aexp',7x,'k(new)')
      iconv = 0
      DO 300 j=1,np
        if ((a(j) .lt. 0) .AND. (NoNegA))  a(j) = 0
        adiff = aexp(j)-a(j)
        if ( (abs(adiff)-epsilon) .LE. 0 ) GO TO 300

C  Create a new value for the absorption index k:
  270   k(j) = k(j) + rstep*adiff/(nu(j)*beta)

C  If the experimentally measured absorbance is negligibly small or <0,
C  approximate the absorption index k for that freq. to zero.
        if ((aexp(j) .lt. 0.00002) .OR. (k(j) .LT. 0)) k(j) = 0
  280   write(*,290) nu(j), adiff, aexp(j), k(j)
  290   format(10X, F6.1, 4X, F9.6, 4X, F9.6, 2X, F9.6)
        iconv = 1
  300 CONTINUE
      write (*, 260)
```

Line# Source Line Microsoft FORTRAN Optimizing Compiler Version 4.10

```
  685
  686       write (*, 320) lstep + 1
  687   320 format (' The program has completed iteration number ', I2,
  688      & ' in the current set.')
  689       if (iconv .EQ. 0) RETURN 1
  690       lstep = lstep + 1
  691       if (lstep .ge. imax) RETURN 2
  692       RETURN
  693       END
```

KCORRS Local Symbols

Name	Class	Type	Size	Offset
LSTEP	param			0006
NP.	param			000a
AEXP.	param			000e
A	param			0012
K	param			0016
NU.	param			001a
J	local	INTEGER*2	2	011c
ADIFF	local	REAL*4	4	011e
ICONV	local	INTEGER*2	2	0122
ITRANS.	TRANS	LOGICAL*4	4	0002
NONEGA.	KCORRC	LOGICAL*4	4	000e
BETA.	KCORRC	REAL*4	4	0000
RSTEP	KCORRC	REAL*4	4	0004
EPSILO.	KCORRC	REAL*4	4	0008
IMAX.	KCORRC	INTEGER*2	2	000c
IPOL.	TRANS	INTEGER*2	2	0000

```
  694
  695 $subtitle:'REVARRAY'
  696 $page
```

Line# Source Line Microsoft FORTRAN Optimizing Compiler Version 4.10

```
  697         subroutine REVARRAY(x,npx)
  698   C  This subroutine simply takes a one-dimensional array of points
  699   C  and reverses the order of its contents.
  700
  701         dimension x(2000)
  702
  703    100  if ( (mod(npx,2)) .eq. 0 ) then
  704           np = npx/2
  705         else
  706           np = (npx-1)/2
  707         endif
  708         DO 450 j=1,np
  709           zx = x(j)
  710           x(j) = x(npx+1-j)
  711           x(npx+1-j) = zx
  712    450  CONTINUE
  713         RETURN
  714         END
```

REVARR Local Symbols

Name	Class	Type	Size	Offset
NPX	param			0006
X	param			000a
J	local	INTEGER*2	2	0124
NP.	local	INTEGER*2	2	0126
ZX.	local	REAL*4	4	0128

Global Symbols

Name	Class	Type	Size	Offset
ASCOUT.	extern	***	***	***
CHKERR.	FFUNCT	INTEGER*2	***	24d1
CSPIN	extern	***	***	***
CSTAK	common	***	48000	0000
FIELDS.	FSUBRT	***	***	3279
ISTKIN.	extern	***	***	***
KCORRC.	common	***	18	0000
KCORRS.	FSUBRT	***	***	543e
KKSUB2.	extern	***	***	***
LABLER.	extern	***	***	***
MVPCOM.	common	***	88	0000
MVPSUB.	FSUBRT	***	***	2786
REVARR.	FSUBRT	***	***	5a05
TRANS	common	***	6	0000
main.	FSUBRT	***	***	0072

Code size = 5c11 (23569)
Data size = 1284 (4740)

```
OPFXNS1                                                    PAGE  21
REVARRAY                                                   07-15-92
                                                           11:46:45

                        Microsoft FORTRAN Optimizing Compiler Version 4.10

Bss size  = 012c (300)

No errors detected
```

b. Subroutine KKSUB2

Line# Source Line Microsoft FORTRAN Optimizing Compiler Version 4.10

```
    1 $title:'KKSUB2'
    2 $pagesize:58
    3 C
    4       subroutine KKSUB2 (NuBr, kOfNu, LastPt, NuLmLo, NuLmHi,
    5      &                   NuRes, nnInf, nOfNu)
    6 C       Parameters passed in subroutine call:
    7 C --> <-- NuBr: frequency nu-bar of i
    8 C --> <-- kOfNu: imag. part of refr. index function
    9 C --> <-- LastPt: number of points in kOfNu
   10 C       (The preceding three variables are overwritten by KKSUB2)
   11 C -->     NuLmLo: lower frequency limit of output data
   12 C -->     NuLmHi: upper limit of frequency data
   13 C -->     NuRes: freq. resolution of output data
   14 C -->     nnInf: scalar value of refr. index in non-absorbing region
   15 C     <-- nOfNu: vector of real refr index function output
   16 C
   17 C This subroutine performs the actual Kramers-Kronig integration.
   18 C
   19
   20       dimension NuBr(2000), kOfNu(2000), nOfNu(2000),
   21      & dKdNu(2000), nuItp(2000), kItp(2000)
   22 C
   23 C  Declarations of data types:
   24       real NuBr, kOfNu, NuLmLo, NuLmHi, NuRes, nnInf
   25
   26       real dKdNu
   27 C         (vector of first derivative of k wrt/ Nu)
   28 C  Variables for area calculation by numerical integration:
   29       real dNu, areasm, apole, deriv, diff
   30 C               NuRes: resolution of final frequency vector
   31 C               dNu: differential element of freq. for integration
   32 C               NuRes = 2 X dNu
   33 C  Variables for interpolated quantities:
   34       real nuItp, nOfNu, kItp
   35 C               nuItp: evenly spaced values of freq.
   36 C               kItp: imag. part of refr. index as function of nuItp
   37 C               nOfNu: vector of real part of refr. index calculated
   38
   39       integer i, j, LastPt, lstitp, jmax
   40 C               lstitp: number of points in interpolated vectors
   41 C                       nuItp and kItp
   42 C               i, j, m: dummy indices
   43 C
   44 C  Data storage address commands (Common block CSTAK contains space
   45 C  for the PORT3 module CSPDI to use.  This is converted from double-
   46 C  precision type to real type by the EQUIVALENCE statement below.):
   47       COMMON/CSTAK/DSTAK
   48       double precision DSTAK(6000)
   49       real RSTAK(12000)
   50       equivalence (DSTAK(1), RSTAK(1))
   51 C
   52       EXTERNAL cspdi
   53 C
```

```
Line#  Source Line          Microsoft FORTRAN Optimizing Compiler Version 4.10

   54  C               Statement function declaration for apole
   55  C               (Taylor's expansion about the pole):
   56        apole(diff, deriv) = 2*deriv*diff
   57
   58  C
   59  C Begin the executable statements.
   60
   61        dNu = NuRes/2
   62  C       Stretch the bounds of the input frequency data , if necessary,
   63  C       to bracket NuLmLo & NuLmHi.  If more than four Nu values are
   64  C       appended, the k values for the endpoints are set equal
   65  C       to zero.  This may cause discontinuities unless the extreme
   66  C       k values of the original data equal zero.  The interpolation
   67  C       routine will fill in gaps in frequency data.
   68
   69        if ((NuBr(1)) .GE. (NuLmLo - dNu - 0.01)) then
   70          if (NuBr(1) .GT. (NuLmLo+5.0*dNu)) kOfNu(1) = 0.0
   71          NuBr(1) = NuLmLo - dNu
   72        end if
   73        if ((NuBr(LastPt)) .LE. (NuLmHi + dNu + 0.01)) then
   74          if (NuBr(LastPt) .LT. (NuLmHi-5.0*dNu)) kOfNu(LastPt) = 0.0
   75          NuBr(LastPt) = NuLmHi + dNu
   76        end if
   77
   78  C       Calculate the number of points in the interpolated
   79  C       frequency array used for the approximation:
   80        lstitp = INT( (NuLmHi - NuLmLo)/dNu + 3.0 )
   81  C       (lstitp is the number of points used for the interpolation.)
   82  C
   83  C       Assign evenly spaced values of freq. to the vector nuItp, such that
   84  C               NuLmLo - dNu < NuItp < NuLmHi + dNu.
   85  C       The vectors k and dk/dNu will be interpolated at these frequencies.
   86        do 210 i = 1, lstitp
   87          nuItp(i) = NuLmLo + dNu*(i - 2)
   88    210 continue
   89  C
   90  C  Call a subroutine from the PORT library, CSPDI (Cubic SPline
   91  C  Differentiation and Interpolation) to interpolate and differentiate
   92  C  the values of k at regular intervals of nu.  There are LastPt
   93  C  input points.  CSPDI interpolates k at frequency values nuItp
   94  C  and outputs k as the vector kItp.  The first derivative of k
   95  C  is also calculated at these freqs. and output as dKdNu.
   96    280 write(*,*) ' PORT3 subprogram CSPDI has been called within KKSUB.'
   97        CALL cspdi (NuBr, kOfNu, LastPt, nuItp, kItp, dKdNu, lstitp)
   98        write(*,*) ' CSPDI is done.'
   99  C
  100  C  Equate negative values of k and its derivative to zero:
  101        DO 320 i = 1, lstitp
  102          if ( kItp(i) .LE. 0.0 ) kItp(i) = 0.0
  103    320 continue
  104  $page
```

Line# Source Line Microsoft FORTRAN Optimizing Compiler Version 4.10

```
C
C  Beginning of the Kramers Kronig calculation.
C       The indices i and j are used for the integration
C                            inf. k(nubar[i])*nubar[i]
C         n(nubar[j])= /       ---------------------- d nubar[i]
C                            0    nubar[i]^2 - nubar[j]^2
C
C       Calculation of Nu(j) is done sequentially for each j.
C For a given j, the point in the calc. for which i=j is a
C discontinuity called a "pole".
C       The counting index j will range from 2 to the nearest
C even number less than the max index of interpolated frequency.
C Call this upper limit "jmax":
      if ( mod(lstitp, 2) .EQ. 1 ) jmax = lstitp - 1
      if ( mod(lstitp, 2) .EQ. 0 ) jmax = lstitp - 2
C
C       The following nested loops calculate nOfNu by numerical
C approximation.  Simpson's rule approximation is used except
C at the poles, where function apole is called.
      do 460, j = 2, jmax, 2
C     [calculate n(j) for all j values]
C       Initialize variable to which partial sum of area accrues:
        areasm = 0.0
        do 420, i = 2, jmax, 2
C       [calculate total area for this j]
          if (i .NE. j) then
C           [do Simpson's rule]
            y1 = nultp(i-1)*kltp(i-1)/(nultp(i-1)**2 - nultp(j)**2)
            y2 = nultp(i)*kltp(i)/(nultp(i)**2 - nultp(j)**2)
            y3 = nultp(i+1)*kltp(i+1)/(nultp(i+1)**2 - nultp(j)**2)
C
            darea = dNu * (y1 + 4*y2 + y3)/3.0
          else
C           [calculate differential area at the pole point by Taylor's
C            expansion]
            deriv = dKdNu(j)
            darea = apole(dNu, deriv)
          end if
C         Increment the accrued area:
          areasm = areasm + darea
  420   continue
C       Calculate n(j) from the area for this j:
        nOfNu(j) = nnInf + areasm*2.0/3.14159
C       (Insert an indicator at the screen of the progress in calcs.:)
        if (mod(j, 20) .EQ. 0) write (*,'(A\)') '-'
  460 continue
C (End of the actual Kramers Kronig calculations)
C
C       Map the calculated vectors onto the output vectors having
C       half the resolution of the former:
      do 520 i = 1, jmax/2, 1
        NuBr(i) = nultp(2*i)
        nOfNu(i) = nOfNu(2*i)
```

```
KKSUB2                                                          PAGE   4
                                                                07-15-92
                                                                11:43:26

 Line#  Source Line          Microsoft FORTRAN Optimizing Compiler Version 4.10

   158          kOfNu(i) = kItp(2*i)
   159          LastPt = i
   160          if (NuBr(i) .GT. NuLmHi) GO TO 550
   161     520 continue
   162     550 RETURN
   163         END


KKSUB2  Local Symbols

Name                      Class   Type              Size   Offset

NOFNU . . . . . . . . . . param                            0006
NNINF . . . . . . . . . . param                            000a
NURES . . . . . . . . . . param                            000e
NULMHI. . . . . . . . . . param                            0012
NULMLO. . . . . . . . . . param                            0016
LASTPT. . . . . . . . . . param                            001a
KOFNU . . . . . . . . . . param                            001e
NUBR. . . . . . . . . . . param                            0022
I . . . . . . . . . . . . local   INTEGER*4            4    0002
Y1. . . . . . . . . . . . local   REAL*4               4    0006
J . . . . . . . . . . . . local   INTEGER*4            4    000a
Y2. . . . . . . . . . . . local   REAL*4               4    000e
Y3. . . . . . . . . . . . local   REAL*4               4    0012
NUITP . . . . . . . . . . local   REAL*4            8000    0016
DIFF. . . . . . . . . . . local   REAL*4               4    1f56
DAREA . . . . . . . . . . local   REAL*4               4    1f5a
LSTITP. . . . . . . . . . local   INTEGER*4            4    1f5e
DNU . . . . . . . . . . . local   REAL*4               4    1f62
JMAX. . . . . . . . . . . local   INTEGER*4            4    1f66
DKDNU . . . . . . . . . . local   REAL*4            8000    1f6a
KITP. . . . . . . . . . . local   REAL*4            8000    3eaa
AREASM. . . . . . . . . . local   REAL*4               4    5dea
DERIV . . . . . . . . . . local   REAL*4               4    5dee
DSTAK . . . . . . . . . . CSTAK   REAL*8           48000    0000
RSTAK . . . . . . . . . . CSTAK   REAL*4           48000    0000


Global Symbols

Name                      Class   Type              Size   Offset

CSPDI . . . . . . . . . . extern  ***                ***    ***
CSTAK . . . . . . . . . . common  ***              48000    0000
KKSUB2. . . . . . . . . . FSUBRT  ***                ***    0000

Code size = 0633 (1587)
Data size = 0078 (120)
Bss size  = 5df2 (24050)

No errors detected
```

c. Module OPF_IO containing subroutines LABLER and ASCII_XYOUT

```
                                                        PAGE   1
                                                        07-15-92
                                                        11:44:40

Line#  Source Line          Microsoft FORTRAN Optimizing Compiler Version 4.10

    1  $title:'OPF_IO'
    2  $subtitle:'LABLER'
    3  $pagesize:58
    4
    5        subroutine LABLER(outfil)
    6
    7  C     This subroutine takes a file of numerical data representing points
    8  C     in two dimensions, counts the number of points, and adds a
    9  C     heading to the top of the file.  The first line of the heading
   10  C     will consist of a title which the user provides when running
   11  C     the subroutine.  The second line will be the number of points in
   12  C     the file.  The file should be an ASCII representation of data
   13  C     in two columns, with 2 spaces separating the two data in each
   14  C     line.
   15
   16  C     One intended use of this subroutine is to convert files generated
   17  C     by the ASCII_XY translator in SpectraCalc into ASCII files that
   18  C     can be read by OPTCON and other programs.  These programs use
   19  C     formatted READ statements that are not compatible with the float-
   20  C     ing point output produced by SpectraCalc.
   21
   22        DIMENSION X(2000), Y(2000)
   23
   24  C                   --THE VARIABLE TYPE DECLARATIONS--
   25        CHARACTER TITLE*70, INFILE*12, outfil*12, ANS*1
   26        REAL X, Y
   27  C     X is the wavelength value and Y is the absorbance value for
   28  C     each point.
   29  C     INDEX and NP are integer variables and are implicitly defined.
   30  C     NP is the total number of points in the file being manipulated.
   31
   32  C                   --THE BODY OF THE subroutine--
   33     40 WRITE (*, 50)
   34     50 FORMAT (1X, 'What is the name of the input file to be read? ')
   35        READ (*, 70) INFILE
   36     70 FORMAT (A)
   37        WRITE (*, 80)
   38     80 FORMAT (1X, 'What is the name of the output file to be created? ')
   39        READ (*, 90) outfil
   40     90 FORMAT (A)
   41        OPEN (19, file= INFILE, status= 'old')
   42
   43  C     Begin a loop to read the points from the input file.
   44        INDEX = 1
   45    100 READ (19, *, end = 400) X(INDEX), Y(INDEX)
   46  C     The subroutine now reads X and Y values from the input file.
   47        INDEX = INDEX + 1
   48        GO TO 100
   49  C     (End of the loop to read points from the input file)
   50
   51    400 NP = INDEX - 1
   52  C     The variable "INDEX" was increased by 1 after reading the points.
   53        WRITE (*,420) NP
```

```
OPF_IO                                                          PAGE   2
LABLER                                                          07-15-92
                                                                11:44:40

 Line#  Source Line          Microsoft FORTRAN Optimizing Compiler Version 4.10

    54   420  FORMAT (1X, 'This subroutine has read', 1X, I4, 1X,
    55       + 'data points in the file.')
    56        WRITE (*, 440) INFILE
    57    440 FORMAT (' Do you want to delete ', A12,' from the disk? ', \)
    58        READ (*, '(A1)') ANS
    59        if((ANS .EQ. 'y')  .OR.  (ANS .EQ. 'Y')) then
    60          CLOSE (19, status= 'delete')
    61        else
    62          CLOSE (19, status= 'keep')
    63        end if
    64
    65        WRITE (*, 510)
    66    510 FORMAT (1X,
    67       + 'With what name do you want to label the output file? ')
    68        READ (*, 530) TITLE
    69    530 FORMAT (A)
    70        OPEN (20, file= outfil, status= 'new')
    71        WRITE (20, 560) TITLE
    72    560  FORMAT (A)
    73        WRITE (20, 600) NP
    74    600  FORMAT (I4)
    75
    76        INDEX = 1
    77  C     Begin a loop to write the data to the output file.
    78    650  WRITE (20, 670) X(INDEX), Y(INDEX)
    79    670  FORMAT (2(F10.5))
    80  C       The above format, 2(F10.5), is compatible with OPTCON.
    81        INDEX = INDEX + 1
    82        IF (INDEX.LE.NP) GO TO 650.
    83  C     (End of the loop to write the data)
    84        CLOSE (20)
    85        WRITE (*, 700)
    86    700  FORMAT (1X, 'Do you want to add a heading to another file?')
    87        WRITE (*, 720)
    88    720  FORMAT (1X, 'Type "y" or "n". ')
    89        READ (*, 740) ANS
    90    740  FORMAT (A)
    91        if((ANS .EQ. 'y')  .OR.  (ANS .EQ. 'Y')) GO TO 40
    92        RETURN
    93
    94        END


LABLER  Local Symbols

Name                    Class   Type            Size   Offset

OUTFIL. . . . . .       param                           0006
TITLE . . . . . .       local   CHAR*70           70    0002
X . . . . . .           local   REAL*4           8000   0048
Y . . . . . .           local   REAL*4           8000   1f88
NP. . . . . .           local   INTEGER*4           4   3ec8
ANS . . . . . .         local   CHAR*1              1   3ecc
```

LABLER Local Symbols

Name	Class	Type	Size	Offset
INFILE.	local	CHAR*12	12	3ece
INDEX	local	INTEGER*4	4	3eda

```
    95  C
    96  $SUBTITLE:'ASCII_XY OUT'
    97  $page
```

```
Line#  Source Line          Microsoft FORTRAN Optimizing Compiler Version 4.10

   98  C                       A S C I I _ X Y O U T    SUBROUTINE
   99  C                       ==================================
  100
  101        SUBROUTINE ASCOUT (nu, an, ak, np)
  102
  103  C  Written in Microsoft FORTRAN for use on an IBM PC-AT.
  104
  105  C               This subroutine will create 2files containing the n & k
  106  C        values so that the program SpectraCalc can read them and plot
  107  C        them.  The files are in "ASCII_XY" format.
  108  C               The main program can be compiled separately and combined
  109  C        with this subroutine at linking time.  This subroutine is in-
  110  C        tended to be combined with the FORTRAN source code program
  111  C        THREEPHASE.
  112
  113  C  Allocation of storage for arrays:
  114        DIMENSION nu(2000), ak(2000), an(2000)
  115  C  Type declarations for variables:
  116        INTEGER NP
  117        REAL nu, ak, an
  118        CHARACTER PREFIX*7, CMPNT*1, SUFFIX*4, nFILE*12, kFILE*12
  119        CHARACTER*1 RESP
  120  C  Format statements for writing to the screen:
  121     41 FORMAT (1X, A)
  122     42 FORMAT ('0', A)
  123     43 FORMAT (1X, A\)
  124  C  Documentation
  125        WRITE (*,42) 'The program will now write ASCII_XY files which can
  126       & be translated by'
  127        WRITE (*,41) 'SpectraCalc.  Two files will be created, called:'
  128        WRITE (*,41) '      *N.PRN      and  *K.PRN'
  129        WRITE (*,41) 'where "*" is a string of seven characters that you
  130       &provide.'
  131        WRITE (*, 4080) NP
  132   4080 FORMAT(1X,'The number of data points is: ', I3,'.')
  133  C  Create the three file names:
  134   4100 WRITE (*,43) 'What is the filename root (type 7 characters)?'
  135        READ (*,'(A7)') PREFIX
  136  $NOTSTRICT
  137  C  [Use concatenation of substrings to generate similar filenames.]
  138        SUFFIX = '.PRN'
  139
  140        CMPNT = 'N'
  141        NFILE(1:7) = PREFIX
  142        NFILE(8:8) = CMPNT
  143        NFILE(9:12) = SUFFIX
  144
  145        CMPNT = 'K'
  146        KFILE(1:7) = PREFIX
  147        KFILE(8:8) = CMPNT
  148        KFILE(9:12) = SUFFIX
  149
  150  C  Confirmation of names:
```

```
OPF_IO                                                          PAGE   5
ASCII_XY OUT                                                    07-15-92
                                                                11:44:40

 Line#  Source Line          Microsoft FORTRAN Optimizing Compiler Version 4.10

   151        WRITE (*,42) 'The program will create the files:'
   152        WRITE (*, 4200) NFILE, KFILE
   153   4200 FORMAT (8X, A12, ' and ', A12, '.')
   154        WRITE (*,43) 'Are these okay (type "y" or "n")? '
   155        READ (*, '(A)') RESP
   156        IF (.NOT. ((RESP.EQ.'y') .OR. (RESP.EQ.'Y'))) GO TO 4100
   157
   158  C                        WRITE THE DATA TO FILES
   159
   160   4300 FORMAT (F9.4, ',', F9.4)
   161
   162        OPEN (11, FILE=NFILE, STATUS='NEW')
   163        DO 4320 I=NP, 1, -1
   164  WRITE (11, 4300) NU(I), AN(I)
   165   4320 CONTINUE
   166        CLOSE(11)
   167        WRITE (*, 42) 'The file for the n-component has been completed.'
   168
   169        OPEN (12, FILE=KFILE, STATUS='NEW')
   170        DO 4420 I=NP, 1, -1
   171  WRITE (12, 4300) NU(I), AK(I)
   172   4420 CONTINUE
   173        CLOSE(12)
   174        WRITE (*, 41) 'The file for the k-component has been completed.'
   175
   176        WRITE (*,'(A)') ' '
   177        RETURN
   178
   179        END


ASCOUT  Local Symbols

Name                      Class   Type            Size   Offset

NP. . . . . . . . . . . . param                          0006
AK. . . . . . . . . . . . param                          000a
AN. . . . . . . . . . . . param                          000e
NU. . . . . . . . . . . . param                          0012
CMPNT . . . . . . . . . . local   CHAR*1             1   3ede
I . . . . . . . . . . . . . local   INTEGER*4          4   3ee0
PREFIX. . . . . . . . . . . local   CHAR*7             7   3ee4
SUFFIX. . . . . . . . . . . local   CHAR*4             4   3eec
KFILE . . . . . . . . . . . local   CHAR*12           12   3ef0
NFILE . . . . . . . . . . . local   CHAR*12           12   3efc
RESP. . . . . . . . . . . . local   CHAR*1             1   3f08


Global Symbols

Name                      Class   Type            Size   Offset

ASCOUT. . . . . . . . . . . FSUBRT  ***              ***   01df
```

Microsoft FORTRAN Optimizing Compiler Version 4.10

Global Symbols

Name	Class	Type	Size	Offset
LABLER.	FSUBRT	***	***	0000

Code size = 046a (1130)
Data size = 0348 (840)
Bss size = 3f09 (16137)

No errors detected

3. Programs for Calculating Infrared Spectra

a. RTCALC


```
Line#  Source Line          Microsoft FORTRAN Optimizing Compiler Version 4.10

    1  $large
    2  $storage:2
    3  $title:'RTCALC'
    4  $SUBTITLE:'Main Program'
    5  $pagesize:58
    6  $linesize:86
    7  $declare
    8
    9                          PROGRAM RTCALC
   10  C                       =============
   11
   12  C              This program computes values of reflectivity and
   13  C       transmissivity for a stratified optical medium of uniform
   14  C       phases separated by parallel planar phase boundaries.
   15  C       One phase is chosen for which to generate spectra (i.e. it is
   16  C       not present in the reference calculation.  Any other phases,
   17  C       except the first, may have variable optical functions,
   18  C       to be input as files of n and k.  All intermediate phases,
   19  C       including the spectral phase, have thicknesses which must be
   20  C       specified in Angstroms.  Transmittance can only be calculated
   21  C       for cases in which the final phase is non-absorbing [k(m)=0.0].
   22  C       Values of R and T for the reference (spectral phase not present)
   23  C       are calculated by setting k = 0.0 and n = nVarInf for the spectral
   24  C       phase; alternatively, the entire stratified medium can be redefined
   25  C       for the reference calculation.
   26  C       The calculation is done in a subroutine by a matrix method which
   27  C       calculates the boundary field strengths.  An algorithm using the
   28  C       mean value theorem is used (hence the program name).
   29  C       The total number of phases, PhzTotal, must be specified
   30  C       and cannot exceed the size specified by the dimension statements.
   31  c       When KBr pellet spectra are calculated set IKBR=true so
   32  c       that N(V) = nVarInf.
   33  C              This program was adapted from SMVP4.FOR in April 1989
   34  C       in order to expand array dimensions and improve reliability.
   35  C       SMVP5 was modified to facilitate separate sample and reference
   36  C       calculations in October 1989 by Darwin D. Popenoe.  The name was
   37  C      changed to "RTCALC" in 1990.
   38
   39  C                         DECLARATION  STATEMENTS
   40  C                         ----------------------
   41
   42        REAL Wdth, w, win, anv, akv, anin, akin
   43        REAL RS, RP, TS, TP, RS0, RP0, TS0, TP0
   44
   45        DIMENSION Wdth(2:5), w(2000), win(2000), anv(2000), akv(2000)
   46        DIMENSION anin(2000), akin(2000)
   47  C               w, anv, akv: optical functions as a fxn of freq. for
   48  C                       spectral phase
   49  C               win, anin, akin: opt. fxns. of freq. for other phases of
   50  C                       variable n,k
   51        DIMENSION RS(2000), RP(2000), TS(2000), TP(2000)
   52        DIMENSION RS0(2000), RP0(2000), TS0(2000), TP0(2000)
   53  C               R, T: components of real reflectivity and transmissivity
```

```
RTCALC                                                          PAGE  2
Main Program                                                    07-15-92
                                                                11:47:09

 Line#  Source Line          Microsoft FORTRAN Optimizing Compiler Version 4.10

    54  C                        for sample and reference phases
    55
    56        LOGICAL ikbr,imore, vPhzs(6)
    57        REAL nVarInf, pi, theta1, ThetaRad
    58        REAL arpmax, warpmax, atpmax, watpmax, arp, ars, atp, ats
    59        INTEGER jarpmax, jatpmax
    60        COMPLEX nCplx(6), nOfNuCplx(2000, 2:6), I, AA(6)
#   61  C       [If memory space is limited, the matrix nOfNuCplx could be eliminated,
#   62  C       by making anv and akv into 5 X 2000 real matrices and releasing space.
#   63  C        AA contains the complex angle of propagation, theta(j), for each phase.
    64        complex UFS(6,6),UBS(6,6),UFP(6,6),UBP(6,6)
    65        CHARACTER TITLE*70, fname*12, TextStr*70, answer*1
    66        INTEGER PhzTotal, iPhzSp, j, jmax, np, npin
    67        INTEGER iPhz, SplRefFlag, SepRefStrata
    68  C               PhzTotal: total no. of phases in stack
    69  C               iPhzSp : ordinal no. of the phase with spectral info.
    70  C               iPhz : ordinal number of a phase used as a pointer.
    71  c               SplRefFlag =0 for sample spectrum and =1 for reference.
    72  C               SepRefStrata =1 for same strata (phases) and =2 for diff. ones.
    73
    74        common/FLDCOM/PhzTotal, ThetaRads, Wdth
    75
    76  C  Data storage address command (Common block CSTAK contains space
    77  C  for the PORT3 modules CSPDI and CSPIN to use.  This is converted from
#   78  C  double-precision type to real type by the EQUIVALENCE statement below.):
    79        COMMON/CSTAK/DSTAK
***** rtcalc.for(79) : warning F4313: DSTAK : not previously declared
    80        double precision DSTAK(6000)
    81        real RSTAK(12000)
    82        equivalence (DSTAK(1), RSTAK(1))
    83
    84        external wnkint, fields, istkin
    85        parameter (PI=3.1415926)
    86  C       [used to echo calculation type via formats 10 & 11]
    87        I=CMPLX(0.0,1.0)
    88
    89  C                        BEGINNING OF EXECUTABLE STATEMENTS
    90  C                        ----------------------------------
    91
    92  C  The PORT3 library subprogram ISTKIN initializes the dynamic storage
    93  C  stack to create enough space for subprograms CSPDI and CSPIN to
    94  C  differentiate 2000 points containing single precision real data.  The
    95  C  parameter ITYPE = 3 represents real numbers.
    96        CALL ISTKIN(12000, 3)
    97  C  The call above initializes the dynamic stack for any and all calls to
    98  C  PORT3 subprograms in the main program or subroutines.
    99
   100  C Global FORMAT statements for input and output:
   101       5 FORMAT (1X, A\)
   102       6 FORMAT (1X, A)
   103       7 FORMAT (BN, I1)
#  104  C Statement echoed to screen to specify calculation for sample or reference:
```

```
 Line#  Source Line          Microsoft FORTRAN Optimizing Compiler Version 4.10

   105     10 FORMAT ('0     Calculation type: SAMPLE')
   106     11 FORMAT ('0     Calculation type: REFERENCE')
   107
   108  C                                  INTRODUCTION:
   109        write(*,6)'This is the program RTCALC, which will calculate spectr
   110       &a from n & k.'
   111        write(*,6)'All real numbers must be typed with explicit decimal po
   112       &int.'
   113        WRITE(*,6)'The experiment is modeled as a stratified optical mediu
   114       &m with parallel planar'
   115        write(*,6)'phase boundaries like this:'
   116        write(*,6)
   117        write(*,6)'     (incident beam)> PHASE 1|PHASE 2| . . . |PHASE N'
   118        write(*,6)
   119
   120  C                          INQUIRE ABOUT CHANGING STRATA:
   121        write(*,6)'Calculation of the reference spectrum may be done in on
   122       &e of the following ways:'
   123        write(*,6)'   1. Substitution of spectral phase with non-absorbing
   124       & phase of constant n.'
   125        write(*,6)'   2. Input of a new set of phases.'
   126        write(*,5)'Choose one of these options (type "1" or "2"): '
   127        read (*,7) SepRefStrata
   128        write (*,*)
   129
   130  C                                  GET RUN NUMBER:
   131        write(*,5) ' Input a run number: '
   132        READ(*,50) IRUN
***** rtcalc.for(132) : warning F4313: IRUN : not previously declared
   133     50 format(bn,i3)
   134        DATA SplRefFlag /0/
   135
   136  C                          RETURN POINT FOR CONTINUING EXECUTION:
   137    220 CONTINUE
   138        iPhzSp = 0
   139  C     [Echo calculation type to which following input applies:]
   140        if (SplRefFlag .EQ. 0) write (*, 10)
   141        if (SplRefFlag .EQ. 1) write (*, 11)
   142        DATA vPhzs /6*.FALSE./
   143
   144  C                          SET UP STRATIFIED PHASES:
   145        write(*,5) 'Input the total number of phases as an integer: '
   146        read (*,7) PhzTotal
   147        write (*,6) 'For each phase, state whether n & k vary with freq.'
   148        write (*,6) '(type "t" for true or "f" for false).'
   149
   150        DO 250 iPhz=2, PhzTotal
   151          write (*, 240) iPhz
   152     240  format (1X, 'Is PHASE ', I1, ' dispersive? (T or F): ', \)
   153          read (*,'(L1)') vPhzs(iPhz)
   154  C       [vPhzs is an array of logical elements.  vPhzs(n) is true if
   155  C       phase n has varying n&k with frequency, and false otherwise.]
```

```
RTCALC                                                          PAGE   4
Main Program                                                    07-15-92
                                                                11:47:09

 Line#  Source Line          Microsoft FORTRAN Optimizing Compiler Version 4.10

   156    250 CONTINUE
   157
   158  C                          INPUT N,K DATA FOR SPECTRAL PHASE:
   159        if (SplRefFlag .EQ. 0) then
   160          write (*,*)
   161          write(*,6) 'Provide info. on file with spectrum of interest.'
   162          write(*,5) 'Input phase number: '
   163          read(*,'(bn,i1)') iPhzSp
   164          write(*,5) 'Input filename: '
   165          read(*,'(bn,a12)') fname
   166          open(09,file=fname,status='old')
   167          read(09,'(a70)') title
   168          write(*, *) '    Heading for this file: '
   169          write (*, '(1X, A70)') title
   170          read(09,'(i4)') np
   171          akvmax=0
***** rtcalc.for(171) : warning F4313: AKVMAX : not previously declared
   172          do 200 j=1,np
   173            read(09,120) w(j),anv(j),akv(j)
   174    120     format(f8.2,2(f8.5))
   175            nOfNuCplx(j, iPhzSp)=cmplx(anv(j),akv(j))
   176            if((akv(j)-akvmax).lt.0) goto 200
   177            akvmax=akv(j)
   178            jmax=j
   179    200   continue
   180          close(09)
   181          write(*,130) akvmax,jmax,w(jmax)
   182    130   FORMAT(10X, 'max. k(nu-bar) = ', F6.4, 2X,
   183       &        'point no. = ', I3, 2X, 'freq.(cm-1) = ', F7.1)
   184
   185          write(*,5)  'Is spectrum for kbr disk? (type "y" or "n")? '
   186          read (*,'(A1)') answer
   187          if(answer .EQ. 'y' .OR. answer .EQ. 'Y') ikbr = .true.
   188          if(ikbr) write (*, 265)
   189    265   format(2x,'-------KBr disk calculation-------')
   190        end if
   191
   192  C               INPUT N,K DATA FOR OTHER DISPERSIVE PHASES
   193        write(*,'(a)') '0Provide data for phases with variable n & k.'
   194        do 400 iPhz= 2, PhzTotal
   195          if ( (vPhzs(iPhz)) .AND. (iPhz .NE. iPhzSp) ) then
   196  C         [Do these steps for dispersive phases except spectral phase]
   197            write (*, 260) iPhz
   198    260     format (6X, 'What file contains n&k data for phase number ',
   199       &           I1, '? ', \)
   200            read (*, '(A12)') fname
   201            open(10,file=fname,status='old')
   202            read(10,'(bn,a70)')  TextStr
   203            write(*, *) '    Heading for this file: '
   204            write (*, '(1X, A70)') TextStr
   205            read(10,'(i4)') npin
   206            do 300 j=1,npin
```

Line# Source Line Microsoft FORTRAN Optimizing Compiler Version 4.10

```
 207              read(10,120) win(j),anin(j),akin(j)
 208    300     continue
 209            close(10)
 210            CALL WNKINT (win, anin, akin, npin, w, anv, akv, np, *1600)
 211            do 350 j=1, np
 212              nOfNuCplx(j, iPhz) = cmplx(anv(j),akv(j))
 213    350     continue
 214           end if
 215    400 continue
 216
 217  C                          INPUT CONSTANT N,K DATA:
 218  C     [Echo calculation type to which following input applies:]
 219    550 if (SplRefFlag .EQ. 0) write (*, 10)
 220        if (SplRefFlag .EQ. 1) write (*, 11)
 221
 222        write(*,6)'    Specify n,k for each phase of const. n (separate by
 223       & a comma):'
 224        DO 590 iPhz=1, PhzTotal
 225          if ( .NOT. (vPhzs(iPhz)) ) then
 226            write(*,570) iPhz
 227    570     format (2x, 'Phase number ', i1, ': '\)
 228            READ(*,'(2f6.3)') nCplx(iPhz)
 229          end if
 230    590 CONTINUE
 231
 232        if (SepRefStrata .EQ. 1) then
 233          write(*,*)
 234          write(*,5)'Input n value of spectral phase for ref. calc.: '
 235          read (*, '(F6.3)') nVarInf
 236        end if
 237
 238  C                          INPUT THICKNESSES:
 239        write(*,'(A)') '0Specify thickness (angstroms) of each phase: '
 240        DO 650 iPhz=2, PhzTotal-1
 241          write(*,570) iPhz
 242          READ(*,'(f9.3)') WdthA
***** rtcalc.for(242) : warning F4313: WDTHA : not previously declared
 243          Wdth(iPhz)=WdthA*1.0E-08
 244    650 CONTINUE
 245
 246  C                          INPUT ANGLE OF INCIDENCE:
 247        write(*,5) ' What is the angle of incidence (degs)? '
 248        READ(*,'(f5.2)') THETA1
 249        ThetaRads=(PI/180)*THETA1
 250
 251    690 CONTINUE
 252
 253  C               (PRINT SUMMARY OF PHASES AT THE SCREEN.)
 254        write(*,*)
 255        if (SplRefFlag .EQ. 0) write (*, 10)
 256        if (SplRefFlag .EQ. 1) write (*, 11)
 257        DO 800 iPhz=1, PhzTotal
```

Line# Source Line Microsoft FORTRAN Optimizing Compiler Version 4.10

```
C     [execute this loop for all phases]
        if (vPhzs(iPhz)) then
C       [execute this command for all absorbing phases only]
          if(iPhz.eq. PhzTotal) then
            write(*,735) iPhz
 735        format(2x,'phase=',i1,':',2x,'VARIABLE N,K')
          else
            write(*,730) iPhz,Wdth(iPhz)*1.0E08
 730        FORMAT(2X, 'PHASE=', I1, ':', 2X, 'VARIABLE N,K', 9X,
     &                 'THICKNESS(A)=', 1P, G10.4)
          end if
        else
C       [in the case of a non-absorbing phase...]
          IF(iPhz.EQ.1 .OR. iPhz.EQ. PhzTotal) then
 740        write(*,750) iPhz, REAL(nCplx(iPhz)),AIMAG(nCplx(iPhz))
 750        FORMAT(2X,'PHASE=',I1,':',2X,'N=',F6.4,2X,'K=',F7.4)
          else
            write (*,710) iPhz, REAL(nCplx(iPhz)), AIMAG(nCplx(iPhz)),
     &                    Wdth(iPhz)*1.0E08
 710        FORMAT(2X,'PHASE=',I1,':',2X,'N=',F6.4,2X,'K=',F7.4,2X,
     &               'THICKNESS(A)=', 1P, G10.4)
          end if
        end if
 800  CONTINUE
$PAGE
```

```
RTCALC                                                          PAGE   7
Main Program                                                    07-15-92
                                                                11:47:09

 Line#  Source Line          Microsoft FORTRAN Optimizing Compiler Version 4.10

   283  C                     BEGIN CALCULATIONS
   284  C                     ------------------
   285
   286    810 DO 1000 J=1,NP
#  287  C [This large DO loop is executed so as to calc. one freq. value at a time.]
   288  C                ESTABLISH COMPLEX N VALUES AT THIS FREQUENCY:
   289         DO 850 iPhz = 2, PhzTotal
   290           if (vPhzs(iPhz)) then
   291             if (iKBr) then
   292  C          (For KBr pellet real(n) is replaced by nVarInf=n(KBr).)
   293    820         nCplx(iPhz)=CMPLX(nVarInf,AIMAG(nOfNuCplx(j,iPhz)))
   294             else
   295               nCplx(iPhz) = nOfNuCplx(j, iPhz)
   296             end if
   297           end if
   298  C        [Go on to next phase in stack.]
   299    850   CONTINUE
   300
   301    860   CALL FIELDS (nCplx, w(j), ufs, ubs, ufp, ubp, AA)
   302  C       [UFS and UFP for final phase boundary = 1.0]
   303
   304    870   IF(SplRefFlag.EQ.0) then
   305  C                        SAMPLE R,T CALCULATION
   306  C                        ----------------------
   307           rp(j)= (UBP(1,2)/UFP(1,2))*CONJG(UBP(1,2)/UFP(1,2))
   308           rs(j)= (UBS(1,2)/UFS(1,2))*CONJG(UBS(1,2)/UFS(1,2))
   309           IF (.NOT. AIMAG(nCplx(PhzTotal)).GT.0) THEN
   310  C              (Do not calculate transmittance if the last phase is
   311  C              absorbing.)
   312             TrFctr=REAL(nCplx(PhzTotal)*AA(PhzTotal))/(nCplx(1)*AA(1))
***** rtcalc.for(312) : warning F4313: TRFCTR : not previously declared
   313             tp(j)= TrFctr*(1.0/UFP(1,2))*CONJG(1.0/UFP(1,2))
   314             ts(j)= TrFctr*(1.0/UFS(1,2))*CONJG(1.0/UFS(1,2))
   315           END IF
   316           nCplx(iPhzSp)=CMPLX(nVarInf,0.0)
   317         else
   318  C                        REFERENCE R,T CALCULATION
   319  C                        -------------------------
   320           rp0(j)= (UBP(1,2)/UFP(1,2))*CONJG(UBP(1,2)/UFP(1,2))
   321           rs0(j)= (UBS(1,2)/UFS(1,2))*CONJG(UBS(1,2)/UFS(1,2))
   322           IF (.NOT. AIMAG(nCplx(PhzTotal)) .GT. 0) then
   323  C              (Do not calculate transmittance if the last phase is
   324  C              absorbing.)
   325             TrFctr=REAL(nCplx(PhzTotal)*AA(PhzTotal))/(nCplx(1)*AA(1))
   326             tp0(j)= TrFctr*(1.0/UFP(1,2))*CONJG(1.0/UFP(1,2))
   327             ts0(j)= TrFctr*(1.0/UFS(1,2))*CONJG(1.0/UFS(1,2))
   328           END IF
   329         end if
   330  C              END OF SAMPLE AND REFERENCE CALCULATIONS
   331  C              ---------------------------------------
   332   1000 continue
   333  $PAGE
```

```
 Line#  Source Line          Microsoft FORTRAN Optimizing Compiler Version 4.10

#  334  C     [If both sample & reference have been calculated, go on to next step.]
   335        if (SplRefFlag .EQ. 1) GO TO 1110
   336  C     Otherwise set up reference calculation:
   337        SplRefFlag = 1
   338
   339  C     If the strata are to be changed, go back and change them:
   340        If (SepRefStrata .EQ. 2) GO TO 220
   341
#  342  C     Otherwise convert the spectral phase to a non-absorbing phase of fixed n
   343        vPhzs(iPhzSp) = .FALSE.
   344        nCplx(iPhzSp) = cmplx(nVarInf, 0.0)
   345  C     ...and go back to calculate the reference spectrum:
   346        GO TO 690
   347
   348   1110 CONTINUE
   349  C                SEARCH FOR POINTS OF MAXIMUM ABSORBANCE:
   350        DATA arpmax, jarpmax, warpmax, atpmax, jatpmax, watpmax /6*0/
   351        DO 1200 j=1, np
   352          if (rp0(j) .GT. 0) then
   353            ARP=-ALOG10(rp(j)/rp0(j))
   354          else
   355            ARP = 999.999
   356          end if
   357          if((arpmax-arp).lt.0) then
   358            arpmax=arp
   359            jarpmax=j
   360            warpmax= w(j)
   361          endif
   362          if (rs0(j) .GT. 0) then
   363            ARS=-ALOG10(rs(j)/rs0(j))
   364          else
   365            ARS = 999.999
   366          end if
   367          IF (.NOT. AIMAG(nCplx(PhzTotal)) .GT. 0) then
   368  C        (Do not calculate transmittance if the last phase is
   369  C        absorbing.)
   370            ATP=-ALOG10(tp(j)/tp0(j))
   371            ats=-alog10(ts(j)/ts0(j))
   372            if((atpmax-atp).lt.0) then
   373              atpmax=atp
   374              jatpmax=j
   375              watpmax= w(j)
   376            end if
   377          END IF
   378   1200 CONTINUE
   379  C                          END OF CALCULATIONS
   380  C                          ___________________
   381
   382  C               WRITE TO OUTPUT FILE:
   383   1400 write (*, '(a\)') 'OWhat is the output filename: '
   384        read (*, '(A12)') fname
   385        open (11, file = fname, status = 'unknown')
   386        WRITE (11, '(i3)') IRUN
```

```
RTCALC                                                          PAGE   9
Main Program                                                    07-15-92
                                                                11:47:09

 Line#  Source Line          Microsoft FORTRAN Optimizing Compiler Version 4.10

   387        WRITE(11,'(a70)') TITLE
   388        WRITE(11,'(i4)') np
   389        write(*, 1420) fname, TITLE
   390   1420 format (1x, 'Writing heading to ', a12, ':', A70)
   391        DO 1450 j=1, np
   392          write (11, '(F8.2)') w(j)
   393          write (11, '(8F10.7)') rp(j),  tp(j),  rs(j),  ts(j),
   394       &                         rp0(j), tp0(j), rs0(j), ts0(j)
   395   1450 CONTINUE
   396        close (11)
   397
   398   C               PRINT INFO. ABOUT MAX. ABSORBANCES:
   399        write(*,1530) arpmax,jarpmax,warpmax
   400   1530 format(3x, '-log(R/Ro)[max.]=', f8.5, 2x, 'point no.=', i3, 2x,
   401       &       'freq.=', f7.1)
   402
   403        if(aimag(nCplx(PhzTotal)).gt.0) go to 1550
   404        write(*,1540) atpmax, jatpmax, watpmax
   405   1540 format(3x, '-log(T/To)[max.]=', f8.5, 2x, 'point no.=', i3, 2x,
   406       &       'freq.=', f7.1)
   407
   408   1550 imore = .false.
   409        if (SepRefStrata .EQ.2) GO TO 1600
   410        write(*,5)' Another calculation with RTCALC (type "y" or "n")? '
   411        read (*,'(A1)') answer
   412        if(answer .EQ. 'y' .OR. answer .EQ. 'Y') imore = .true.
   413        if (imore) then
#  414   C       [use same strata to calculate another set of sample & ref. spectra]
   415          SplRefFlag = 0
   416          vPhzs(iPhzSp) = .TRUE.
   417          IRUN=IRUN+1
   418          GO TO 550
   419        end if
   420   1600 STOP
   421        END

main  Local Symbols

Name                    Class   Type          Size   Offset

NOFNUC. . . . . local   COMPLEX*8    80000   0000
AA. . . . . local   COMPLEX*8       48   0000
TITLE . . . . . local   CHAR*70        70   0002
NCPLX . . . . . local   COMPLEX*8       48   0030
SEPREF. . . . . local   INTEGER*2        2   0048
AKVMAX. . . . . local   REAL*4           4   004a
I . . . . . local   COMPLEX*8        8   004e
J . . . . . local   INTEGER*2        2   0056
NVARIN. . . . . local   REAL*4           4   0058
ANSWER. . . . . local   CHAR*1           1   005c
TRFCTR. . . . . local   REAL*4           4   005e
AKV . . . . . local   REAL*4        8000   0060
```

main Local Symbols

Name	Class	Type	Size	Offset
NP.	local	INTEGER*2	2	0062
IPHZSP.	local	INTEGER*2	2	0064
ARP	local	REAL*4	4	0066
ATP	local	REAL*4	4	006a
ARS	local	REAL*4	4	006e
FNAME	local	CHAR*12	12	0072
THETA1.	local	REAL*4	4	007e
ATS	local	REAL*4	4	0082
IKBR.	local	LOGICAL*2	2	0086
TEXTST.	local	CHAR*70	70	0088
JMAX.	local	INTEGER*2	2	00ce
NPIN.	local	INTEGER*2	2	00d0
WDTHA	local	REAL*4	4	00d2
IPHZ.	local	INTEGER*2	2	00d6
IMORE	local	LOGICAL*2	2	00d8
IRUN.	local	INTEGER*2	2	00da
SPLREF.	local	INTEGER*2	2	0536
ARPMAX.	local	REAL*4	4	0756
JARPMA.	local	INTEGER*2	2	075a
WARPMA.	local	REAL*4	4	075c
ATPMAX.	local	REAL*4	4	0760
JATPMA.	local	INTEGER*2	2	0764
WATPMA.	local	REAL*4	4	0766
AKIN.	local	REAL*4	8000	1fa0
RPO	local	REAL*4	8000	3880
TP.	local	REAL*4	8000	3ee0
TPO	local	REAL*4	8000	57c0
RS.	local	REAL*4	8000	5e20
RSO	local	REAL*4	8000	7700
ANV	local	REAL*4	8000	7d60
TSO	local	REAL*4	8000	9640
ANIN.	local	REAL*4	8000	9ca0
W	local	REAL*4	8000	b580
TS.	local	REAL*4	8000	bbe0
RP.	local	REAL*4	8000	d4c0
WIN	local	REAL*4	8000	db20
UBP	local	COMPLEX*8	288	f400
UBS	local	COMPLEX*8	288	f520
UFP	local	COMPLEX*8	288	f640
UFS	local	COMPLEX*8	288	f760
VPHZS	local	LOGICAL*2	12	f8e2
DSTAK	CSTAK	REAL*8	48000	0000
RSTAK	CSTAK	REAL*4	48000	0000
WDTH.	FLDCOM	REAL*4	16	0006
THETAR.	FLDCOM	REAL*4	4	0002
PHZTOT.	FLDCOM	INTEGER*2	2	0000

Microsoft FORTRAN Optimizing Compiler Version 4.10

Symbolic Constant	Type	Value
PI.	REAL*4	3.1415925E+000

```
   422  $NODECLARE
   423  $subtitle:'FIELDS subroutine'
   424  $page
```

Line# Source Line Microsoft FORTRAN Optimizing Compiler Version 4.10

```
      SUBROUTINE FIELDS(nCplx,W,ufs,ubs,ufp,ubp, AA)

      COMPLEX nCplx(6),TFS(6),TFP(6),RFS(6),RFP(6),UFS(6,6),UBS(6,6),
     1     UFP(6,6),UBP(6,6),AA(6),DELTA,ZCD,I
      integer PhzTotal
      DIMENSION Wdth(2:5)
      common/fldcom/PhzTotal, ThetaRads, Wdth
      parameter (PI=3.1415926)
      I=CMPLX(0.0,1.0)

      UFS(PhzTotal,PhzTotal-1)=1.0
      UFP(PhzTotal,PhzTotal-1)=1.0
      UBS(PhzTotal,PhzTotal-1)=0.0
      UBP(PhzTotal,PhzTotal-1)=0.0
      DO 100 LCOUNT=1,PhzTotal
        iPhz=(PhzTotal+1)-LCOUNT
        AA(iPhz) =
     & ( ((nCplx(iPhz))**2)-(nCplx(1)**2)*((SIN(ThetaR))**2) )**0.5/
     &                  nCplx(iPhz)
        IF(iPhz.EQ.PhzTotal) GO TO 100
        IF(iPhz.EQ.1) GO TO 50
        ZCD=W*Wdth(iPhz)*nCplx(iPhz)*AA(iPhz)
        ZID=AIMAG(ZCD)
        ZRD=REAL(ZCD)
        ZRD=ZRD-AINT(ZRD)
        DELTA=2*PI*CMPLX(ZRD,ZID)
   50   RFS(iPhz) = (nCplx(iPhz)*AA(iPhz)-nCplx(iPhz+1)*AA(iPhz+1))/
     &         (nCplx(iPhz)*AA(iPhz)+nCplx(iPhz+1)*AA(iPhz+1))
        RFP(iPhz) = (nCplx(iPhz+1)*AA(iPhz)-nCplx(iPhz)*AA(iPhz+1))/
     &         (nCplx(iPhz+1)*AA(iPhz)+nCplx(iPhz)*AA(iPhz+1))
        TFS(iPhz) = (2*nCplx(iPhz)*AA(iPhz))/
     &              (nCplx(iPhz)*AA(iPhz)+nCplx(iPhz+1)*AA(iPhz+1))
        TFP(iPhz) = (2*nCplx(iPhz)*AA(iPhz))/
     &              (nCplx(iPhz)*AA(iPhz+1)+nCplx(iPhz+1)*AA(iPhz))
        UFS(iPhz,iPhz+1) = (1.0/TFS(iPhz))*(UFS(iPhz+1,iPhz) +
     &                     RFS(iPhz)*UBS(iPhz+1,iPhz))
        UBS(iPhz,iPhz+1) = (1.0/TFS(iPhz))*(RFS(iPhz)*UFS(iPhz+1,iPhz)+
     &                      UBS(iPhz+1,iPhz))
        UFP(iPhz,iPhz+1) = (1.0/TFP(iPhz))*(UFP(iPhz+1,iPhz) +
     &                      RFP(iPhz)*UBP(iPhz+1,iPhz))
        UBP(iPhz,iPhz+1) = (1.0/TFP(iPhz))*(RFP(iPhz)*UFP(iPhz+1,iPhz)+
     &                      UBP(iPhz+1,iPhz))
        IF(iPhz.EQ.1) GO TO 100
        UFS(iPhz,iPhz-1) = CEXP(-I*DELTA) * UFS(iPhz,iPhz+1)
        UBS(iPhz,iPhz-1) = CEXP( I*DELTA) * UBS(iPhz,iPhz+1)
        UFP(iPhz,iPhz-1) = CEXP(-I*DELTA) * UFP(iPhz,iPhz+1)
        UBP(iPhz,iPhz-1) = CEXP( I*DELTA) * UBP(iPhz,iPhz+1)
  100  CONTINUE
       RETURN
       END
```

Microsoft FORTRAN Optimizing Compiler Version 4.10

FIELDS Local Symbols

Name	Class	Type	Size	Offset
AA.	param			0006
UBP	param			000a
UFP	param			000e
UBS	param			0012
UFS	param			0016
W	param			001a
NCPLX	param			001e
I	local	COMPLEX*8	8	00dc
LCOUNT.	local	INTEGER*2	2	00e4
ZCD	local	COMPLEX*8	8	00e6
ZID	local	REAL*4	4	00ee
DELTA	local	COMPLEX*8	8	00f2
ZRD	local	REAL*4	4	00fa
IPHZ.	local	INTEGER*2	2	00fe
RFP	local	COMPLEX*8	48	fbba
TFP	local	COMPLEX*8	48	fbea
RFS	local	COMPLEX*8	48	fc1a
TFS	local	COMPLEX*8	48	fc4a
PHZTOT.	FLDCOM	INTEGER*2	2	0000
WDTH.	FLDCOM	REAL*4	16	0006
THETAR.	FLDCOM	REAL*4	4	0002

Symbolic Constant	Type	Value
PI.	REAL*4	3.1415925E+000

```
  475  $subtitle:'WNKINT subroutine'
  476  $page
```

Line# Source Line Microsoft FORTRAN Optimizing Compiler Version 4.10

```
      subroutine wnkint(w1, an1, ak1, np1, w3, an3, ak3, np3, *)

      real w1, w3, an1, an3, ak1, ak3, wmesh, bmesh, bf
C       w1, an1, and ak1 are for phase of variable n,k on input
C       w3, an3, and ak3 contain the matrix of complex n on input,
C               and the interpolated values for the selected phase
C               on output

      dimension w1(2000), w3(2000), an1(2000), an3(2000)
      dimension ak1(2000),ak3(2000)
      dimension wmesh(2000),bmesh(4000),bf(4000)

      integer np1, np3
      common/cstak/dstak(6000)
      double precision dstak
      real rstak(12000)
      equivalence (dstak(1), rstak(1))
      external cspin, umb, mnpb, dl2sf, spline
      character answer*1
      logical iout

c     test to see if w1 array increases in value from w1(1) to w1(np1).
      if(w1(1).gt.w1(np1)) THEN
c       (reverse array order if necessary)
  100   if((mod(np1,2)).eq.0) then
          np=np1/2
        else
          np=(np1-1)/2
        endif
        do 150 j=1,np
          z=w1(j)
          w1(j)=w1(np1+1-j)
          w1(np1+1-j)=z
          z=an1(j)
          an1(j)=an1(np1+1-j)
          an1(np1+1-j)=z
          z=ak1(j)
          ak1(j)=ak1(np1+1-j)
          ak1(np1+1-j)=z
  150   continue
      END IF

  200 if(w1(1).gt.w3(1)) go to 900
      if(w1(np1).lt.w3(np3)) goto 900
      write(*, '(1X, A\)')
     &     'Enter the approx. resolution (integ.) of n,k file: '
      read(*,'(bn,i4)') kz1
      nab=int((w1(np1)-w1(1))/kz1) + 1

c     generate uniform w mesh
      write(*, '(1X, A\)') 'Select spline order (>2): '
      read(*,'(bn,i2)') k
      CALL umb(w1(1),w1(np1),nab,k,wmesh,nwmesh)
```

```
RTCALC                                                          PAGE  15
WNKINT subroutine                                               07-15-92
                                                                11:47:09

 Line#  Source Line          Microsoft FORTRAN Optimizing Compiler Version 4.10

   530        write(*,'(2i4)') nab,nwmesh
   531
   532  c     generate b-spline mesh
   533        kz2=np1
   534        CALL mnpb(wmesh,nwmesh,kz2,k,bmesh,nbmesh)
   535        write(*,'(2i4)') nbmesh,np1
   536
   537  c     generate leastsquares spline fit to w1,an1 data.
   538        write(*,*) ' Calculating spline and interpolation.'
   539        CALL dl2sf(w1,an1,np1,k,bmesh,nbmesh,bf)
   540
   541  c     interpolate spline function for values of an3.
   542        CALL splne(k,bmesh,nbmesh,bf,w3,np3,an3)
   543
   544  c     generate leastsquares spline fit to w1,ak1 data.
   545        CALL dl2sf(w1,ak1,np1,k,bmesh,nbmesh,bf)
   546
   547  c     interpolate spline function for values of ak3.
   548        CALL splne(k,bmesh,nbmesh,bf,w3,np3,ak3)
   549
   550        write (*, '(1X, A\)')
   551       &  'Want to see interpolated n,k data (type "y" or "n")? '
   552        read (*,'(A1)') answer
   553        if(answer .EQ. 'y' .OR. answer .EQ. 'Y') iout = .true.
   554        if(iout) then
   555          do 400 j=1,np3
   556            write(*,'(f8.2,2f9.5)') w3(j),an3(j),ak3(j)
   557   400    continue
   558        endif
   559
   560        goto 1000
   561   900  write(*,*) 'Range of data set to be interpolated is improper.'
   562        return 1
   563   1000 return
   564        end


WNKINT  Local Symbols

Name                        Class   Type              Size   Offset

NP3 . . . . . .  param                                      0006
AK3 . . . . . .  param                                      000a
AN3 . . . . . .  param                                      000e
W3. . . . . .  param                                        0012
NP1 . . . . . .  param                                      0016
AK1 . . . . . .  param                                      001a
AN1 . . . . . .  param                                      001e
W1. . . . . .  param                                        0022
WMESH . . . . . .  local   REAL*4                 8000     0000
IOUT. . . . . .  local   LOGICAL*2                   2     0100
J . . . . . .  local   INTEGER*2                     2     0102
K . . . . . .  local   INTEGER*2                     2     0104
```

Microsoft FORTRAN Optimizing Compiler Version 4.10

WNKINT Local Symbols

Name	Class	Type	Size	Offset
ANSWER.	local	CHAR*1	1	0106
NAB	local	INTEGER*2	2	0108
NWMESH.	local	INTEGER*2	2	010a
KZ1	local	INTEGER*2	2	010c
KZ2	local	INTEGER*2	2	010e
Z	local	REAL*4	4	0110
NP.	local	INTEGER*2	2	0114
NBMESH.	local	INTEGER*2	2	0116
BF.	local	REAL*4	16000	1f40
BMESH	local	REAL*4	16000	5dc0
DSTAK	CSTAK	REAL*8	48000	0000
RSTAK	CSTAK	REAL*4	48000	0000

Global Symbols

Name	Class	Type	Size	Offset
CSTAK	common	***	48000	0000
DL2SF	extern	***	***	***
FIELDS.	FSUBRT	***	***	14c1
FLDCOM.	common	***	22	0000
ISTKIN.	extern	***	***	***
MNPB.	extern	***	***	***
SPLNE	extern	***	***	***
UMB	extern	***	***	***
WNKINT.	FSUBRT	***	***	2230
main.	FSUBRT	***	***	0000

Code size = 2812 (10258)
Data size = 09bb (2491)
Bss size = 0118 (280)

No errors detected

b. SPECTRA_PREP (SPREP)

```
                                                                PAGE   1
                                                                07-15-92
                                                                11:47:36

Line#  Source Line          Microsoft FORTRAN Optimizing Compiler Version 4.10

    1  $Title:'SPECTRA_PREP'
    2  $Debug
    3  $pagesize:58
    4  $linesize:86
    5  $declare
    6  C
    7                            PROGRAM       SPREP
    8  C                         ______________________
    9  $LARGE:w,axp,axs,axu,xP,xP0,xS,xS0,xU,xU0
   10  C
   11  C       This program, SPREP (for "spectra preparation") was created by
   12  C       modifiying the FORTRAN program SDUMP.FOR in Jan. & April 1989 at
   13  C       Ames Lab.  The program is intended to take data of calculated
   14  C       reflectivity and transmissivity from the program RTCALC and change
   15  C       them to spectra.  There are options of output format which allow
   16  C       the data to be read directly by SpectraCalc and generic graph
   17  C       programs such as PicSure on the VMS operating system.  Note that
   18  C      RTCALC was formerly SMVP6.
   19  C       REFLECTANCE IS CALCULATED RELATIVE TO A BASELINE VALUE.
   20  C       Values OF I/I0 OR -LOG(I/I0) ARE calculated.  If TrType IS TRUE
   21  C       I/I0 WILL BE calculated.;FALSE, -LOG(I/I0).
   22  C       CALCULATIONS ARE MADE FOR BOTH POLARIZATIONS AND UNPOLARIZED
   23  C       LIGHT.  Only spectra of one polarization are written into
   24  C       the output file.
   25  C
   26  C                           Declaration Statements
   27  C                           ______________________
   28  C
   29        real w, axp, axs, axu, xP, xP0, xS, xS0, xU, xU0
   30
   31        dimension w(2000), axp(2000), axs(2000), axu(2000)
   32        DIMENSION xP(2000), xP0(2000), xS(2000), xS0(2000)
   33        dimension xU(2000), xU0(2000)
   34  C
   35        CHARACTER TITLE*70, INFILE*12, OUTFIL*12
   36        CHARACTER*1 resp
   37        INTEGER choice, type, irun, np
   38        LOGICAL TrType, reflsp, oldfil
   39        REAL rp, tp, rs, ts, rp0, tp0, rs0, ts0
   40  C
   41  C                 Beginning of the Executable Statements
   42  C                 ______________________________________
   43     5  format (1X, A)
   44        write (*,5)'This program SPREP converts output from RTCALC into sp
   45       &ectra that can'
   46        write (*,5)'be read by Spectra Calc and other graphing programs.'
   47        write (*,5) ' '
   48    10  write(*,20) 'Are these reflection or transmission data (type "r"
   49       &or "t")? '
   50    20  format (1x, A\)
   51        read (*, '(A1)') resp
   52        if ((resp .EQ. 'r') .OR. (resp .EQ. 'R')) then
   53           reflsp = .TRUE.
```

Line# Source Line Microsoft FORTRAN Optimizing Compiler Version 4.10

```
    54        else
    55          reflsp = .FALSE.
    56        end if
    57     40 write(*,5) 'Do you want to calculate:'
    58        write(*,5)'  1. Transmittance or its reflection analogue (-I/Io)'
    59        write(*,5)'  2. Absorbance or its analogue [-log(I/Io)]'
    60        write(*,20) '(Type "1" or "2")? '
    61        read (*, '(I1)') type
    62        if ((type .NE. 1) .AND. (type .NE. 2)) GO TO 40
    63        if (type .EQ. 1) TrType = .TRUE.
    64        write(*,20)'What is the name of the file from RTCALC that you want
    65       & to read? '
    66        read (*, '(A12)') infile
    67        open (10, file = infile, status='old')
    68        write (*, 5) ' '
    69  C Begin reading the heading information at the top of the input file:
    70        read (10, 80) irun
    71     80 format(i3)
    72        write(*,90) irun
    73     90 format (10x, 'This is run number ', i3, '.')
    74        read (10, 100) title
    75    100 format(a70)
    76        write(*,5) 'The heading on the top of the input file is:'
    77        write(*,110) title
    78    110 format (5x, a70)
    79        read (10, 120) np
    80    120 format(i4)
    81        write(*,130) np
    82    130 format(10x,'Number of data points= ',i4)
    83        DO 290 I=1,NP
***** sprep.for(83) : warning F4313: I : not previously declared
    84          read (10, 135) w(i)
    85     135  format(f8.2)
    86  C Read the data for reflectance and transmittance from the input file:
    87          READ (10,140)RP,TP,RS,TS,RP0,TP0,RS0,TS0
    88     140  format(8(f10.7))
    89          if(reflsp) then
    90     150    xp(i)=rp
    91            xs(i)=rs
    92            xp0(i)=rp0
    93            xs0(i)=rs0
    94          else
    95     200    xp(i)=tp
    96            xs(i)=ts
    97            xp0(i)=tp0
    98            xs0(i)=ts0
    99          end if
   100     250  xU(I)=(xS(i)+xP(i))/2
   101          xU0(I)=(xS0(i)+xP0(i))/2
   102          IF ( .NOT. (TrType)) THEN
   103            AxP(I)=-ALOG10(xP(i)/xP0(i))
   104            AxS(I)=-ALOG10(xS(i)/xS0(i))
```

Line# Source Line Microsoft FORTRAN Optimizing Compiler Version 4.10

```
105           AxU(I)=-ALOG10(xU(i)/xU0(i))
106         end if
107   290 CONTINUE
108 C
109   300 write (*,5) ' '
110       write(*,5)'The program will write a single file for input by Spect
111      &raCalc without heading info.'
112       write (*, 5) 'Do you want to use data for:'
113       write (*, 5) '     1. p-polarization (normal for refl. expts.),'
114       write (*, 5) '     2. s-polarization, or'
115       write (*, 5) '     3. unpolarized light'
116       write (*,20) '(enter "1", "2", or "3")? '
117       read (*, '(I1)') choice
118       if ((choice .NE. 1) .AND. (choice .NE. 2) .AND. (choice .NE. 3))
119      &          GO TO 300
120 C
121   340 write(*,20)'What do you want to name the file for output? '
122       read (*, '(A12)') outfil
123       inquire (FILE = outfil, EXIST = oldfil)
124       if (oldfil) then
125         write (*, 360) outfil
126   360   format (1X, 'The file ', A12, ' ALREADY EXISTS on this dir. ',
127      &          ' Choose another name.')
128         go to 340
129       end if
130       open (11, file = outfil, status = 'new')
131       write (*,5) ' '
132 C
133       if (TrType) write (*,370)
134   370   FORMAT(10X,'WAVENUMBER',10X,'I/I0')
135       if (.NOT. (TrType)) write (*,380)
136   380   FORMAT(10X,'WAVENUMBER',10X,'-LOG(I/I0)')
137 C Write a summary of the data at the terminal:
138       write (*, 390)
139   390 FORMAT(22X,'P',9X,'S',9X,'UNPOLARIZED')
140   410 FORMAT(10X,F6.1,4X,3(2X,F8.5))
141       if (TrType) then
142         write(*,410) W(1), xp(1)/xp0(1), xs(1)/xs0(1), xu(1)/xu0(1)
143         write(*,410) W(np), xp(np)/xp0(np),
144      &               xs(np)/xs0(np), xu(np)/xu0(np)
145       else
146         write(*,410) W(1), AxP(1), AxS(1), AxU(1)
147         write(*,410) W(np), AxP(np), AxS(np), AxU(np)
148       end if
149
150 C       The following format is used for the output files.  It is
151 C       equivalent to, and can be read by, the format (2F10.5).
152   430 format(F10.5, 1X, F9.5)
153 C  Write the data to the output file in two columns:
154 C                         P-POLARIZED data
155       if (choice .EQ. 1) then
156         DO 500 I=1,NP
157           IF(TrType) then
```

Line# Source Line Microsoft FORTRAN Optimizing Compiler Version 4.10

```
158             write(11,430) w(i), xp(i)/xp0(i)
159           else
160             write(11,430) w(i), Axp(i)
161           end if
162    500   CONTINUE
163       end if
164   C                          S-POLARIZED data
165       if (choice .EQ. 2) then
166         DO 520 I=1,NP
167           IF(TrType) then
168             write(11,430) w(i), xs(i)/xs0(i)
169           else
170             write(11,430) w(i), Axs(i)
171           end if
172    520   CONTINUE
173       end if
174   C                          UNPOLARIZED data
175       if (choice .EQ. 3) then
176         DO 540 I=1,NP
177           IF(TrType) then
178             write(11,430) w(i), xu(i)/xu0(i)
179           else
180             write(11,430) w(i), Axu(i)
181           end if
182    540   CONTINUE
183       end if
184   C End of writing data to files
185   C Allow the user several options regarding file disposition:
186       write (*, 5) ' '
187       write(*,560) infile
188    560 format(1X, ' Make another spectrum file from ', A20)
189       write (*,20) '(type "y" or "n")? '
190       read (*, '(A1)') resp
191       if ((resp .EQ. 'Y') .OR. (resp .EQ. 'y')) then
192         CLOSE(11)
193         GO TO 300
194       end if
195   C
196       write (*, 580) infile
197    580 format(1X, 'Do you want to delete the file ', A20, '?', \)
198       read (*, '(A1)') resp
199       if ((resp .EQ. 'Y') .OR. (resp .EQ. 'y')) then
200         CLOSE (10, status='DELETE')
201         write (*,5) 'The file has been deleted from your directory.'
202       else
203         CLOSE (10, status='KEEP')
204       end if
205       write(*,20)'Do you want to use this program on another file (type
206      &"y" or "n")? '
207       read (*, '(A1)') resp
208       if ((resp .EQ. 'Y') .OR. (resp .EQ. 'y')) then
209         close(11)
210         go to 10
```

```
SPECTRA_PREP                                                    PAGE   5
                                                                07-15-92
                                                                11:47:36

 Line#  Source Line          Microsoft FORTRAN Optimizing Compiler Version 4.10

   211        end if
   212        write(*,5) 'Remember to install the ASCII_XY translator before'
   213        write(*,5) 'using SpectraCalc to import the data file.'
   214        write(*,5) ' '
   215  C
   216   1000 STOP
   217        END

main  Local Symbols

Name                          Class   Type            Size   Offset

W . . . . . . . . . . . . . . local   REAL*4          8000   0000
XU. . . . . . . . . . . . . . local   REAL*4          8000   0000
TYPE. . . . . . . . . . . . . local   INTEGER*4          4   0002
TITLE . . . . . . . . . . . . local   CHAR*70            70   0006
I . . . . . . . . . . . . . . local   INTEGER*4          4   004c
REFLSP. . . . . . . . . . . . local   LOGICAL*4          4   0050
RPO . . . . . . . . . . . . . local   REAL*4             4   0054
OUTFIL. . . . . . . . . . . . local   CHAR*12           12   0058
TPO . . . . . . . . . . . . . local   REAL*4             4   0064
RSO . . . . . . . . . . . . . local   REAL*4             4   0068
TSO . . . . . . . . . . . . . local   REAL*4             4   006c
NP. . . . . . . . . . . . . . local   INTEGER*4          4   0070
RP. . . . . . . . . . . . . . local   REAL*4             4   0074
TP. . . . . . . . . . . . . . local   REAL*4             4   0078
RS. . . . . . . . . . . . . . local   REAL*4             4   007c
TS. . . . . . . . . . . . . . local   REAL*4             4   0080
TRTYPE. . . . . . . . . . . . local   LOGICAL*4          4   0084
CHOICE. . . . . . . . . . . . local   INTEGER*4          4   0088
INFILE. . . . . . . . . . . . local   CHAR*12           12   008c
OLDFIL. . . . . . . . . . . . local   LOGICAL*4          4   0098
RESP. . . . . . . . . . . . . local   CHAR*1             1   009c
IRUN. . . . . . . . . . . . . local   INTEGER*4          4   009e
AXU . . . . . . . . . . . . . local   REAL*4          8000   1f40
XPO . . . . . . . . . . . . . local   REAL*4          8000   1f40
XSO . . . . . . . . . . . . . local   REAL*4          8000   3e80
XUO . . . . . . . . . . . . . local   REAL*4          8000   5dc0
XP. . . . . . . . . . . . . . local   REAL*4          8000   7d00
AXP . . . . . . . . . . . . . local   REAL*4          8000   9c40
XS. . . . . . . . . . . . . . local   REAL*4          8000   bb80
AXS . . . . . . . . . . . . . local   REAL*4          8000   dac0

Global Symbols

Name                          Class   Type            Size   Offset

main. . . . . . . . . . . . . FSUBRT  ***              ***   0048

Code size = 1799 (6041)
Data size = 06c2 (1730)
```

Microsoft FORTRAN Optimizing Compiler Version 4.10

Bss size = 00a2 (162)

No errors detected

4. Other Programs Relating to Infrared Spectroscopy

a. CAUCHY to generate synthetic absorbance profiles

```
                                                          PAGE   1
                                                          07-15-92
                                                          11:42:40

Line#  Source Line          Microsoft FORTRAN Optimizing Compiler Version 4.10

    1  $title:'CAUCHY'
    2  $pagesize: 58
    3  $linesize: 86
    4  C Set printer font size to 12-point before printing a listing file.
    5  $DECLARE
    6
    7                          Program  CAUCHY
    8  C                       ===============
    9
   10  C       Synthetic absorbance profiles can be generated using a Cauchy
   11  C function to calculate the absorption index k as a function of
   12  C frequency in wavenumbers using this program.  The old program
   13  C MAKECURV (nee' GAUSS) provided inspiration for this; however, this
   14  C program is different in that it allows component peaks to have
   15  C varying heights, widths, and spacing.
   16  C       The algorithm for this program comes directly from:
   17  C   J.P. Hawranek, P. Neelakantan, R.P. Young and R.N. Jones
   18  C   SPECTROCHIM. ACTA vol. 32A (1976) pp. 85-98.
   19  C Source code was written in Microsoft FORTRAN Version 4.1 by Darwin
   20  C D. Popenoe in June 1989.
   21
   22  C               DECLARATION STATEMENTS
   23  C               ----------------------
   24
   25        real Nu, KofNu
   26        dimension Nu(2000), KofNu(2000)
   27  C       Nu, KofNu: vectors of absorption index as a function of
   28  C       wavenumber.
   29
   30  C Parameters for individual peaks:
   31        real kMax, Numax, bPeak
   32  C       (bPeak equals one-half the FWHM.)
   33        dimension kMax(9), Numax(9), bPeak(9)
   34
   35        integer LastNu, LastPk, NuOrd, PkOrd, GoodLoLm, GoodHiLm
   36  C       NuOrd, PkOrd: ordinal numbers to index the frequency and peak arrays.
   37        real NuLmHi, NuLmLo, NuGap, FWHM
   38        character resp*1
   39
   40        external SumOfKs, AscOut
   41        data LastPk/0/
   42
   43  C               BEGINNING OF EXECUTABLE STATEMENTS
   44  C               ----------------------------------
   45
   46     5 format (1X, A)
   47     7 format (1X, A\)
   48    10 format (f7.2)
   49       WRITE (*,5)'Welcome to the program Cauchy, which calculates a synt
   50      &hetic absorption'
   51       write (*,5)'index k as a function of wavenumber.  Up to 9 componen
   52      &t peaks in the form'
   53       write (*,5)'of a Cauchy (Lorentzian) function can be specified by
```

Line# Source Line Microsoft FORTRAN Optimizing Compiler Version 4.10

```
     &the user.'
      write (*,7) 'How many peaks do you want? '
      read (*,'(I1)') LastPk
      write (*,*) ' '
      write(*,5)'Peak parameters should be listed in order of increasing
     & frequency.'
      write (*,5)'Type all input parameters as real numbers with decimal
     & points.'
  110 do 190 PkOrd = 1, LastPk
        write (*, 130) PkOrd
  130   format (1X, 'Provide parameters for peak number ', I1, ': ')
        write (*,7)'What is the peak freq. (1/cm)? '
        read (*,10) Numax(PkOrd)
        write (*,7)'What is the maximum k value for this peak? '
        read (*, '(F8.5)') kMax(PkOrd)
        write (*,7)'What is the FWHM of this peak (1/cm)? '
        read (*,10) FWHM
        bPeak(PkOrd) = FWHM/2.0
        write (*,*) ' '
  190 CONTINUE
      write (*, 230) LastPk
  230 format (1X, '...that takes care of all ', I1, ' peaks.')
      write (*,*) ' '

      write (*,5) 'Now you must specify the range and density of freq.
     &values.'
      GoodLoLm = INT(Numax(1) - 2.0*bPeak(1))
      GoodHiLm = INT(Numax(LastPk) + 2.0*bPeak(LastPk))
      write (*,250) GoodLoLm, GoodHiLm
  250 format (1X, 'The wavenumber range should span at least ',
     &        I4, ' to ', I4, ' cm-1.')
  270 write (*,7)'Input the minimum frequency (1/cm): '
      read (*, 10) NuLmLo
      write (*,7) 'Input the maximum frequency (1/cm): '
      read (*, 10) NuLmHi
      write (*,7) 'What resolution do you want (1/cm)? '
      read (*, 10) NuGap

      if ( (NuLmHi - NuLmLo)/NuGap .GT. 1999.0) then
        write(*,5)'The freq. parameters you entered require > 2000 pts.'
        write(*,5)'Please adjust them!'
        write(*,*) ' '
        GO TO 270
      end if
      write (*,5) '                [CALCULATING]'
C Create the vector of freq. values:
      LastNu = INT((NuLmHi - NuLmLo)/NuGap + 0.999) + 1
C               The first point in the array has freq. = NuLmLo.  If points
C       separated by the specified resolution do not land exactly on NuLmHi,
C       then one more point will be taken with freq. > NuLmHi.
```

```
CAUCHY                                                          PAGE   3
                                                                07-15-92
                                                                11:42:40

 Line#  Source Line          Microsoft FORTRAN Optimizing Compiler Version 4.10

    107        DO 350 NuOrd = 1, LastNu
    108          Nu(NuOrd) = NuLmLo + (NuOrd - 1)*NuGap
    109    350 CONTINUE
    110
#   111  C  Calculate the vector of k values at all freqs. in the specified range:
    112        DO 400 NuOrd = 1, LastNu
    113          KofNu(NuOrd) = SumOfKs (kMax, Numax, bPeak, LastPk, Nu(NuOrd))
    114    400 CONTINUE
    115        write (*,*) ' '
    116        write (*,5) 'The calculations are complete.'
    117
    118        CALL AscOut (Nu, KofNu, LastNu)
    119
    120        STOP
    121        END


main  Local Symbols

Name                          Class    Type              Size   Offset

PKORD . . . . . . . . . . .   local    INTEGER*4            4     0002
KOFNU . . . . . . . . . . .   local    REAL*4            8000     0006
LASTPK. . . . . . . . . . .   local    INTEGER*4            4     030a
GOODLO. . . . . . . . . . .   local    INTEGER*4            4     1f46
NUORD . . . . . . . . . . .   local    INTEGER*4            4     1f4a
NUMAX . . . . . . . . . . .   local    REAL*4              36     1f4e
NULMHI. . . . . . . . . . .   local    REAL*4               4     1f72
NULMLO. . . . . . . . . . .   local    REAL*4               4     1f76
LASTNU. . . . . . . . . . .   local    INTEGER*4            4     1f7a
BPEAK . . . . . . . . . . .   local    REAL*4              36     1f7e
NU. . . . . . . . . . . . .   local    REAL*4            8000     1fa2
KMAX. . . . . . . . . . . .   local    REAL*4              36     3ee2
FWHM. . . . . . . . . . . .   local    REAL*4               4     3f06
GOODHI. . . . . . . . . . .   local    INTEGER*4            4     3f0a
NUGAP . . . . . . . . . . .   local    REAL*4               4     3f0e

    122
    123  $subtitle:'Sum Of ks function'
    124  $page
```

```
CAUCHY                                                          PAGE   4
Sum Of ks function                                              07-15-92
                                                                11:42:40

 Line#  Source Line          Microsoft FORTRAN Optimizing Compiler Version 4.10

   125        REAL FUNCTION SumOfKs (kMax, Numax, bPeak, LastPk, Nu)
   126
   127        real kMax, Numax, bPeak, Nu, PrtSum
   128        dimension kMax(*), Numax(*), bPeak(*)
   129        integer LastPk
   130
   131        PrtSum = 0.0
   132        DO 1090 i = 1, LastPk
***** cauchy.for(132) : warning F4313: I : not previously declared
   133          PrtSum = PrtSum + kMax(i) / (1 + (Nu-Numax(i))**2/bPeak(i)**2)
   134   1090 CONTINUE
   135        SumOfKs = PrtSum
   136        END


SUMOFK  Local Symbols

Name                      Class   Type              Size   Offset

SUMOFK. . . . . . . . . . param                            0006
NU. . . . . . . . . . . . param                            0008
LASTPK. . . . . . . . . . param                            000c
BPEAK . . . . . . . . . . param                            0010
NUMAX . . . . . . . . . . param                            0014
KMAX. . . . . . . . . . . param                            0018
I . . . . . . . . . . . . local   INTEGER*4            4    3f12
PRTSUM. . . . . . . . . . local   REAL*4               4    3f16

   137
   138  $SUBTITLE:'ASCII_XY OUT'
   139  $page
```

```
 Line#  Source Line          Microsoft FORTRAN Optimizing Compiler Version 4.10

  140  C                       A S C I I _ X Y O U T    SUBROUTINE
  141  C                       ==================================
  142
  143        SUBROUTINE AscOut  (freq, kIndex, NoPts)
  144  C  Written in Microsoft FORTRAN for use on an IBM PC-AT.
  145
  146  C  Type declarations for variables:
  147        real freq, kIndex
  148        dimension freq(*), kIndex(*)
  149        INTEGER NoPts, i
  150        CHARACTER PREFIX*7, outfil*11, kfile*11
  151        CHARACTER*1 RESP
  152        logical RevOrder
  153
  154  C  Format statements for writing to the screen:
  155     41 FORMAT (1X, A)
  156     42 FORMAT ('0', A)
  157     43 FORMAT (1X, A\)
  158  C  Documentation
  159        WRITE (*,42) 'The program will now write an ASCII_XY files which c
  160       &an be translated by'
  161        WRITE (*,41) 'SpectraCalc.  One file will be created, called:'
  162        WRITE (*,41) '     *.PRN,'
  163        WRITE (*,41) 'where "*" is a string of seven characters that you
  164       &provide.'
  165        WRITE (*, 4080) NoPts
  166   4080 FORMAT(1X,'The numbers of data points is: ', I4,'.')
  167        write (*, 43) 'Do you want data in decreasing freq. order? '
  168        read (*, '(A1)') resp
  169        IF ((RESP.EQ.'y') .OR. (RESP.EQ.'Y')) RevOrder = .true.
  170  C  Create the file name:
  171   4100 WRITE (*,43) 'What is the filename root (type 7 characters)?'
  172        READ (*,'(A7)') PREFIX
  173        kfile = prefix // '.PRN'
  174
  175  C  Confirmation of names:
  176        WRITE (*,42) 'The program will create the file:'
  177        WRITE (*, 4200) KFILE
  178   4200 FORMAT (8X, A12, '.')
  179        WRITE (*,43) 'Is this okay (type "y" or "n")? '
  180        READ (*, '(A)') RESP
  181        IF (.NOT. ((RESP.EQ.'y') .OR. (RESP.EQ.'Y'))) GO TO 4100
  182
  183  C                          WRITE THE DATA TO FILES
  184
  185   4300 FORMAT ($P, F9.1, ',', S, F7.4)
  186
  187        OPEN (11, FILE=KFILE, STATUS='NEW')
  188        if (RevOrder) then
  189          DO 4320 I= NoPts, 1, -1
  190            WRITE (11, 4300) freq(I), kIndex(I)
  191   4320   CONTINUE
  192        else
```

```
CAUCHY                                                          PAGE   6
ASCII_XY OUT                                                    07-15-92
                                                                11:42:40

 Line#  Source Line          Microsoft FORTRAN Optimizing Compiler Version 4.10

   193          do 4340 I= 1, NoPts, +1
   194            write (11, 4300) freq(i), kIndex(i)
   195   4340   CONTINUE
   196        end if
   197        CLOSE(11)
   198
   199        write (*, 4380) kfile
   200   4380 format (1X, 'The program has written data to ', A11, ' .')
   201
   202        RETURN
   203
   204        END


ASCOUT  Local Symbols

Name                      Class   Type              Size   Offset

NOPTS . . . . . . . . . . param                            0006
KINDEX. . . . . . . . . . param                            000a
FREQ. . . . . . . . . . . param                            000e
I . . . . . . . . . . . . local   INTEGER*4           4     3f1a
PREFIX. . . . . . . . . . local   CHAR*7              7     3f1e
REVORD. . . . . . . . . . local   LOGICAL*4           4     3f26
KFILE . . . . . . . . . . local   CHAR*11            11     3f2a
RESP. . . . . . . . . . . local   CHAR*1              1     3f35


Global Symbols

Name                      Class   Type              Size   Offset

ASCOUT. . . . . . . . . . FSUBRT  ***               ***    0584
SUMOFK. . . . . . . . . . FFUNCT  REAL*4            ***    0458
main. . . . . . . . . . . FSUBRT  ***               ***    0000

Code size = 07f9 (2041)
Data size = 066e (1646)
Bss size  = 3f36 (16182)

No errors detected
```

b. KTON to calculate $n(\nu)$ given a function $k(\nu)$ using Kramers-Kronig integration

```
                                                                PAGE   1
                                                                07-15-92
                                                                11:43:49

Line#  Source Line          Microsoft FORTRAN Optimizing Compiler Version 4.10

    1  $storage:2
    2  $title:'kTOn'
    3  $subtitle:'MainProgram'
    4  $pagesize:58
    5  $large
    6  C
    7                       PROGRAM  kTOn
    8  C                    =======  ====
    9  C
   10  C       This program calculates the real refractive index function,
   11  C n(freq.), from the absorptive index, k(freq.), using a numerical
   12  C approximation to the Kramers Kronig integration.  Data are
   13  C input as a file containing frequency in wavenumbers in the first
   14  C column and k in the second.  The actual calculations are
   15  C performed by the subroutine KKSUB2.
   16  C       Output is similar to that from the program OPTCON5 and
   17  C OPTFXNS1.  A single file with a heading may be generated; or the
   18  C program may make separate ASCII_XY-type files compatible with
   19  C SpectraCalc -- one containing n(freq.) and the other k(freq.).
   20  C       This program should be linked with the subroutine KKSUB2.
   21  C This program was written for the IBM PC/AT in April 1989.
   22  C
   23        dimension NuBr(2000), kOfNu(2000), nOfNu(2000)
   24  C
   25  C Data type declarations:
   26        real NuBr, kOfNu, NuLmLo, NuLmHi, NuRes, nnInf, nOfNu
   27
   28        integer ifrmt, j
   29
   30        character title*70, FILNAM*12, outfil*12, ANSWER*1, BELL*1
   31
   32  C  Data storage address command (Common block CSTAK contains space
   33  C  for the PORT3 modules CSPDI and CSPIN to use.  This is converted from
#  34  C  double-precision type to real type by the EQUIVALENCE statement below.):
   35        COMMON/CSTAK/DSTAK
   36        double precision DSTAK(6000)
   37        real RSTAK(12000)
   38        equivalence (DSTAK(1), RSTAK(1))
   39
   40        external KKSUB2, REVARRAY, ASCOUT, ISTKIN
   41  C       The above units are subroutines declared within this program
   42  C       or from PORT3.  ASCOUT is contained in module OPF_IO.OBJ.
   43
   44        bell = char(007)
   45
   46  C Beginning of the executable statements
   47        write(*,*) ' This program, n TO k, calculates the function n'
   48        write(*,*) ' given k as a function of frequency using Kramers Kron
   49       &nig integration.'
   50        write(*,*) ' '
   51
   52  C  The PORT3 library subprogram ISTKIN initializes the dynamic storage
   53  C  stack to create enough space for subprograms CSPDI and CSPIN to
```

```
Line#  Source Line          Microsoft FORTRAN Optimizing Compiler Version 4.10

   54  C  differentiate 2000 points containing single precision real data.  The
   55  C  parameter ITYPE = 3 represents real numbers.
   56         CALL ISTKIN(12000, 3)
   57  C  The call above initializes the dynamic stack for any and all calls to
   58  C  PORT3 subprograms in the main program or subroutines.
   59
   60  C Global FORMAT statement to be used for prompting user input:
   61       5 format (1X, A\)
   62
   63  C                 INPUT OF DATA FROM FILES
   64  C                 ------------------------
   65
   66      50 write(*,5) 'What is the name of the input file? '
   67         read (*, '(A12)') FILNAM
   68      70 OPEN(09, file= FILNAM, status='old')
   69  C
   70      75 write(*,*) ' Is file (1) floating type [from SpectraCalc],'
   71         write(*,*) ' or (2) fixed pt. with heading [from LABELER],'
   72         write(*,5) 'Type "1" or "2":'
   73         read(*, '(I1)') ifmt
   74         if (ifmt .EQ. 1) then
   75  C        (Read a floating point, not decimal-formatted, file)
   76           write(*,5) 'Do you want to skip the first line ("y" or "n")?:'
   77           read(*,'(A1)') answer
   78           if ((answer .EQ. 'y') .OR. (answer .EQ. 'Y')) read(09,*)
   79           DO 100 j=1, 2000
   80             read (09, *, END = 110) NuBr(j),kOfNu(j)
   81  C          (The program reads in data unformatted)
   82  C          (The program sets negative exptl. absorbance values equal to
   83  C          zero:)
   84             if (kOfNu(j).lt.0) kOfNu(j)=0
   85             LastPt = j
   86     100   CONTINUE
   87     110   CLOSE(9)
   88           write (*, 120) LastPt
   89     120   format (1X, 'This program has read', 1X, I4, 1X,
   90        &          'data points from the file.')
   91  C
   92         elseif (ifmt .EQ. 2) then
   93  C        (Read a fixed point headed file)
   94           read(09, 130) title
   95     130   FORMAT (A70)
   96           write (*,'(A)') ' The heading on the top of the file is:'
   97           write (*, '(6X, A70)') title
   98           write (*,*) ' '
   99     145   read(09,'(I4)') LastPt
  100           write (*,160) LastPt
  101     160   FORMAT(1X,'The number of data points in the input file = ',I4)
  102           write(*,*) ' '
  103           DO 190 j=1,LastPt
  104             read (09,170) NuBr(j),kOfNu(j)
  105     170     format(2f10.5)
  106  C          (The program sets negative exptl. absorbance values equal to
```

Line# Source Line Microsoft FORTRAN Optimizing Compiler Version 4.10

```
107  C         zero:)
108            if (kOfNu(j).lt.0) kOfNu(j)=0
109    190   CONTINUE
110          CLOSE(9)
111  C
112         elseif ((ifrmt .NE. 1) .AND. (ifrmt .NE. 2)) then
113           write(*,*) ' You have not entered a valid choice.'
114           GO TO 75
115  C
116         end if
117
118  C      NuBr must be entered in increasing order for input into KKSUB.
119    245 if (NuBr(2).lt.NuBr(1)) then
120           write(*,*) ' The input points were in decreasing freq. order.'
121           write(*,*) ' Therefore, the subroutine REVARRAY has been called
122       &to reverse their order.'
123           CALL REVARRAY (NuBr,LastPt)
124           CALL REVARRAY (kOfNu,LastPt)
125         endif
126
127  C                ESTABLISHING USER-INPUT PARAMETERS
128  C                ----------------------------------
129
130         write (*,*) ' '
131    260  format(f7.2)
132         write(*,5) 'Supply lower freq. limit nu in final data set: '
133         read(*,260) NuLmLo
134         write(*,5) 'Supply upper freq. limit nu in final data set: '
135         read(*,260) NuLmHi
136         write(*,5) 'Input resolution in cm-1 of final nu set: '
137         read(*,420) NuRes
138    420  format(f5.2)
139         write(*,*) ' OPFXNS1 must have a zero-freq. n value for the phase
140        &of interest.'
141         write(*,5)'Input a value of n out of the integration range: '
142         read(*,430) nnInf
143  C       The value nnInf goes into the function call to KKSUB2.
144    430  format(f7.5)
145
146         write(*,*) ' The subroutine KKSUB2 has been called.'
147         CALL KKSUB2 (NuBr, kOfNu, LastPt, NuLmLo, NuLmHi, NuRes,
148        &            nnInf, nOfNu)
149         write(*,*) BELL
150
151  C        WRITING THE DATA TO OUTPUT FILES
152  C        --------------------------------
153    900  write(*,*) ' '
154         write(*,*) ' Do you want to create (1) a headed three-column file'
155         write(*,*) ' or (2) separate files for SpectraCalc?'
156         write(*,5) 'Type "1" or "2":'
157         read (*,'(I1)') ifrmt
158         if (ifrmt .EQ. 1) then
159      910  write(*,5) ' What is the name of the output file? '
```

```
kTOn                                                              PAGE   4
MainProgram                                                       07-15-92
                                                                  11:43:49

 Line#  Source Line          Microsoft FORTRAN Optimizing Compiler Version 4.10

   160          read (*, '(A12)') FILNAM
   161          OPEN (10, file= FILNAM, status='new')
   162          write(10, 130) title
   163          write(10,'(i4)')LastPt
   164          do 950 j=1,LastPt
   165            write(10,920) NuBr(j),nOfNu(j),kOfNu(j)
   166    920     format(f8.2,2f8.5)
   167    950   continue
   168  C
   169        elseif (ifrmt .EQ. 2) then
   170   CALL ASCOUT (NuBr, nOfNu, kOfNu, LastPt)
   171  C
   172        elseif ((ifrmt .NE. 1) .AND. (ifrmt .NE. 2)) then
   173          write (*,*) ' You have not entered a valid answer.'
   174          write (*,*)
   175          GO TO 900
   176  C
   177        end if
   178  C  Echo the values of the first and last points written at the screen:
   179        write (*, '(A)') ' The first and last points written to the output
   180       & have these values: '
   181        write (*,960) NuBr(1), nOfNu(1), kOfNu(1)
   182        write (*,960) NuBr(LastPt), nOfNu(LastPt), kOfNu(LastPt)
   183   960  format(2x,'nu= ',f8.2,2x,'n= ',f8.5,2x,'k= ',f8.5)
   184  C
   185   1500 stop
   186        END

main  Local Symbols

Name                    Class   Type            Size   Offset

KOFNU . . . . . . . . . local   REAL*4          8000    0000
TITLE . . . . . . . . . local   CHAR*70           70    0002
IFRMT . . . . . . . . . local   INTEGER*2          2    0048
J . . . . . . . . . . . local   INTEGER*2          2    004a
NURES . . . . . . . . . local   REAL*4             4    004c
NULMHI. . . . . . . . . local   REAL*4             4    0050
ANSWER. . . . . . . . . local   CHAR*1             1    0054
NULMLO. . . . . . . . . local   REAL*4             4    0056
LASTPT. . . . . . . . . local   INTEGER*2          2    005a
BELL. . . . . . . . . . local   CHAR*1             1    005c
FILNAM. . . . . . . . . local   CHAR*12           12    005e
NNINF . . . . . . . . . local   REAL*4             4    006a
NOFNU . . . . . . . . . local   REAL*4          8000    1f40
NUBR. . . . . . . . . . local   REAL*4          8000    3e80
DSTAK . . . . . . . . . CSTAK   REAL*8         48000    0000
RSTAK . . . . . . . . . CSTAK   REAL*4         48000    0000

   187  C                                --SUBLIST--
   188  $SUBTITLE:'ASCII_XY OUT'
   189  $page
```

```
kTOn                                                              PAGE   5
ASCII_XY OUT                                                      07-15-92
                                                                  11:43:49

Line#  Source Line          Microsoft FORTRAN Optimizing Compiler Version 4.10

  190  C                       A S C I I _ X Y O U T    SUBROUTINE
  191  C                       ====================================
  192
  193        SUBROUTINE ASCOUT (nu, an, ak, np)
  194
  195  C  Written in Microsoft FORTRAN for use on an IBM PC-AT.
  196
  197  C                This subroutine will create 2files containing the n & k
  198  C        values so that the program SpectraCalc can read them and plot
  199  C        them.  The files are in "ASCII_XY" format.
  200  C                The main program can be compiled separately and combined
  201  C        with this subroutine at linking time.  This subroutine is in-
  202  C        tended to be combined with the FORTRAN source code program
  203  C        THREEPHASE.
  204
  205  C  Allocation of storage for arrays:
  206        DIMENSION nu(2000), ak(2000), an(2000)
  207  C  Type declarations for variables:
  208        INTEGER NP
  209        REAL nu, ak, an
  210        CHARACTER PREFIX*7, CMPNT*1, SUFFIX*4, nFILE*12, kFILE*12
  211        CHARACTER*1 RESP
  212  C  Format statements for writing to the screen:
  213     41 FORMAT (1X, A)
  214     42 FORMAT ('0', A)
  215     43 FORMAT (1X, A\)
  216  C  Documentation
  217        WRITE (*,42) 'The program will now write ASCII_XY files which can
  218       & be translated by'
  219        WRITE (*,41) 'SpectraCalc.  Two files will be created, called:'
  220        WRITE (*,41) '      *N.PRN     and  *K.PRN'
  221        WRITE (*,41) 'where "*" is a string of seven characters that you
  222       &provide.'
  223        WRITE (*, 4080) NP
  224   4080 FORMAT(1X,'The number of data points is: ', I3,'.')
  225  C  Create the three file names:
  226   4100 WRITE (*,43) 'What is the filename root (type 7 characters)?'
  227        READ (*,'(A7)') PREFIX
  228  $NOTSTRICT
  229  C  [Use concatenation of substrings to generate similar filenames.]
  230        SUFFIX = '.PRN'
  231
  232        CMPNT = 'N'
  233        NFILE(1:7) = PREFIX
  234        NFILE(8:8) = CMPNT
  235        NFILE(9:12) = SUFFIX
  236
  237        CMPNT = 'K'
  238        KFILE(1:7) = PREFIX
  239        KFILE(8:8) = CMPNT
  240        KFILE(9:12) = SUFFIX
  241
  242  C  Confirmation of names:
```

```
kTOn                                                              PAGE   6
ASCII_XY OUT                                                      07-15-92
                                                                  11:43:49

 Line#  Source Line          Microsoft FORTRAN Optimizing Compiler Version 4.10

   243        WRITE (*,42) 'The program will create the files:'
   244        WRITE (*, 4200) NFILE, KFILE
   245   4200 FORMAT (8X, A12, ' and ', A12, '.')
   246        WRITE (*,43) 'Are these okay (type "y" or "n")? '
   247        READ (*, '(A)') RESP
   248        IF (.NOT. ((RESP.EQ.'y') .OR. (RESP.EQ.'Y'))) GO TO 4100
   249
   250  C                        WRITE THE DATA TO FILES
   251
   252   4300 FORMAT (F9.4, ',', F9.4)
   253
   254        OPEN (11, FILE=NFILE, STATUS='NEW')
   255        DO 4320 I=NP, 1, -1
   256  WRITE (11, 4300) NU(I), AN(I)
   257   4320 CONTINUE
   258        CLOSE(11)
   259        WRITE (*, 42) 'The file for the n-component has been completed.'
   260
   261        OPEN (12, FILE=KFILE, STATUS='NEW')
   262        DO 4420 I=NP, 1, -1
   263  WRITE (12, 4300) NU(I), AK(I)
   264   4420 CONTINUE
   265        CLOSE(12)
   266        WRITE (*, 41) 'The file for the k-component has been completed.'
   267
   268        WRITE (*,'(A)') ' '
   269        RETURN
   270
   271        END

ASCOUT  Local Symbols

Name                          Class   Type              Size   Offset

NP. . . . . . . . . . . . . . param                            0006
AK. . . . . . . . . . . . . . param                            000a
AN. . . . . . . . . . . . . . param                            000e
NU. . . . . . . . . . . . . . param                            0012
CMPNT . . . . . . . . . . . . local   CHAR*1              1     006e
I . . . . . . . . . . . . . . local   INTEGER*2           2     0070
PREFIX. . . . . . . . . . . . local   CHAR*7              7     0072
SUFFIX. . . . . . . . . . . . local   CHAR*4              4     007a
KFILE . . . . . . . . . . . . local   CHAR*12            12     007e
NFILE . . . . . . . . . . . . local   CHAR*12            12     008a
RESP. . . . . . . . . . . . . local   CHAR*1              1     0096

   272
   273  $subtitle:'REVARRAY'
   274        subroutine REVARRAY(x,lastx)
   275  C  This subroutine simply takes a one-dimensional array of points
   276  C  and reverses the order of its contents.
   277
```

```
kTOn                                                          PAGE   7
REVARRAY                                                      07-15-92
                                                              11:43:49

 Line#  Source Line          Microsoft FORTRAN Optimizing Compiler Version 4.10

   278        dimension x(2000)
   279
   280   100  if ( (mod(lastx,2)) .eq. 0 ) then
   281          LastPt = lastx/2
   282        else
   283          LastPt = (lastx-1)/2
   284        endif
   285        DO 450 j=1,LastPt
   286          zx = x(j)
   287          x(j) = x(lastx+1-j)
   288          x(lastx+1-j) = zx
   289   450  CONTINUE
   290        RETURN
   291        END


REVARR  Local Symbols

Name                    Class   Type            Size   Offset

LASTX . . . . . . . . . param                          0006
X . . . . . . . . . . . param                          000a
J . . . . . . . . . . . local   INTEGER*2          2    0098
LASTPT. . . . . . . . . local   INTEGER*2          2    009a
ZX. . . . . . . . . . . local   REAL*4             4    009c


Global Symbols

Name                    Class   Type            Size   Offset

ASCOUT. . . . . . . . . FSUBRT  ***             ***    05c4
CSTAK . . . . . . . . . common  ***           48000    0000
ISTKIN. . . . . . . . . extern  ***             ***     ***
KKSUB2. . . . . . . . . extern  ***             ***     ***
REVARR. . . . . . . . . FSUBRT  ***             ***    0893
main. . . . . . . . . . FSUBRT  ***             ***    0000

Code size = 097c (2428)
Data size = 08ac (2220)
Bss size  = 00a0 (160)

No errors detected
```

c. MAKECURVE to calculate Gaussian or Lorentzian bands

```
                                                          PAGE   1
                                                          07-15-92
                                                          11:44:10

Line#  Source Line          Microsoft FORTRAN Optimizing Compiler Version 4.10

    1  C
    2  C              M A K E C U R V E
    3  C              ==================
    4  C       ... a program to generate synthetic model absorbance spectra
    5  C           from Gaussian or Lorentzian curves.
    6  C
    7  C Written for the IBM-PC originally as the program GAUSS.
    8  C Adapted for use with SpectraCalc in March 1989 by Darwin D. Popenoe.
    9  C
   10  $FLOATCALLS
   11  $debug
   12  $TITLE:'MAKECURVE'
   13  c
   14  c  PROGRAM gauss
   15  c
   16        real Ab(2000),wavnum(2000),Abmax,w(20)
   17        character fname*12, title*70, resp*1
   18        integer kount
   19
   20        external ASCOUT
   21        intrinsic ABS
   22
   23  C       Set the frequency and Absorbance vectors equal to 0 initially:
   24        DATA Ab/2000*0.0/, wavnum/2000*0.0/
   25
   26        write(*,*) ' Spectral synthesis program'
   27        write(*,*) ' Is spectral synthesis gaussian(1) or lorentzian(2)'
   28        read(*,10)iflag
   29     10 format(i4)
   30        write(*,*) ' Input number of bands (max=20)'
   31        read(*,10)iband
   32        write(*,*) ' Input FWHM'
   33        read(*,20)fwhm
   34     20 format(f10.5)
   35        write(*,*) ' Input desired resolution'
   36        read(*,20)res
   37        write(*,*) ' Input band separation as integer'
   38        read(*,10)isep
   39        write(*,*) ' Input absorbance maximum (little k)'
   40        read(*,20)Abmax
   41        write(*,*) ' Input wavenumber maximum for lowest energy band'
   42        read(*,20)wmax
   43        num=int(12.0*fwhm/res)
   44          do 14 i=1,iband
   45          w(i)=wmax+(i-1)*isep
   46     14 continue
   47  c setup constants
   48        if(iflag.eq.2)goto 500
   49  c gaussian calculation
   50        c1=1.0/(sqrt(3.1451927*fwhm))
   51        step=wmax-res*num
   52        kount=int(iband*isep/res+2.0*num)
   53        do 100 i=1,kount
```

Line# Source Line Microsoft FORTRAN Optimizing Compiler Version 4.10

```
      wavnum(i)=step
      do 21 j=1,iband
        dx=abs(w(j)-wavnum(i))
        Ab(i)=c1*exp(-0.5*dx*dx/(fwhm*fwhm/4.0))+Ab(i)
   21 continue
      step=step+res
  100 continue
      goto 1000
c
c lorentzian calculation
c
  500 c2=fwhm/2.0
      c2sq=c2*c2
      c3=1.0/3.1415927
      step=wmax-res*num
      kount=int(iband*isep/res+2.0*num)
      do 750 i=1,kount
        wavnum(i)=step
        do 740 j=1,iband
          dx=abs(w(j)-wavnum(i))
          Ab(i)=Ab(i)+c2*c3/(dx*dx+c2sq)
  740   continue
        step=step+res
  750 continue

 1000 peak=0.0
      do 1010 i=1,kount
        if (Ab(i).ge.peak) peak=Ab(i)
 1010 continue
      factor=Abmax/peak
      do 1050 i=1,kount
        Ab(i)=factor*Ab(i)
 1050 continue

C Write the data to output files:
 1100 write (*,'(A\)') ' Do you want to create files to be read by Spect
     &ra Calc (type "y" or "n")? '
      read (*,'(A)') RESP
      if ((RESP .EQ. 'y') .OR. (RESP .EQ. 'Y')) then
        CALL ASCOUT (wavnum, Ab, kount)
      else
        write(*,*)'output filename'
        read (*, 1205) fname
 1205   format(a8)
        write(*,*)'file description  (a70)'
        read (*, 1207) title
 1207   format(a70)
 1300   open(11,file=fname,status='new')
        write(11,1207) title
        write(11,10)kount
        write(11,1500)(wavnum(i),Ab(i),i=1,kount)
 1500   format(2(f10.5))
        close(11)
```

```
MAKECURVE                                                    PAGE   3
                                                             07-15-92
                                                             11:44:10

 Line#  Source Line          Microsoft FORTRAN Optimizing Compiler Version 4.10

   107        end if
   108  C
   109        stop
   110        end


main  Local Symbols

Name                    Class   Type            Size   Offset

TITLE . . . . . local   CHAR*70           70    0002
I . . . . . local   INTEGER*4          4    0048
J . . . . . local   INTEGER*4          4    004c
KOUNT . . . . . local   INTEGER*4          4    0050
W . . . . . local   REAL*4            80    0054
C2SQ. . . . . local   REAL*4           4    00a4
DX. . . . . local   REAL*4           4    00a8
IBAND . . . . . local   INTEGER*4          4    00ac
PEAK. . . . . local   REAL*4           4    00b0
IFLAG . . . . . local   INTEGER*4          4    00b4
FNAME . . . . . local   CHAR*12          12    00b8
ABMAX . . . . . local   REAL*4           4    00c4
RES . . . . . local   REAL*4           4    00c8
NUM . . . . . local   INTEGER*4          4    00cc
ISEP. . . . . local   INTEGER*4          4    00d0
FWHM. . . . . local   REAL*4           4    00d4
C1. . . . . local   REAL*4           4    00d8
C2. . . . . local   REAL*4           4    00dc
C3. . . . . local   REAL*4           4    00e0
RESP. . . . . local   CHAR*1           1    00e4
STEP. . . . . local   REAL*4           4    00e6
WMAX. . . . . local   REAL*4           4    00ea
FACTOR. . . . . local   REAL*4           4    00ee
AB. . . . . local   REAL*4        8000    0186
WAVNUM. . . . . local   REAL*4        8000    20c6

   111
   112  C                      A S C I I _ X Y O U T    SUBROUTINE
   113  C                      ====================================
   114
   115        SUBROUTINE ASCOUT (WAVNUM, Ab, KOUNT)
   116
   117  $SUBTITLE:'ASCII_XY OUT'
   118  C  Written in Microsoft FORTRAN for use on an IBM PC-AT.
   119
   120  C               This subroutine will create A file containing the data
   121  C       values so that the program SpectraCalc can read them and plot
   122  C       them.  The files are in "ASCII_XY" format.  In each, the first
   123  C       line contains the x-label and y-label.    Subsequent lines contain
   124  C       ASCII representations of data in 2 columns to be read by the
   125  C       translator.
   126
   127  C  Allocation of storage for arrays:
```

Line# Source Line Microsoft FORTRAN Optimizing Compiler Version 4.10

```
      DIMENSION wavnum(2000), Ab(2000)
C  Type declarations for variables:
      CHARACTER PREFIX*7, SUFFIX*4, outfil*11, YFILE*11
      CHARACTER*1 RESP
      INTEGER KOUNT

C  Format statements for writing to the screen:
   41 FORMAT (1X, A)
   42 FORMAT ('0', A)
   43 FORMAT (1X, A\)
C  Documentation
      WRITE (*,42) 'The program will now write ASCII_XY files which can
     & be translated by'
      WRITE (*,41) 'SpectraCalc.  One file will be created, called:'
      WRITE (*,41) '     *.PRN'
      WRITE (*,41) 'where "*" is a string of seven characters that you
     &provide.'
      WRITE (*, 4080) KOUNT
 4080 FORMAT(1X,'The number of data points is: ', I4,'.')
C  Create the file name:
 4100 WRITE (*,43) 'What is the filename root (type 7 characters)?'
      READ (*,'(A7)') PREFIX
$NOTSTRICT
C  [Use concatenation of substrings to generate filenames.]
      SUFFIX = '.PRN'

      YFILE(1:7) = PREFIX
      YFILE(8:11) = SUFFIX

C  Confirmation of names:
      WRITE (*,42) 'The program will create the file:'
      WRITE (*, 4200) YFILE
 4200 FORMAT (8X, A11, '.')
      WRITE (*,43) 'Is this okay (type "y" or "n")? '
      READ (*, '(A)') RESP
      IF (.NOT. ((RESP.EQ.'y') .OR. (RESP.EQ.'Y'))) GO TO 4100

C                          WRITE THE DATA TO FILES

 4300 FORMAT (F9.4, ',', F9.4)

      OPEN (11, FILE=YFILE, STATUS='NEW')
      WRITE (11, '(A)') 'Wavenumbers, Absorbance'
      DO 4320 I=KOUNT, 1, -1
WRITE (11, 4300) wavnum(I), Ab(I)
 4320 CONTINUE
      CLOSE(11)
      WRITE (*, 42) 'The file for output has been completed.'

      WRITE (*,'(A)') ' '
      RETURN

      END
```

Microsoft FORTRAN Optimizing Compiler Version 4.10

ASCOUT Local Symbols

Name	Class	Type	Size	Offset
KOUNT	param			0006
AB.	param			000a
WAVNUM.	param			000e
I	local	INTEGER*4	4	00f2
PREFIX.	local	CHAR*7	7	00f6
SUFFIX.	local	CHAR*4	4	00fe
YFILE	local	CHAR*11	11	0102
RESP.	local	CHAR*1	1	010d

Global Symbols

Name	Class	Type	Size	Offset
ASCOUT.	FSUBRT	***	***	0d1d
main.	FSUBRT	***	***	0024

Code size = 108b (4235)
Data size = 4340 (17216)
Bss size = 010e (270)

No errors detected

d. FRINGE.AB (Array Basic program) to estimate thickness of polymer film from interference fringes in spectra

```
        REM     FRINGE.AB Array Basic Program
        REM This program generates synthetic absorption spectra for
        REM transparent (i.e. non-absorbing) thin films.  The result
        REM is an interference fringe pattern.
        REM
        REM Program assumes a transmission experiment in which a thin
        REM film is suspended perpendicular to IR beam in surrounding
        REM medium of n = 1.00.
        REM Formula used is derived from Fresnel coefficients.
        REM Spectra must be displayed in "x-flip" mode, with highest frequency
        REM at the left.
        REM
        REM Written by Darwin D. Popenoe in September 1989.

1000    PRINTLINE 24: PAUSEOFF
1010    PRINT "FRINGE synthesizes fringe patterns (trans. spectra) of thin"
1020    PAUSEON
1030    PRINT "transparent films. (PRESS SPACEBAR TO CONTINUE)"
1040    free                    'clear all variables and arrays
1050
1100    menu lims,"Okay_to_use_current_window_limits? YES NO"
1110    IF lims = 1 THEN GOTO 1120 ELSE GOTO 1200
1120      INPUT "Type YMAX, YMIN in 1/cm:", ymax, ymin
1130      GOTO 1300
1195    REM If answer was yes then obtain current screen window limits:
1200    \ ymin = getright()
1210      ymax = getleft()
1220    REM YMAX is the freq. value at the beginning (left side) of the
1230    REM spectrum--conversely for YMIN.
1300    INPUT "What is film thickness in micrometers (microns)?", dmicrom
1310    dcm = dmicrom * 1.0E-04
1340    INPUT "What is film's refractive index?", nfilm

1400    REM Dimension the new spectrum that will contain fringe pattern:
1405    REM (INCR is the increment for the new spectrum; it is negative,
1406    REM since the spectrum is generated starting from the left.)
1410    incr = (getflp() - getffp())/(npts(#s) - 1)       'freq. interval
1414    PRINTLINE 24: PAUSEOFF
1415    PRINT "Spacing between points in 1/cm = ", incr
1416    PAUSEON: PRINT "  PRESS ANY KEY TO CONTINUE"
1420    REM Set parameters for FILL command, which generates function:
1420    fillinc incr
1430    fillbeg ymax                                      'begin new spect.
1440    points = int((ymin - ymax)/incr)          '# pts new spect.
1446    PRINTLINE 24: PAUSEOFF
1447    PRINT "No. of points in spectrum = ", points
1448    PAUSEON: PRINT "  PRESS ANY KEY TO CONTINUE"
1450    newspc tempsp(points)                             'new memory file
1470    setleft ymax, ymin                                'new screen limits
1480    setffp ymax, ymin                                 'new file endpoints
1500    PAUSEOFF: PRINT "          calculating. . . ": PAUSEON

2000    REM             -CALCULATIONS-
2010    REM Calculate the coefficients for the transmittance expression:
2030    aa = 16 * (nfilm^2)
2040    bb = ((1 + nfilm)^4) + ((1 - nfilm)^4)
2050    cc = -2.0 * ((1 - (nfilm^2))^2)
2060    dd = 4.0 * 3.1415927 * dcm * nfilm
```

```
2100    tempsp = cos(fill(tempsp)*dd)
2110    tempsp = tempsp*cc + bb
2120    tempsp = (inverse(tempsp)) * aa 'transmittance!
2125    tempsp = tempsp*100
2130    tempsp = T2A(tempsp)            'convert to absorbance
2150    dim sname(8), descr(3)
2160    INPUT "Give three chars. for file descr. (may be an integer):", $descr
2170    string $sname(0,4) = "frnge"
2174    string $sname(5,7) = $descr
2178    string $sname(0,7), -3

3000    see
3100    end
```

APPENDIX 2. TABLES OF EXPERIMENTALLY DETERMINED OPTICAL FUNCTIONS OF COMPOUNDS

1. Deuterium Oxide

wavenumber	n	k	1976	1.3754	0.0031	2054	1.3870	0.0036
1900	1.3703	0.0022	1978	1.3755	0.0031	2056	1.3873	0.0036
1902	1.3697	0.0023	1980	1.3758	0.0030	2058	1.3878	0.0037
1904	1.3695	0.0024	1982	1.3760	0.0030	2060	1.3882	0.0038
1906	1.3694	0.0024	1984	1.3764	0.0030	2062	1.3886	0.0039
1908	1.3694	0.0023	1986	1.3767	0.0031	2064	1.3890	0.0040
1910	1.3694	0.0023	1988	1.3769	0.0033	2066	1.3893	0.0041
1912	1.3695	0.0024	1990	1.3772	0.0034	2068	1.3898	0.0041
1914	1.3696	0.0024	1992	1.3773	0.0035	2070	1.3902	0.0042
1916	1.3696	0.0023	1994	1.3775	0.0036	2072	1.3907	0.0043
1918	1.3698	0.0023	1996	1.3775	0.0036	2074	1.3911	0.0044
1920	1.3700	0.0024	1998	1.3778	0.0035	2076	1.3915	0.0046
1922	1.3700	0.0024	2000	1.3782	0.0036	2078	1.3919	0.0047
1924	1.3702	0.0023	2002	1.3784	0.0037	2080	1.3923	0.0048
1926	1.3703	0.0023	2004	1.3785	0.0039	2082	1.3928	0.0049
1928	1.3705	0.0022	2006	1.3785	0.0040	2084	1.3932	0.0050
1930	1.3708	0.0022	2008	1.3785	0.0040	2086	1.3936	0.0051
1932	1.3711	0.0023	2010	1.3787	0.0041	2088	1.3941	0.0052
1934	1.3713	0.0024	2012	1.3775	0.0041	2090	1.3945	0.0054
1936	1.3713	0.0026	2014	1.3778	0.0024	2092	1.3949	0.0055
1938	1.3713	0.0025	2016	1.3796	0.0024	2094	1.3954	0.0056
1940	1.3716	0.0025	2018	1.3799	0.0025	2096	1.3959	0.0057
1942	1.3717	0.0025	2020	1.3805	0.0026	2098	1.3963	0.0058
1944	1.3720	0.0024	2022	1.3808	0.0026	2100	1.3968	0.0059
1946	1.3722	0.0025	2024	1.3813	0.0026	2102	1.3973	0.0061
1948	1.3724	0.0025	2026	1.3817	0.0027	2104	1.3978	0.0062
1950	1.3726	0.0025	2028	1.3821	0.0027	2106	1.3982	0.0063
1952	1.3728	0.0026	2030	1.3824	0.0028	2108	1.3987	0.0065
1954	1.3730	0.0026	2032	1.3828	0.0028	2110	1.3992	0.0066
1956	1.3732	0.0026	2034	1.3832	0.0029	2112	1.3996	0.0068
1958	1.3735	0.0026	2036	1.3836	0.0030	2114	1.4001	0.0069
1960	1.3738	0.0027	2038	1.3840	0.0030	2116	1.4007	0.0070
1962	1.3739	0.0028	2040	1.3843	0.0031	2118	1.4012	0.0072
1964	1.3741	0.0027	2042	1.3847	0.0031	2120	1.4018	0.0074
1966	1.3743	0.0028	2044	1.3851	0.0032	2122	1.4023	0.0075
1968	1.3746	0.0028	2046	1.3855	0.0033	2124	1.4028	0.0077
1970	1.3747	0.0029	2048	1.3858	0.0034	2126	1.4033	0.0079
1972	1.3750	0.0029	2050	1.3862	0.0035	2128	1.4038	0.0080
1974	1.3754	0.0030	2052	1.3866	0.0035	2130	1.4044	0.0082

2132	1.4050	0.0084	2234	1.4444	0.0287	2336	1.4985	0.1115
2134	1.4055	0.0086	2236	1.4453	0.0294	2338	1.4989	0.1150
2136	1.4060	0.0087	2238	1.4462	0.0301	2340	1.4992	0.1183
2138	1.4066	0.0089	2240	1.4472	0.0308	2342	1.4995	0.1218
2140	1.4072	0.0091	2242	1.4481	0.0316	2344	1.4994	0.1254
2142	1.4078	0.0093	2244	1.4491	0.0323	2346	1.4984	0.1288
2144	1.4083	0.0095	2246	1.4502	0.0331	2348	1.4985	0.1313
2146	1.4089	0.0097	2248	1.4512	0.0339	2350	1.4988	0.1351
2148	1.4095	0.0099	2250	1.4523	0.0347	2352	1.4976	0.1385
2150	1.4102	0.0100	2252	1.4534	0.0356	2354	1.4970	0.1414
2152	1.4108	0.0103	2254	1.4544	0.0366	2356	1.4965	0.1445
2154	1.4114	0.0105	2256	1.4555	0.0375	2358	1.4958	0.1477
2156	1.4120	0.0106	2258	1.4566	0.0384	2360	1.4944	0.1506
2158	1.4127	0.0109	2260	1.4578	0.0394	2362	1.4944	0.1527
2160	1.4134	0.0111	2262	1.4589	0.0405	2364	1.4951	0.1563
2162	1.4140	0.0113	2264	1.4600	0.0414	2366	1.4941	0.1601
2164	1.4147	0.0115	2266	1.4612	0.0425	2368	1.4932	0.1634
2166	1.4155	0.0117	2268	1.4624	0.0437	2370	1.4925	0.1670
2168	1.4162	0.0120	2270	1.4636	0.0448	2372	1.4918	0.1708
2170	1.4169	0.0122	2272	1.4648	0.0460	2374	1.4894	0.1748
2172	1.4177	0.0124	2274	1.4660	0.0473	2376	1.4875	0.1773
2174	1.4185	0.0126	2276	1.4672	0.0486	2378	1.4868	0.1807
2176	1.4195	0.0128	2278	1.4684	0.0499	2380	1.4858	0.1843
2178	1.4203	0.0131	2280	1.4697	0.0513	2382	1.4836	0.1886
2180	1.4224	0.0133	2282	1.4709	0.0527	2384	1.4802	0.1918
2182	1.4232	0.0152	2284	1.4721	0.0542	2386	1.4783	0.1945
2184	1.4227	0.0156	2286	1.4734	0.0557	2388	1.4747	0.1979
2186	1.4232	0.0159	2288	1.4746	0.0573	2390	1.4719	0.1990
2188	1.4238	0.0160	2290	1.4758	0.0589	2392	1.4712	0.2018
2190	1.4247	0.0164	2292	1.4770	0.0606	2394	1.4684	0.2050
2192	1.4255	0.0168	2294	1.4782	0.0624	2396	1.4649	0.2071
2194	1.4262	0.0172	2296	1.4794	0.0641	2398	1.4625	0.2085
2196	1.4270	0.0176	2298	1.4806	0.0660	2400	1.4614	0.2108
2198	1.4277	0.0180	2300	1.4818	0.0679	2402	1.4587	0.2140
2200	1.4285	0.0184	2302	1.4829	0.0699	2404	1.4541	0.2157
2202	1.4293	0.0188	2304	1.4840	0.0719	2406	1.4517	0.2160
2204	1.4302	0.0192	2306	1.4851	0.0739	2408	1.4506	0.2174
2206	1.4311	0.0197	2308	1.4861	0.0761	2410	1.4495	0.2195
2208	1.4319	0.0201	2310	1.4872	0.0781	2412	1.4460	0.2222
2210	1.4328	0.0206	2312	1.4882	0.0803	2414	1.4437	0.2225
2212	1.4337	0.0210	2314	1.4896	0.0824	2416	1.4423	0.2248
2214	1.4346	0.0215	2316	1.4907	0.0852	2418	1.4391	0.2259
2216	1.4355	0.0219	2318	1.4911	0.0874	2420	1.4384	0.2273
2218	1.4366	0.0224	2320	1.4927	0.0897	2422	1.4360	0.2298
2220	1.4376	0.0230	2322	1.4937	0.0929	2424	1.4328	0.2308
2222	1.4388	0.0235	2324	1.4940	0.0955	2426	1.4311	0.2320
2224	1.4397	0.0240	2326	1.4948	0.0983	2428	1.4293	0.2333
2226	1.4420	0.0246	2328	1.4956	0.1012	2430	1.4274	0.2346
2228	1.4430	0.0268	2330	1.4949	0.1042	2432	1.4267	0.2359
2230	1.4426	0.0274	2332	1.4951	0.1055	2434	1.4249	0.2387
2232	1.4436	0.0280	2334	1.4973	0.1081	2436	1.4220	0.2402

2438	1.4201	0.2418	2540	1.2566	0.2695	2642	1.1197	0.1749
2440	1.4180	0.2433	2542	1.2543	0.2686	2644	1.1183	0.1712
2442	1.4161	0.2449	2544	1.2518	0.2676	2646	1.1170	0.1676
2444	1.4142	0.2463	2546	1.2494	0.2667	2648	1.1157	0.1639
2446	1.4136	0.2481	2548	1.2469	0.2657	2650	1.1147	0.1604
2448	1.4114	0.2513	2550	1.2446	0.2647	2652	1.1136	0.1569
2450	1.4079	0.2531	2552	1.2422	0.2639	2654	1.1126	0.1532
2452	1.4059	0.2546	2554	1.2399	0.2630	2656	1.1118	0.1498
2454	1.4040	0.2566	2556	1.2374	0.2624	2658	1.1108	0.1463
2456	1.4015	0.2587	2558	1.2348	0.2614	2660	1.1099	0.1426
2458	1.3987	0.2606	2560	1.2325	0.2606	2662	1.1095	0.1391
2460	1.3965	0.2624	2562	1.2301	0.2600	2664	1.1088	0.1357
2462	1.3940	0.2646	2564	1.2274	0.2593	2666	1.1079	0.1322
2464	1.3911	0.2664	2566	1.2247	0.2585	2668	1.1075	0.1286
2466	1.3897	0.2685	2568	1.2220	0.2577	2670	1.1071	0.1252
2468	1.3865	0.2722	2570	1.2192	0.2569	2672	1.1065	0.1216
2470	1.3813	0.2739	2572	1.2163	0.2561	2674	1.1062	0.1180
2472	1.3780	0.2751	2574	1.2133	0.2550	2676	1.1060	0.1146
2474	1.3753	0.2768	2576	1.2107	0.2539	2678	1.1055	0.1112
2476	1.3716	0.2788	2578	1.2077	0.2531	2680	1.1053	0.1077
2478	1.3677	0.2801	2580	1.2046	0.2518	2682	1.1041	0.1043
2480	1.3652	0.2818	2582	1.2021	0.2506	2684	1.1039	0.0994
2482	1.3606	0.2845	2584	1.1989	0.2497	2686	1.1049	0.0959
2484	1.3556	0.2852	2586	1.1958	0.2482	2688	1.1050	0.0922
2486	1.3516	0.2864	2588	1.1931	0.2471	2690	1.1054	0.0888
2488	1.3471	0.2870	2590	1.1895	0.2458	2692	1.1053	0.0851
2490	1.3430	0.2877	2592	1.1866	0.2440	2694	1.1058	0.0812
2492	1.3386	0.2882	2594	1.1836	0.2427	2696	1.1063	0.0776
2494	1.3343	0.2883	2596	1.1806	0.2410	2698	1.1069	0.0738
2496	1.3314	0.2887	2598	1.1773	0.2398	2700	1.1065	0.0701
2498	1.3262	0.2901	2600	1.1730	0.2376	2702	1.1075	0.0649
2500	1.3205	0.2891	2602	1.1707	0.2349	2704	1.1098	0.0613
2502	1.3176	0.2886	2604	1.1687	0.2337	2706	1.1108	0.0576
2504	1.3127	0.2889	2606	1.1641	0.2321	2708	1.1128	0.0540
2506	1.3076	0.2872	2608	1.1612	0.2292	2710	1.1134	0.0507
2508	1.3051	0.2859	2610	1.1579	0.2278	2712	1.1150	0.0460
2510	1.3009	0.2856	2612	1.1535	0.2246	2714	1.1180	0.0426
2512	1.2975	0.2836	2614	1.1507	0.2216	2716	1.1203	0.0393
2514	1.2954	0.2831	2616	1.1475	0.2186	2718	1.1219	0.0364
2516	1.2918	0.2825	2618	1.1445	0.2153	2720	1.1244	0.0324
2518	1.2887	0.2816	2620	1.1419	0.2119	2722	1.1280	0.0299
2520	1.2856	0.2809	2622	1.1396	0.2086	2724	1.1295	0.0274
2522	1.2823	0.2802	2624	1.1371	0.2052	2726	1.1325	0.0237
2524	1.2789	0.2791	2626	1.1350	0.2017	2728	1.1367	0.0216
2526	1.2759	0.2780	2628	1.1330	0.1984	2730	1.1397	0.0200
2528	1.2728	0.2770	2630	1.1319	0.1949	2732	1.1415	0.0184
2530	1.2698	0.2759	2632	1.1298	0.1927	2734	1.1444	0.0156
2532	1.2671	0.2749	2634	1.1268	0.1891	2736	1.1484	0.0142
2534	1.2632	0.2739	2636	1.1251	0.1857	2738	1.1511	0.0130
2536	1.2605	0.2715	2638	1.1231	0.1822	2740	1.1539	0.0119
2538	1.2591	0.2705	2640	1.1213	0.1785	2742	1.1566	0.0110

2744	1.1592	0.0102	2846	1.2243	0.0013	2948	1.2482	0.0007
2746	1.1616	0.0093	2848	1.2249	0.0012	2950	1.2485	0.0006
2748	1.1640	0.0086	2850	1.2256	0.0012	2952	1.2489	0.0007
2750	1.1662	0.0079	2852	1.2262	0.0012	2954	1.2492	0.0007
2752	1.1684	0.0073	2854	1.2268	0.0011	2956	1.2495	0.0006
2754	1.1706	0.0068	2856	1.2275	0.0011	2958	1.2498	0.0006
2756	1.1727	0.0063	2858	1.2281	0.0011	2960	1.2501	0.0007
2758	1.1747	0.0059	2860	1.2286	0.0011	2962	1.2503	0.0006
2760	1.1766	0.0054	2862	1.2292	0.0010	2964	1.2507	0.0004
2762	1.1786	0.0051	2864	1.2298	0.0009	2966	1.2511	0.0004
2764	1.1805	0.0048	2866	1.2305	0.0009	2968	1.2515	0.0005
2766	1.1821	0.0046	2868	1.2310	0.0010	2970	1.2518	0.0005
2768	1.1837	0.0042	2870	1.2315	0.0009	2972	1.2520	0.0006
2770	1.1854	0.0039	2872	1.2321	0.0008	2974	1.2522	0.0005
2772	1.1871	0.0037	2874	1.2328	0.0009	2976	1.2525	0.0004
2774	1.1886	0.0035	2876	1.2332	0.0009	2978	1.2529	0.0005
2776	1.1902	0.0034	2878	1.2337	0.0008	2980	1.2530	0.0005
2778	1.1915	0.0033	2880	1.2342	0.0008	2982	1.2533	0.0004
2780	1.1929	0.0031	2882	1.2348	0.0008	2984	1.2536	0.0004
2782	1.1944	0.0029	2884	1.2354	0.0008	2986	1.2539	0.0004
2784	1.1957	0.0028	2886	1.2358	0.0008	2988	1.2542	0.0004
2786	1.1970	0.0028	2888	1.2363	0.0008	2990	1.2544	0.0004
2788	1.1983	0.0027	2890	1.2368	0.0007	2992	1.2548	0.0003
2790	1.1994	0.0026	2892	1.2373	0.0008	2994	1.2551	0.0004
2792	1.2005	0.0025	2894	1.2377	0.0008	2996	1.2553	0.0004
2794	1.2017	0.0024	2896	1.2382	0.0007	2998	1.2556	0.0003
2796	1.2028	0.0022	2898	1.2387	0.0007	3000	1.2558	0.0003
2798	1.2040	0.0022	2900	1.2392	0.0007	3002	1.2561	0.0003
2800	1.2051	0.0021	2902	1.2396	0.0008	3004	1.2563	0.0003
2802	1.2061	0.0020	2904	1.2400	0.0008	3006	1.2566	0.0003
2804	1.2071	0.0020	2906	1.2405	0.0007	3008	1.2569	0.0003
2806	1.2082	0.0019	2908	1.2409	0.0008	3010	1.2571	0.0003
2808	1.2091	0.0019	2910	1.2413	0.0008	3012	1.2574	0.0003
2810	1.2100	0.0018	2912	1.2418	0.0008	3014	1.2577	0.0003
2812	1.2110	0.0017	2914	1.2422	0.0008	3016	1.2580	0.0003
2814	1.2120	0.0017	2916	1.2425	0.0008	3018	1.2582	0.0004
2816	1.2129	0.0016	2918	1.2429	0.0008	3020	1.2582	0.0004
2818	1.2137	0.0017	2920	1.2434	0.0008	3022	1.2585	0.0002
2820	1.2145	0.0016	2922	1.2437	0.0008	3024	1.2589	0.0003
2822	1.2154	0.0015	2924	1.2441	0.0008	3026	1.2590	0.0003
2824	1.2163	0.0014	2926	1.2444	0.0008	3028	1.2592	0.0002
2826	1.2171	0.0014	2928	1.2447	0.0008	3030	1.2594	0.0002
2828	1.2179	0.0014	2930	1.2451	0.0007	3032	1.2596	0.0002
2830	1.2187	0.0014	2932	1.2455	0.0007	3034	1.2599	0.0001
2832	1.2194	0.0014	2934	1.2460	0.0007	3036	1.2602	0.0002
2834	1.2202	0.0014	2936	1.2463	0.0008	3038	1.2603	0.0001
2836	1.2209	0.0014	2938	1.2466	0.0008	3040	1.2606	0.0001
2838	1.2215	0.0013	2940	1.2469	0.0008	3042	1.2609	0.0001
2840	1.2223	0.0012	2942	1.2472	0.0007	3044	1.2611	0.0001
2842	1.2231	0.0012	2944	1.2475	0.0007	3046	1.2613	0.0002
2844	1.2238	0.0013	2946	1.2479	0.0007	3048	1.2615	0.0002

3050	1.2617	0.0002	3068	1.2634	0.0001	3086	1.2652	0.0002
3052	1.2620	0.0002	3070	1.2638	0.0001	3088	1.2653	0.0002
3054	1.2622	0.0002	3072	1.2640	0.0002	3090	1.2655	0.0002
3056	1.2623	0.0002	3074	1.2641	0.0002	3092	1.2656	0.0002
3058	1.2625	0.0001	3076	1.2643	0.0002	3094	1.2658	0.0001
3060	1.2628	0.0002	3078	1.2645	0.0001	3096	1.2661	0.0001
3062	1.2630	0.0002	3080	1.2647	0.0002	3098	1.2663	0.0002
3064	1.2632	0.0002	3082	1.2648	0.0002	3100	1.2663	0.0002
3066	1.2633	0.0002	3084	1.2650	0.0002			

2. Hexanethiol

wavenumber	n	k	2790.0	1.4632	0.0030	2882.5	1.4593	0.0246
2700.0	1.4574	0.0029	2792.5	1.4638	0.0031	2885.0	1.4633	0.0257
2702.5	1.4565	0.0029	2795.0	1.4645	0.0032	2887.5	1.4659	0.0261
2705.0	1.4562	0.0029	2797.5	1.4651	0.0033	2890.0	1.4694	0.0274
2707.5	1.4562	0.0029	2800.0	1.4658	0.0035	2892.5	1.4721	0.0292
2710.0	1.4562	0.0030	2802.5	1.4667	0.0037	2895.0	1.4745	0.0315
2712.5	1.4562	0.0031	2805.0	1.4675	0.0039	2897.5	1.4764	0.0340
2715.0	1.4562	0.0032	2807.5	1.4683	0.0042	2900.0	1.4784	0.0363
2717.5	1.4561	0.0032	2810.0	1.4692	0.0044	2902.5	1.4808	0.0389
2720.0	1.4562	0.0033	2812.5	1.4701	0.0047	2905.0	1.4850	0.0422
2722.5	1.4564	0.0033	2815.0	1.4712	0.0049	2907.5	1.4885	0.0483
2725.0	1.4565	0.0035	2817.5	1.4724	0.0052	2910.0	1.4902	0.0548
2727.5	1.4565	0.0037	2820.0	1.4737	0.0057	2912.5	1.4911	0.0625
2730.0	1.4564	0.0038	2822.5	1.4751	0.0061	2915.0	1.4924	0.0708
2732.5	1.4563	0.0039	2825.0	1.4768	0.0066	2917.5	1.4901	0.0826
2735.0	1.4562	0.0038	2827.5	1.4786	0.0073	2920.0	1.4842	0.0930
2737.5	1.4561	0.0038	2830.0	1.4818	0.0082	2922.5	1.4732	0.1045
2740.0	1.4562	0.0035	2832.5	1.4844	0.0108	2925.0	1.4579	0.1104
2742.5	1.4565	0.0034	2835.0	1.4861	0.0127	2927.5	1.4410	0.1140
2745.0	1.4568	0.0034	2837.5	1.4889	0.0153	2930.0	1.4228	0.1110
2747.5	1.4569	0.0035	2840.0	1.4917	0.0188	2932.5	1.4073	0.1040
2750.0	1.4570	0.0034	2842.5	1.4944	0.0236	2935.0	1.3951	0.0920
2752.5	1.4573	0.0033	2845.0	1.4954	0.0297	2937.5	1.3908	0.0779
2755.0	1.4575	0.0033	2847.5	1.4964	0.0363	2940.0	1.3947	0.0656
2757.5	1.4579	0.0032	2850.0	1.4921	0.0451	2942.5	1.4017	0.0587
2760.0	1.4582	0.0034	2852.5	1.4855	0.0497	2945.0	1.4095	0.0551
2762.5	1.4583	0.0035	2855.0	1.4776	0.0545	2947.5	1.4183	0.0566
2765.0	1.4585	0.0035	2857.5	1.4678	0.0544	2950.0	1.4239	0.0631
2767.5	1.4589	0.0036	2860.0	1.4595	0.0525	2952.5	1.4228	0.0729
2770.0	1.4579	0.0038	2862.5	1.4532	0.0466	2955.0	1.4115	0.0812
2772.5	1.4582	0.0022	2865.0	1.4538	0.0408	2957.5	1.3964	0.0823
2775.0	1.4600	0.0023	2867.5	1.4573	0.0385	2960.0	1.3823	0.0790
2777.5	1.4604	0.0024	2870.0	1.4584	0.0397	2962.5	1.3686	0.0701
2780.0	1.4611	0.0026	2872.5	1.4537	0.0402	2965.0	1.3622	0.0570
2782.5	1.4616	0.0027	2875.0	1.4489	0.0359	2967.5	1.3607	0.0451
2785.0	1.4621	0.0028	2877.5	1.4499	0.0301	2970.0	1.3640	0.0332
2787.5	1.4626	0.0029	2880.0	1.4539	0.0264	2972.5	1.3699	0.0262

2975.0	1.3741	0.0202	3017.5	1.4107	0.0044	3060.0	1.4201	0.0023
2977.5	1.3803	0.0159	3020.0	1.4115	0.0041	3062.5	1.4205	0.0023
2980.0	1.3847	0.0142	3022.5	1.4123	0.0039	3065.0	1.4207	0.0023
2982.5	1.3871	0.0120	3025.0	1.4130	0.0038	3067.5	1.4210	0.0023
2985.0	1.3906	0.0099	3027.5	1.4137	0.0035	3070.0	1.4212	0.0022
2987.5	1.3938	0.0087	3030.0	1.4144	0.0034	3072.5	1.4214	0.0021
2990.0	1.3973	0.0078	3032.5	1.4150	0.0033	3075.0	1.4217	0.0020
2992.5	1.3994	0.0084	3035.0	1.4156	0.0032	3077.5	1.4222	0.0019
2995.0	1.4000	0.0077	3037.5	1.4162	0.0031	3080.0	1.4224	0.0021
2997.5	1.4018	0.0070	3040.0	1.4166	0.0030	3082.5	1.4226	0.0020
3000.0	1.4034	0.0065	3042.5	1.4171	0.0029	3085.0	1.4228	0.0022
3002.5	1.4046	0.0062	3045.0	1.4177	0.0028	3087.5	1.4227	0.0021
3005.0	1.4058	0.0058	3047.5	1.4181	0.0027	3090.0	1.4229	0.0020
3007.5	1.4070	0.0054	3050.0	1.4186	0.0027	3092.5	1.4230	0.0020
3010.0	1.4081	0.0051	3052.5	1.4188	0.0027	3095.0	1.4230	0.0019
3012.5	1.4090	0.0049	3055.0	1.4191	0.0025	3097.5	1.4231	0.0018
3015.0	1.4099	0.0046	3057.5	1.4196	0.0024	3100.0	1.4227	0.0018

3. Dodecanethiol

wavenumber	n	k	2770.0	1.4648	0.0019	2842.5	1.5297	0.0384
2700.0	1.4612	0.0028	2772.5	1.4668	0.0020	2845.0	1.5346	0.0533
2702.5	1.4603	0.0028	2775.0	1.4674	0.0021	2847.5	1.5322	0.0721
2705.0	1.4601	0.0027	2777.5	1.4683	0.0023	2850.0	1.5216	0.0908
2707.5	1.4602	0.0027	2780.0	1.4690	0.0024	2852.5	1.4952	0.1065
2710.0	1.4602	0.0028	2782.5	1.4698	0.0025	2855.0	1.4603	0.1044
2712.5	1.4603	0.0028	2785.0	1.4706	0.0027	2857.5	1.4390	0.0895
2715.0	1.4605	0.0029	2787.5	1.4713	0.0028	2860.0	1.4300	0.0722
2717.5	1.4605	0.0030	2790.0	1.4722	0.0029	2862.5	1.4318	0.0555
2720.0	1.4606	0.0030	2792.5	1.4731	0.0031	2865.0	1.4394	0.0459
2722.5	1.4609	0.0030	2795.0	1.4740	0.0032	2867.5	1.4464	0.0404
2725.0	1.4610	0.0032	2797.5	1.4750	0.0034	2870.0	1.4516	0.0387
2727.5	1.4610	0.0033	2800.0	1.4762	0.0036	2872.5	1.4526	0.0369
2730.0	1.4611	0.0034	2802.5	1.4773	0.0038	2875.0	1.4544	0.0330
2732.5	1.4612	0.0034	2805.0	1.4785	0.0040	2877.5	1.4605	0.0297
2735.0	1.4613	0.0033	2807.5	1.4799	0.0042	2880.0	1.4662	0.0295
2737.5	1.4614	0.0032	2810.0	1.4813	0.0045	2882.5	1.4708	0.0289
2740.0	1.4617	0.0031	2812.5	1.4830	0.0048	2885.0	1.4780	0.0297
2742.5	1.4620	0.0031	2815.0	1.4848	0.0051	2887.5	1.4838	0.0331
2745.0	1.4624	0.0031	2817.5	1.4881	0.0054	2890.0	1.4887	0.0367
2747.5	1.4627	0.0031	2820.0	1.4905	0.0076	2892.5	1.4927	0.0420
2750.0	1.4630	0.0030	2822.5	1.4916	0.0084	2895.0	1.4948	0.0466
2752.5	1.4633	0.0030	2825.0	1.4943	0.0094	2897.5	1.4973	0.0514
2755.0	1.4637	0.0030	2827.5	1.4972	0.0107	2900.0	1.5001	0.0561
2757.5	1.4642	0.0030	2830.0	1.5007	0.0123	2902.5	1.5033	0.0617
2760.0	1.4646	0.0032	2832.5	1.5049	0.0145	2905.0	1.5072	0.0681
2762.5	1.4648	0.0034	2835.0	1.5101	0.0178	2907.5	1.5122	0.0766
2765.0	1.4652	0.0034	2837.5	1.5148	0.0226	2910.0	1.5162	0.0880
2767.5	1.4643	0.0035	2840.0	1.5215	0.0280	2912.5	1.5200	0.1019

2915.0	1.5224	0.1216	2977.5	1.3760	0.0121	3040.0	1.4121	0.0021
2917.5	1.5123	0.1453	2980.0	1.3810	0.0099	3042.5	1.4128	0.0019
2920.0	1.4974	0.1674	2982.5	1.3842	0.0101	3045.0	1.4134	0.0019
2922.5	1.4682	0.1855	2985.0	1.3858	0.0088	3047.5	1.4139	0.0018
2925.0	1.4213	0.1922	2987.5	1.3885	0.0079	3050.0	1.4144	0.0018
2927.5	1.3858	0.1798	2990.0	1.3906	0.0072	3052.5	1.4148	0.0018
2930.0	1.3608	0.1625	2992.5	1.3925	0.0066	3055.0	1.4152	0.0016
2932.5	1.3433	0.1408	2995.0	1.3942	0.0060	3057.5	1.4157	0.0015
2935.0	1.3329	0.1183	2997.5	1.3959	0.0054	3060.0	1.4162	0.0015
2937.5	1.3323	0.0946	3000.0	1.3976	0.0050	3062.5	1.4166	0.0014
2940.0	1.3386	0.0770	3002.5	1.3989	0.0048	3065.0	1.4171	0.0014
2942.5	1.3484	0.0625	3005.0	1.4001	0.0044	3067.5	1.4174	0.0014
2945.0	1.3607	0.0553	3007.5	1.4014	0.0041	3070.0	1.4176	0.0014
2947.5	1.3705	0.0523	3010.0	1.4026	0.0038	3072.5	1.4179	0.0012
2950.0	1.3783	0.0540	3012.5	1.4037	0.0036	3075.0	1.4183	0.0011
2952.5	1.3796	0.0579	3015.0	1.4048	0.0034	3077.5	1.4188	0.0010
2955.0	1.3749	0.0603	3017.5	1.4056	0.0033	3080.0	1.4192	0.0011
2957.5	1.3676	0.0588	3020.0	1.4064	0.0031	3082.5	1.4194	0.0011
2960.0	1.3612	0.0537	3022.5	1.4074	0.0029	3085.0	1.4197	0.0011
2962.5	1.3564	0.0461	3025.0	1.4081	0.0028	3087.5	1.4199	0.0011
2965.0	1.3567	0.0367	3027.5	1.4089	0.0026	3090.0	1.4201	0.0010
2967.5	1.3587	0.0298	3030.0	1.4096	0.0025	3092.5	1.4204	0.0009
2970.0	1.3626	0.0223	3032.5	1.4104	0.0024	3095.0	1.4206	0.0009
2972.5	1.3683	0.0182	3035.0	1.4110	0.0023	3097.5	1.4207	0.0009
2975.0	1.3721	0.0148	3037.5	1.4116	0.0022	3100.0	1.4207	0.0008

4. Octadecanethiol

wavenumber	n	k	2740	1.4918	0.0040	2782	1.5011	0.0049
2700	1.4906	0.0036	2742	1.4916	0.0040	2784	1.5017	0.0059
2702	1.4890	0.0035	2744	1.4923	0.0040	2786	1.5013	0.0059
2704	1.4893	0.0032	2746	1.4918	0.0045	2788	1.5017	0.0055
2706	1.4891	0.0037	2748	1.4921	0.0037	2790	1.5036	0.0052
2708	1.4888	0.0035	2750	1.4927	0.0043	2792	1.5042	0.0062
2710	1.4888	0.0038	2752	1.4924	0.0037	2794	1.5047	0.0056
2712	1.4888	0.0035	2754	1.4935	0.0036	2796	1.5061	0.0061
2714	1.4889	0.0038	2756	1.4942	0.0038	2798	1.5073	0.0060
2716	1.4885	0.0035	2758	1.4947	0.0040	2800	1.5085	0.0071
2718	1.4891	0.0031	2760	1.4948	0.0043	2802	1.5087	0.0071
2720	1.4902	0.0035	2762	1.4951	0.0041	2804	1.5100	0.0071
2722	1.4893	0.0043	2764	1.4956	0.0042	2806	1.5112	0.0073
2724	1.4893	0.0034	2766	1.4962	0.0042	2808	1.5130	0.0075
2726	1.4902	0.0039	2768	1.4968	0.0045	2810	1.5144	0.0084
2728	1.4898	0.0039	2770	1.4971	0.0045	2812	1.5151	0.0086
2730	1.4907	0.0039	2772	1.4974	0.0045	2814	1.5171	0.0086
2732	1.4901	0.0046	2774	1.4984	0.0043	2816	1.5190	0.0094
2734	1.4893	0.0037	2776	1.4994	0.0050	2818	1.5208	0.0096
2736	1.4905	0.0032	2778	1.4992	0.0053	2820	1.5232	0.0102
2738	1.4915	0.0034	2780	1.4995	0.0050	2822	1.5261	0.0108

2824	1.5290	0.0123	2926	1.3097	0.1740	3028	1.4344	0.0047
2826	1.5315	0.0136	2928	1.3090	0.1411	3030	1.4340	0.0045
2828	1.5342	0.0148	2930	1.3153	0.1147	3032	1.4352	0.0041
2830	1.5381	0.0156	2932	1.3217	0.0954	3034	1.4351	0.0049
2832	1.5434	0.0173	2934	1.3284	0.0773	3036	1.4346	0.0038
2834	1.5490	0.0198	2936	1.3374	0.0629	3038	1.4364	0.0035
2836	1.5565	0.0231	2938	1.3490	0.0507	3040	1.4365	0.0042
2838	1.5655	0.0287	2940	1.3599	0.0442	3042	1.4362	0.0036
2840	1.5753	0.0363	2942	1.3684	0.0380	3044	1.4374	0.0033
2842	1.5904	0.0477	2944	1.3790	0.0343	3046	1.4381	0.0036
2844	1.6084	0.0702	2946	1.3887	0.0337	3048	1.4381	0.0037
2846	1.6248	0.1081	2948	1.3971	0.0360	3050	1.4383	0.0035
2848	1.6078	0.1662	2950	1.3999	0.0408	3052	1.4392	0.0035
2850	1.5223	0.2030	2952	1.3990	0.0435	3054	1.4390	0.0040
2852	1.4359	0.1770	2954	1.3964	0.0455	3056	1.4390	0.0035
2854	1.4099	0.1295	2956	1.3911	0.0444	3058	1.4396	0.0036
2856	1.4140	0.0941	2958	1.3883	0.0407	3060	1.4396	0.0035
2858	1.4242	0.0706	2960	1.3863	0.0367	3062	1.4401	0.0033
2860	1.4346	0.0558	2962	1.3854	0.0310	3064	1.4402	0.0036
2862	1.4443	0.0445	2964	1.3881	0.0258	3066	1.4396	0.0032
2864	1.4557	0.0374	2966	1.3901	0.0225	3068	1.4407	0.0023
2866	1.4659	0.0345	2968	1.3925	0.0182	3070	1.4421	0.0030
2868	1.4732	0.0341	2970	1.3969	0.0159	3072	1.4412	0.0033
2870	1.4776	0.0342	2972	1.3989	0.0143	3074	1.4421	0.0026
2872	1.4809	0.0340	2974	1.4015	0.0120	3076	1.4427	0.0037
2874	1.4834	0.0330	2976	1.4049	0.0110	3078	1.4419	0.0037
2876	1.4881	0.0312	2978	1.4063	0.0102	3080	1.4416	0.0036
2878	1.4933	0.0315	2980	1.4085	0.0085	3082	1.4417	0.0029
2880	1.4985	0.0316	2982	1.4115	0.0081	3084	1.4425	0.0030
2882	1.5041	0.0338	2984	1.4126	0.0079	3086	1.4419	0.0031
2884	1.5080	0.0361	2986	1.4145	0.0067	3088	1.4422	0.0023
2886	1.5120	0.0389	2988	1.4166	0.0067	3090	1.4435	0.0025
2888	1.5159	0.0420	2990	1.4181	0.0063	3092	1.4433	0.0031
2890	1.5185	0.0458	2992	1.4190	0.0064	3094	1.4429	0.0032
2892	1.5211	0.0485	2994	1.4207	0.0056	3096	1.4426	0.0032
2894	1.5242	0.0519	2996	1.4215	0.0062	3098	1.4421	0.0030
2896	1.5279	0.0548	2998	1.4224	0.0048	3100	1.4415	0.0028
2898	1.5321	0.0592	3000	1.4248	0.0052			
2900	1.5349	0.0628	3002	1.4250	0.0054			
2902	1.5426	0.0659	3004	1.4265	0.0052			
2904	1.5514	0.0732	3006	1.4263	0.0058			
2906	1.5618	0.0813	3008	1.4269	0.0044			
2908	1.5748	0.0952	3010	1.4289	0.0047			
2910	1.5910	0.1137	3012	1.4293	0.0049			
2912	1.6132	0.1476	3014	1.4295	0.0049			
2914	1.6192	0.2034	3016	1.4301	0.0042			
2916	1.5802	0.2669	3018	1.4316	0.0042			
2918	1.4827	0.3020	3020	1.4323	0.0045			
2920	1.4010	0.2791	3022	1.4322	0.0047			
2922	1.3579	0.2512	3024	1.4327	0.0040			
2924	1.3222	0.2131	3026	1.4341	0.0042			

5. Eicosanoic Acid

wavenumber	n	k	2630	1.4458	0.0091	2814	1.4725	0.0104
2450	1.4446	0.0025	2634	1.4447	0.0082	2818	1.4766	0.0116
2454	1.4446	0.0025	2638	1.4461	0.0087	2822	1.4791	0.0128
2458	1.4452	0.0032	2642	1.4447	0.0093	2826	1.4850	0.0133
2462	1.4428	0.0042	2646	1.4451	0.0082	2830	1.4914	0.0167
2466	1.4432	0.0022	2650	1.4458	0.0093	2834	1.4995	0.0195
2470	1.4448	0.0038	2654	1.4439	0.0089	2838	1.5135	0.0263
2474	1.4422	0.0035	2658	1.4456	0.0080	2842	1.5427	0.0443
2478	1.4444	0.0024	2662	1.4451	0.0094	2846	1.5695	0.1020
2482	1.4441	0.0045	2666	1.4444	0.0079	2850	1.4566	0.1622
2486	1.4428	0.0031	2670	1.4462	0.0085	2854	1.3695	0.0900
2490	1.4452	0.0037	2674	1.4444	0.0088	2858	1.4074	0.0517
2494	1.4429	0.0047	2678	1.4455	0.0074	2862	1.4231	0.0372
2498	1.4436	0.0029	2682	1.4466	0.0088	2866	1.4391	0.0321
2502	1.4449	0.0045	2686	1.4449	0.0084	2870	1.4472	0.0334
2506	1.4431	0.0041	2690	1.4462	0.0079	2874	1.4494	0.0324
2510	1.4451	0.0037	2694	1.4456	0.0085	2878	1.4576	0.0301
2514	1.4443	0.0052	2698	1.4459	0.0071	2882	1.4675	0.0334
2518	1.4436	0.0039	2702	1.4474	0.0080	2886	1.4728	0.0384
2522	1.4457	0.0045	2706	1.4460	0.0080	2890	1.4775	0.0433
2526	1.4443	0.0055	2710	1.4473	0.0070	2894	1.4819	0.0490
2530	1.4447	0.0045	2714	1.4477	0.0080	2898	1.4866	0.0542
2534	1.4455	0.0059	2718	1.4469	0.0070	2902	1.4974	0.0609
2538	1.4438	0.0058	2722	1.4492	0.0067	2906	1.5128	0.0746
2542	1.4453	0.0052	2726	1.4487	0.0077	2910	1.5509	0.1067
2546	1.4446	0.0067	2730	1.4493	0.0065	2914	1.5421	0.1872
2550	1.4439	0.0054	2734	1.4506	0.0077	2918	1.4150	0.2291
2554	1.4457	0.0061	2738	1.4493	0.0072	2922	1.3191	0.1736
2558	1.4439	0.0066	2742	1.4515	0.0064	2926	1.3175	0.1179
2562	1.4452	0.0055	2746	1.4521	0.0078	2930	1.3309	0.0853
2566	1.4455	0.0075	2750	1.4515	0.0072	2934	1.3422	0.0664
2570	1.4436	0.0066	2754	1.4534	0.0072	2938	1.3508	0.0524
2574	1.4454	0.0065	2758	1.4530	0.0078	2942	1.3614	0.0417
2578	1.4440	0.0075	2762	1.4543	0.0067	2946	1.3744	0.0364
2582	1.4440	0.0058	2766	1.4556	0.0079	2950	1.3866	0.0386
2586	1.4459	0.0068	2770	1.4552	0.0075	2954	1.3822	0.0449
2590	1.4442	0.0072	2774	1.4575	0.0075	2958	1.3759	0.0391
2594	1.4456	0.0063	2778	1.4576	0.0085	2962	1.3760	0.0357
2598	1.4456	0.0079	2782	1.4582	0.0074	2966	1.3738	0.0285
2602	1.4444	0.0069	2786	1.4610	0.0080	2970	1.3785	0.0217
2606	1.4465	0.0073	2790	1.4609	0.0088	2974	1.3849	0.0182
2610	1.4449	0.0085	2794	1.4628	0.0080	2978	1.3888	0.0170
2614	1.4450	0.0071	2798	1.4651	0.0094	2982	1.3917	0.0153
2618	1.4464	0.0083	2802	1.4653	0.0094	2986	1.3957	0.0146
2622	1.4443	0.0085	2806	1.4685	0.0093	2990	1.3976	0.0148
2626	1.4458	0.0075	2810	1.4703	0.0107	2994	1.3994	0.0138

2998	1.4022	0.0138	3202	1.4203	0.0123	3406	1.4219	0.0223
3002	1.4033	0.0141	3206	1.4206	0.0117	3410	1.4228	0.0223
3006	1.4049	0.0139	3210	1.4214	0.0119	3414	1.4215	0.0235
3010	1.4060	0.0146	3214	1.4210	0.0121	3418	1.4209	0.0226
3014	1.4060	0.0142	3218	1.4215	0.0117	3422	1.4210	0.0234
3018	1.4078	0.0138	3222	1.4216	0.0124	3426	1.4199	0.0230
3022	1.4086	0.0146	3226	1.4213	0.0118	3430	1.4208	0.0231
3026	1.4087	0.0143	3230	1.4224	0.0121	3434	1.4197	0.0242
3030	1.4096	0.0145	3234	1.4219	0.0126	3438	1.4189	0.0236
3034	1.4092	0.0144	3238	1.4220	0.0123	3442	1.4190	0.0242
3038	1.4102	0.0135	3242	1.4220	0.0126	3446	1.4173	0.0242
3042	1.4109	0.0141	3246	1.4216	0.0121	3450	1.4170	0.0235
3046	1.4109	0.0134	3250	1.4236	0.0121	3454	1.4174	0.0237
3050	1.4124	0.0135	3254	1.4222	0.0135	3458	1.4159	0.0241
3054	1.4119	0.0139	3258	1.4220	0.0118	3462	1.4157	0.0231
3058	1.4127	0.0129	3262	1.4236	0.0130	3466	1.4153	0.0237
3062	1.4138	0.0137	3266	1.4220	0.0129	3470	1.4148	0.0227
3066	1.4130	0.0136	3270	1.4227	0.0122	3474	1.4148	0.0233
3070	1.4138	0.0131	3274	1.4236	0.0127	3478	1.4134	0.0226
3074	1.4141	0.0134	3278	1.4226	0.0129	3482	1.4142	0.0223
3078	1.4139	0.0130	3282	1.4238	0.0121	3486	1.4134	0.0228
3082	1.4150	0.0128	3286	1.4239	0.0135	3490	1.4126	0.0219
3086	1.4149	0.0133	3290	1.4233	0.0126	3494	1.4129	0.0219
3090	1.4152	0.0127	3294	1.4244	0.0131	3498	1.4121	0.0217
3094	1.4157	0.0131	3298	1.4238	0.0131	3502	1.4122	0.0211
3098	1.4156	0.0128	3302	1.4249	0.0129	3506	1.4119	0.0214
3102	1.4163	0.0129	3306	1.4251	0.0139	3510	1.4112	0.0208
3106	1.4158	0.0132	3310	1.4245	0.0137	3514	1.4115	0.0206
3110	1.4163	0.0124	3314	1.4254	0.0138	3518	1.4110	0.0206
3114	1.4174	0.0130	3318	1.4249	0.0145	3522	1.4110	0.0202
3118	1.4160	0.0134	3322	1.4253	0.0139	3526	1.4110	0.0206
3122	1.4162	0.0122	3326	1.4262	0.0148	3530	1.4098	0.0206
3126	1.4174	0.0125	3330	1.4256	0.0149	3534	1.4085	0.0197
3130	1.4169	0.0126	3334	1.4266	0.0151	3538	1.4094	0.0185
3134	1.4173	0.0122	3338	1.4266	0.0163	3542	1.4099	0.0190
3138	1.4174	0.0124	3342	1.4260	0.0163	3546	1.4092	0.0189
3142	1.4174	0.0121	3346	1.4266	0.0168	3550	1.4085	0.0188
3146	1.4179	0.0120	3350	1.4259	0.0175	3554	1.4082	0.0180
3150	1.4178	0.0120	3354	1.4258	0.0171	3558	1.4083	0.0177
3154	1.4182	0.0117	3358	1.4268	0.0178	3562	1.4080	0.0172
3158	1.4181	0.0118	3362	1.4260	0.0187	3566	1.4087	0.0170
3162	1.4184	0.0111	3366	1.4264	0.0186	3570	1.4081	0.0175
3166	1.4196	0.0113	3370	1.4266	0.0201	3574	1.4070	0.0168
3170	1.4191	0.0117	3374	1.4249	0.0205	3578	1.4076	0.0162
3174	1.4197	0.0111	3378	1.4245	0.0202	3582	1.4070	0.0165
3178	1.4203	0.0119	3382	1.4248	0.0203	3586	1.4063	0.0155
3182	1.4194	0.0117	3386	1.4253	0.0209	3590	1.4066	0.0150
3186	1.4202	0.0113	3390	1.4242	0.0220	3594	1.4066	0.0145
3190	1.4207	0.0117	3394	1.4234	0.0216	3598	1.4071	0.0142
3194	1.4209	0.0117	3398	1.4237	0.0222	3602	1.4067	0.0143
3198	1.4212	0.0123	3402	1.4227	0.0226	3606	1.4065	0.0136

3610	1.4071	0.0135	3694	1.4083	0.0070	3778	1.4102	0.0053
3614	1.4059	0.0137	3698	1.4087	0.0069	3782	1.4101	0.0054
3618	1.4057	0.0123	3702	1.4088	0.0069	3786	1.4100	0.0050
3622	1.4063	0.0122	3706	1.4091	0.0068	3790	1.4102	0.0051
3626	1.4064	0.0117	3710	1.4084	0.0070	3794	1.4100	0.0049
3630	1.4064	0.0118	3714	1.4088	0.0061	3798	1.4100	0.0047
3634	1.4057	0.0112	3718	1.4093	0.0066	3802	1.4103	0.0044
3638	1.4061	0.0104	3722	1.4089	0.0061	3806	1.4102	0.0047
3642	1.4063	0.0103	3726	1.4099	0.0062	3810	1.4102	0.0042
3646	1.4064	0.0097	3730	1.4087	0.0065	3814	1.4106	0.0044
3650	1.4066	0.0094	3734	1.4096	0.0052	3818	1.4103	0.0045
3654	1.4075	0.0091	3738	1.4100	0.0064	3822	1.4100	0.0044
3658	1.4072	0.0097	3742	1.4098	0.0056	3826	1.4098	0.0041
3662	1.4068	0.0089	3746	1.4096	0.0065	3830	1.4103	0.0039
3666	1.4069	0.0088	3750	1.4090	0.0053	3834	1.4101	0.0044
3670	1.4066	0.0080	3754	1.4097	0.0054	3838	1.4096	0.0040
3674	1.4078	0.0075	3758	1.4098	0.0049	3842	1.4096	0.0041
3678	1.4079	0.0079	3762	1.4103	0.0051	3846	1.4090	0.0041
3682	1.4077	0.0074	3766	1.4106	0.0050	3850	1.4075	0.0041
3686	1.4083	0.0073	3770	1.4109	0.0055			
3690	1.4082	0.0073	3774	1.4101	0.0057			

6. Poly(styrene/acrylonitrile)

wavenumber	n	k						
630	1.5606	0.0023	726	1.4957	0.0079	826	1.5033	0.0043
634	1.5617	0.0030	730	1.5121	0.0080	830	1.5055	0.0043
638	1.5614	0.0034	734	1.5297	0.0127	834	1.5079	0.0051
642	1.5627	0.0021	738	1.5411	0.0225	838	1.5095	0.0067
646	1.5660	0.0020	742	1.5472	0.0316	842	1.5092	0.0084
650	1.5685	0.0023	746	1.5562	0.0419	846	1.5077	0.0089
654	1.5714	0.0023	750	1.5644	0.0592	850	1.5066	0.0081
658	1.5754	0.0025	754	1.5652	0.0838	854	1.5066	0.0068
662	1.5807	0.0033	758	1.5419	0.1121	858	1.5079	0.0055
666	1.5860	0.0057	762	1.4917	0.1206	862	1.5094	0.0052
670	1.5894	0.0078	766	1.4506	0.1005	866	1.5104	0.0053
674	1.5940	0.0077	770	1.4384	0.0721	870	1.5105	0.0052
678	1.6043	0.0072	774	1.4406	0.0497	874	1.5115	0.0042
682	1.6184	0.0088	778	1.4473	0.0326	878	1.5133	0.0044
686	1.6440	0.0123	782	1.4572	0.0210	882	1.5141	0.0046
690	1.6744	0.0236	786	1.4667	0.0143	886	1.5152	0.0047
694	1.8024	0.0679	790	1.4746	0.0105	890	1.5164	0.0051
698	1.8307	0.2730	794	1.4804	0.0086	894	1.5176	0.0056
702	1.5240	0.3865	798	1.4849	0.0073	898	1.5193	0.0065
706	1.2961	0.2446	802	1.4881	0.0063	902	1.5217	0.0087
710	1.3218	0.1032	806	1.4916	0.0049	906	1.5218	0.0128
714	1.3918	0.0341	810	1.4950	0.0048	910	1.5166	0.0158
718	1.4462	0.0128	814	1.4972	0.0045	914	1.5108	0.0144
722	1.4768	0.0082	818	1.4997	0.0043	918	1.5089	0.0110
			822	1.5017	0.0044	922	1.5098	0.0081

926	1.5116	0.0065	1130	1.5164	0.0016	1334	1.5222	0.0093
930	1.5133	0.0059	1134	1.5172	0.0014	1338	1.5223	0.0092
934	1.5146	0.0058	1138	1.5188	0.0012	1342	1.5228	0.0096
938	1.5155	0.0059	1142	1.5200	0.0020	1346	1.5222	0.0103
942	1.5160	0.0062	1146	1.5212	0.0024	1350	1.5216	0.0102
946	1.5161	0.0063	1150	1.5237	0.0044	1354	1.5218	0.0105
950	1.5167	0.0060	1154	1.5220	0.0081	1358	1.5214	0.0110
954	1.5175	0.0060	1158	1.5167	0.0080	1362	1.5207	0.0114
958	1.5192	0.0062	1162	1.5156	0.0052	1366	1.5197	0.0117
962	1.5201	0.0080	1166	1.5174	0.0039	1370	1.5184	0.0116
966	1.5188	0.0091	1170	1.5187	0.0035	1374	1.5169	0.0109
970	1.5175	0.0090	1174	1.5204	0.0037	1378	1.5157	0.0095
974	1.5174	0.0083	1178	1.5221	0.0053	1382	1.5157	0.0077
978	1.5183	0.0082	1182	1.5203	0.0076	1386	1.5166	0.0063
982	1.5186	0.0087	1186	1.5172	0.0068	1390	1.5175	0.0054
986	1.5180	0.0089	1190	1.5177	0.0052	1394	1.5185	0.0046
990	1.5177	0.0086	1194	1.5192	0.0052	1398	1.5196	0.0040
994	1.5179	0.0079	1198	1.5193	0.0059	1402	1.5209	0.0035
998	1.5202	0.0076	1202	1.5186	0.0062	1406	1.5223	0.0033
1002	1.5211	0.0097	1206	1.5181	0.0061	1410	1.5238	0.0032
1006	1.5195	0.0102	1210	1.5176	0.0058	1414	1.5253	0.0033
1010	1.5196	0.0099	1214	1.5174	0.0052	1418	1.5271	0.0036
1014	1.5206	0.0103	1218	1.5171	0.0047	1422	1.5287	0.0040
1018	1.5218	0.0112	1222	1.5176	0.0036	1426	1.5315	0.0041
1022	1.5245	0.0138	1226	1.5186	0.0035	1430	1.5361	0.0055
1026	1.5234	0.0200	1230	1.5192	0.0035	1434	1.5412	0.0090
1030	1.5104	0.0226	1234	1.5196	0.0038	1438	1.5458	0.0150
1034	1.5034	0.0138	1238	1.5198	0.0039	1442	1.5494	0.0233
1038	1.5084	0.0087	1242	1.5199	0.0041	1446	1.5528	0.0359
1042	1.5117	0.0073	1246	1.5194	0.0042	1450	1.5506	0.0581
1046	1.5138	0.0071	1250	1.5196	0.0035	1454	1.4925	0.0739
1050	1.5151	0.0073	1254	1.5202	0.0034	1458	1.4604	0.0302
1054	1.5161	0.0078	1258	1.5206	0.0033	1462	1.4883	0.0116
1058	1.5171	0.0086	1262	1.5212	0.0033	1466	1.4980	0.0072
1062	1.5178	0.0101	1266	1.5216	0.0034	1470	1.5049	0.0051
1066	1.5172	0.0121	1270	1.5221	0.0036	1474	1.5104	0.0048
1070	1.5137	0.0134	1274	1.5227	0.0039	1478	1.5151	0.0050
1074	1.5102	0.0120	1278	1.5230	0.0044	1482	1.5214	0.0064
1078	1.5089	0.0097	1282	1.5233	0.0048	1486	1.5304	0.0111
1082	1.5095	0.0075	1286	1.5230	0.0052	1490	1.5492	0.0288
1086	1.5103	0.0064	1290	1.5233	0.0050	1494	1.5059	0.0592
1090	1.5108	0.0053	1294	1.5240	0.0054	1498	1.4649	0.0258
1094	1.5118	0.0046	1298	1.5243	0.0060	1502	1.4865	0.0081
1098	1.5124	0.0042	1302	1.5246	0.0067	1506	1.4955	0.0041
1102	1.5130	0.0038	1306	1.5246	0.0075	1510	1.5003	0.0031
1106	1.5136	0.0034	1310	1.5243	0.0082	1514	1.5030	0.0027
1110	1.5142	0.0032	1314	1.5237	0.0086	1518	1.5050	0.0024
1114	1.5150	0.0031	1318	1.5231	0.0088	1522	1.5066	0.0022
1118	1.5149	0.0034	1322	1.5228	0.0088	1526	1.5079	0.0022
1122	1.5146	0.0026	1326	1.5229	0.0089	1530	1.5089	0.0021
1126	1.5155	0.0019	1330	1.5227	0.0093	1534	1.5100	0.0023

1538	1.5107	0.0025	1742	1.5156	0.0013	1946	1.5184	0.0024
1542	1.5116	0.0027	1746	1.5156	0.0014	1950	1.5179	0.0027
1546	1.5117	0.0034	1750	1.5154	0.0014	1954	1.5174	0.0027
1550	1.5114	0.0032	1754	1.5152	0.0013	1958	1.5171	0.0025
1554	1.5117	0.0030	1758	1.5151	0.0011	1962	1.5169	0.0023
1558	1.5121	0.0026	1762	1.5150	0.0009	1966	1.5167	0.0021
1562	1.5128	0.0023	1766	1.5152	0.0006	1970	1.5167	0.0019
1566	1.5136	0.0022	1770	1.5154	0.0004	1974	1.5167	0.0017
1570	1.5147	0.0022	1774	1.5158	0.0002	1978	1.5167	0.0015
1574	1.5159	0.0026	1778	1.5160	0.0002	1982	1.5169	0.0014
1578	1.5186	0.0039	1782	1.5163	0.0000	1986	1.5169	0.0014
1582	1.5172	0.0074	1786	1.5168	0.0000	1990	1.5169	0.0013
1586	1.5130	0.0065	1790	1.5173	0.0002	1994	1.5170	0.0012
1590	1.5149	0.0044	1794	1.5177	0.0006	1998	1.5170	0.0011
1594	1.5194	0.0059	1798	1.5180	0.0011	2002	1.5172	0.0010
1598	1.5225	0.0116	1802	1.5179	0.0017	2006	1.5173	0.0010
1602	1.5117	0.0183	1806	1.5174	0.0021	2010	1.5174	0.0010
1606	1.5002	0.0114	1810	1.5169	0.0022	2014	1.5173	0.0011
1610	1.5034	0.0049	1814	1.5162	0.0022	2018	1.5174	0.0010
1614	1.5069	0.0030	1818	1.5159	0.0016	2022	1.5171	0.0011
1618	1.5084	0.0022	1822	1.5161	0.0014	2026	1.5172	0.0007
1622	1.5098	0.0019	1826	1.5161	0.0012	2030	1.5175	0.0007
1626	1.5104	0.0020	1830	1.5162	0.0010	2034	1.5176	0.0007
1630	1.5106	0.0017	1834	1.5164	0.0008	2038	1.5177	0.0007
1634	1.5111	0.0015	1838	1.5166	0.0007	2042	1.5177	0.0007
1638	1.5115	0.0013	1842	1.5165	0.0007	2046	1.5178	0.0007
1642	1.5120	0.0011	1846	1.5167	0.0003	2050	1.5179	0.0007
1646	1.5124	0.0011	1850	1.5174	0.0003	2054	1.5179	0.0007
1650	1.5127	0.0010	1854	1.5177	0.0004	2058	1.5180	0.0007
1654	1.5131	0.0009	1858	1.5181	0.0006	2062	1.5180	0.0008
1658	1.5135	0.0010	1862	1.5184	0.0009	2066	1.5181	0.0008
1662	1.5139	0.0011	1866	1.5186	0.0014	2070	1.5181	0.0008
1666	1.5140	0.0012	1870	1.5185	0.0019	2074	1.5181	0.0008
1670	1.5145	0.0013	1874	1.5181	0.0023	2078	1.5181	0.0008
1674	1.5145	0.0018	1878	1.5177	0.0025	2082	1.5182	0.0008
1678	1.5141	0.0018	1882	1.5169	0.0025	2086	1.5182	0.0008
1682	1.5141	0.0017	1886	1.5166	0.0020	2090	1.5182	0.0008
1686	1.5141	0.0016	1890	1.5168	0.0018	2094	1.5183	0.0008
1690	1.5143	0.0015	1894	1.5167	0.0017	2098	1.5183	0.0008
1694	1.5144	0.0015	1898	1.5167	0.0014	2102	1.5183	0.0008
1698	1.5146	0.0014	1902	1.5168	0.0012	2106	1.5183	0.0008
1702	1.5147	0.0016	1906	1.5169	0.0010	2110	1.5184	0.0008
1706	1.5149	0.0017	1910	1.5171	0.0009	2114	1.5184	0.0007
1710	1.5145	0.0020	1914	1.5174	0.0008	2118	1.5184	0.0007
1714	1.5138	0.0016	1918	1.5177	0.0008	2122	1.5185	0.0007
1718	1.5141	0.0011	1922	1.5179	0.0009	2126	1.5186	0.0007
1722	1.5144	0.0008	1926	1.5182	0.0010	2130	1.5189	0.0007
1726	1.5148	0.0007	1930	1.5184	0.0012	2134	1.5189	0.0010
1730	1.5151	0.0006	1934	1.5186	0.0015	2138	1.5186	0.0010
1734	1.5157	0.0007	1938	1.5184	0.0019	2142	1.5186	0.0010
1738	1.5158	0.0012	1942	1.5184	0.0020	2146	1.5186	0.0009

2150	1.5186	0.0009	2354	1.5186	0.0001	2558	1.5206	0.0009
2154	1.5187	0.0009	2358	1.5187	0.0001	2562	1.5206	0.0009
2158	1.5187	0.0008	2362	1.5187	0.0001	2566	1.5206	0.0009
2162	1.5187	0.0008	2366	1.5188	0.0001	2570	1.5207	0.0009
2166	1.5188	0.0008	2370	1.5188	0.0000	2574	1.5207	0.0010
2170	1.5189	0.0007	2374	1.5190	0.0000	2578	1.5207	0.0010
2174	1.5190	0.0007	2378	1.5191	0.0000	2582	1.5207	0.0011
2178	1.5191	0.0007	2382	1.5192	0.0000	2586	1.5207	0.0011
2182	1.5192	0.0007	2386	1.5193	0.0000	2590	1.5207	0.0011
2186	1.5192	0.0007	2390	1.5194	0.0001	2594	1.5207	0.0011
2190	1.5192	0.0007	2394	1.5195	0.0002	2598	1.5207	0.0012
2194	1.5193	0.0006	2398	1.5195	0.0003	2602	1.5204	0.0013
2198	1.5195	0.0005	2402	1.5196	0.0004	2606	1.5204	0.0010
2202	1.5200	0.0005	2406	1.5193	0.0004	2610	1.5206	0.0010
2206	1.5202	0.0008	2410	1.5193	0.0002	2614	1.5206	0.0009
2210	1.5202	0.0008	2414	1.5196	0.0002	2618	1.5208	0.0009
2214	1.5205	0.0008	2418	1.5196	0.0003	2622	1.5209	0.0010
2218	1.5211	0.0008	2422	1.5197	0.0004	2626	1.5209	0.0010
2222	1.5220	0.0010	2426	1.5197	0.0004	2630	1.5209	0.0011
2226	1.5237	0.0016	2430	1.5195	0.0005	2634	1.5209	0.0012
2230	1.5266	0.0042	2434	1.5195	0.0002	2638	1.5208	0.0011
2234	1.5253	0.0095	2438	1.5198	0.0003	2642	1.5208	0.0011
2238	1.5170	0.0115	2442	1.5198	0.0003	2646	1.5208	0.0011
2242	1.5115	0.0077	2446	1.5199	0.0003	2650	1.5209	0.0011
2246	1.5120	0.0038	2450	1.5199	0.0004	2654	1.5209	0.0011
2250	1.5137	0.0019	2454	1.5199	0.0004	2658	1.5210	0.0011
2254	1.5150	0.0011	2458	1.5199	0.0005	2662	1.5210	0.0011
2258	1.5160	0.0008	2462	1.5200	0.0005	2666	1.5210	0.0011
2262	1.5165	0.0009	2466	1.5197	0.0006	2670	1.5210	0.0011
2266	1.5166	0.0007	2470	1.5198	0.0003	2674	1.5211	0.0011
2270	1.5169	0.0006	2474	1.5201	0.0003	2678	1.5211	0.0011
2274	1.5171	0.0005	2478	1.5201	0.0004	2682	1.5211	0.0011
2278	1.5173	0.0004	2482	1.5202	0.0004	2686	1.5211	0.0010
2282	1.5174	0.0003	2486	1.5202	0.0005	2690	1.5212	0.0010
2286	1.5177	0.0003	2490	1.5203	0.0005	2694	1.5212	0.0010
2290	1.5178	0.0003	2494	1.5203	0.0006	2698	1.5213	0.0010
2294	1.5182	0.0002	2498	1.5203	0.0006	2702	1.5214	0.0010
2298	1.5183	0.0005	2502	1.5204	0.0007	2706	1.5214	0.0010
2302	1.5181	0.0005	2506	1.5204	0.0007	2710	1.5217	0.0009
2306	1.5182	0.0004	2510	1.5204	0.0008	2714	1.5217	0.0012
2310	1.5182	0.0005	2514	1.5204	0.0009	2718	1.5215	0.0012
2314	1.5182	0.0005	2518	1.5203	0.0009	2722	1.5216	0.0012
2318	1.5182	0.0004	2522	1.5200	0.0009	2726	1.5216	0.0011
2322	1.5186	0.0003	2526	1.5201	0.0006	2730	1.5216	0.0011
2326	1.5186	0.0006	2530	1.5203	0.0006	2734	1.5216	0.0010
2330	1.5185	0.0005	2534	1.5204	0.0007	2738	1.5217	0.0010
2334	1.5186	0.0006	2538	1.5205	0.0007	2742	1.5218	0.0009
2338	1.5185	0.0006	2542	1.5205	0.0007	2746	1.5219	0.0009
2342	1.5183	0.0005	2546	1.5205	0.0008	2750	1.5220	0.0009
2346	1.5182	0.0003	2550	1.5205	0.0008	2754	1.5221	0.0008
2350	1.5184	0.0002	2554	1.5205	0.0008	2758	1.5222	0.0008

2762	1.5224	0.0008	2966	1.5089	0.0048	3170	1.5147	0.0009
2766	1.5225	0.0008	2970	1.5103	0.0037	3174	1.5148	0.0009
2770	1.5227	0.0008	2974	1.5118	0.0030	3178	1.5149	0.0009
2774	1.5229	0.0008	2978	1.5130	0.0027	3182	1.5150	0.0009
2778	1.5230	0.0008	2982	1.5141	0.0023	3186	1.5151	0.0009
2782	1.5234	0.0008	2986	1.5155	0.0022	3190	1.5151	0.0009
2786	1.5235	0.0011	2990	1.5167	0.0023	3194	1.5151	0.0009
2790	1.5234	0.0010	2994	1.5183	0.0026	3198	1.5152	0.0009
2794	1.5236	0.0010	2998	1.5199	0.0040	3202	1.5150	0.0010
2798	1.5237	0.0010	3002	1.5191	0.0055	3206	1.5151	0.0007
2802	1.5239	0.0010	3006	1.5180	0.0052	3210	1.5153	0.0007
2806	1.5242	0.0010	3010	1.5191	0.0045	3214	1.5154	0.0007
2810	1.5244	0.0010	3014	1.5220	0.0048	3218	1.5154	0.0007
2814	1.5247	0.0010	3018	1.5256	0.0077	3222	1.5155	0.0007
2818	1.5250	0.0010	3022	1.5265	0.0133	3226	1.5155	0.0007
2822	1.5255	0.0010	3026	1.5198	0.0186	3230	1.5156	0.0007
2826	1.5260	0.0010	3030	1.5099	0.0172	3234	1.5157	0.0007
2830	1.5269	0.0011	3034	1.5067	0.0117	3238	1.5157	0.0007
2834	1.5277	0.0016	3038	1.5085	0.0078	3242	1.5157	0.0007
2838	1.5286	0.0021	3042	1.5107	0.0060	3246	1.5158	0.0007
2842	1.5298	0.0033	3046	1.5130	0.0053	3250	1.5158	0.0007
2846	1.5303	0.0050	3050	1.5151	0.0059	3254	1.5159	0.0007
2850	1.5296	0.0069	3054	1.5160	0.0075	3258	1.5159	0.0007
2854	1.5278	0.0080	3058	1.5151	0.0094	3262	1.5159	0.0006
2858	1.5259	0.0082	3062	1.5121	0.0101	3266	1.5160	0.0006
2862	1.5246	0.0075	3066	1.5094	0.0085	3270	1.5160	0.0006
2866	1.5242	0.0064	3070	1.5093	0.0064	3274	1.5160	0.0006
2870	1.5247	0.0055	3074	1.5108	0.0051	3278	1.5160	0.0006
2874	1.5258	0.0051	3078	1.5126	0.0055	3282	1.5161	0.0006
2878	1.5272	0.0052	3082	1.5119	0.0068	3286	1.5161	0.0006
2882	1.5281	0.0060	3086	1.5092	0.0064	3290	1.5161	0.0005
2886	1.5286	0.0067	3090	1.5084	0.0043	3294	1.5162	0.0005
2890	1.5291	0.0076	3094	1.5097	0.0029	3298	1.5162	0.0005
2894	1.5294	0.0084	3098	1.5111	0.0026	3302	1.5163	0.0005
2898	1.5301	0.0093	3102	1.5116	0.0028	3306	1.5165	0.0005
2902	1.5310	0.0105	3106	1.5112	0.0028	3310	1.5165	0.0007
2906	1.5316	0.0124	3110	1.5109	0.0022	3314	1.5163	0.0007
2910	1.5320	0.0146	3114	1.5114	0.0016	3318	1.5163	0.0006
2914	1.5319	0.0176	3118	1.5119	0.0012	3322	1.5163	0.0006
2918	1.5301	0.0210	3122	1.5124	0.0011	3326	1.5163	0.0006
2922	1.5263	0.0236	3126	1.5126	0.0011	3330	1.5163	0.0006
2926	1.5217	0.0247	3130	1.5129	0.0008	3334	1.5163	0.0005
2930	1.5175	0.0244	3134	1.5134	0.0008	3338	1.5163	0.0005
2934	1.5140	0.0234	3138	1.5136	0.0008	3342	1.5163	0.0005
2938	1.5108	0.0217	3142	1.5138	0.0008	3346	1.5163	0.0004
2942	1.5081	0.0195	3146	1.5140	0.0008	3350	1.5164	0.0004
2946	1.5064	0.0167	3150	1.5142	0.0008	3354	1.5164	0.0004
2950	1.5054	0.0139	3154	1.5144	0.0008	3358	1.5164	0.0003
2954	1.5051	0.0109	3158	1.5145	0.0009	3362	1.5164	0.0003
2958	1.5060	0.0082	3162	1.5146	0.0009	3366	1.5165	0.0003
2962	1.5074	0.0062	3166	1.5146	0.0009	3370	1.5165	0.0002

3374	1.5166	0.0002	3434	1.5171	0.0000	3494	1.5173	0.0000
3378	1.5166	0.0002	3438	1.5171	0.0002	3498	1.5173	0.0000
3382	1.5168	0.0002	3442	1.5170	0.0002	3502	1.5174	0.0000
3386	1.5168	0.0004	3446	1.5170	0.0001	3506	1.5174	0.0000
3390	1.5167	0.0003	3450	1.5170	0.0001	3510	1.5174	0.0000
3394	1.5167	0.0003	3454	1.5170	0.0000	3514	1.5175	0.0000
3398	1.5167	0.0002	3458	1.5171	0.0000	3518	1.5175	0.0001
3402	1.5167	0.0002	3462	1.5171	0.0000	3522	1.5174	0.0001
3406	1.5167	0.0002	3466	1.5172	0.0000	3526	1.5174	0.0000
3410	1.5167	0.0001	3470	1.5172	0.0000	3530	1.5174	0.0000
3414	1.5168	0.0001	3474	1.5172	0.0000	3534	1.5175	0.0000
3418	1.5168	0.0001	3478	1.5173	0.0000	3538	1.5175	0.0000
3422	1.5169	0.0000	3482	1.5173	0.0001	3542	1.5175	0.0000
3426	1.5169	0.0000	3486	1.5172	0.0001	3546	1.5176	0.0000
3430	1.5170	0.0000	3490	1.5173	0.0000	3550	1.5176	0.0000

7. Poly(vinylidene chloride/acrylonitrile)

wavenumber	n	k	655	1.4209	0.0638	717	1.3978	0.0289
595	1.4672	0.0141	657	1.4180	0.0634	719	1.3978	0.0282
597	1.4648	0.0156	659	1.4158	0.0632	721	1.3977	0.0275
599	1.4626	0.0171	661	1.4132	0.0629	723	1.3975	0.0267
601	1.4618	0.0165	663	1.4106	0.0624	725	1.3978	0.0258
603	1.4659	0.0170	665	1.4075	0.0616	727	1.3981	0.0252
605	1.4680	0.0211	667	1.4047	0.0598	729	1.3984	0.0246
607	1.4673	0.0236	669	1.4040	0.0586	731	1.3987	0.0240
609	1.4688	0.0260	671	1.4004	0.0587	733	1.3992	0.0235
611	1.4698	0.0297	673	1.3962	0.0557	735	1.3996	0.0232
613	1.4694	0.0335	675	1.3948	0.0528	737	1.4000	0.0229
615	1.4684	0.0369	677	1.3932	0.0500	739	1.4004	0.0228
617	1.4675	0.0399	679	1.3921	0.0471	741	1.4007	0.0228
619	1.4673	0.0431	681	1.3905	0.0440	743	1.4008	0.0227
621	1.4663	0.0475	683	1.3915	0.0396	745	1.4009	0.0227
623	1.4634	0.0514	685	1.3939	0.0378	747	1.4011	0.0227
625	1.4591	0.0542	687	1.3946	0.0362	749	1.4010	0.0229
627	1.4577	0.0558	689	1.3960	0.0349	751	1.4006	0.0230
629	1.4531	0.0598	691	1.3972	0.0341	753	1.4002	0.0230
631	1.4488	0.0590	693	1.3978	0.0336	755	1.3997	0.0229
633	1.4472	0.0609	695	1.3985	0.0330	757	1.3990	0.0226
635	1.4428	0.0612	697	1.3993	0.0327	759	1.3982	0.0222
637	1.4411	0.0612	699	1.3995	0.0327	761	1.3974	0.0214
639	1.4385	0.0621	701	1.3993	0.0325	763	1.3970	0.0205
641	1.4361	0.0619	703	1.3993	0.0319	765	1.3966	0.0196
643	1.4344	0.0626	705	1.3997	0.0318	767	1.3963	0.0185
645	1.4316	0.0629	707	1.3994	0.0318	769	1.3962	0.0174
647	1.4297	0.0628	709	1.3988	0.0313	771	1.3963	0.0163
649	1.4275	0.0634	711	1.3985	0.0307	773	1.3966	0.0152
651	1.4250	0.0631	713	1.3985	0.0301	775	1.3970	0.0141
653	1.4235	0.0633	715	1.3982	0.0297	777	1.3974	0.0131

779	1.3982	0.0122	881	1.4235	0.0197	983	1.4167	0.0282
781	1.3975	0.0115	883	1.4240	0.0204	985	1.4172	0.0280
783	1.3985	0.0089	885	1.4245	0.0212	987	1.4178	0.0279
785	1.4011	0.0084	887	1.4250	0.0222	989	1.4184	0.0279
787	1.4023	0.0080	889	1.4253	0.0234	991	1.4191	0.0279
789	1.4037	0.0078	891	1.4253	0.0246	993	1.4198	0.0281
791	1.4048	0.0078	893	1.4252	0.0259	995	1.4207	0.0282
793	1.4057	0.0078	895	1.4248	0.0271	997	1.4214	0.0285
795	1.4067	0.0078	897	1.4242	0.0284	999	1.4234	0.0288
797	1.4076	0.0080	899	1.4233	0.0294	1001	1.4240	0.0306
799	1.4084	0.0081	901	1.4222	0.0302	1003	1.4235	0.0309
801	1.4092	0.0083	903	1.4211	0.0308	1005	1.4244	0.0314
803	1.4098	0.0085	905	1.4199	0.0312	1007	1.4251	0.0319
805	1.4105	0.0086	907	1.4189	0.0314	1009	1.4259	0.0325
807	1.4112	0.0089	909	1.4179	0.0315	1011	1.4268	0.0332
809	1.4119	0.0092	911	1.4171	0.0314	1013	1.4278	0.0340
811	1.4124	0.0096	913	1.4163	0.0314	1015	1.4288	0.0350
813	1.4128	0.0099	915	1.4154	0.0311	1017	1.4299	0.0361
815	1.4132	0.0102	917	1.4147	0.0307	1019	1.4309	0.0374
817	1.4136	0.0105	919	1.4140	0.0302	1021	1.4320	0.0389
819	1.4140	0.0108	921	1.4148	0.0296	1023	1.4331	0.0406
821	1.4144	0.0111	923	1.4145	0.0306	1025	1.4341	0.0426
823	1.4146	0.0114	925	1.4129	0.0299	1027	1.4349	0.0448
825	1.4149	0.0115	927	1.4128	0.0293	1029	1.4354	0.0472
827	1.4153	0.0118	929	1.4126	0.0288	1031	1.4355	0.0497
829	1.4156	0.0121	931	1.4125	0.0284	1033	1.4354	0.0519
831	1.4159	0.0124	933	1.4125	0.0279	1035	1.4353	0.0542
833	1.4162	0.0127	935	1.4126	0.0276	1037	1.4352	0.0562
835	1.4164	0.0130	937	1.4127	0.0272	1039	1.4356	0.0586
837	1.4165	0.0131	939	1.4128	0.0269	1041	1.4358	0.0611
839	1.4169	0.0133	941	1.4132	0.0266	1043	1.4363	0.0639
841	1.4170	0.0135	943	1.4135	0.0264	1045	1.4367	0.0674
843	1.4174	0.0137	945	1.4138	0.0262	1047	1.4368	0.0713
845	1.4177	0.0140	947	1.4143	0.0262	1049	1.4364	0.0758
847	1.4179	0.0142	949	1.4146	0.0261	1051	1.4357	0.0805
849	1.4182	0.0144	951	1.4150	0.0262	1053	1.4347	0.0861
851	1.4185	0.0146	953	1.4153	0.0263	1055	1.4320	0.0925
853	1.4189	0.0149	955	1.4157	0.0265	1057	1.4277	0.0989
855	1.4192	0.0152	957	1.4160	0.0267	1059	1.4212	0.1054
857	1.4194	0.0155	959	1.4163	0.0270	1061	1.4117	0.1102
859	1.4197	0.0158	961	1.4165	0.0272	1063	1.4011	0.1123
861	1.4200	0.0162	963	1.4168	0.0276	1065	1.3910	0.1117
863	1.4202	0.0165	965	1.4170	0.0280	1067	1.3829	0.1094
865	1.4204	0.0168	967	1.4169	0.0284	1069	1.3767	0.1067
867	1.4206	0.0171	969	1.4167	0.0288	1071	1.3714	0.1041
869	1.4210	0.0174	971	1.4165	0.0289	1073	1.3666	0.1018
871	1.4213	0.0177	973	1.4163	0.0290	1075	1.3617	0.0995
873	1.4215	0.0180	975	1.4162	0.0290	1077	1.3564	0.0970
875	1.4219	0.0183	977	1.4161	0.0288	1079	1.3509	0.0939
877	1.4224	0.0187	979	1.4162	0.0286	1081	1.3457	0.0899
879	1.4230	0.0191	981	1.4164	0.0284	1083	1.3410	0.0853

1085	1.3370	0.0802	1187	1.3832	0.0048	1289	1.3841	0.0057
1087	1.3336	0.0744	1189	1.3841	0.0052	1291	1.3841	0.0056
1089	1.3326	0.0684	1191	1.3851	0.0058	1293	1.3842	0.0052
1091	1.3314	0.0641	1193	1.3861	0.0066	1295	1.3845	0.0049
1093	1.3293	0.0585	1195	1.3869	0.0076	1297	1.3849	0.0047
1095	1.3293	0.0529	1197	1.3874	0.0088	1299	1.3853	0.0045
1097	1.3298	0.0479	1199	1.3874	0.0100	1301	1.3857	0.0044
1099	1.3305	0.0430	1201	1.3873	0.0109	1303	1.3860	0.0044
1101	1.3319	0.0384	1203	1.3870	0.0119	1305	1.3863	0.0042
1103	1.3339	0.0342	1205	1.3866	0.0126	1307	1.3867	0.0041
1105	1.3362	0.0307	1207	1.3860	0.0133	1309	1.3871	0.0041
1107	1.3385	0.0276	1209	1.3854	0.0139	1311	1.3874	0.0040
1109	1.3410	0.0248	1211	1.3846	0.0142	1313	1.3879	0.0039
1111	1.3438	0.0227	1213	1.3837	0.0144	1315	1.3883	0.0039
1113	1.3461	0.0211	1215	1.3828	0.0142	1317	1.3887	0.0040
1115	1.3484	0.0195	1217	1.3822	0.0139	1319	1.3890	0.0040
1117	1.3508	0.0185	1219	1.3819	0.0135	1321	1.3894	0.0040
1119	1.3530	0.0178	1221	1.3817	0.0132	1323	1.3899	0.0040
1121	1.3549	0.0174	1223	1.3816	0.0129	1325	1.3904	0.0041
1123	1.3565	0.0172	1225	1.3806	0.0127	1327	1.3909	0.0042
1125	1.3577	0.0171	1227	1.3807	0.0113	1329	1.3914	0.0043
1127	1.3587	0.0170	1229	1.3817	0.0112	1331	1.3920	0.0046
1129	1.3594	0.0170	1231	1.3818	0.0111	1333	1.3927	0.0049
1131	1.3598	0.0169	1233	1.3822	0.0110	1335	1.3933	0.0053
1133	1.3600	0.0167	1235	1.3823	0.0111	1337	1.3939	0.0059
1135	1.3601	0.0163	1237	1.3824	0.0111	1339	1.3946	0.0067
1137	1.3601	0.0157	1239	1.3823	0.0112	1341	1.3949	0.0077
1139	1.3601	0.0149	1241	1.3822	0.0111	1343	1.3950	0.0087
1141	1.3601	0.0140	1243	1.3821	0.0111	1345	1.3947	0.0098
1143	1.3604	0.0129	1245	1.3820	0.0109	1347	1.3941	0.0107
1145	1.3607	0.0117	1247	1.3818	0.0108	1349	1.3935	0.0114
1147	1.3611	0.0104	1249	1.3817	0.0105	1351	1.3928	0.0119
1149	1.3619	0.0091	1251	1.3817	0.0103	1353	1.3920	0.0124
1151	1.3629	0.0079	1253	1.3818	0.0100	1355	1.3911	0.0127
1153	1.3640	0.0068	1255	1.3818	0.0098	1357	1.3902	0.0127
1155	1.3652	0.0058	1257	1.3818	0.0096	1359	1.3893	0.0127
1157	1.3666	0.0049	1259	1.3819	0.0094	1361	1.3886	0.0125
1159	1.3680	0.0043	1261	1.3820	0.0092	1363	1.3878	0.0123
1161	1.3695	0.0038	1263	1.3819	0.0090	1365	1.3866	0.0119
1163	1.3709	0.0035	1265	1.3819	0.0088	1367	1.3857	0.0110
1165	1.3722	0.0033	1267	1.3820	0.0085	1369	1.3845	0.0099
1167	1.3734	0.0032	1269	1.3820	0.0083	1371	1.3845	0.0078
1169	1.3746	0.0031	1271	1.3821	0.0080	1373	1.3858	0.0069
1171	1.3758	0.0032	1273	1.3822	0.0078	1375	1.3863	0.0061
1173	1.3768	0.0033	1275	1.3823	0.0076	1377	1.3870	0.0054
1175	1.3777	0.0034	1277	1.3825	0.0074	1379	1.3878	0.0049
1177	1.3787	0.0036	1279	1.3818	0.0072	1381	1.3886	0.0044
1179	1.3796	0.0038	1281	1.3821	0.0059	1383	1.3895	0.0040
1181	1.3805	0.0040	1283	1.3832	0.0058	1385	1.3904	0.0037
1183	1.3814	0.0043	1285	1.3835	0.0057	1387	1.3914	0.0035
1185	1.3822	0.0045	1287	1.3839	0.0057	1389	1.3925	0.0034

1391	1.3936	0.0034	1493	1.3835	0.0021	1595	1.3893	0.0021
1393	1.3950	0.0035	1495	1.3838	0.0020	1597	1.3892	0.0021
1395	1.3966	0.0039	1497	1.3841	0.0019	1599	1.3892	0.0020
1397	1.3983	0.0046	1499	1.3844	0.0019	1601	1.3891	0.0020
1399	1.4000	0.0057	1501	1.3846	0.0019	1603	1.3892	0.0019
1401	1.4016	0.0075	1503	1.3849	0.0018	1605	1.3892	0.0019
1403	1.4026	0.0096	1505	1.3851	0.0018	1607	1.3892	0.0018
1405	1.4030	0.0120	1507	1.3853	0.0017	1609	1.3892	0.0018
1407	1.4027	0.0144	1509	1.3856	0.0016	1611	1.3892	0.0018
1409	1.4016	0.0166	1511	1.3866	0.0016	1613	1.3892	0.0017
1411	1.4004	0.0183	1513	1.3867	0.0025	1615	1.3892	0.0017
1413	1.3990	0.0198	1515	1.3860	0.0025	1617	1.3892	0.0016
1415	1.3971	0.0209	1517	1.3862	0.0024	1619	1.3893	0.0015
1417	1.3955	0.0214	1519	1.3862	0.0024	1621	1.3894	0.0015
1419	1.3943	0.0218	1521	1.3863	0.0024	1623	1.3894	0.0014
1421	1.3932	0.0221	1523	1.3863	0.0023	1625	1.3895	0.0014
1423	1.3924	0.0225	1525	1.3864	0.0023	1627	1.3895	0.0013
1425	1.3917	0.0230	1527	1.3865	0.0022	1629	1.3896	0.0013
1427	1.3910	0.0238	1529	1.3866	0.0023	1631	1.3897	0.0012
1429	1.3900	0.0249	1531	1.3866	0.0022	1633	1.3898	0.0012
1431	1.3883	0.0261	1533	1.3867	0.0022	1635	1.3898	0.0011
1433	1.3859	0.0272	1535	1.3868	0.0021	1637	1.3906	0.0011
1435	1.3826	0.0277	1537	1.3869	0.0021	1639	1.3906	0.0019
1437	1.3788	0.0272	1539	1.3869	0.0021	1641	1.3899	0.0018
1439	1.3752	0.0256	1541	1.3870	0.0020	1643	1.3899	0.0018
1441	1.3724	0.0229	1543	1.3872	0.0019	1645	1.3897	0.0017
1443	1.3711	0.0199	1545	1.3873	0.0019	1647	1.3896	0.0015
1445	1.3707	0.0172	1547	1.3873	0.0019	1649	1.3898	0.0015
1447	1.3706	0.0147	1549	1.3874	0.0019	1651	1.3897	0.0015
1449	1.3709	0.0124	1551	1.3874	0.0018	1653	1.3896	0.0014
1451	1.3717	0.0104	1553	1.3875	0.0018	1655	1.3897	0.0012
1453	1.3727	0.0088	1555	1.3876	0.0017	1657	1.3897	0.0012
1455	1.3740	0.0076	1557	1.3877	0.0017	1659	1.3897	0.0011
1457	1.3751	0.0069	1559	1.3878	0.0016	1661	1.3898	0.0010
1459	1.3758	0.0064	1561	1.3879	0.0016	1663	1.3898	0.0009
1461	1.3761	0.0058	1563	1.3880	0.0016	1665	1.3899	0.0008
1463	1.3766	0.0050	1565	1.3880	0.0016	1667	1.3899	0.0008
1465	1.3773	0.0043	1567	1.3881	0.0016	1669	1.3899	0.0007
1467	1.3781	0.0038	1569	1.3882	0.0015	1671	1.3901	0.0006
1469	1.3789	0.0034	1571	1.3883	0.0015	1673	1.3902	0.0006
1471	1.3796	0.0032	1573	1.3884	0.0015	1675	1.3902	0.0005
1473	1.3801	0.0031	1575	1.3885	0.0015	1677	1.3903	0.0005
1475	1.3806	0.0030	1577	1.3886	0.0014	1679	1.3904	0.0004
1477	1.3810	0.0028	1579	1.3887	0.0014	1681	1.3904	0.0004
1479	1.3815	0.0027	1581	1.3888	0.0014	1683	1.3905	0.0004
1481	1.3818	0.0027	1583	1.3890	0.0014	1685	1.3905	0.0003
1483	1.3821	0.0026	1585	1.3891	0.0013	1687	1.3906	0.0003
1485	1.3824	0.0025	1587	1.3892	0.0013	1689	1.3907	0.0003
1487	1.3827	0.0024	1589	1.3900	0.0013	1691	1.3908	0.0002
1489	1.3830	0.0023	1591	1.3900	0.0022	1693	1.3909	0.0002
1491	1.3832	0.0022	1593	1.3892	0.0021	1695	1.3909	0.0002

1697	1.3910	0.0001	1723	1.3919	0.0008	1749	1.3918	0.0000
1699	1.3911	0.0001	1725	1.3918	0.0008	1751	1.3919	0.0000
1701	1.3912	0.0000	1727	1.3918	0.0009	1753	1.3920	0.0000
1703	1.3914	0.0000	1729	1.3916	0.0008	1755	1.3920	0.0000
1705	1.3915	0.0001	1731	1.3916	0.0008	1757	1.3921	0.0000
1707	1.3916	0.0002	1733	1.3915	0.0008	1759	1.3922	0.0000
1709	1.3917	0.0002	1735	1.3914	0.0006	1761	1.3922	0.0000
1711	1.3918	0.0003	1737	1.3914	0.0005	1763	1.3923	0.0000
1713	1.3919	0.0004	1739	1.3914	0.0004	1765	1.3923	0.0000
1715	1.3919	0.0004	1741	1.3915	0.0003	1767	1.3924	0.0000
1717	1.3919	0.0005	1743	1.3915	0.0002	1769	1.3924	0.0000
1719	1.3919	0.0006	1745	1.3916	0.0002			
1721	1.3920	0.0007	1747	1.3917	0.0001			

8. Cellulose Acetate

wavenumber	n	k	950	1.6180	0.0357	1115	1.3912	0.1489
790	1.5596	0.0000	955	1.6249	0.0359	1120	1.3999	0.1493
795	1.5649	0.0000	960	1.6326	0.0367	1125	1.3990	0.1477
800	1.5677	0.0027	965	1.6437	0.0368	1130	1.3946	0.1379
805	1.5694	0.0043	970	1.6584	0.0417	1135	1.3984	0.1216
810	1.5715	0.0060	975	1.6692	0.0499	1140	1.4146	0.1064
815	1.5730	0.0074	980	1.6767	0.0582	1145	1.4397	0.0995
820	1.5754	0.0083	985	1.6827	0.0652	1150	1.4641	0.1046
825	1.5793	0.0102	990	1.6892	0.0698	1155	1.4759	0.1177
830	1.5823	0.0138	995	1.7001	0.0722	1160	1.4715	0.1279
835	1.5821	0.0177	1000	1.7210	0.0768	1165	1.4613	0.1267
840	1.5796	0.0192	1005	1.7442	0.0896	1170	1.4572	0.1157
845	1.5787	0.0180	1010	1.7683	0.1055	1175	1.4635	0.0997
850	1.5815	0.0161	1015	1.7996	0.1298	1180	1.4818	0.0828
855	1.5867	0.0157	1020	1.8337	0.1677	1185	1.5142	0.0694
860	1.5925	0.0170	1025	1.8672	0.2251	1190	1.5595	0.0659
865	1.5989	0.0200	1030	1.8754	0.3070	1195	1.6158	0.0764
870	1.6047	0.0259	1035	1.8293	0.3891	1200	1.6831	0.1087
875	1.6055	0.0328	1040	1.7554	0.4408	1205	1.7509	0.1747
880	1.6036	0.0367	1045	1.6869	0.4713	1210	1.7830	0.2759
885	1.6056	0.0386	1050	1.6120	0.4896	1215	1.7521	0.3817
890	1.6127	0.0438	1055	1.5306	0.4831	1220	1.6845	0.4623
895	1.6157	0.0557	1060	1.4757	0.4552	1225	1.6183	0.5260
900	1.6047	0.0669	1065	1.4456	0.4332	1230	1.5180	0.5882
905	1.5879	0.0674	1070	1.4076	0.4169	1235	1.3766	0.6064
910	1.5800	0.0600	1075	1.3629	0.3898	1240	1.2413	0.5754
915	1.5808	0.0535	1080	1.3302	0.3516	1245	1.1411	0.5043
920	1.5824	0.0494	1085	1.3101	0.3109	1250	1.0852	0.4205
925	1.5836	0.0449	1090	1.2989	0.2678	1255	1.0600	0.3360
930	1.5875	0.0397	1095	1.3012	0.2242	1260	1.0630	0.2581
935	1.5946	0.0357	1100	1.3210	0.1867	1265	1.0860	0.1952
940	1.6032	0.0340	1105	1.3480	0.1640	1270	1.1160	0.1487
945	1.6117	0.0344	1110	1.3724	0.1518	1275	1.1467	0.1144

1280	1.1767	0.0901	1535	1.3866	0.0038	1790	1.2944	0.0212
1285	1.2044	0.0735	1540	1.3888	0.0036	1795	1.3073	0.0173
1290	1.2279	0.0629	1545	1.3910	0.0035	1800	1.3176	0.0146
1295	1.2470	0.0548	1550	1.3932	0.0034	1805	1.3247	0.0127
1300	1.2654	0.0482	1555	1.3952	0.0034	1810	1.3315	0.0098
1305	1.2838	0.0449	1560	1.3971	0.0031	1815	1.3385	0.0084
1310	1.2993	0.0451	1565	1.3994	0.0029	1820	1.3436	0.0073
1315	1.3099	0.0467	1570	1.4016	0.0029	1825	1.3484	0.0065
1320	1.3164	0.0470	1575	1.4037	0.0029	1830	1.3525	0.0058
1325	1.3223	0.0448	1580	1.4059	0.0028	1835	1.3563	0.0053
1330	1.3303	0.0408	1585	1.4082	0.0029	1840	1.3585	0.0050
1335	1.3417	0.0371	1590	1.4105	0.0030	1845	1.3615	0.0033
1340	1.3558	0.0350	1595	1.4128	0.0032	1850	1.3654	0.0031
1345	1.3726	0.0349	1600	1.4152	0.0035	1855	1.3679	0.0029
1350	1.3975	0.0387	1605	1.4177	0.0039	1860	1.3704	0.0028
1355	1.4340	0.0576	1610	1.4202	0.0045	1865	1.3726	0.0027
1360	1.4604	0.1034	1615	1.4225	0.0053	1870	1.3746	0.0026
1365	1.4348	0.1604	1620	1.4247	0.0062	1875	1.3765	0.0025
1370	1.3639	0.1855	1625	1.4270	0.0072	1880	1.3782	0.0025
1375	1.3044	0.1706	1630	1.4277	0.0084	1885	1.3799	0.0025
1380	1.2722	0.1414	1635	1.4295	0.0077	1890	1.3815	0.0025
1385	1.2569	0.1061	1640	1.4327	0.0084	1895	1.3829	0.0026
1390	1.2639	0.0717	1645	1.4345	0.0091	1900	1.3842	0.0027
1395	1.2850	0.0501	1650	1.4366	0.0094	1905	1.3854	0.0029
1400	1.3054	0.0404	1655	1.4390	0.0094	1910	1.3855	0.0031
1405	1.3205	0.0382	1660	1.4423	0.0094	1915	1.3865	0.0020
1410	1.3304	0.0387	1665	1.4449	0.0096	1920	1.3885	0.0021
1415	1.3375	0.0405	1670	1.4492	0.0085	1925	1.3895	0.0021
1420	1.3427	0.0431	1675	1.4555	0.0091	1930	1.3906	0.0022
1425	1.3453	0.0471	1680	1.4612	0.0102	1935	1.3915	0.0023
1430	1.3430	0.0508	1685	1.4677	0.0117	1940	1.3923	0.0023
1435	1.3365	0.0509	1690	1.4756	0.0139	1945	1.3932	0.0024
1440	1.3312	0.0465	1695	1.4829	0.0171	1950	1.3939	0.0024
1445	1.3301	0.0402	1700	1.4928	0.0195	1955	1.3946	0.0024
1450	1.3318	0.0347	1705	1.5067	0.0251	1960	1.3953	0.0024
1455	1.3338	0.0303	1710	1.5209	0.0336	1965	1.3960	0.0024
1460	1.3348	0.0260	1715	1.5399	0.0454	1970	1.3967	0.0023
1465	1.3364	0.0207	1720	1.5625	0.0664	1975	1.3974	0.0023
1470	1.3404	0.0152	1725	1.5834	0.0978	1980	1.3980	0.0022
1475	1.3459	0.0112	1730	1.6001	0.1426	1985	1.3987	0.0022
1480	1.3515	0.0087	1735	1.6001	0.2029	1990	1.3995	0.0022
1485	1.3564	0.0072	1740	1.5610	0.2685	1995	1.4001	0.0023
1490	1.3607	0.0063	1745	1.4872	0.3138	2000	1.4007	0.0024
1495	1.3646	0.0056	1750	1.4034	0.3348	2005	1.4013	0.0025
1500	1.3680	0.0052	1755	1.2998	0.3304	2010	1.4018	0.0026
1505	1.3712	0.0048	1760	1.1934	0.2750	2015	1.4023	0.0028
1510	1.3742	0.0045	1765	1.1490	0.1810	2020	1.4027	0.0029
1515	1.3770	0.0044	1770	1.1759	0.1009	2025	1.4030	0.0030
1520	1.3795	0.0042	1775	1.2214	0.0584	2030	1.4034	0.0031
1525	1.3820	0.0040	1780	1.2541	0.0387	2035	1.4028	0.0032
1530	1.3844	0.0039	1785	1.2770	0.0275	2040	1.4032	0.0020

2045	1.4047	0.0020	2300	1.4162	0.0024	2555	1.4242	0.0018
2050	1.4051	0.0021	2305	1.4162	0.0023	2560	1.4243	0.0017
2055	1.4057	0.0021	2310	1.4162	0.0021	2565	1.4244	0.0017
2060	1.4063	0.0022	2315	1.4162	0.0018	2570	1.4246	0.0017
2065	1.4067	0.0023	2320	1.4164	0.0014	2575	1.4247	0.0017
2070	1.4072	0.0024	2325	1.4167	0.0010	2580	1.4248	0.0017
2075	1.4077	0.0025	2330	1.4173	0.0007	2585	1.4248	0.0016
2080	1.4082	0.0026	2335	1.4178	0.0006	2590	1.4249	0.0016
2085	1.4086	0.0028	2340	1.4186	0.0005	2595	1.4250	0.0016
2090	1.4090	0.0030	2345	1.4193	0.0011	2600	1.4252	0.0015
2095	1.4094	0.0033	2350	1.4184	0.0015	2605	1.4253	0.0015
2100	1.4096	0.0035	2355	1.4181	0.0005	2610	1.4254	0.0014
2105	1.4097	0.0037	2360	1.4192	0.0000	2615	1.4256	0.0014
2110	1.4098	0.0039	2365	1.4203	0.0000	2620	1.4257	0.0014
2115	1.4099	0.0040	2370	1.4214	0.0005	2625	1.4259	0.0014
2120	1.4099	0.0040	2375	1.4218	0.0013	2630	1.4260	0.0013
2125	1.4099	0.0040	2380	1.4216	0.0020	2635	1.4262	0.0013
2130	1.4100	0.0039	2385	1.4212	0.0022	2640	1.4263	0.0013
2135	1.4101	0.0039	2390	1.4211	0.0023	2645	1.4271	0.0012
2140	1.4103	0.0037	2395	1.4211	0.0023	2650	1.4272	0.0021
2145	1.4104	0.0036	2400	1.4211	0.0024	2655	1.4265	0.0020
2150	1.4106	0.0035	2405	1.4211	0.0024	2660	1.4266	0.0019
2155	1.4108	0.0034	2410	1.4211	0.0025	2665	1.4266	0.0018
2160	1.4110	0.0033	2415	1.4211	0.0025	2670	1.4266	0.0017
2165	1.4112	0.0032	2420	1.4211	0.0024	2675	1.4267	0.0016
2170	1.4115	0.0030	2425	1.4212	0.0023	2680	1.4269	0.0015
2175	1.4118	0.0029	2430	1.4213	0.0023	2685	1.4270	0.0015
2180	1.4121	0.0029	2435	1.4214	0.0023	2690	1.4272	0.0014
2185	1.4124	0.0028	2440	1.4214	0.0022	2695	1.4273	0.0014
2190	1.4126	0.0028	2445	1.4215	0.0022	2700	1.4275	0.0014
2195	1.4129	0.0028	2450	1.4216	0.0022	2705	1.4277	0.0014
2200	1.4131	0.0028	2455	1.4217	0.0021	2710	1.4279	0.0014
2205	1.4134	0.0027	2460	1.4218	0.0021	2715	1.4280	0.0014
2210	1.4137	0.0027	2465	1.4219	0.0020	2720	1.4282	0.0014
2215	1.4139	0.0027	2470	1.4220	0.0020	2725	1.4283	0.0014
2220	1.4141	0.0027	2475	1.4221	0.0019	2730	1.4290	0.0014
2225	1.4143	0.0027	2480	1.4222	0.0018	2735	1.4290	0.0022
2230	1.4145	0.0027	2485	1.4223	0.0018	2740	1.4283	0.0020
2235	1.4148	0.0027	2490	1.4224	0.0017	2745	1.4285	0.0019
2240	1.4149	0.0028	2495	1.4226	0.0016	2750	1.4285	0.0018
2245	1.4151	0.0028	2500	1.4227	0.0015	2755	1.4286	0.0017
2250	1.4152	0.0028	2505	1.4229	0.0015	2760	1.4288	0.0016
2255	1.4154	0.0028	2510	1.4231	0.0014	2765	1.4290	0.0015
2260	1.4155	0.0028	2515	1.4234	0.0013	2770	1.4292	0.0014
2265	1.4156	0.0028	2520	1.4235	0.0012	2775	1.4294	0.0014
2270	1.4157	0.0028	2525	1.4245	0.0012	2780	1.4297	0.0014
2275	1.4158	0.0028	2530	1.4246	0.0021	2785	1.4299	0.0013
2280	1.4159	0.0028	2535	1.4239	0.0020	2790	1.4308	0.0014
2285	1.4159	0.0027	2540	1.4240	0.0020	2795	1.4309	0.0022
2290	1.4160	0.0026	2545	1.4240	0.0019	2800	1.4303	0.0022
2295	1.4161	0.0025	2550	1.4241	0.0018	2805	1.4305	0.0021

2810	1.4306	0.0021	3065	1.4284	0.0012	3320	1.4357	0.0032
2815	1.4307	0.0021	3070	1.4287	0.0012	3325	1.4358	0.0034
2820	1.4309	0.0020	3075	1.4290	0.0012	3330	1.4359	0.0036
2825	1.4312	0.0020	3080	1.4292	0.0012	3335	1.4361	0.0038
2830	1.4316	0.0019	3085	1.4294	0.0012	3340	1.4362	0.0040
2835	1.4321	0.0020	3090	1.4296	0.0013	3345	1.4363	0.0042
2840	1.4326	0.0022	3095	1.4298	0.0013	3350	1.4364	0.0044
2845	1.4333	0.0026	3100	1.4299	0.0014	3355	1.4365	0.0046
2850	1.4338	0.0031	3105	1.4301	0.0015	3360	1.4366	0.0048
2855	1.4342	0.0038	3110	1.4302	0.0015	3365	1.4367	0.0051
2860	1.4343	0.0046	3115	1.4303	0.0016	3370	1.4368	0.0054
2865	1.4342	0.0055	3120	1.4303	0.0017	3375	1.4368	0.0056
2870	1.4338	0.0062	3125	1.4304	0.0018	3380	1.4368	0.0059
2875	1.4333	0.0068	3130	1.4298	0.0018	3385	1.4368	0.0062
2880	1.4327	0.0072	3135	1.4299	0.0011	3390	1.4369	0.0065
2885	1.4320	0.0074	3140	1.4307	0.0011	3395	1.4363	0.0068
2890	1.4314	0.0074	3145	1.4309	0.0012	3400	1.4364	0.0064
2895	1.4309	0.0072	3150	1.4311	0.0012	3405	1.4371	0.0067
2900	1.4305	0.0069	3155	1.4312	0.0013	3410	1.4371	0.0071
2905	1.4306	0.0066	3160	1.4314	0.0013	3415	1.4372	0.0074
2910	1.4307	0.0064	3165	1.4316	0.0014	3420	1.4373	0.0078
2915	1.4310	0.0063	3170	1.4317	0.0015	3425	1.4373	0.0083
2920	1.4315	0.0064	3175	1.4318	0.0016	3430	1.4374	0.0087
2925	1.4322	0.0067	3180	1.4318	0.0017	3435	1.4373	0.0092
2930	1.4331	0.0077	3185	1.4319	0.0018	3440	1.4372	0.0097
2935	1.4332	0.0094	3190	1.4314	0.0018	3445	1.4371	0.0102
2940	1.4315	0.0109	3195	1.4315	0.0011	3450	1.4369	0.0108
2945	1.4293	0.0112	3200	1.4323	0.0012	3455	1.4366	0.0114
2950	1.4279	0.0107	3205	1.4324	0.0013	3460	1.4362	0.0120
2955	1.4272	0.0103	3210	1.4326	0.0013	3465	1.4357	0.0126
2960	1.4263	0.0101	3215	1.4328	0.0014	3470	1.4350	0.0130
2965	1.4248	0.0096	3220	1.4330	0.0015	3475	1.4343	0.0134
2970	1.4236	0.0083	3225	1.4332	0.0016	3480	1.4336	0.0137
2975	1.4235	0.0068	3230	1.4333	0.0017	3485	1.4328	0.0139
2980	1.4242	0.0058	3235	1.4334	0.0018	3490	1.4320	0.0140
2985	1.4247	0.0053	3240	1.4336	0.0019	3495	1.4312	0.0140
2990	1.4248	0.0050	3245	1.4337	0.0020	3500	1.4305	0.0139
2995	1.4248	0.0045	3250	1.4338	0.0021	3505	1.4298	0.0137
3000	1.4250	0.0039	3255	1.4339	0.0022	3510	1.4292	0.0135
3005	1.4254	0.0035	3260	1.4340	0.0024	3515	1.4286	0.0133
3010	1.4259	0.0033	3265	1.4340	0.0025	3520	1.4280	0.0130
3015	1.4262	0.0032	3270	1.4341	0.0026	3525	1.4274	0.0127
3020	1.4262	0.0032	3275	1.4336	0.0027	3530	1.4269	0.0124
3025	1.4261	0.0029	3280	1.4337	0.0021	3535	1.4264	0.0120
3030	1.4261	0.0025	3285	1.4345	0.0022	3540	1.4259	0.0116
3035	1.4264	0.0021	3290	1.4346	0.0023	3545	1.4254	0.0112
3040	1.4267	0.0018	3295	1.4349	0.0025	3550	1.4250	0.0106
3045	1.4271	0.0015	3300	1.4350	0.0026	3555	1.4246	0.0101
3050	1.4274	0.0014	3305	1.4352	0.0027	3560	1.4243	0.0095
3055	1.4278	0.0013	3310	1.4354	0.0029	3565	1.4240	0.0088
3060	1.4281	0.0012	3315	1.4355	0.0031	3570	1.4239	0.0082

3575	1.4238	0.0075
3580	1.4238	0.0069
3585	1.4240	0.0063
3590	1.4242	0.0058
3595	1.4244	0.0053
3600	1.4247	0.0049
3605	1.4250	0.0045
3610	1.4252	0.0042
3615	1.4255	0.0040
3620	1.4257	0.0038
3625	1.4260	0.0036
3630	1.4262	0.0034
3635	1.4264	0.0033
3640	1.4265	0.0031
3645	1.4267	0.0030
3650	1.4269	0.0029
3655	1.4270	0.0028
3660	1.4272	0.0026
3665	1.4274	0.0025
3670	1.4276	0.0024
3675	1.4277	0.0023
3680	1.4278	0.0022
3685	1.4281	0.0021
3690	1.4282	0.0021
3695	1.4283	0.0020
3700	1.4285	0.0020
3705	1.4287	0.0020
3710	1.4288	0.0020
3715	1.4289	0.0020
3720	1.4290	0.0020
3725	1.4291	0.0020
3730	1.4292	0.0019
3735	1.4294	0.0019
3740	1.4295	0.0020
3745	1.4296	0.0020
3750	1.4296	0.0021
3755	1.4295	0.0020
3760	1.4297	0.0019
3765	1.4298	0.0019
3770	1.4298	0.0020
3775	1.4298	0.0019
3780	1.4299	0.0019
3785	1.4300	0.0019
3790	1.4300	0.0019
3795	1.4301	0.0019
3800	1.4302	0.0019
3805	1.4302	0.0019
3810	1.4302	0.0019
3815	1.4303	0.0019
3820	1.4303	0.0019
3825	1.4303	0.0018
3830	1.4304	0.0018
3835	1.4305	0.0018
3840	1.4304	0.0018
3845	1.4305	0.0018
3850	1.4306	0.0018
3855	1.4305	0.0018
3860	1.4305	0.0018
3865	1.4306	0.0017
3870	1.4307	0.0017
3875	1.4307	0.0017
3880	1.4307	0.0017
3885	1.4308	0.0017
3890	1.4308	0.0017
3895	1.4308	0.0016
3900	1.4309	0.0016
3905	1.4309	0.0016
3910	1.4309	0.0016
3915	1.4310	0.0016
3920	1.4310	0.0015
3925	1.4311	0.0015
3930	1.4311	0.0015
3935	1.4312	0.0015
3940	1.4312	0.0015
3945	1.4313	0.0015
3950	1.4313	0.0015
3955	1.4314	0.0015
3960	1.4314	0.0015
3965	1.4315	0.0015
3970	1.4315	0.0015
3975	1.4316	0.0015
3980	1.4316	0.0015
3985	1.4316	0.0014
3990	1.4321	0.0014
3995	1.4321	0.0020
4000	1.4316	0.0019